ANALYTICA CHIMICA ACTA

International monthly devoted to all branches of analytical chemistry
Revue mensuelle internationale consacrée à tous les domaines de la chimie analytique
Internationale Monatsschrift für alle Gebiete der analytischen Chemie

ELSEVIER SCIENTIFIC PUBLISHING COMPANY

AMSTERDAM

Anal. Chim. Acta, Vol. 80, 1–208, November 1975

Published monthly

Complete in one issue

ANALYTICA CHIMICA ACTA

Publication Schedule for 1975

Vol. 74, No. 1	January 1975	
Vol. 74, No. 2	February 1975	**(completing Vol. 74)**
Vol. 75. No. 1	March 1975	
Vol. 75, No. 2	April 1975	**(completing Vol. 75)**
Vol. 76, No. 1	May 1975	
Vol. 76, No. 2	June 1975	**(completing Vol. 76)**
Vol. 77	July 1975	**(complete in one issue)**
Vol. 78, No. 1	August 1975	
Vol. 78, No. 2	September 1975	**(completing Vol. 78)**
Vol. 79	October 1975	**(complete in one issue)**
Vol. 80, No. 1	November 1975	
Vol. 80, No. 2	December 1975	**(completing Vol. 80)**

Subscription price for 1975 (covering Vols. 74–79): Dfl. 570.00 plus Dfl. 54.00 postage. US$ 265.53 inclusive of postage. Subscribers in the U.S.A. and Canada receive their copies by airmail. Additional charges for airmail to other countries are available on request. For advertising rates apply to the publishers.

Subscriptions should be sent to:
Elsevier Scientific Publishing Company, P.O. Box 211, Amsterdam, The Netherlands.

GENERAL INFORMATION

Languages

Papers will be published in English, French or German.

Detailed information

Authors should consult Vol. 73, p. 435 for detailed instructions. Reprints of this information are obtainable from Dr. Macdonald or from: Elsevier Editorial Series Ltd., Mayfield House, 256 Banbury Road, Oxford (Great Britain).

Submission of papers

Papers should be sent to:

Prof. Philip W, West,
Coates Chemical Laboratories,
College of Chemistry and Physics,
Louisiana State University,
Baton Rouge 3,
La. 70803 (U.S.A.)

or to:

Dr. A.M.G. MacDonald,
Department of Chemistry,
The University,
P.O. Box 363
Birmingham B15 2TT (Great Britain)

Reprints

Fifty reprints will be supplied free of charge. Additional reprints (minimum 100) can be ordered at quoted prices. They must be ordered on order forms which are sent together with the proofs.

Deuteration degree: min. 99.5%
^{12}C content: min. 99.95%

No interfering solvent signals in the ^{1}H and ^{13}C NMR spectra from deuterated ^{12}C solvents[1,2].

10718 ^{12}C-Chloroform-d_1
10717 ^{12}C-Dichloromethane-d_2
10781 ^{12}C-Dimethyl sulfoxide-d_6
10682 ^{12}C-Methanol-d_4
2205 ^{12}C-Carbon tetrachloride

Further ^{12}C solvents and new ^{12}C preparations for synthesis and for isotope labelling 3 are in preparation.

1. L. Pohl, KONTAKTE Merck 2/73, 9-11
2. L. Pohl, R. Unger and W. Theysohn, CZ-Chemie-Technik 2 (1973), No. 8, 335/36
3. J. Prestin and H. Günther, Angew. Chem. 86, 7, 278 (1974)

ANALYTICA CHIMICA ACTA
Vol. 80 (1975)

ANALYTICA CHIMICA ACTA

International monthly devoted to all branches of analytical chemistry
Revue mensuelle internationale consacrée à tous les domaines de la chimie analytique
Internationale Monatsschrift für alle Gebiete der analytischen Chemie

ELSEVIER SCIENTIFIC PUBLISHING COMPANY

AMSTERDAM

PRINTED IN THE NETHERLANDS

Analytica Chimica Acta, 80 (1975) 1—8

OBSERVATIONS ON THE CALIBRATION OF SOLID-STATE SILVER SULPHIDE MEMBRANE ION-SELECTIVE ELECTRODES

D. J. CROMBIE, G. J. MOODY and J. D. R. THOMAS

Chemistry Department, University of Wales Institute of Science and Technology, Cardiff CF1 3NU (Wales)

(Received 13th June 1975)

SUMMARY

By adding known increments of standardizing solution to the contents of an e.m.f. measuring cell and taking precautions against oxidation of sulphide ions, solid-state Orion 94-16A silver sulphide membrane electrodes, may be calibrated with near-Nernstian response down to ca. 10^{-7} M silver and ca. $2 \cdot 10^{-7}$ M sulphide ions, respectively. These and associated data suggest that the detection limits for these ions are dictated by the solubility of the membrane material and that an alternative mechanism based on silver defects does not have a significant role in the practical measuring situation. Standard reduction potentials for the electrode with respect to silver and sulphide are +800 mV and −660 mV, respectively.

The capability of ion-selective electrodes based on silver sulphide sensing membranes for monitoring low levels of sulphide ion activity has been demonstrated by potentiometric titrations [1—6], alkaline pulp liquor analysis [4, 7, 8] and stability constant determination [3]. However, calibration curves for total sulphide in solutions varying in sodium sulphide concentration in a constant background of 1.0 M sodium hydroxide (to establish a constant fraction of total sulphide in the form of sulphide ion) are claimed [4] to establish a lower Nernstian linear relation limit of 10^{-4} M for such electrodes. Of course, because of the appreciable hydrolysis of the sulphide ion according to

$$S^{2-} + H_2O \rightleftharpoons HS^- + OH^- \quad (1)$$

$$HS^- + H_2O \rightleftharpoons H_2S + OH^- \quad (2)$$

of which only the first step affects the sulphide ion concentration in alkaline solutions, the actual sulphide ion activity, $[S^{2-}]$, which will be sensed by the electrode is lower than the total level, $[S^{2-}]_T$, and may be calculated [3, 9] from the relation

$$[S^{2-}] = f_{S^{2-}} [S^{2-}]_T \Big/ \left(1 + \frac{[H^+]}{K_2}\right) \quad (3)$$

where K_2 is the ionization constant of HS^- and $f_{S^{2-}}$ the activity coefficient of the sulphide ion.

Equation (3) indicates that at constant total sulphide ion concentration and constant ionic strength, the actual sulphide ion activity will increase with increasing pH values [3]; moreover, the sulphide ion-selective electrode can be used to determine either the concentration of free sulphide ions or the total sulphide concentration if the pH value of the sample solution is determined simultaneously in aqueous solution [3]. Thus, in the discussion by Hseu and Rechnitz [3], total sulphide concentrations in the 10^{-1}—$3 \cdot 10^{-5}$ M range correspond to free sulphide ion activity in the $10^{-2.2}$—10^{-7} M range at pH 11.4—11.8 in 0.1 M, 0.3 M and 0.5 M ionic strength solutions. While it is reassuring to know that the sulphide ion-selective electrode can detect low levels of free sulphide ion activity, calibrations by the method of Hseu and Rechnitz [3] are made tedious by the need for parallel pH measurements in order to compute the sulphide ion activity corresponding to the standard total sulphide calibrating solutions; also, such calibrations are restricted to the higher ranges of total sulphide.

A simpler calibration for sulphide, recommended by Orion Research [1], involves very basic solutions where the total sulphide exists mainly as free sulphide ions; only 10^{-1} M and 10^{-2} M sodium sulphide solutions in 1.0 M sodium hydroxide are used and the e.m.f.—$\log[S^{2-}]$ relation is extrapolated to the required sulphide ion range. This extrapolation is a rather sweeping recommendation in view of the recent claim [10] that the detection limits of silver compound solid-state electrodes are governed by either the solubility of the membrane material or the activity of the silver defects in the membrane surface, according to which effect is larger. For the silver sulphide membrane electrode, silver defects are shown [10] to dominate; in support of this, an e.m.f. response diagram for sulphide ions shows a potential change of about +820 mV in passing from 10^{-5} M sulphide to 10^{-6} M sulphide and a further change of about +90 mV in passing to 10^{-7} M sulphide [10]. These are staggeringly large e.m.f. changes over one decade and the reading of +100 mV vs. a double junction reference electrode (with potassium nitrate junction) for the 10^{-6} M sulphide solution is nearly 500 mV more positive than the reading of around −400 mV expected of a ca. 10^{-17} M sulphide system as represented by the normal solubility of silver sulphide ($K_{SO} \approx 10^{-51}$).

In view of this anomaly and the importance of measuring low sulphide ion levels, the present investigation was undertaken to assess the direct calibration of the Orion model 94-16A sulphide/silver ion-selective electrode.

EXPERIMENTAL

An Orion model 94-16A sulphide/silver ion-selective electrode was used in various test solutions at 25 °C in conjunction with an Orion model 90-02-00 double-junction reference electrode with an outer 10 % potassium nitrate filler. The e.m.f. was recorded with a Radiometer pHM 64, digital pH meter, to 0.1 mV used in conjunction with a Servoscribe Model RE 541 potentiometric recorder.

Calibration solutions were prepared from Analar silver nitrate for silver ion calibrations and Analar sodium sulphide nonahydrate for sulphide ion calibrations. The salts were dissolved in deionized water through which purified nitrogen had previously been bubbled. Proper sulphide ion calibrations were, however, made on alkaline solutions prepared from Analar sodium sulphide dissolved in 1.0 M Analar sodium hydroxide, or in 1.0 M Analar sodium hydroxide containing Analar ascorbic acid (20 mg ml^{-1}) in deionized water also presaturated with purified nitrogen.

E.m.f. calibrating measurements were made as appropriate on fresh solutions prepared by direct weighing or by serial dilution with nitrogen-saturated deionized water; but, for low sulphide levels, measurements were made on solutions prepared in the measuring cell by adding small increments of fresh standardizing solution from an Agla micrometer syringe burette to a known volume of nitrogen-saturated deionized water. Stock sodium sulphide solutions were standardized by titration with silver nitrate [1].

Standard silver solutions in PTFE, light-protected measuring cells were mixed by magnetic stirrer, but for sulphide ion solutions mixing was effected by bubbling with white-spot nitrogen.

RESULTS AND DISCUSSION

Electrode response to silver ions

Serial dilution of 0.1 M silver nitrate solution gives a characteristic e.m.f.—log a_{Ag} calibration that is linear (slope 59.2 mV pAg^{-1}) to 10^{-5} M followed by a breakaway non-linear region in the direction of 10^{-6} and 10^{-7} M (Fig. 1, curve A). Since the electrode ought to give a longer linear range, extended calibrations at high pIon were made with small increments of 10^{-2} M silver nitrate solution from an Agla micrometer syringe burette in the manner described above. A longer linear e.m.f.—log a_{Ag} calibration was thus readily obtained for silver ions to 10^{-7} M (Fig. 1, curve B). This confirms the silver part per billion calibration obtained by Müller et al. [11] for an Orion model 94-16 silver sulphide membrane electrode by a similar procedure, and the calibration to 10^{-7} M of a Crytur model 16-17 and other laboratory-prepared silver sulphide membrane electrodes by Veselý et al. [9] with diluted silver nitrate.

Durst and Duhart [12] observed linearity to ca. $4 \cdot 10^{-7}$ M for serially diluted 10^{-4} M silver nitrate for an Orion Model 94-16 electrode and showed that because of silver ion adsorption, containers made of Vycor, polyethylene, Teflon, Desicoted Pyrex and Pyrex were unsuitable for the long-term storage of solutions containing low levels of silver. However, while the other materials, and especially Pyrex, showed appreciable silver ion adsorption from $2 \cdot 10^{-6}$ M solution even after a very short time, silver losses on Teflon for comparable periods were minimal and were of the order of only 2 % after one day [12]. These facts and other studies [13—14] place the problems of calibrating ion-selective electrodes at low ion levels in perspective. In the

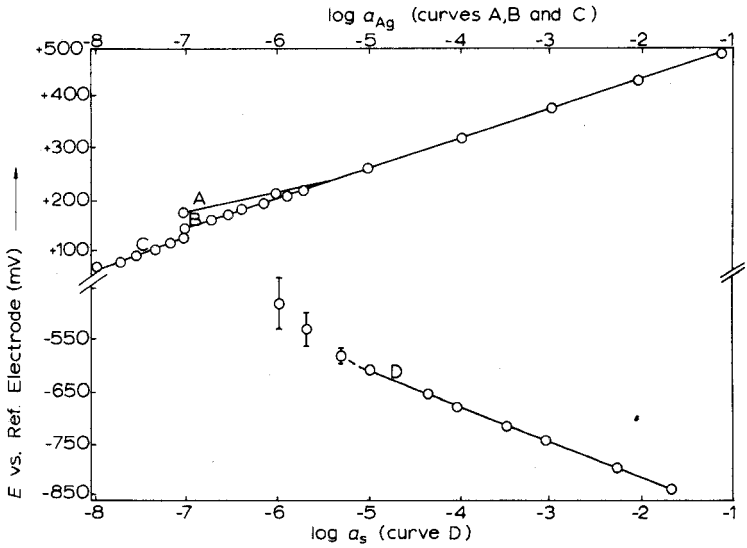

Fig. 1. Response of an Orion model 94-16A ion-selective electrode to silver ions and sulphide ions in aqueous solution. Curve A; response to silver ions by serial dilution. Curve B; response to silver ions in standard solutions and in solutions prepared by adding known increments of 10^{-2} M silver nitrate. Curve C; response to silver ions in solutions prepared by adding known increments of 10^{-3} M silver nitrate. Curve D; response to sulphide ions in standard solutions and in solutions prepared by adding known increments of 10^{-2} M sodium sulphide.

present study, attempts to continue the electrode calibration to 10^{-8} M silver ions with 10^{-3} M silver nitrate solution in the Agla burette failed (Fig. 1, curve C), the fall-off indicating a silver ion level lower than expected, which may have been due to the sorption of silver ions by container materials including the glass of the Agla syringe.

Long response times create their own problems in such measurements. Thus, while the Orion model 94-16A electrode reaches an equilibrium reading in under 1 min at $2 \cdot 10^{-7}$ M silver ions, up to 5 min are required at 10^{-7} M, and 20 min or more at lower levels of silver ions.

Despite limitations in respect of more extended calibrations, the above examples clearly confirm a linear e.m.f.—log a_{Ag} calibration to 10^{-7} M silver ions for solid-state silver sulphide membrane electrodes. It should, however, be noted that the linear range of Morf et al. [10] for membrane electrodes made from pressed silver sulphide discs falls far short by breaking away between 10^{-4} M and 10^{-5} M silver ion activity, while Hseu and Rechnitz quote a calibration down to only 10^{-4} M silver ion for an Orion model 94-16 electrode.

Electrode response to sulphide ions in deionized water treated with nitrogen

Curve D in Fig. 1 was obtained by direct calibration with specially prepared 10^{-1} M, 10^{-2} M and 10^{-3} M sodium sulphide solutions and at more dilute sulphide levels with solutions prepared from increments taken from an Agla micrometer syringe burette. The calibration gives a considerably steeper e.m.f.—log a_S slope (76 mV/pS^{2-}) than the expected 29.6 mV/pS^{2-} but this is consistent with eqn. (3), for the increasingly lower pH values with dilution lead to consumption of sulphide ions by equilibrium (1) supported by equilibrium (2). Thus, the pH changes from 12.5 at 10^{-1} M sodium sulphide concentration to 8.7 at 10^{-5} M. Rechnitz and Hseu [3] counteracted the effect of equilibrium (2), prominent at low pH, with sodium hydroxide to keep the pH at 11.4—11.8; they were thus able to use eqn. (3) to compute the true sulphide ion levels.

Electrode response to sulphide ions in alkaline media

The apparent lower limit of 10^{-4} M in the calibration for total sulphide observed by Light and Swartz [4] is attributed to the difficulty in preparing dilute sulphide solutions without loss of sulphide, even when precautions are taken to exclude air by purging with inert gas. Also, while e.m.f. readings were found to be stable to ca. 1 mV over several hours at ambient temperatures in 10^{-1} M sodium sulphide plus 1.0 M sodium hydroxide, at lower sulphide levels, oxidation problems limit the reproducibility of the sulphide ion-selective electrode in alkaline sulphide solutions [4].

The present work confirms the lower calibration limit of 10^{-4} M as the best obtainable with solutions prepared by serial dilution in sodium hydroxide, but a combination of directly prepared calibrating solutions and solutions prepared in the measuring cell by additions of calibrating solution from an Agla syringe burette gives a reproducible linear e.m.f.—log[S^{2-}] relation down to ca. 10^{-6} M sulphide with a slope of 29.4 mV/pS^{2-} (curve A, Fig. 2).

Attempts to extend the calibration to below 10^{-6} M sulphide led to rather more positive e.m.f. readings than those demanded by the linear portion of curve A (Fig. 2). Such readings indicate lower sulphide ion levels than those computed from the contents of the measuring cell and can be explained by oxidation of sulphide ions. The ascorbic acid in Sulphide Anti-Oxidant Buffer (SAOB) greatly retards atmospheric oxidation of sulphide solutions [15] but although this was claimed to permit the determination of sulphide concentrations down to $3 \cdot 10^{-6}$ M, SAOB is not mentioned in a more recent Orion model 94-16 sulphide ion-selective electrode instruction manual [1].

Compared with curve A (Fig. 2), $3 \cdot 10^{-6}$ M sulphide is not a particularly ambitious linear limit for the e.m.f.—log[S^{2-}] relation, but the use of ascorbic acid (20 mg ml^{-1}) in the background 1.0 M sodium hydroxide extends the linear e.m.f.—log[S^{2-}] plot to ca. $2 \cdot 10^{-7}$ M sulphide

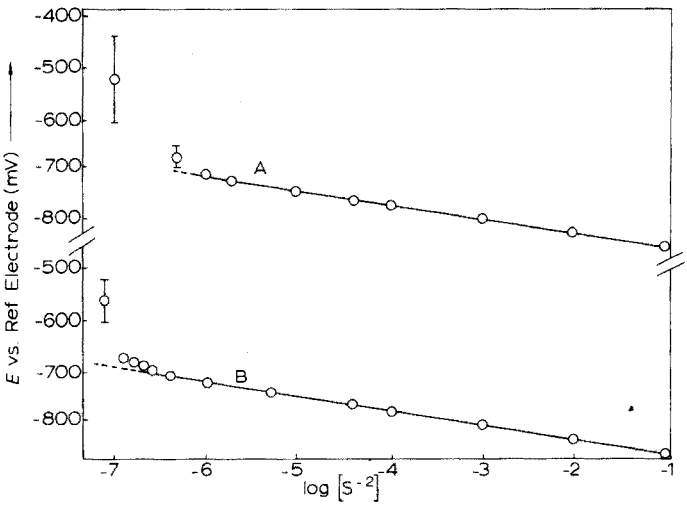

Fig. 2. Response of an Orion model 94-16A ion-selective electrode to sulphide ions in alkaline solution. Curve A, response to sulphide ions in 1.0 M sodium hydroxide. Curve B, response to sulphide ions in solutions of 1.0 M sodium hydroxide containing ascorbic acid.

(Fig. 2, curve B). This represents an improvement by an order of magnitude; furthermore, the calibration in solutions with ascorbic acid can be superimposed on the calibration in 1.0 M sodium hydroxide (which is shown separately in Fig. 2 for illustrative convenience).

Despite the presence of the antioxidant ascorbic acid, attempts to calibrate the electrode to below 10^{-7} M sulphide lead to e.m.f. values which are more positive than predicted as noted above, and suggest oxidation of sulphide. Moreover, while electrode response (< 2 min) at higher sulphide levels is sufficiently fast for stable e.m.f. readings to be recorded for a long time before oxidative consumption of sulphide ions becomes extensive, dependable e.m.f. readings cannot be achieved at sulphide levels below 10^{-7} M. This is because of the combined effects of traces of oxygen in the bubbling nitrogen and of sluggish electrode response which becomes evident below 10^{-6} M, but inconveniently long ($\gg$ 15 min) below 10^{-7} M, making serious inroads into the now very small sulphide ion levels. Additionally, adsorption and other effects noted above for silver can also have their roles.

The suggestion of an oxidative consumption of sulphide ions was confirmed by the rapid change of cell e.m.f. to more positive values on replacing the nitrogen stream into the cell by oxygen. However, even under these drastic oxidative conditions, both in the presence and absence of ascorbic acid, the cell e.m.f. values consistently settled at values more negative than −400 mV and in no case did the calibration pattern span e.m.f. values in the range + 100 to +200 mV for 10^{-6} M and 10^{-7} M sulphide as quoted previously [10].

Standard potentials

Standard potentials with respect to both silver and sulphide may be found by extrapolating the appropriate e.m.f.—$\log a_{Ion}$ line to $\log a_{Ion} = 0$ and correcting with 242 mV as the potential of the reference electrode at 25 °C. If junction potentials are ignored, a value of $E^\circ = +800$ mV is obtained for silver which is in close agreement with that predicted [16] +799 mV vs. NHE.

By extrapolating to $\log[S^{2-}] = 0$ and correcting for the reference electrode potential, a value of −648 mV is obtained for sulphide. After due allowance is made for the activity of sulphide in the sodium hydroxide/ascorbic acid system, a slightly more negative value holds for the true E° but a value of this order, namely, −660 mV, corresponds to E° in base solutions for the following system [17]

$$Ag_2S + 2e^- \rightleftharpoons 2Ag + S^{2-} \qquad (4)$$

which is consistent with the electrode having silver as the contact material to the silver sulphide membrane [16].

CONCLUSIONS

The results of this study on an Orion model 94-16A sulphide/silver ion-selective electrode were duplicated on a second electrode of the same model, and confirm that this kind of electrode can be calibrated to ca. $2 \cdot 10^{-7}$ M sulphide and ca. 10^{-7} M silver ions, respectively. Such a calibration extends to the part per billion (10^9) range; only manipulative and interference limitations prevent calibration to the even lower levels that would be expected on the basis of the detection limit being largely dictated by the solubility [13, 14] of the membrane material.

On the present evidence, the activity of silver defects in the membrane surface does not play any substantial part in governing detection limits of silver compound membrane electrodes, at least in the case of the Orion model 94-16A sulphide/silver ion-selective electrodes. Indeed, the experimental evidence upon which such a thesis was based may partly be attributed to oxidation effects as shown by this work and previously noted and observed for the solid-state sulphide [18], and iodide [19, 20] ion-selective electrodes.

Finally, it is pertinent to note that the characteristic detection limit of an ion-selective electrode leads to a region of little or no change in cell e.m.f. with increasing dilution of the species under study. An oxidizable anion, on the other hand, leads to a region of much more positive cell e.m.f. values than are suggested by normal Nernstian or near-Nernstian response, but such effects can be lessened with ascorbic acid anti-oxidant as noted here for sulphide and elsewhere for iodide [19, 20].

The authors thank the Esso Petroleum Company Ltd. for valuable discussion and for financial support including a research award (to D. J. C.).

REFERENCES

1 Orion Research Inc., Instruction Manual, Sulphide Ion Electrode, Silver Ion Electrode, Model 94-16, 1970.
2 E. Pungor, Anal. Chem., 39 (1967) 28A.
3 T. M. Hseu and G. A. Rechnitz, Anal. Chem., 40 (1968) 1054.
4 T. S. Light and J. L. Swartz, Paper presented at the Pittsburgh Conference on Analytical Chemistry and Applied Spectroscopy, Cleveland, Ohio, March 3—8, 1968. Extracts appear in Anal. Lett., 1 (13) (1968) 825.
5 L. C. Gruen and B. S. Harrap, J. Soc. Leather Trades' Chem., 55 (1971) 131.
6 R. Naumann and Ch. Weber, Z. Anal. Chem., 253 (1971) 111.
7 J. L. Swartz and T. S. Light, J. Tech. Ass. Pulp Paper Ind., 53 (1970) 90.
8 M. S. Frant and J. W. Ross, J. Tech. Ass. Pulp Paper Ind., 53 (1970) 1753.
9 J. Veselý, O. J. Jensen and B. Nicolaisen, Anal. Chim. Acta, 62 (1972) 1.
10 W. E. Morf, G. Kahr and W. Simon, Anal. Chem., 46 (1974) 1538.
11 D. C. Müller, P. W. West and R. H. Müller, Anal. Chem., 41 (1969) 2038.
12 R. A. Durst and B. T. Duhart, Anal. Chem., 42 (1970) 1002.
13 N. Parthasarathy, J. Buffle and D. Monnier, Anal. Chim. Acta, 68 (1974) 185.
14 J. Buffle, N. Parthasarathy and W. Haerdi, Anal. Chim. Acta, 68 (1974) 253.
15 Orion Research Inc., Applications Bulletin No. 12, 1969.
16 M. Koebel, Anal. Chem., 46 (1974) 1559.
17 J. E. Huheey, Inorganic Chemistry: Principles of Structure and Reactivity, Harper and Row, New York, 1972, p. 265.
18 R. Bock and H. J. Puff, Z. Anal. Chem., 240 (1968) 381.
19 M. N. Khayat, Ph. D. Thesis, University of Manchester, 1974.
20 J. Kontoyannakos, G. J. Moody and J. D. R. Thomas, unpublished results.

Analytica Chimica Acta, 80 (1975) 9—16

THE SUITABILITY OF VARIOUS CALCIUM ELECTRODES BASED ON METAL SALTS OF Di-(n-OCTYLPHENYL)PHOSPHORIC ACID AND SOME DERIVATIVES FOR THE MEASUREMENT OF CALCIUM IN SEA WATER

DANIEL JAGNER* and J. P. ØSTERGAARD-JENSEN

Department of Inorganic Chemistry, Aarhus University, DK-8000 Aarhus C (Denmark)

(Received 23rd June 1975)

SUMMARY

The calcium salts of di-(n-octylphenyl)-phosphoric acid, di-(*p*-n-octyl-*o*-nitrophenyl)-phosphoric acid and di-(*p*-n-octyl-*o*-bromophenyl)-phosphoric acid have been investigated as calcium sensors in membrane electrodes. The electrodes have been used for potentiometric titrations of calcium in sea water. The effect of varying the membrane solvent and the chelate metal has been studied.

Since the development of the first calcium-selective membrane electrode by Ross [1], two major improvements have been made. The PVC membrane technique, suggested by Moody et al. [2, 3], has resulted in membrane electrodes which are much easier to handle than the Orion [1] electrodes and have much longer life-times. The use of the calcium salt of di-(n-octyl-phenyl)phosphoric acid has been shown by Růžička et al. [4] to give considerably improved calcium selectivity, particularly in acidic and sodium-containing solutions. This is largely due to the more electrophilic character of the n-octylphenyl group compared with the n-decyl group used previously [1].

In connection with previous investigations on the determination of calcium in sea water [5—7], it was considered interesting to test the suitability of the Růžička electrode for this purpose. These investigations were extended to include the effects caused by electrophilic substitution in the n-octylphenyl group, and by the use of different solvents.

*Present address: Department of Analytical Chemistry, University of Göteborg, Fack, S-402 20 Göteborg 5, Sweden.

EXPERIMENTAL

Electrodes

Selectrode [4, 8] electrode bodies were used in all investigations. A mixture of the relevant metal sulphate, mercury(I) chloride and mercury was used as inner-reference paste. PVC membranes were prepared as described by Moody et al. [2, 3] with only minor modifications.

Calcium activity changes in sea water were measured with the cell

$$\text{SCE}\,||\,\text{Standard Sea Water}\,|\,\text{membrane}\,|\,\underset{+\ \text{calcium increment}}{\text{Standard Sea Water}}\,||\,\text{SCE} \qquad (1)$$

where the reference electrodes were Radiometer K401. The circular membrane had a diameter of ca. 10 mm.

Apparatus

Calcium in sea water was titrated with a computerized titrator [9]. A Radiometer PHM 4 meter was used for all other potential measurements.

Reagents

Di-(n-octylphenyl)phosphoric acid (HDOPP) was prepared as described by Růžička et al. [4] Di-(*p*-n-octyl-*o*-nitrophenyl)phosphoric acid (NO_2-HDOPP) was prepared as follows: a solution of 0.05 moles of *p*-n-octylphenol in 10 g of carbon tetrachloride was added dropwise to a 0.3 M solution of nitric acid in carbon tetrachloride at 10 °C; the carbon tetrachloride fraction was washed with water, dried and evaporated, and the resulting *p*-n-octyl-*o*-nitrophenol was treated with phosphorus oxide trichloride as described elsewhere [4]. The corresponding bromine derivative (Br-HDOPP) was prepared by allowing HDOPP to react with bromine in the presence of iron powder; the product contained appreciable amounts of HDOPP.

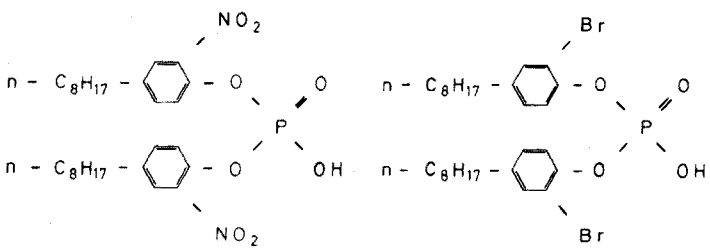

NO_2 - HDOPP Br - HDOPP

The solvent di-(n-octyl)phenylphosphonate (DOPP-n) was prepared as described by Griffiths et al. [10] and purified by Sephadex LH20 gel filtration. All other reagents were used as purchased. Standard Sea Water was obtained from Charlottenlund Slot, Copenhagen, Denmark.

The composition of the different membranes prepared is shown in Table 1 together with a summary of the experiments carried out.

Calibration

The membrane electrodes were calibrated by means of compleximetric titrations with EDTA or EGTA at varying total calcium, sodium and magnesium concentrations and at different pH values. The experimental titration curves were compared with theoretical titration curves computed by means of the program HALTAFALL [11]. From this comparison, the range of Nernstian response and the selectivity coefficients could be evaluated. This procedure [12] is in all essential aspects equivalent to the use of calcium buffers [4].

RESULTS AND CONCLUSIONS

$Ca(DOPP)_2$ membranes

Membranes of $Ca(DOPP)_2$ in DOPP-n (membrane I in Table 1) were investigated with respect to the range of Nernstian response and sodium selectivity. The same experiments were carried out on corresponding membranes prepared in Růžička's laboratory. All membranes showed similar behaviour and the results obtained agreed well with those published previously [4]. This shows that preparation of $Ca(DOPP)_2$ membranes can easily be reproduced and, moreover, that in practice the titration procedure [12] yields the same results as the calcium buffer procedure [4].

Sea water titrations

Membranes I were used for the potentiometric titration of calcium in Standard Sea Water samples, with EGTA as titrant and boric acid/borate as buffer system. The data were evaluated by the linear regression method of Gran [13], based on the theoretical value for the Nernst slope, 29.6 mV/decade.

Thirty consecutive titrations on 40—60-g samples yielded a relative standard deviation of 0.8 %. Although this is a considerably better precision than that obtainable with the Orion electrode [1, 5, 14], it is less satisfactory than that of the photometric titration procedure based on the zinc—zincon indicator system [7]. In routine analysis, the photometric method yields relative standard deviations better than 0.3 %. Moreover, even when the same computerized titrator [7] is used, a potentiometric titration takes

TABLE 1

Composition of PVC membranes prepared in this investigation

Membrane no.	Electroactive agent	Solvent	Investigations	Comments
I	$Ca(DOPP)_2$	DOPP-n	Ca titration, calcium activity measurements, pH dependence	Similar membrane obtained from Růžička
II	$Mg(DOPP)_2$	DOPP-n	Ca and Mg titrations	$Mg(DOPP)_2$ only slightly soluble in DOPP-n
III	$Zn(DOPP)_2$	DOPP-n	Ca and Zn titrations	
IV	$Ca(NO_2\text{-}DOPP)_2$	DOPP-n	Ca titration, pH dependence	$Ca(NO_2\text{-}DOPP)_2$ only slightly soluble in DOPP-n
V	$Ca(Br\text{-}DOPP)_2$	DOPP-n	Ca titration, pH dependence	Br-HDOPP contained appreciable amounts HDOPP
VI	none	DOPP-n	Ca titration	
VII	none	none	Ca titration	Pure PVC membrane
VIII	$Ca(DOPP)_2$	$(CH_3O)_3P{=}O$	Ca titration	
IX	$Ca(DOPP)_2$	$(C_2H_5O)_2P(S)Cl$	Ca titration	
X	none	$(C_6H_5O)_3P{=}O$	Ca titration	M.p. 50 °C. No crystal formation in membranes
XI	none	Sat. soln. of $(C_6H_5{-}O)_3P{=}O$ in DOPP-n	Ca titration, calcium activity measurement	

considerably longer than a photometric titration; after each addition of titrant, the membrane potential takes much longer to stabilize than the photocell signal. It can therefore be concluded that photometric titration is superior to potentiometric titration for oceanographic calcium determinations.

pH-dependence for different membranes

At constant calcium activity, an e.m.f. vs. pH plot shows a minimum for any calcium membrane electrode. The position of this minimum is related to the acidity of the electroactive substance. Membranes I, IV and V of Table 1 were tested for pH response by the addition of increments of dilute hydrochloric acid to a solution with pCa = 2. Membranes I were also compared with corresponding membranes obtained from Růžička [4].

Membranes containing $Ca(DOPP)_2$ as electroactive substance and DOPP-n as solvent (membrane I) yielded a potential minimum at pH 3.1. The same value was obtained with Růžička's membranes. This is almost half a unit lower than the value obtained previously [4], but hydrochloric acid was added slowly in a continuous stream, in the earlier study.

Membrane IV containing $Ca(NO_2\text{-}DOPP)_2$ was expected to have its potential minimum at a lower pH value than membrane I, but, the potential minimum actually occurred at a pH value 0.4 units higher than that of membrane I. The bromine-containing membrane, V, showed a pH response very similar to that of membrane I.

The calcium responses of membranes IV and V were also tested. When these membranes were used as sensors for the complexiметric titration of calcium in sea water, they showed a range of Nernstian response one to two decades smaller than that obtained with membranes containing unsubstituted electroactive agents. Moreover, less stable potential readings were obtained probably because of the low solubility of the nitro and bromine compounds in the DOPP-n solvent.

It can thus be concluded that a simple electrophilic substitution in the n-octylphenyl group will not increase the useful pH range of a calcium membrane electrode based on the calcium salt of di-(n-octylphenyl)phosphoric acid. Nor will such a substitution improve the calcium detection limit.

$Mg(DOPP)_2$ and $Zn(DOPP)_2$ membranes

Membranes containing the magnesium and zinc salts of di-(n-octylphenyl)-phosphoric acid (membranes II and III, respectively) were prepared in the same way as the corresponding calcium salt membranes. These membranes were used to investigate whether or not the calcium interference on the $Mg(DOPP)_2$ and $Zn(DOPP)_2$ membranes was related to a simple exchange equilibrium to the magnesium and zinc interferences on a $Ca(DOPP)_2$ membrane.

On calibration, by means of complexiметric titrations of magnesium or

zinc in solutions containing different concentrations of calcium, both the magnesium and the zinc salt membranes gave irreproducible results. Values of the selectivity coefficients could therefore be estimated only roughly. These values did not indicate a straightforward relationship between the selectivity coefficients for magnesium and zinc, obtained from a calcium salt membrane, and the selectivity coefficients for calcium, obtained from magnesium and zinc salt membranes. Obviously, the solvent, which was the same for all membranes, is of prime importance in the establishment of sensitivity and selectivity for calcium.

Effect of solvent

The mechanism of the solvent in calcium-selective membrane electrodes has never been completely clarified. Its importance has been indicated by several authors and is clearly demonstrated by the titration curve shown in Fig. 1. Here a PVC membrane containing DOPP-n only (membrane VI) was used for the titration of a 0.01 M calcium solution with EGTA solution. Although the titration curve is inferior to those obtained with membranes I, the membrane shows several decades of almost Nernstian response, as is indicated by the Gran plot which is also shown. A pure PVC membrane gave no calcium response.

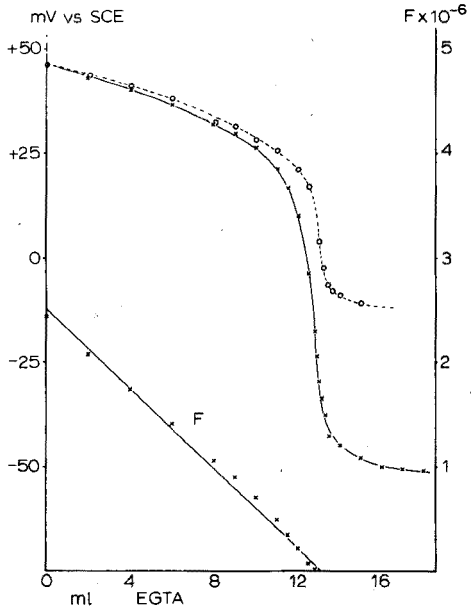

Fig. 1. Titration of 25 ml of 0.0100 M calcium and 0.01 M sodium with v ml of 0.0195 M EGTA at pH 9. PVC membranes prepared from di-(n-octyl)-phenyl phosphonate (—) and triphenylphosphate (---) were used. For comparison, the latter curve has been displaced so that both curves start at the same e.m.f. value. The corresponding Gran plot $F = (25 + v)\,10\exp((200 + E)/29.6)$ is shown for the di-(n-octyl)phenylphosphonate membrane.

The calcium sensitivity of membranes containing di-(n-octyl)phenylphosphonate has previously [4] been explained by the presence of appreciable amounts of protolytic impurities capable of complex formation with calcium. Since, in the present investigation, the solvent was purified by gel filtration, this explanation seems less likely.

The importance of using DOPP-n as solvent in achieving calcium sensitivity is further illustrated by the results obtained with membranes X, where DOPP-n was replaced by triphenylphosphate and no electroactive agent was added. When these membranes were used in complexiметric calcium titrations, the range of calcium sensitivity shown was considerably less than that of the DOPP-n membranes (Fig. 1). However, membranes prepared from a mixture of triphenylphosphate and DOPP-n (XI) yielded titration curves equivalent to that shown for the DOPP-n membrane in Fig. 1.

That the choice of solvent is of major importance for achieving calcium sensitivity with membranes based on the calcium salt of di-(n-octylphenyl)-phosphoric acid is further emphasized by the results obtained with membranes VIII and IX; here trimethylphosphate and O,O-diethylthiophosphorochloridate were used as solvents and $Ca(DOPP)_2$ as the "electroactive agent". While the trimethylphosphate membranes yielded titration curves similar to that shown for triphenylphosphate in Fig. 1, the thiophosphonyl solvent membranes showed hardly any calcium sensitivity at all. This means that the presence of a phosphonyl group in the solvent is essential for obtaining calcium sensitivity.

Measurement of small changes in calcium activity

Titration procedures give accurate results for the total calcium concentration in a sea-water sample, but they do not yield any direct information on the calcium activity. In order to give useful information, activity differences, for example, between Standard Sea Water and the sample, of 1 % or less must be detectable. For a calcium-selective electrode this corresponds to an e.m.f. difference of 0.12 mV. Despite this, the calcium-selective membranes I were examined to establish if they could detect variations of this order of magnitude when the symmetrical cell arrangement (1) above was used. In these experiments, three increments of calcium standard solution were added to the Standard Sea Water sample in one of the cell compartments. These increments corresponded to total increases in the calcium concentration of 1, 2 and 5 %, the total calcium concentration in Standard Sea Water being ca. 0.01 M. Dilution effects could thus be neglected and the activity variations were assumed to be equal to the small concentration variations.

Ten consecutive experiments showed that activity variations of the order of magnitude of 2 % and less did not result in reproducible membrane potential variations. The main reason for this was the slow continuous drift in membrane potential. Calibrations confirmed that this drift could not be attributed to changes in reference electrode potentials. It was therefore

concluded that the cell arrangement (1) is not capable of detecting very small calcium activity variations in a sea-water sample.

The authors wish to express their gratitude to Dr. J. Růžička for the gift of calcium membranes prepared at his laboratory, and to Mrs. Lynne Monkman for skilful technical assistance. A guest professorship for one of us (D. J.) provided by the Danish Natural Science Research Council is gratefully acknowledged.

REFERENCES

1 J. W. Ross, Science, 156 (1967) 1378.
2 G. J. Moody, R. B. Oke and J. D. R. Thomas, Analyst (London), 95 (1970) 910.
3 G. H. Griffiths, G. J. Moody and J. D. R. Thomas, Analyst (London), 97 (1972) 420.
4 J. Růžička, E. H. Hansen and J. C. Tjell, Anal. Chim. Acta, 67 (1973) 155.
5 D. Dyrssen, D. Jagner and H. Johansson, Report on the Chemistry of Sea Water V, Dept. Anal. Chem., University of Göteborg, 1967.
6 D. Jagner and K. Årén, Anal. Chim. Acta, 57 (1971) 185.
7 D. Jagner, Anal. Chim. Acta, 68 (1974) 83.
8 J. Růžička, C. G. Lamm and J. C. Tjell, Anal. Chim. Acta, 62 (1972) 15.
9 T. Anfält and D. Jagner, Anal. Chim. Acta, 57 (1971) 177.
10 G. H. Griffiths, G. J. Moody and J. D. R. Thomas, J. Inorg. Nucl. Chem., 34 (1972) 3043.
11 N. Ingri, W. Kakotowicz, L. G. Sillén and B. Warnqvist, Talanta, 14 (1967) 1261.
12 T. Anfält and D. Jagner, Anal. Chim. Acta, 55 (1971) 477.
13 G. Gran, Analyst (London), 77 (1952) 661.
14 M. Mascini and A. Liberti, Anal. Chim. Acta, 53 (1971) 202.

Analytica Chimica Acta, 80(1975)17—30

THE POLAROGRAPHIC DETERMINATION OF SOME THIAZIDE DIURETICS IN COMPOUND TABLETS

EFTYCHIOS KKOLOS* and JOHN WALKER

Pharmacy Department, Chelsea College, University of London, Manresa Road, London, SW3 6LX (England)

(Received 19th April 1975)

Derivatives of benzothiadiazine include compounds used as diuretics and mild antihypertensives; two main groups exist, the thiazides (I), 2H-1, 2, 4-benzothiadiazine-1,1-dioxides and the hydrothiazides (II), 3, 4-dihydro-(2H)-1, 2, 4-benzothiadiazine-1, 1-dioxides exemplified by chlorothiazide (Ia), hydrochlorothiazide (IIa) and methylclothiazide (IIb). Tablets of these and related substances are frequently formulated in combination with antihypertensives such as methyldopa (III) reserpine (IVa) and deserpidine (IVb), for the treatment of hypertension. General methods for the assay of thiazides and hydrothiazides include spectrophotometry [1—3], colorimetry [4—6], non-aqueous titrimetry [1,7—11] and polarography [11]. This paper describes the application of a polarographic method to the determination of hydrochlorothiazide and methylclothiazide in some proprietary compound tablets, i.e. Tablets A (hydrochlorothiazide 15 mg, methyldopa 250 mg), Tablets B (hydrochlorothiazide 12.5 mg, reserpine 0.0625 mg, potassium chloride 572 mg), Tablets C (hydrochlorothiazide 10 mg, reserpine 0.15 mg), and Tablets D (methylclothiazide 5 mg, deserpidine 0.25 mg).

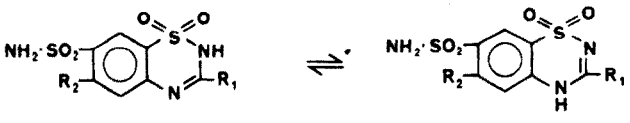

I

a) R_1 = H , R_2 = Cl

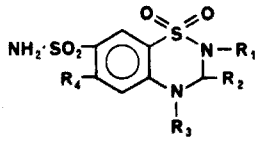

II

a) R_1 = R_2 = R_3 = H , R_4 = Cl

b) R_1 = CH_3 , R_2 = CH_2Cl , R_3 = H

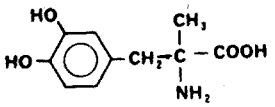

III

*Present address: Government Analytical Laboratory, 44 Kimonos Street, Nicosia, Cyprus.

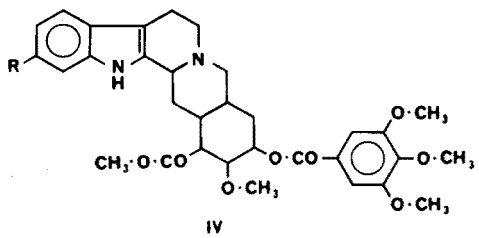

IV

a) R = CH_3O

b) R = H

Both hydrochlorothiazide and methyldopa possess overlapping u.v. spectra and the high content of methyldopa with respect to hydrochlorothiazide in Tablet A rules out a spectrophotometric procedure applicable to two-component mixtures. Colorimetric procedures are also liable to interference from the methyldopa, and differentiating non-aqueous titrimetry could also be expected to produce difficulties. Chromatographic and ion-exchange separation followed by spectrophotometric determination of the thiazide has been reported [12]. In the presence of reserpine, hydrochlorothiazide has been determined by non-aqueous titrimetry and by a u.v. spectrophotometric method reported as giving high results [9]; low concentrations of reserpine have also been reported as not interfering in a u.v. spectrophotometric assay of hydrochlorothiazide [13]. Recently, high-pressure liquid chromatography has been used to determine both components of a hydrochlorothiazide-reserpine mixture [14]. Both reserpine and deserpidine respond polarographically in a non-aqueous system [15]. No polarographic method for the determination of methylclothiazide either alone or in the presence of deserpidine has been reported.

The polarographic reduction of 1, 2, 4-benzothiadiazine-1, 1-dioxides has been studied in formdimethylamide, aqueous methanol or ethanol with tetramethylammonium halides, and in borate buffer with potassium chloride or tetramethylammonium halides; the process involves the halogen atom at position 6, two electrons being transferred [16,17]. Correlations between structure and polarographic behaviour have also been discussed [16].

EXPERIMENTAL

All experiments were performed on a Cambridge pen-recording polarograph, with a dropping mercury electrode and a saturated calomel reference electrode. The drop time (t) was 3.3 s, and the mercury flow rate through the capillary (m) was 1.577 mg s^{-1}. All $E_{1/4}$ values quoted are related to the SCE.

Michaelis borate buffers [18] were made 0.1M with respect to tetramethylammonium bromide (TMAB, 15.41 g l^{-1}) and adjusted to the pH value stated. Unless otherwise indicated, it was found that minor deviations from the pH values quoted did not significantly affect the i_d values.

All experiments were performed at 21 ° ± 0.2 °C and all solutions were deoxygenated by means of a stream of nitrogen previously passed through the appropriate buffer solution. Samples of hydrochlorothiazide and methylclothiazide used in preliminary experiments and for preparing calibration curves were dried at 105 °C for 2 h before use.

RESULTS AND DISCUSSION

Preliminary experiments with hydrochlorothiazide in aqueous 20% (v/v) ethanol and aqueous 10% (v/v) formdimethylamide with 0.1M TMAB as supporting electrolyte resulted in distorted polarographic waves. Since hydrochlorothiazide was readily soluble above pH 9.5, a solution was prepared containing 0.15 mg cm^{-3} in borax buffer pH 9.9. Portions of this solution, made 0.1M with respect to potassium chloride or TMAB as supporting electrolyte, gave $E_{½}$ values of −1.78 V and −1.675 V, respectively; with TMAB, there was an accompanying flattening of the plateau, which enhanced its suitability for quantitative work (Fig. 1). The influence of supporting electrolytes on the reduction of chlorobenzene has been reported [19,20]. With methylclothiazide solutions in borax buffer pH 10.3, the $E_{½}$ values were −1.75 V in 0.1M KCl and −1.64 V in 0.1M TMAB.

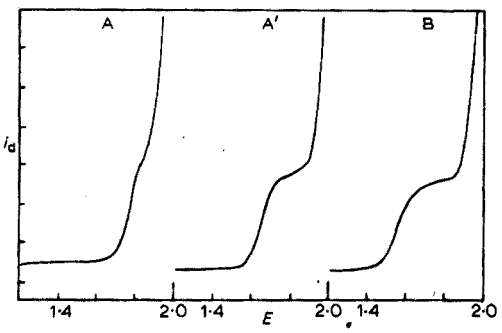

Fig. 1. Polarographic curves. A, Hydrochlorothiazide 0.15 mg cm^{-3}; borax buffer pH 9.9+ 0.1 M KCl. $E_{½}$−1.78 V. A', Hydrochlorothiazide 0.15 mg cm^{-3}; borax buffer pH 9.9+ 0.1 M TMAB. $E_{½}$−1.675 V. B, Methylclothiazide 0.2 mg cm^{-3}; borax buffer pH 10.3+0.1 M TMAB. $E_{½}$−1.64 V.

Effect of pH on $E_{½}$ values

Non-ionizable halogen compounds have $E_{½}$ values virtually independent of pH, whereas the $E_{½}$ values for ionizable halogen derivatives are pH-dependent [18]. Polythiazide has a constant $E_{½}$ value between pH 6 and 9.4, but the value increases by 60mV/pH unit above this [17]. The polarographic curves for hydrochlorothiazide (0.3 mg cm^{-3} in buffer pH 9.9) were obtained at different pH values, which were changed by the addition of either 0.05M

borax or 0.1M sodium hydroxide. Since methylclothiazide dissolved more readily at higher pH (see below) the initial solution was prepared in buffer solution pH 10.3. Results are shown in Fig. 2. The influence of pH on the $E_{1/2}$ of thiazide derivatives has been explained [16] in terms of the effect of ring substituents on the lability of the carbon—halogen bond (C_6).

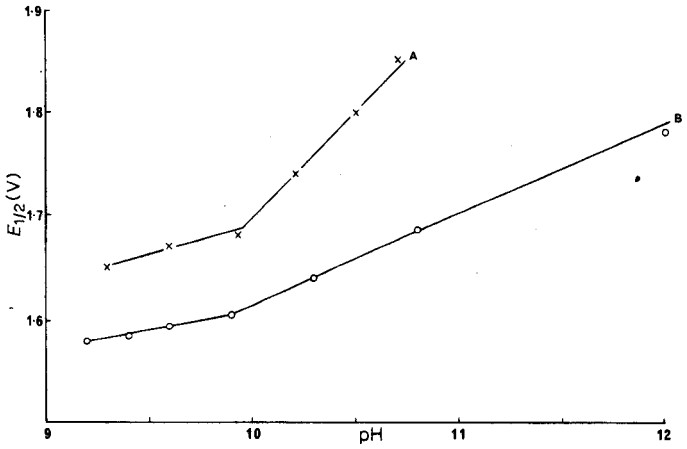

Fig. 2. $E_{1/2}$ vs. pH. A, Hydrochlorothiazide. B, Methylclothiazide.

Although hydrochlorothiazide in 0.1M sodium hydroxide solution is hydrolysed [21—23] to the extent of only 1% in 300 h, the possibility of hydrolysis affecting the polarographic wave was examined. A solution of hydrochlorothiazide (0.5 mg cm^{-3}) in buffer pH 9.9 was prepared and the i_d measured at −1.8V at intervals for 1 h; no significant change was observed. Because methylclothiazide was not readily soluble in borax buffer solution below pH 11.5, the effect of possible hydrolysis was studied at pH 12; it was found that when a solution (1.0 mg cm^{-3}) was prepared at pH 12 and then quickly adjusted to pH 9.4, the methylclothiazide remained in solution for at least 48 h, the wave at this lower pH being better defined. Since it was considered necessary during tablet assays to extract the methylclothiazide as rapidly as possible, borax buffer pH 12 was chosen, and the effect of time on the polarographic wave at this pH was studied for a solution containing 0.4 mg cm^{-3}. The limiting current remained constant at 3.85 μA during the period 5—30 min, but then decreased gradually to 3.41 μA, i.e. a decrease of ca. 9%, after 2 h. To overcome this source of error during the assay of methylclothiazide, both standard and sample were treated for the same length of time at pH 12. At pH 9.4 no change in i_d with time was observed. The effect at pH 12 is attributed to hydrolysis. For the assay of methylclothiazide, therefore, both sample and standard were shaken with buffer at pH 12 for the same time, and brought to pH 9.4 for polarography.

Linearity of calibration graphs

A solution containing 1.0 mg cm^{-3} of hydrochlorothiazide in buffer pH 9.9 was prepared, suitable dilutions (0.1—0.6 mg cm^{-3}) were made in the same buffer and the i_d values were measured at −1.8V. For methylclothiazide, a solution containing 1 mg cm^{-3} in borax buffer pH 12 was prepared; immediately 3, 4 and 5-cm^3 aliquots were transferred to each of three 20 cm^3 graduated flasks, and 3, 4 and 5 cm^3 respectively of the same buffer were added, thus ensuring that the final concentrations (0.15—0.25 mg cm^{-3}) were comparable to those expected during the tablet assay, to allow for the possibility that the variation of i_d with time was concentration-dependent. The flasks were shaken for 20 min and adjusted to volume with 0.05 M borax solution containing 0.1 M TMAB (final pH 9.4). The i_d was measured at −1.76 V. With both hydrochlorothiazide and methylclothiazide, linear relationships between i_d and concentration were observed over the concentration ranges studied.

Effects of other tablet components on i_d value of hydrochlorothiazide

The i_d value at −1.8 V of a 0.5-mg cm^{-3} solution of hydrochlorothiazide in buffer pH 9.9 was not affected by the addition of methyldopa to give a concentration of 8.33 mg cm^{-3}; the hydrochlorothiazide and methyldopa were in the same ratio as in the tablets to be assayed, i.e. 1:16.7. There was no significant change in the i_d value for times up to 1 h. When 5 solutions of hydrochlorothiazide and methyldopa were measured after 5 min, the average i_d value was 10.88 μA (s = 0.05, s_r = 0.45), whereas the i_d for a solution without methyldopa was 10.875 μA. However, with methyldopa, two small waves appeared with time, having $E_{1/4}$ values of −0.4 V and −1.04 V, respectively. Since the plateau between −1.2 and −2 V was horizontal, it was possible to measure the i_d of hydrochlorothiazide ($E_{1/4}$ −1.68 V, pH 9.9) without difficulty. These extra waves were thought to be due to the reduction of an oxidation product of methyldopa since a freshly prepared solution (5 mg cm^{-3}) in buffer solution pH 9.9 showed no wave. After being shaken for 1 h the solution gave a polarographic curve with two waves comparable to those seen in the previous experiments (Fig. 3) and the solution had turned pale brown. These observations can be explained by air oxidation of methyldopa to a quinonoid derivative in a similar manner to epinephrine, quinones being reducible at the dropping mercury electrode [18].

To study the effect of reserpine two solutions of hydrochlorothiazide at pH 9.9 were prepared, containing 0.5 and 0.25 mg cm^{-3} respectively. Addition of 1.0 mg of reserpine to 10-cm^3 aliquots of these solutions did not affect the polarographic curves. (The ratio of reserpine to hydrochlorothiazide was much greater than that usual in commercial formulations.) The pH of the solutions was unaffected by the addition of reserpine which was apparently insoluble.

The relative advantage of TMAB over potassium chloride as supporting electrolyte has already been discussed, but it was considered desirable to ob-

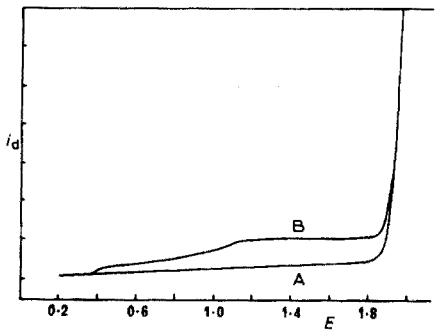

Fig. 3. Polarographic curve of methyldopa solution (5 mg cm^{-3}, pH 9.9). A, Freshly prepared. B, After 1 h.

serve the effects of the presence of potassium chloride in the system chosen. Polarographic curves of a solution of hydrochlorothiazide (0.5 mg cm^{-3}) in buffer solution pH 9.9 (and 0.1 M TMAB) were taken before and after the addition of potassium chloride (23 mg cm^{-3}) to produce a solution in which the ratio of potassium chloride to hydrochlorothiazide was approximately equivalent to that in the tablets to be assayed. No interference was observed.

Effects of other tablet components on i_d value of methylclothiazide

Sufficient methylclothiazide was dissolved in borax buffer solution pH 12, adjusted to pH 9.4 as soon as solution was complete, so that the solution when adjusted to an appropriate volume gave a final concentration of 0.2 mg cm^{-3}. The addition of deserpidine (0.5 mg cm^{-3}) to this solution did not affect the i_d value for methylclothiazide.

Determination of hydrochlorothiazide in tablets A

The above study had shown that the polarographic wave was suitable for quantitative measurements, and was unaffected by the presence of methyldopa. Samples of Tablet A stated to contain hydrochlorothiazide (15 mg) and methyldopa (250 mg) were therefore studied. These were salmon-pink film coated tablets, and the possible interference of excipient and film coating and the time required for complete extraction of the hydrochlorothiazide were therefore investigated.

The film coating prevented rapid filtration of a tablet extract; reduced pressure filtration produced a turbid solution with a rather ill-defined polarographic wave, unsuitable for quantitative work. A small moistened cotton-wool swab on the end of a stick was used to remove carefully the coating of 12 tablets and the cotton wool with the removed coating was shaken for 30 min in 100 cm^3 of buffer solution pH 9.9. The resulting extract gave a wave ($E_{1/4}$ −1.6 V) which was independent of pH indicating that it was not due to hydro-

chlorothiazide and that no detectable amount had been removed in the combined coatings of 12 tablets (Fig. 4). At pH 9.9 the hydrochlorothiazide wave appears between −1.6 and −1.7 V and would have distorted the wave caused by the reducible substance in the film coating. This reducible substance was also

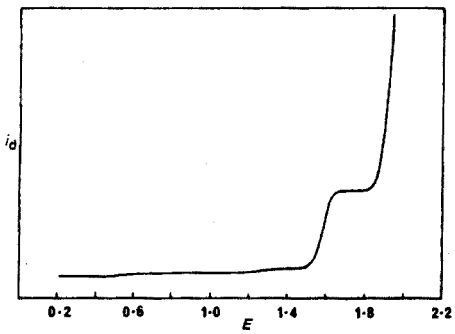

Fig. 4. Polarographic curve of film coating of 12 tablets A/100 cm³; pH 9.9. $E_{½}$—1.6 V.

present in the tablet extract, and unsuccessful attempts were made to eliminate it by extracting the tablets with acetone and alcohol. The pH dependence of the hydrochlorothiazide wave could be used to avoid the interference. The addition of 1—2 drops of 20% sodium hydroxide solution to the buffered tablet extract in the polarographic cell resulted in a pH shift from 9.8 to 11.5, with an accompanying shift of the hydrochlorothiazide wave to more negative potentials uncovering the interfering wave. Such interfering substances may be present only in certain formulations. However, although the interference of the film coating could be obviated in this way, there was still some distortion of the wave, and the initial filtration of the solution was slow. The film coating was therefore removed in the final method.

To study the effect of the excipient, two tablets from which the film coating had been removed, were crushed and extracted with buffer solution pH 10.3 (since methyldopa lowered the pH significantly), the solution was filtered and the residue was washed with buffer solution and dried. The polarographic curve of a solution containing 0.5 mg cm^{-3} of hydrochlorothiazide in buffer pH 9.9 was not affected by the addition of approximately 50 mg of the dried residue, i.e. by the insoluble or sparingly soluble excipients in the tablets. It has been reported that lactose, mannitol and cornstarch do not affect the i_d of glyceryl trinitrate [24].

The time required for complete extraction was studied by shaking a powdered tablet with buffer solution (pH 10.3, 20 cm^3) and recording the curve at 5-min intervals. No increase in i_d was observed after shaking for 15 min or longer, showing that complete extraction had occurred. Subsequently 25 min was allowed for extraction.

This investigation led to the development of the procedure described below.

Preparation of calibration curve

This was prepared as described under *Linearity of calibration graphs* for

the range of 0.1—0.6 mg cm^{-3} with buffer pH 9.9 and measurement at −1.8 V. Polarographic curves were recorded in duplicate for each concentration.

Assay procedure

Fifteen tablets were individually weighed, the film coating was removed with a moistened cotton-wool swab, and the tablets were reweighed. Each tablet was powdered in a small glass mortar and transferred quantitatively to a 20 cm^3 graduated flask with buffer solution pH 10.3; the mixture was adjusted to volume with the same solution, and shaken mechanically for 25 min. The solutions were then filtered, the first 5 cm^3 of filtrate being discarded and 5 cm^3 of each solution was diluted to 20 cm^3 with buffer solution pH 10.3 in a graduated flask. The pH of the final solution was 9.9. Each dilution was prepared in duplicate and polarographic curves were recorded between −1.2 and −2.0 V. After the initial recording, 1—2 drops of 20% sodium hydroxide were added to each solution in the polarographic cell to give pH 11.5—11.8 and the curves were recorded again. The residual currents of both curves were extrapolated, the i_d values measured at −1.8 V were subtracted, and the i_d for hydrochlorothiazide calculated (Fig. 5). The content of hydrochlorothiazide per tablet was calculated using the calibration curve and expressed as a percentage of the stated amount of 15 mg per tablet (Table 1). The standard deviation (s) was found to be 0.89 and the relative standard deviation 5.86.

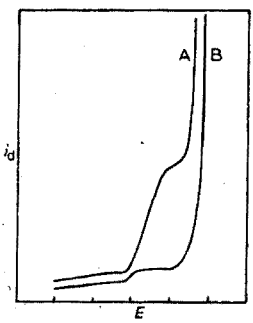

Fig. 5. Tablets A. Typical polarogram from assay of single tablet. A, pH 9.9. B, pH 11.8.

A composite assay was also performed as follows. The film coating of 10 tablets was removed as before, the tablets were weighed and powdered, and the powder was mixed thoroughly. A quantity of powder equivalent to one tablet of average weight was analysed in the same way as were individual tablets. The results are recorded at the foot of Table 1. These results indicate that polarography offers a convenient method for the determination of hydrochlorothiazide in the present of methyldopa and is suitable for the assay of single tablets.

Removal of the film coating is advisable and introduces no significant error.

TABLE 1

Hydrochlorothiazide content of tablets A

Tablet	Original wt. (mg)	Final wt. (mg)	Wt. of coating removed (mg)	Hydrochlorothiazide content	
				mg/tab	% recovery
1	449.4	434.6	14.8	15.04	100.2
2	447.0	431.8	15.2	13.68	91.2
3	452.0	432.2	19.8	16.32	108.8
4	450.0	433.6	16.4	15.76	105.0
5	452.6	437.2	15.4	14.32	95.5
6	452.1	437.2	14.9	14.96	99.7
7	447.6	429.8	17.8	14.95	94.7
8	450.6	434.5	16.1	16.30	108.7
9	451.4	436.4	15.0	15.68	104.5
10	451.8	436.2	15.6	15.04	100.2
11	450.5	432.9	17.6	16.72	111.5
12	451.8	439.0	12.8	14.96	99.7
13	449.0	434.1	14.9	14.56	97.0
14	456.7	437.4	19.3	13.92	93.0
15	455.8	439.5	15.7	14.56	97.0
Average	451.2	435.1	16.1	15.12	100.8
Composite assay of 10 tablets	451.2	435.1	16.1	14.88	99.2

It removes a high proportion of the substance with $E_{½}$ −1.6 V. The wave caused by an oxidation product of methyldopa is, under the experimental conditions, very small with $E_{½}$ 0.68 V more positive than that of hydrochlorothiazide at pH 9.8 and with a horizontal plateau so that extrapolation does not introduce a significant error. The most serious potential source of interference was considered to be the soluble polarographically reducible substance ($E_{½}$ −1.6 V). However, this could be avoided by taking advantage of the pH dependence of the $E_{½}$ value of hydrochlorothiazide, and when 7 cm^3 or more of solution was used in the polarographic cell, the addition of 1—2 drops of 20% sodium hydroxide solution to increase the pH did not introduce a significant error. The possibility that differences in viscosity between the solutions used to obtain the calibration curve and sample solutions might introduce an error was investigated by standard addition of some hydrochlorothiazide to a tablet extract with no detectable error.

Of the methods published [12] for the assay of hydrochlorothiazide in the presence of methyldopa, one method involves chromatography and does not determine methyldopa; the second method involves an ion-exchange separation with subsequent spectrophotometric determination of both components, the recoveries from prepared mixtures being 96.4% (*s* 2.30) for methyldopa and 98.8% (*s* 2.92) for hydrochlorothiazide.

Determination of hydrochlorothiazide in tablets B

The tablets are stated to contain hydrochlorothiazide (12.5 mg), reserpine (0.625 mg) and potassium chloride (572 mg) in an enteric-coated core. It was shown above that neither reserpine nor potassium chloride interfere with the polarographic wave of hydrochlorothiazide.

To examine the possible interference of the enteric coating, two tablets were crushed in a mortar, and the enteric coating was removed and extracted first with buffer solution pH 9.9 then with ethanol, to remove hydrochlorothiazide. The polarographic curves of two solutions of hydrochlorothiazide containing 0.4 and 0.5 mg cm^{-3}, respectively, were recorded; to each solution was then added an amount of enteric coating approximately equivalent to one quarter of that present in one tablet and the polarograms were again recorded. No change in i_d was observed.

To investigate the effect of excipient, one tablet was powdered and a suspension was prepared in a 25-cm^3 volumetric flask with buffer solution pH 9.9 by shaking for 30 min; after filtration, 8 cm^3 of the solution was polarographed. The solution was then made more alkaline (pH 11.6) with 1—2 drops of 20% sodium hydroxide solution and the curve again recorded. The increase in alkalinity, by shifting the hydrochlorothiazide wave to more negative potentials, uncovered a wave ($E_{½}$ −1.6 V) analogous to that obtained by similar treatment of the extract from tablets A, but of greater magnitude. The same procedure was therefore adopted to calculate the i_d value for hydrochlorothiazide.

TABLE 2

Hydrochlorothiazide content of tablets B

Tablet no.	Weight (mg)	Content (mg)	% Content
1	930.4	11.59	92.7
2	888.8	14.07	112.6
3	932.5	13.92	111.4
4	907.9	11.91	95.3
5	903.2	12.75	102.0
6	913.0	12.41	99.3
7	888.6	13.56	108.5
8	869.1	12.84	102.7
9	900.6	11.90	95.2
10	883.0	10.59	84.7
11	911.9	14.67	117.4
12	845.2	10.54	84.3
Average	897.8	12.56	100.5
Composite assay of 10 tablets	902	12.46	99.6

Detailed procedure

A calibration curve was prepared in buffer solution pH 9.9 as described earlier. Twelve tablets were individually assayed. Each tablet was weighed, powdered and quantitatively transferred to a 25-cm^3 volumetric flask; the mixtures were adjusted to volume with buffer solution pH 9.9. A procedure similar to that used for tablets A was followed, polarographic curves being recorded before and after the tablet extract had been adjusted to pH 11.8. In this instance, because of the higher proportion of interfering substance present, a correction was made to allow for dilution of the solution by the addition of the 20% sodium hydroxide solution: this correction was applied individually for each tablet, because the current constituted a different proportion in each case (average value 0.65%). The results of the assays are shown in Table 2 (s 1.33, s_r 10.6). The result of a composite assay of ten tablets is also given. This was performed similarly to the individual tablet assays, the powder from ten tablets being extracted with 300 cm^3 of buffer solution.

Determination of hydrochlorothiazide in tablets C

Each tablet was stated to contain hydrochlorothiazide (10 mg) and reserpine (0.15 mg). To examine any interference of excipient, 5 tablets were powdered and extracted with 50 ml of buffer solution pH 9.9 for 30 min, and the insoluble excipient was collected and washed as described for previous assays. The polarographic curves of two standard solutions of hydrochlorothiazide (0.15 and 0.2 mg cm^{-3}) were not affected by the addition of excipient (1 mg cm^{-3}). A polarographic curve of the filtrate from the tablet extraction, adjusted to pH 11.8, showed no additional wave, in contrast to the tablets previously assayed.

TABLE 3

Hydrochlorothiazide content of tablets C

Tablet no.	Weight (mg)	Content (mg)	% Content
1	142.9	10.40	104.0
2	139.8	10.52	105.2
3	138.4	10.81	108.1
4	139.8	11.30	113.0
5	139.5	9.00	90.0
6	136.7	11.80	118.0
7	138.6	9.55	95.5
8	140.6	10.35	103.5
9	142.1	11.00	110.0
10	139.0	9.80	98.0
Average	139.7	10.45	104.5
Composite assay of 10 tablets	140.6	10.57	105.7

Detailed procedure

A calibration curve was prepared as described above. Ten tablets were individually weighed, powdered and transferred quantitatively to 50-cm^3 graduated flasks. After being filled with buffer solution pH 9.9, the flasks were shaken for 25 min and the hydrochlorothiazide content was determined as described for previous assays, the i_d value being measured at −1.8 V. The results are shown in Table 3 (s 0.84, s_r 8.02), together with the result of a composite assay of ten tablets.

This method might be considered less satisfactory than a u.v. spectrophotometric determination, but it should be pointed out that reports differ as to the extent of interference of reserpine in the spectrophotometric determination of hydrochlorothiazide. Urbanyi and O'Connell [13] claimed no interference, whereas Chiang [9] reported an error of ca. 3%. The present method is reproducible, comparatively rapid and not subject to interference from reserpine

Determination of methylclothiazide in tablets D

Each tablet is stated to contain methylclothiazide (5 mg) and deserpidine (0.25 mg). The preliminary experiments established the suitability of a borax buffer solution adjusted to pH 9.4 after preliminary dissolution of methylclothiazide at pH 12, and the non-interference of deserpidine.

The possible interference of excipient was investigated as described previously a standard solution of methylclothiazide (0.2 mg cm^{-3}) was used, to which was added excipient (1 mg cm^{-3}) obtained from the extraction of five tablets with 25 cm^3 of buffer and subsequent filtration. The addition had no apparent effect on the magnitude of the i_d value.

Detailed procedure

A procedure modified from that used for hydrochlorothiazide was adopted as described under *Linearity of calibration graph.*

For assay, 10 tablets were individually weighed and transferred to 25 cm^3 graduated flasks, borax buffer (pH 12; 10 cm^3) was added, the flasks were shaken for 20 min, and the contents were adjusted to volume with borax solution 0.05 M containing 0.1 M TMAB to reduce the pH to 9.4. After filtration (discarding the first 5 cm^3), the polarographic curves were obtained between −1.0 and −2.0 V in the order of preparation of the solutions, i_d being measured at −1.76 V. The content of methylclothiazide was calculated from the calibration curve.

The results are shown in Table 4 (s 0.10; s_r 2.13), together with the result of a composite assay of ten tablets.

In this assay, because of solubility difficulties, the methylclothiazide was dissolved at pH 12 and the solution subsequently adjusted to pH 9.4, preliminary experiments having indicated that at the concentrations used, methylclothiazide remained in solution. Since at pH 12, the magnitude of i_d decreased with time,

TABLE 4

Methylclothiazide content of tablets D

Tablet no.	Weight (mg)	Content (mg)	% Content
1	194.3	4.77	95.4
2	196.7	4.95	99.0
3	194.9	4.89	97.8
4	193.1	5.07	101.4
5	195.2	5.00	100.0
6	196.3	5.02	100.4
7	194.3	4.84	96.8
8	192.3	4.82	96.4
9	196.8	4.95	99.0
10	199.1	5.07	101.4
Average	195.3	4.94	98.8
Composite assay of 10 tablets	193.4	5.020	100.40

it was considered important to treat standard and sample at this pH for the same period, preferably for not more than 20 min. The method has the advantage that no time-consuming separation of methylclothiazide and deserpidine is required.

We thank Abbott Laboratories and Merck, Sharp and Dohme Limited for gifts of the pure substances used in this investigation. One of us (E.K.) thanks the W.H.O. for the award of a Fellowship, during the tenure of which this investigation was carried out.

SUMMARY

Methods are described for the polarographic assay of hydrochlorothiazide in the presence of methyldopa and reserpine, and for methylclothiazide with deserpidine; borax buffer solutions are used with 0.1 M TMAB as supporting electrolyte. The methods appear to have advantages over existing ones, since no separation of the components is necessary, the problem of interference from excipients, etc. can be overcome readily, and the procedures are applicable to single tablet assays.

REFERENCES

1 British Pharmacopoeia, 1973.
2 C.R. Rehm and J.B. Smith, J. Amer. Pharm. Ass., Sci. Ed., 49 (1960) 386.
3 F.R. Fazzari, J. Ass. Offic. Anal. Chem. 53, (1970) 582.
4 J.F. Magalhaes and M.G. Prios, Rev. Farm. Biochim, 8, (1971) 273; Anal. Abst., 21 (1971) 3723.

5 H. Sheppard, T.F. Mowles and A.J. Plummer, J. Amer. Pharm. Ass., Sci. Ed., 49 (1960) 722.
6 J. Vachnek, Ceskoslov. Farm., 10, (1961) 515; Anal. Abst., 9 (1962) 3428.
7 J. Kracmer and M. Lastovkova, Pharmazie, 25 (1970) 464.
8 A. Stark and M. Wagler, Zentralbl. Pharm. Pharmakother., 109 (1970) 921.
9 H.C. Chiang, J. Pharm. Sci., 50 (1961) 885.
10 D.C. Garratt, The Quantitative Analysis of Drugs, Chapman and Hall, London, 3rd edn., 1964.
11 United States Pharmacopoeia, XVIII, 1970.
12 R. Chu, J. Ass. Offic. Anal. Chem., 54 (1971) 603.
13 T. Urbanyi and A. O'Connell. Anal. Chem., 44 (1972) 565.
14 J.L. Honigberg, J.T. Stewart, A.P. Smith, R.D. Plunkett, and D.W. Hester, J. Pharm. Sci., 63 (1974) 1762.
15 A.L. Woodson, Anal. Chem., 42 (1970) 244.
16 A.I. Cohen, B.T. Keeler, N.H. Coy and H.L. Yale, Anal. Chem., 34 (1962) 216.
17 P. Gantes and J. Barat, Ann. Pharm. Fr., 25 (1967) 447.
18 M. Brezina and P. Zuman, Polarography in Medicine, Biochemistry and Pharmacy, Revised English Ed., Interscience, New York, 1958.
19 F.L. Lambert and K. Kobayashi, J. Org. Chem., 23 (1958) 773.
20 H.A. Laitinen and C.J. Nyman, J. Amer. Chem. Soc., 70 (1948) 3002.
21 T. Yamana and Y. Mizakami. J. Pharm. Sci., 54 (1965) 1057.
22 J.A. Mollica, C.R. Rehm and J.B. Smith, J. Pharm. Sci., 58 (1969) 635.
23 J.A. Mollica, C.R. Rehm, J.B. Smith and H.K. Govan, J. Pharm. Sci., 60 (1971) 1380.
24 B.C. Flann, J. Pharm. Sci., 58 (1969) 122.

Analytica Chimica Acta, 80(1975)31—37

TURBULENT HYDRODYNAMIC VOLTAMMETRY. PART I. THE DISTRIBUTION OF VOLTAMMETRIC CURRENT ON ELECTRODE SURFACES

M. VARADI* and E. PUNGOR

Institute for General and Analytical Chemistry, Technical University Budapest (Hungary)

(Received 14th May 1975)

The effects of hydrodynamic parameters in flowing systems on voltammetric currents have been thoroughly studied by several workers. For the case of an electrode surface perpendicular to the direction of laminar flow, Matsuda [1] gave the following correlation between the diffusion current and the various hydrodynamic parameters

$$I_d = \text{const.}\ n\ FACD^{2/3}\ \nu^{-1/6}\ (U/L)^{1/2} \qquad (1)$$

where I_d is the diffusion limiting current, n the number of electrons taking part in the electrochemical reaction, F the Faraday constant, A the electrode surface area, C the concentration of the electroactive component, D the diffusion constant, ν the kinematic viscosity, U the linear flow rate, and L the characteristic size of the electrode (e.g. in the case of disc-shaped electrodes $L = \pi r/2$, where r is the radius of the disc)..

The validity of the above equation was also confirmed by the experimental data of Dikusar and Bardin [2,3] who studied on cone and disc-shaped electrodes, the effects of shape and size on the formation of mass transport.

In further investigations, Matsuda and Yamada [4] determined under well defined geometrical conditions the value of the constants shown in eqn. (1) and proved experimentally the correctness of their equations. They found that when the electrode is arranged so that the electrolyte flows through a jet onto the surface of the disc electrode, the minimum electrode radius which can still be used for the measurements, is 1.5 mm.

In the work described here the optimal size of the electrode surface area and the distribution of the mass transport on the electrode surface were investigated empirically for a system in which the electrolyte flows directly from a nozzle onto the electrode surface. In front of the electrode is placed a jet which causes an increase in the linear flow rate of the liquid; because the flow is perpendicular to the surface, a turbulent liquid flow is ensured in the vicinity of the electrode. The construction of the cell and its application to liquid chromatography, have been described in an earlier paper [5]. Since in the case of a single electrode,

---

* Permanent address: LABOR MIM Laboratory Instruments and Equipment Works, Budapest, Hungary.

the current densities originating from electrochemical reactions taking place on different parts of the electrode surface could not be established, the single electrode was replaced by a multichannel electrode consisting of several symmetrically placed electrodes. In this way it was possible to study the mass transport defined at the various points of the electrode by the flow conditions.

EXPERIMENTAL

Reagents

The solution examined was a 10^{-3} M potassium hexacyanoferrate(II) solution in 10^{-1} M KCl. The chemicals used were of analytical grade (Reanal, Budapest).

Equipment

The experimental arrangement is shown in Fig. 1. To transport the liquid, an LMIM LS-204 type micropump with piston was used, thus ensuring a precision of ± 0.5% in the liquid flow rate in the range of 20—250 ml h^{-1} to a pressure of 50 atm.

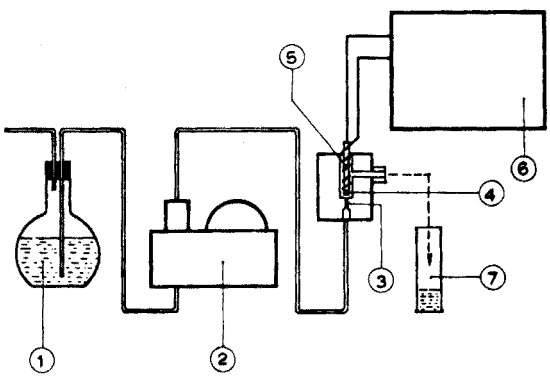

Fig. 1. Schematic diagram of the experimental device: 1, electrolyte reservoir; 2, pump; 3, jet; 4, indicator electrode; 5, reference electrode; 6, electric unit; 7, calibrated receiver.

The electric unit contained the equipment necessary to apply a voltage to the cell and to measure the current. Initially, a Radelkis type OH 102 polarograph was used for this purpose; the sensitivity of the polarograph could be adjusted between $8 \cdot 10^{-11}$ and $6.4 \cdot 10^{-7}$ A mm^{-1}. Later, the polarizing voltage was obtained from a 3-V battery, and the signal was recorded by means of a Philips oscilloscope type PM 3251. The sensitivity of the oscilloscope and its resolution in time could be adjusted between 2 mV/div—20 V/div and 0.05 μs/div—1 s/div. For the fitting of the oscilloscope, a Keithley differential electrometer type 604 was connected into the circuit.
The construction of the measuring cell was identical to that described earlier

[5]; the diameter of the jet opposite the indicator electrode was 0.5 mm or 0.3 mm. Silicone rubber-based graphite electrodes of various sizes served as indicator electrodes [6] for practical purposes, but for theoretical purposes a multichannel electrode was used. A Ag/AgCl reference electrode was employed.

The construction of the multichannel electrode is shown in Fig. 2. The body of the electrode is a teflon rod of 9-mm diameter which is supplied with five bores, each 1.2 mm in diameter. One of these bores is placed centrally while the other four are made at identical distances approximately 3.5 mm from the central electrode. The sensing surface of the electrode consists of silicone rubber-based graphite polymerized into the bores.

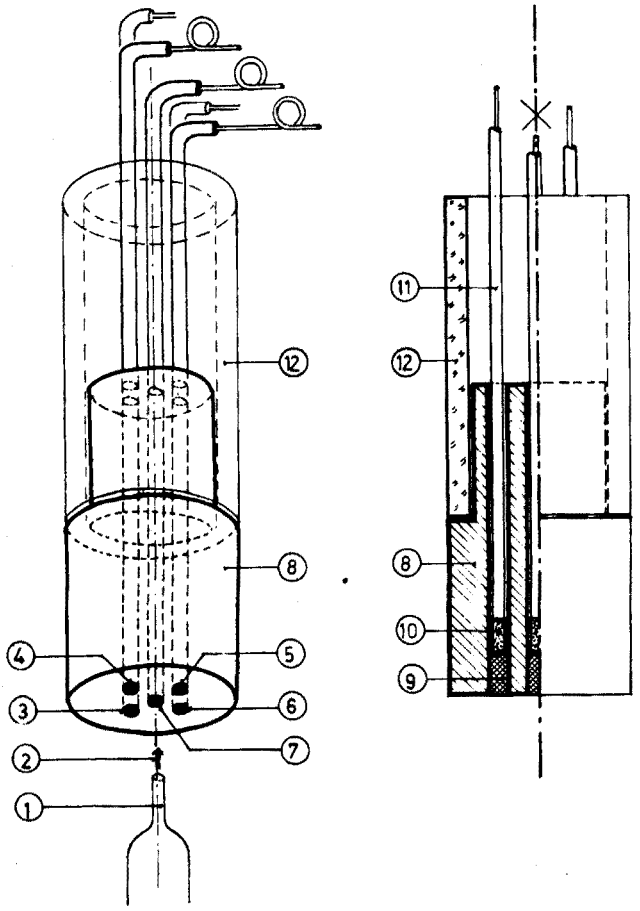

Fig. 2. Construction of the multichannel electrode: 1, jet; 2, direction of the fluid streaming; 3—7, indicator electrode; 8, teflon body; 9, silicone rubber-based graphite; 10, graphite powder; 11, electric connexions; 12, glass tube.

RESULTS AND DISCUSSION

Effect of the surface area of the electrode on the voltammetric current

The effect of the sensing area on the voltammetric signal was studied. Graphite electrodes of different sizes were used with the arrangement shown in Fig. 1, and the current intensities were measured in both stationary and flowing solutions by means of a polarograph. The linear flow rate of the electrolyte was 6.6 cm s^{-1}. In the flowing system the measurements were made at 0.76 V vs. the Ag/AgCl electrode. The results obtained are given in Table 1. The maximum values of current intensities measured on the electrode in the stationary solution served as a basis of comparison. As the data in Table 1 show, the maximum increase in current intensity in the flowing system was observed for the electrode with the smallest surface area. In the case of larger surface areas, only a small part of the electrode comes in contact with the fresh solution streaming at high speed from the 0.5-mm jet, and most of the other parts of the electrode receive the liquid transport through a Prandtl layer, the thickness of which depends on the distance from the point where the flow stream hits the electrode. Consequently, increasing the surface of the electrode decreases the current intensity using the same jet system.

TABLE 1

Relationship between the geometrical size of the electrode and the voltammetric current

Electrode diameter (mm)	2	5	7	9
$\frac{i_{flowing}}{i_{stat.}}$	2.31	1.79	0.58	0.50

Investigation of current distribution with a multichannel electrode

For the examination of the current distribution on the electrode surface, the multichannel electrode shown in Fig. 2 was used. The electrode was connected to the system shown in Fig. 1.

First, the values of the current intensities were examined by means of a polarograph. The current intensity on each of the microelectrodes was measured separately, and after the five electrodes had been connected, the total current intensity was established. The applied flow rate was 13.2 cm s^{-1}. The results obtained are summarized in Table 2. As in the earlier experiments, the tabulated data prove that the current intensities of the electrodes placed on the periphery are in fact lower than that on the electrode placed opposite the jet. The current intensities for the peripheral electrodes are nearly equivalent because of their almost symmetrical positions; the small differences

occurred because the positioning was not exactly symmetrical. When the flow rate was reduced to 6.6 cm s^{-1}, the results obtained became less reproducible, and the differences found between the current intensities measured on the electrodes at different positions became significantly smaller.

TABLE 2

The values of the current intensities on electrodes in different positions

Position of electrode[a]	$i_{stat.}$ (10^{-8} A)	$i_{flowing}$ (10^{-8} A)	$i = \frac{i_{flowing}}{i_{stat.}}$	$\frac{i}{i_{mean}}$
3	204.0	190.8	0.93	0.84
4	189.3	198.8	1.05	0.95
5	238.0	249.9	1.05	0.95
6	181.0	180.0	0.98	0.88
7	216.0	334.8	1.55	1.39
Total	1028.3	1154.3	$\frac{1154.3}{1028.3} = 1.12$	1
Connected electrodes	935.6	1043.1	$\frac{1043.1}{935.6} = 1.11$	1

[a]Positions as indicated in Fig. 2. Position 7 is central, and the others peripheral.

The formation of the momentary current intensities on the electrode surface was then examined. The experimental conditions were the same as before, except that, instead of the polarograph, a memory oscilloscope was used to record the signal; also, the diameter of the jet was 0.3 mm, so that the applied flow rate was increased to 107.9 cm s^{-1}. The results obtained are shown in Fig. 3. The current on the central electrode follows, with only a small distortion, the flow rate of the liquid controlled by the pump. At the peripheral electrodes, the signals are distorted and of reduced amplitude. By tracing the momentary current intensities, the differences between electrodes in different positions are even more striking.

When the distance between the electrode and the jet was increased, even the central electrode produced a strongly distorted signal, which was similar to those for the peripheral electrodes; the differences between the amplitudes were then less significant than in Fig. 3. The signals obtained are shown in Fig. 4.

The momentary current intensities obtained in the course of the oscilloscopic examination are shown in Table 3; the data are the arithmetical mean values calculated on the basis of 15 curves. Since it was established in the previous experiment that electrodes situated at the periphery were nearly equivalent, the measurement was performed only with one of these. The data in

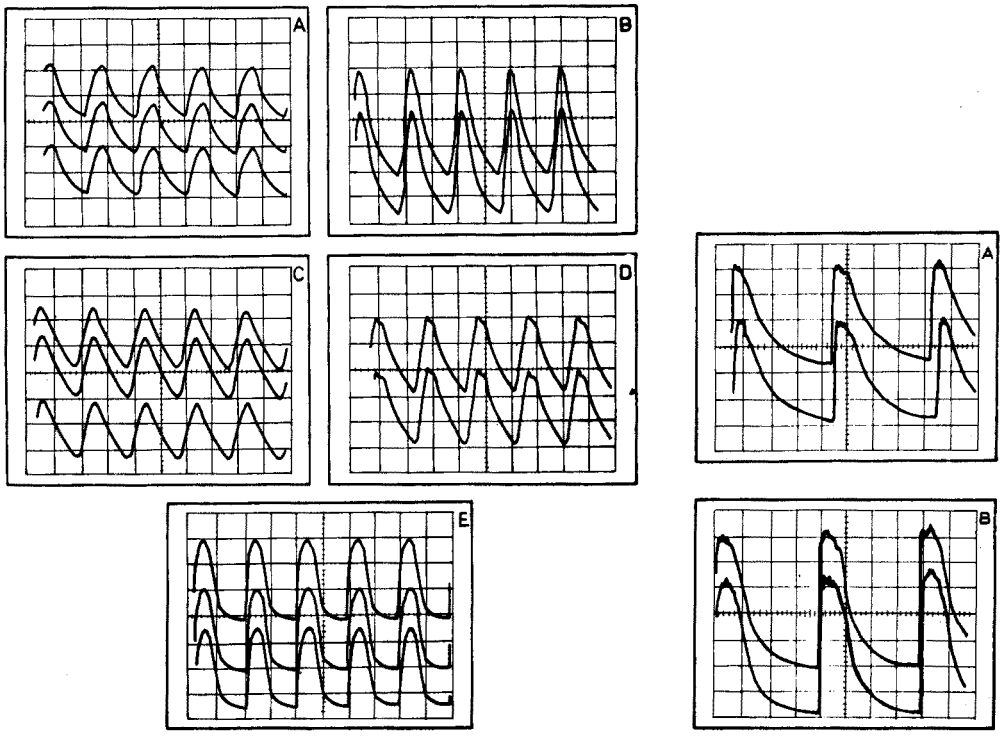

Fig. 3. Oscilloscope results obtained by means of differently placed electrodes situated near the jet. (A) Peripheral electrode, 3. Amplification, 35; sensitivity, 0.2 V/div; time axis, 1 s/div. (B) Peripheral electrode, 4. Amplification, 35; sensitivity, 0.1 V/div; time axis, 1 s/div. (C) Peripheral electrode, 5. Amplification, 35; sensitivity, 0.2 V/div; time axis, 1 s/div. (D) Peripheral electrode, 6. Amplification, 35; sensitivity, 0.1 V/div; time axis, 1 s/div. (E) Central electrode, 7. Amplification, 10; sensitivity, 0.5 V/div; time axis, 1 s/div.

Fig. 4. Oscilloscope results obtained by means of differently placed electrodes situated 4—5 mm from the jet. (A) Peripheral electrode, 4. Amplification, 35; sensitivity, 0.1 V/div; time axis, 0.5 s/div. (B) Central electrode, 7. Amplification, 35; sensitivity, 0.1 v/div; time axis, 0.5 s/div.

Table 3 show that the electrode placed opposite the jet not only closely follows the flow rate but also produces a large signal in cases when its size is smaller than the diameter of the liquid jet and the flow of the jet is not retarded by the medium in front of the electrode.

In conclusion, when turbulent flows are used, efficiency can be increased by reducing the surface area of the electrode. Thus, in contrast to earlier literary data, it was established that for the measurement of very low concentrations, the surface area of the electrode must be decreased to an optimal extent.

The analysis of the distortion of the electrode signals will be discussed in a separate paper.

TABLE 3

Momentary signal levels on electrodes in different positions

Position of electrode[a]	U_1[b] (mV)	U_2[c] (mV)
3	9.7	—
4	11.6	10.8
5	13.5	—
6	7.8	—
7	157.5	15.1

[a]See footnote, Table 2.
[b]U_1 is the measured signal when the electrode is placed directly by the jet.
[c]U_2 is the measured signal when the distance between jet and electrode is 4—5 mm.

SUMMARY

In voltammetric analysis, when turbulent flows are used, i.e. the electrolyte passes through a jet on to the surface of an indicator electrode placed perpendicularly to the direction of flow, the current can be increased by decreasing the electrode surface area. When a system of this type was examined with a multichannel electrode, the momentary signal on the electrode placed opposite the jet was about 15 times larger than the signal measured on the electrode placed on the periphery about 3.5 mm from the central electrode.

REFERENCES

1 H. Matsuda, J. Electroanal. Chem., 15 (1967) 109.
2 A.J. Dikusar and M.B. Bardin, Zh. Anal. Khim., 26 (1971) 1059.
3 M.B. Bardin and A.J. Dikusar, Zh. Anal. Khim., 26 (1971) 1068.
4 H. Matsuda and J. Yamada, J. Electroanal. Chem. Interfacial Electrochem., 30 (1971) 261, 271; 44 (1973) 189.
5 M. Váradi, Zs. Fehér and E. Pungor, J. Chromatogr., 90 (1974) 259.
6 E. Pungor and É. Szepesvàry, Anal. Chim. Acta, 43 (1968) 289.

Analytica Chimica Acta, 80(1975)39—45

RAPID DETERMINATION OF CADMIUM IN BIOLOGICAL TISSUES BY MICROSAMPLING-CUP ATOMIC ABSORPTION SPECTROMETRY

KENNETH W. JACKSON and DOUGLAS G. MITCHELL

Division of Laboratories and Research, New York State Department of Health, New Scotland Avenue, Albany, New York 12201 (U.S.A.)

(Received 2nd April 1975)

Cadmium, a widespread environmental health hazard, is virtually absent from the body at birth; but it accumulates with age in the kidneys, liver and other tissues at the expense of zinc, an essential element. Cadmium is thought to contribute to hypertension in humans [1].

Atomic absorption spectrometry (a.a.s.) is the commonest method for determining cadmium and other trace metals in tissues. This would be a highly satisfactory technique if current sample preparation procedures could be simplified. Dry-ashing of samples at 400—500 °C for up to 24 h is time-consuming, and metals such as cadmium may volatilize. Low-temperature dry-ashing [2] gives less likelihood of loss of volatile metals, but the method is slow and requires expensive apparatus. Wet-ashing is generally quicker than dry-ashing, but the hazardous nature of the reagents (oxidizing acids) necessitates constant surveillance, and high-purity reagents must be used to avoid high blanks. The simplest method of sample preparation reported to date involves solubilizing the tissue with a quaternary ammonium hydroxide [3,4]; digestion time can be reduced to as little as 1 h.

Micromethods of a.a.s. offer greatly improved sensitivity over flame nebulization techniques. One of these procedures is the microsampling-cup technique, originally developed by Delves [5], which has two very important advantages for tissue analysis: (a) the microsample is aliquoted directly into an analysis cup, which is automatically cleaned during use, so that the risk of contamination is minimized; and (b) sample pretreatment is minimal. The tissue is homogenized with water to produce a uniform suspension, and suitable dilutions of the homogenate are pipetted into the analysis cups. The cups are oven-dried and injected into an air—acetylene flame. Ashing and atomization occur together at this stage, and there is no interference with the spectrometric measurement.

A microsampling-cup a.a.s. procedure for determining cadmium in biological tissues is described here. It was developed as a pilot study of the feasibility of determining several trace metals by this method.

EXPERIMENTAL

Instrumentation

The atomic absorption spectrometer used has been described in detail by Aldous et al. [6]. The instrument differs somewhat from commercially available spectrometers having the Delves microsampling-cup assembly. A very stable cup-injector unit and noncorroding ceramic absorption tube (Coors Porcelain Co., Golden, Colo.) are used. A photon-counting signal-processing system enables measurement of integrated rather than peak absorbance. The instrument is interfaced to a computer, which provides automated calibration, a number of quality-control checks and a direct print-out of analyte concentration. However, these features are not indispensable to the method described; any commercial microsampling-cup system should give satisfactory data.

Sample preparation

Whole organs (kidney, liver and lung) were collected at autopsy, packed individually in polyethylene bags, and stored at −5 °C. A stainless steel surgical knife was used to remove connective tissues. The knife blade was ruled out as a source of cadmium contamination by soaking it overnight in (1+1) nitric acid and then analyzing the acid solution for cadmium by the microsampling-cup technique. No signal was detected at 228.8 nm.

Trace metals are usually not distributed evenly throughout tissues. In the kidney particularly, a large concentration gradient occurs [7]. Accordingly, large cross-sectional slices of tissue were taken, avoiding any surface which might have contacted the pathologist's knife. These sections (up to 100 g) were frozen, cut into approximately 10-mm cubes and weighed into a 600-ml laboratory mixer (Omnimixer, Ivan Sorvall Inc., Norwalk, Conn.). Four times their weight in water was then added, and the mixture was homogenized at maximum (16,000) r.p.m. for 10 min.

This (1+4) homogenate was further diluted with deionized water to give a cadmium concentration which would be within the linear part of the calibration curve. For kidney tissue the final dilution (by weight) was (1+4999); for liver and lung, the dilution was (1+1249).

Preparation of standards

A stock solution (10,000 μg Cd ml^{-1}) was prepared by dissolving 27.44 g $Cd(NO_3)_2 \cdot 4H_2O$ (reagent grade) in 1 l of deionized water. Suitable dilutions yielded aqueous standards from 0 to 0.01 μg Cd ml^{-1}.

Procedure

Aliquots (50 μl) of the suitably diluted homogenates were transferred in

triplicate to nickel microsampling cups, with an Eppendorf micropipette (Brinkmann Instruments Inc.). The cups had been burned off in the flame to ensure that there was no residual cadmium. Aqueous standards were similarly aliquoted in duplicate. The cups and their contents were oven-dried at 105 °C for 10 min.

A stoichiometric air—acetylene flame was used. After 10-min burning to allow the absorption tube to reach equilibrium temperature, the two sets of cups containing the standards were injected into the flame. Integrated absorbances at 228.8 nm were then measured, the computer calculated the least-squares regression line, and the correlation coefficient and the equation of the line were printed out. If the correlation coefficient was less than 0.98, the calibration standards were automatically rejected, and recalibration was necessary. The three replicate samples were then injected into the flame, and a print-out of their integrated absorbance was obtained. The cadmium concentration was automatically calculated from the mean of the three absorbance measurements.

RESULTS AND DISCUSSION

Nonspecific absorption interference

When biological materials are volatilized from a microsampling cup, nonspecific absorption signals from organic material entering the light path are usually observed. This often necessitates chemical pretreatment to destroy the organic matrix and/or the use of deuterium background correction.

In order to test for nonspecific absorption, aliquots (50 μl) of kidney homogenates at dilutions from (1+4) to (1+79) were pipetted into cups, dried, and injected into the flame. Measurements were made at the cobalt 240.7-nm line, which is a nonabsorbing wavelength, since cobalt will not volatilize from the cup with this flame. Nonspecific absorption was negligible at dilutions of (1+49) and above (Fig. 1). At the dilutions used in this cadmium study, destruction of the organic matrix and/or background correction are unnecessary.

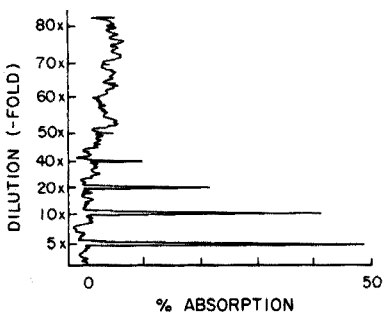

Fig. 1. Nonspecific absorption signals from kidney homogenates (50 μl). λ = 240.7 nm.

Calibration procedures

Ideally, standards should contain the analyte element bound in the same chemical form and in the same matrix as the samples. The best currently available standard, a lyophilized bovine liver (SRM 1577, National Bureau of Standards), contains only 0.27 μg Cd g^{-1} dried tissue (ca. 0.1 μg g^{-1} wet tissue). Normal levels in human kidney, liver and lung are higher, especially in kidney, where concentrations are of the order of 30 μg g^{-1}. At the small dilutions required for adequate sensitivity the NBS material is not suitable, since it gives a large unresolved nonspecific absorption peak because of the high concentration of organic material.

The standard matrix would be expected to be less critical for cadmium than for many other elements, since cadmium does not form refractory compounds and is readily volatilized. Four tests were carried out to check whether matrix effects were significant.

(1) A beef kidney which was low in cadmium was spiked to concentrations typical of human kidney with aqueous standard solutions. Pure aqueous standards were also prepared. Calibration curves obtained from these two sets of standards are shown in Fig. 2. The slopes are almost parallel, and if the spiked kidney curve is corrected for the residual cadmium in the kidney (i.e., if the intercept is subtracted), the two curves are almost identical. Any matrix interference would result in an increased or decreased slope. A human kidney was found to contain 24 μg Cd g^{-1} when determined against the spiked bovine curve and 26 μg Cd g^{-1} against the aqueous curve.

(2) In further tests, the integrated absorbances were plotted for various aliquots (0—100 μl) of a (1+4999) human kidney homogenate, and an excellent rectilinear plot was obtained. The concentration of organic matrix increases as the cadmium concentration increases, and the plot would be curved if the matrix were interfering.

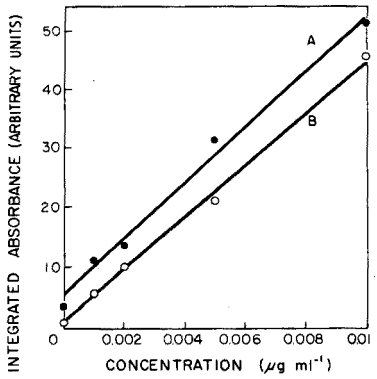

Fig. 2. Calibration curves for cadmium. λ = 228.8 nm. (A) Spiked beef kidney, (B) aqueous standards.

TABLE 1

Results obtained from aqueous calibration curve and by standard additions (All results are $\mu g\ Cd\ g^{-1}$)

Liver							
Aq. curve	1.6	4.1	2.8	5.7	1.9	2.4	4.2
Std. addn.	1.3	4.4	3.3	6.5	1.4	2.5	3.5
Kidney							
Aq. curve	10.3	11.3	10.4	48.2	30.6	3.5	
Std. addn.	10.2	12.8	10.7	50.5	34.0	4.5	
Lung							
Aq. curve	1.2	0.9	1.6				
Std. addn.	1.2	1.2	1.6				

(3) Three (1+4999) kidney homogenates were analyzed for cadmium against aqueous standards. Each homogenate was analyzed after oven-drying. Then the samples were heated in the microsampling cups at 400 °C for 24 h to remove the organic matrix, and the analysis was repeated. The concentrations obtained ($\mu g\ g^{-1}$) were comparable by the two methods (homogenate A, 19.9, 20.1; B, 12.8, 15.2; C, 16.5, 15.3), so that the results seem to be independent of the matrix.

(4) The method of standard additions was used to analyze 16 tissues, with each homogenate spiked at six concentrations between 0 and 0.01 $\mu g\ Cd\ ml^{-1}$. The tissues were also analyzed against a curve derived from aqueous standards. The comparative results (Table 1) show good agreement.

The results of these four tests confirm that aqueous cadmium standards can be used for tissue analysis. At 228.8 nm the sensitivity (1 % absorption) is 0.0002 $\mu g\ Cd\ ml^{-1}$ aqueous solution. The linear range is 0.0003—0.03 $\mu g\ ml^{-1}$, where the lower figure is the detection limit ($S/N = 2$), obtained from the standard deviation of 10 replicates of a solution.

Typical concentration ranges for cadmium in wet tissue are given in Table 2. The homogenate dilutions used in this study gave a linear range which includes all typical tissues. Any tissues not within the linear range can be further diluted

TABLE 2

Typical concentrations of cadmium in wet tissues and linear ranges obtained

	Kidney	Liver	Lung
Typical concentration range ($\mu g\ g^{-1}$)[a]	5—73	0.4—12	0.4—2.5
Linear range obtained ($\mu g\ g^{-1}$)	1.5—150[b]	0.38—38[c]	0.38—38[c]

[a] See reference 8.
[b] (1+4999) Homogenate.
[c] (1+1249) Homogenate.

or concentrated. The lowest detection limit obtainable (by using a (1+49) homogenate is 0.015 μg Cd g^{-1} wet tissue.

Precision

A sample of each type of tissue at a typical cadmium concentration was homogenized and suitably diluted. Ten replicate aliquots were pipetted into microsampling cups, which were dried and injected into the flame. Peak absorbances and integrated absorbances were measured, and relative standard deviations were determined. The results (Table 3) confirm an earlier report [6] that improved precision can be obtained by measuring integrated rather than peak absorbances. When transient signals are measured (as in all micro atomization systems), the rate of atom formation must be constant if peak absorbance measurements are to yield optimal precision data. In practice, the rate of atom

TABLE 3

Relative standard deviations for typical tissues

Tissue	μg Cd g^{-1} wet tissue	s_r	
		Peak absorbance	Integrated absorbance
Kidney	30.6	5.0	3.7
Liver	2.4	4.8	2.6
Lung	1.2	10.5	5.5

formation varies with cup heating rate, which may vary with cup thickness, cup injection rate and several other factors. Integrated absorbance measurements are independent of this parameter and are consequently more precise.

Conclusions

Tissue analysis procedures are generally time-consuming and prone to error, mainly because large amounts of sample are handled and because sample preparation is tedious.

The procedure described here is simple, rapid and precise. After homogenization, small sample volumes are required, with no further pretreatment. Sensitivity is high, enabling large dilutions, with consequent elimination of matrix effects. Thus aqueous standards are suitable, and background correction is not required. Since no reagents are used and very few steps are involved in sample pretreatment, the risk of contamination is minimal. Samples are prepared at room temperature, so that no volatilization losses occur.

It has recently been shown that a nitrous oxide—acetylene flame greatly increases the number of elements which can be determined by the micro-

sampling-cup method [9]. This should enable the development of simple, rapid and sensitive methods for other important trace elements in tissues.

SUMMARY

A microsampling-cup method of atomic absorption spectrometry has been applied to the determination of cadmium in biological tissues. Sample preparation involves homogenizing a known weight of the tissue with a known volume of water, pipetting a suitable dilution of the homogenate into a microsampling cup and drying. Aqueous calibration standards are used. Sensitivity, linear range and reproducibility are adequate for this application. Simplicity and speed make this method preferable to any other reported to date.

REFERENCES

1 H.A. Schroeder and A.P. Nason, Clin. Chem., 17 (1971) 461.
2 H. Sanui, Anal. Biochem., 42 (1971) 21.
3 L. Murthy, E.E. Menden, P.M. Eller and H.G. Petering, Anal. Biochem., 53 (1973) 365.
4 S.B. Gross and E.S. Parkinson, At. Absorption Newslett., 13 (1974) 107.
5 H.T. Delves, Analyst (London), 95 (1970) 431.
6 K.M. Aldous, D.G. Mitchell and F.J. Ryan, Anal. Chem., 45 (1973) 1990.
7 H.D. Livingston, Clin. Chem., 18 (1972) 67.
8 I.H. Tipton, in M.J. Seven and L.A. Johnson (Eds.), Metal Binding in Medicine, Lippincott, Philadelphia, 1960, p. 27.
9 D.G. Mitchell, A.F. Ward and M. Kahl, Anal. Chim. Acta, 76 (1975) 456.

Analytica Chimica Acta, 80 (1975) 47—59

THE ATOMIC ABSORPTION SPECTROMETRIC DETERMINATION OF INDIUM IN PREMIXED INERT GAS (ENTRAINED AIR)—HYDROGEN FLAMES

TAKETOSHI NAKAHARA and SÔICHIRÔ MUSHA

Department of Applied Chemistry, College of Engineering, University of Osaka Prefecture, Mozu-umemachi, Sakai 591 (Japan)

(Received 13th May 1975)

SUMMARY

Indium can be determined more sensitively in argon (entrained air)— and nitrogen (entrained air)—hydrogen flames than in air—acetylene or air—hydrogen flames. The indium sensitivity (for 1% absorption) is 0.075—0.082 p.p.m. at 303.9 nm and the calibration graphs are linear up to 10 p.p.m. Many foreign elements interfere with the determination, but the addition of magnesium halides is very effective in eliminating interferences from other elements, with the exception of silicon and vanadium. This finding was satisfactorily applied to the determination of indium in some semi-conducting III—V compounds. It is suggested that indium atoms are produced in the cool flames by dissociation of InH molecules, the production of which is enhanced by a large amount of magnesium halide.

The determination of indium by atomic absorption spectrometry has been reported by many workers. Several lines for indium and their sensitivities and detection limits in conventional a.a.s. have been listed [1—3]; a continuum source has also been studied [4, 5]. Detection limits for indium in air—acetylene flames have been reported as 0.05 p.p.m. at 303.9 nm [6], and 0.3 p.p.m. at 325.6 nm [7]; the detection limit is 0.7 p.p.m. at 325.6 nm in the nitrous oxide—acetylene flame [7]. Spitzer and Tesik [8] described the determination of indium by a.a.s. after extraction of indium bromide with diisopropyl ether and then methyl isobutyl ketone. Haraguchi et al. [9, 10] reported the molecular flame absorption spectrometry of indium compounds in an air—acetylene flame. The use of a long-path absorption quartz tube has also been discussed [11]. Detection limits of $1—2.6 \cdot 10^{-10}$ g of indium at 303.9 nm have been found with non-flame atomic absorption spectrometry [12, 13].

Cool flames — usually inert gas (entrained air)—hydrogen flames — have become quite commonly used in a.a.s., as has been outlined in an earlier paper [14]. The premixed inert gas (entrained air)—hydrogen flames produced with a "multi-flame" burner [15] can be used as atom reservoirs in the a.a.s. determination of tin, zinc, bismuth, arsenic and selenium (see ref. 14),

as well as gallium [14] and lead [16].

This paper describes the flame characteristics for indium in the premixed argon (entrained air)— and nitrogen (entrained air)—hydrogen flames produced with the specially designed "multi-flame" burner [15], and the various interferences with the indium atomic absorption in these flames. Several acids and many diverse elements interfered, but a large amount of magnesium (as halide) eliminated most of these interferences. The method was successfully applied to the determination of indium in some semiconducting III—V compounds. Furthermore, the molecular flame absorption and emission band spectra were measured in these low-temperature flames, and a mechanism for the production of indium atoms in the flame and for the elemination of interferences is suggested.

EXPERIMENTAL

Apparatus

The spectrophotometer, long-path "multi-flame" burner [15], and nebulizer-chamber were the same as those used in the studies of gallium [14]. Premixed argon (entrained air)— and nitrogen (entrained air)—hydrogen flames were used; the height in the flame was taken as zero when the light beam just touched the top of the burner head. The analytical wavelength was 303.9 nm, and the light source was an indium hollow-cathode lamp (Westinghouse, Type WL 22996A), operated at 8 mA. In the measurement of the molecular flame absorption spectra, a deuterium lamp of the hollow-cathode type (Hamamatsu TV Co. Ltd., Type L233), operated at 18 mA, was used as a continuous light source. Gas flow rates were carefully regulated and monitored on calibrated flow meters.

Reagents

A stock solution of indium (1000 p.p.m.) was prepared by gently heating 1.000 g of high-purity indium metal (99.99%, Wako Pure Chemical Industries Co. Ltd.) in 20 ml of concentrated nitric acid until dissolved. This solution was diluted to 1 l with distilled water. Working solutions were prepared by appropriate dilution. All the other reagents were of either analytical-reagent grade or the purest grade available and used without further purification. Blanks were run on each solution for the interference study.

RESULTS AND DISCUSSION

Selection of wavelength and sensitivities in different flames

Table 1 shows the various spectral lines of indium which, according to transition probabilities [17], should be applicable for atomic absorption;

TABLE 1

Line intensities and sensitivities of indium spectral lines in the premixed inert gas (entrained air)—hydrogen flames

Indium line (nm)	Relative line intensity[a]	Sensitivity for 1% absorption (p.p.m.)	
		Ar(air)—H_2	N_2 (air)—H_2
256.0[b]	0.044	1.36	2.21
271.0	0.133	6.75	26.6
271.3	0.088	64.0	125
275.3[b]	0.029	3.09	4.49
277.5[b]	0.100	63.2	87.6
283.6	0.232	142	226
285.8[b]	0.130	26.9	42.9
293.2	0.088	23.6	59.5
295.7	0.228	978	603
303.9[b]	0.912	0.075	0.082
325.6	1.000	0.267	0.512
410.4[b]	0.118	0.500	1.34
451.1	0.138	2.52	13.0

[a] Arbitrary units; 10 mV f.s.d. for recorder.
[b] Resonance lines.

the relative line intensities from the hollow-cathode lamp and the sensitivities for 1% absorption observed under identical flame conditions are also listed. The indium 303.9-nm resonance line was the most sensitive and had a relatively higher intensity, and was therefore selected as the analytical line.

The indium sensitivities at 303.9 nm for 1% absorption in aqueous solutions were obtained in several different flames produced with the "multi-flame" burner [15] under optimal flame conditions. The sensitivities obtained were 0.234, 0.786, 0.252, 1.48, 0.075 and 0.082 p.p.m. in the premixed air—acetylene, nitrous oxide—acetylene, air—hydrogen, nitrous oxide—hydrogen, argon (entrained air)—hydrogen and nitrogen (entrained air)—hydrogen flames, respectively. The inert gas (entrained air)—hydrogen flames gave much better sensitivity than the other hydrogen or acetylene flames; this may be explained in terms of the formation of indium hydride (InH) during the production of indium atoms in these low-temperature flames (see below). As has been shown previously [14—16], many relatively volatile elements are sufficiently atomized to provide good sensitivity even in cool flames.

Effect of flame composition and flame height

At a fixed flow rate of argon or nitrogen nebulizing gas, the hydrogen flow rates were varied from 3.6 to 12.6 l min^{-1} and the signals for 5 p.p.m. of indium were measured at various flame heights. The optimal flame conditions were found to be :

for the argon (entrained air)—hydrogen flame: 5.4 l min^{-1} of hydrogen, 4.5 l min^{-1} (1.5 kg cm^{-2}) of argon, with a height in the flame of 4 mm above the top of the burner head; for the nitrogen (entrained air)—hydrogen flame: 5.4 l min^{-1} of hydrogen, 5.0 l min^{-1} (1.5 kg cm^{-2}) of nitrogen, with a height in the flame of 5 nm above the top of the burner head.

Both these flames were almost invisible; the sample aspiration rates were 8.9 ml min^{-1} with the former flame and 9.0 ml min^{-1} with the latter. Unless otherwise stated, these flame parameters were used in the following study.

Detection limits and calibration graphs for indium

Under the above optimal conditions, the detection limit (signal/noise = 2 : 1) for indium was 0.025 p.p.m. and the sensitivity (for 1% absorption) was 0.075 p.p.m. in the argon (entrained air)—hydrogen flame; the detection limit was 0.027 p.p.m. and the sensitivity 0.082 p.p.m. in the nitrogen (entrained air)—hydrogen flame. The calibration graphs for indium at 303.9 nm in both flames were linear for the concentration range 0—10 p.p.m. of indium.

Effect of acids

Popham and Schrenk [7] have shown that hydrochloric, nitric, phosphoric and sulfuric acids at concentrations below 0.1 M do not seriously affect indium atomic absorption in air—acetylene and nitrous oxide—acetylene flames, though the effects were smaller in the hotter nitrous oxide flame.

In the cool flames used here, the effects of acids normally used in the dissolution of various samples were examined over the concentration range 0.1—2.0 M. In the argon (entrained air)—hydrogen flame, phosphoric acid caused a large depressing interference (Fig. 1), probably owing to the

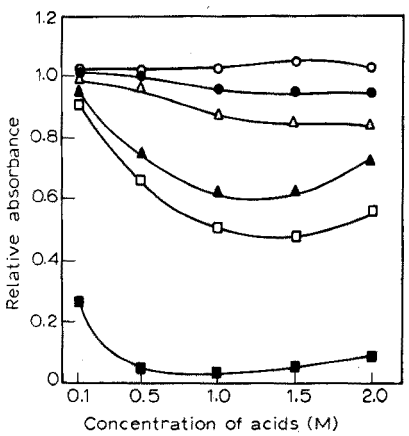

Fig. 1. Effect of acids on indium absorption. Concentration of indium, 5 p.p.m. Flame, argon (entrained air)—hydrogen. (○) Hydrofluoric acid; (●) nitric acid; (△) sulfuric acid; (▲) hydrochloric acid; (□) perchloric acid; (■) phosphoric acid.

formation of a species which was more difficult to vaporize or dissociate in the cool flame. Other acids below 0.1 M did not interfere, but hydrochloric, perchloric or sulfuric acids above 0.1 M caused increasing depression with an increase in the acid concentration. The nitrogen (entrained air)—hydrogen flame produced the same results as the argon (entrained air)—hydrogen flame.

Effect of various other elements

Mulford [6] found that aluminum, magnesium, copper and zinc at concentrations 100 times that of indium depressed the absorption of indium in air—acetylene flames. Popham and Schrenk [7] reported that indium was relatively free from major interferences, with only nickel causing a severe depression in the air—acetylene flame; in the nitrous oxide—acetylene flame only bismuth caused a depression, while most other elements caused some enhancement.

The effects of various other elements on the indium atomic absorption in both the hydrogen flames were investigated at constant concentration levels of indium and diverse elements. Many elements caused a depressing interference (Table 2), the deviation of the absorbance for indium being greater than 5%. Some elements such as calcium, cobalt, magnesium, sodium etc. did not interfere, but no element enhanced the indium atomic absorption. The higher temperature of the argon (entrained air)—hydrogen flame compared to the corresponding nitrogen flame [18] probably explains the difference in the interference effects described in Table 2. The depressing interferences depended on the fuel (hydrogen) flow rate and on the flame

TABLE 2

Effect of other elements on indium atomic absorption
(5 p.p.m. In; 100 p.p.m. interfering element)

	Ar(air)—H_2	N_2 (air)—H_2
No interference	Ag[a], As[b], Au[c], Ba[c], Bi[a], Ca[c], Cd[a], Ce[d], Co[c], Cs[c], Cu[d], Fe[c], Ga[c], La[c], Li[c], Mg[c], Na[c], Ni[d], Pb[a], Sb[c], Sn[c], Sr[a], Ti[c], Zn[a]	As[b], Au[c], Bi[a], Ca[c], Cd[a], Ce[d], Co[c], Cu[d], Fe[c], Ga[c], La[c], Mg[c], Na[c], Ni[d], Pb[a], Sb[c], Sn[c], Sr[a], Ti[c], Tl[a], W[b], Zn[a]
Depression	Al[c], B[d], Be[d], Cr[c], Hg[c], K[c], Mn[a], Mo[e], Pd[c], Pt[c], Rb[c], Se[b], Si[b], Te[b], Th[a], Tl[a], V[e], W[b], Y[a], Zr[a]	Ag[a], Al[c], B[b], Ba[c], Be[d], Cr[c], Cs[c], Hg[c], K[c], Li[c], Mn[a], Mo[e], Pd[c], Pt[c], Rb[c], Se[b], Si[b], Te[b], Th[a], V[e], Y[a], Zr[a]
Enhancement	None	None

[a]Added as nitrate.
[b]Added as sodium salt.
[c]Added as chloride.
[d]Added as sulfate.
[e]Added as ammonium salt.

height, as happens in other flames [19], and as happened with gallium in cool flames [14]. The type of compound used also had some effect on the magnitude of interferences. But the depressing interferences from other elements did not show linear relationships with their concentrations.

Elimination of interferences

The above interferences depend on the concentration of the diverse element, the flame composition and the flame height. In an attempt to eliminate these interferences, the effect of adding a non-interfering element was examined. Calcium, cobalt, magnesium and sodium eliminated the depressing interferences, magnesium being the most effective (Table 3). When the standard and sample solutions contained 1000 p.p.m. of magnesium as a releasing element, the interferences were almost removed, and this could be applied to practical samples.

Further experiments on eliminating the interferences were made with different magnesium compounds, i.e., magnesium iodide, bromide, chloride, nitrate and sulfate (Fig. 2). Magnesium halides were more effective. The interference-eliminating efficiency of the halides decreased in the order: iodide > bromide > chloride. This order was expected from considerations

TABLE 3

Suppression of interferences from other elements in cool flames (5 p.p.m. In; 500 p.p.m. interfering element; 2000 p.p.m. Ca, Na, Co or Mg. Results are expressed as the ratio of the absorbance for indium in the presence of the interfering element to the absorbance in the absence of the interfering element)

Element	Relative absorbance in Ar(air)—H_2					Relative absorbance in N_2 (air)—H_2				
	None	Ca	Na	Co	Mg	None	Ca	Na	Co	Mg
Al	0.15	1.09	1.00	1.06	1.02	0.17	1.02	0.98	1.03	1.02
B	0.79	1.02	1.01	1.04	1.03	0.73	0.96	1.03	1.03	1.00
Be	0.11	0.39	0.48	1.01	1.01	0.09	0.75	0.38	0.96	0.97
Cr	0.81	1.04	1.04	1.04	1.01	0.19	1.01	0.99	0.98	1.00
Hg	0.61	1.02	0.54	1.03	1.01	0.48	1.01	0.39	1.00	1.01
K	0.82	1.01	0.98	1.04	1.03	0.76	1.01	0.92	0.99	1.03
Mn	0.72	1.04	0.58	0.99	0.98	0.52	1.05	0.46	0.99	0.97
Mo	0.45	0.99	0.48	0.99	0.98	0.25	0.97	0.32	0.90	0.98
Pd	0.77	0.29	0.11	0.65	0.97	0.68	0.39	0.06	0.32	0.96
Pt	0.74	1.04	0.17	1.01	0.98	0.58	0.94	0.21	0.91	0.97
Rb	0.93	1.04	0.93	0.99	0.98	0.83	1.01	0.85	0.96	0.99
Se	0.81	0.04	0.74	0.02	0.97	0.76	0.07	0.65	0.05	0.98
Si	0.64	0.04	0.99	0.03	0.90	0.52	0.07	0.94	0.05	0.92
Te	0.70	0.03	0.78	0.02	0.96	0.57	0.06	0.51	0.04	0.97
Th	0.45	1.04	0.90	1.00	1.01	0.38	1.02	0.87	0.98	1.00
V	0.48	1.04	0.64	0.68	0.75	0.26	0.37	0.38	0.53	0.68
Y	0.81	1.01	1.00	1.04	1.02	0.71	1.01	0.95	0.96	1.03
Zr	0.52	1.02	1.05	1.01	1.03	0.37	1.05	0.99	1.04	1.01

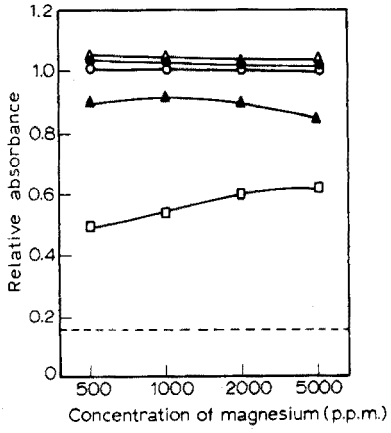

Fig. 2. Effect of some magnesium compounds on the interference of aluminum. Concentration of indium, 5 p.p.m. Flame, argon (entrained air)—hydrogen. Concentration of aluminum, 500 p.p.m. Magnesium added as (△) magnesium iodide, (●) magnesium bromide, (○) magnesium chloride, (▲) magnesium nitrate, (□) magnesium sulfate. (---) The interference from aluminum in the absence of magnesium.

of molecular weight and electronegativity; magnesium fluoride was not examined because of its small solubility in water. Thus the halide ions as well as magnesium ion may contribute to the formation of species which are stable in cool flames, e.g. InI, InBr, InCl, and these species favour the formation of InH which decomposes directly to produce indium atoms, as will be described below.

Mechanism for production of indium atoms and for interference elimination

The premixed cool flames employed here are considered to contain fewer oxygen molecules and/or atoms and more hydrogen molecules and/or atoms in the flame than the other acetylene or hydrogen flames produced with a "multi-flame" burner [15]. Therefore the production of indium atoms in the flame may be different in the cool flames and the other flames. Indium oxide, one of the species which may be formed in the flame, has a dissociation energy [20] of 3.3 eV, while the dissociation energy of indium hydride (InH) [20], which is expected to be produced in the low-temperature flames, is 2.5 eV. Therefore, the production of indium atoms in the flame may be outlined as follows

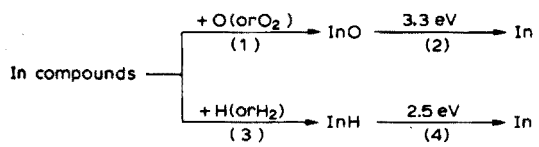

Scheme 1

In the cool flames, processes (3) and (4) may be promoted much more than processes (1) and (2), although the difference in dissociation energies between InO and InH is very small (0.8 eV). This may contribute to the fact that the cool flames used here give much better sensitivity than the other hydrogen or acetylene flames. The indium hydride emission spectral band [21] headed at 454.1 nm is shown in Fig. 3. The indium oxide absorption spectral band [21] headed at 273.0 nm is shown in Fig. 4; the broad absorption band at about 207 nm, which is observed only on nebulizing nitric acid solutions of indium, may be attributed to ZnO. As is shown in Fig. 4, the hydrochloric acid solution of indium gave the absorption bands of indium chloride (InCl), by which the existence of InCl is indicated in the cool flames.

As has been described above (Table 2 and Fig. 2), the presence of magnesium halides removes the depressing interferences in the indium atomic absorption in the cool flames used here. The intensities of the InH emission band (headed at 454.1 nm) with and without the addition of magnesium halides (iodide, bromide and chloride) in indium solutions containing aluminum as a depressing element were measured in the flames. The results obtained in both the hydrogen flames are shown in Table 4. The relative intensities of the InH emission band in the presence of magnesium halides decreased in the order: iodide > bromide > chloride; this order was expected from the interference-eliminating efficiency described above (Fig. 2). Other interfering elements gave the same results as those shown for aluminum in Table 4. The results indicate that the interference elimination may

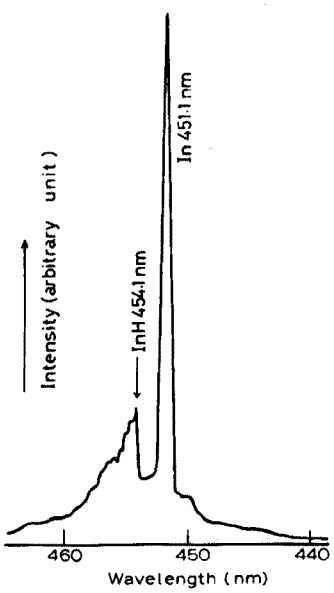

Fig. 3. Molecular emission band of InH. Flame, argon (entrained air)—hydrogen; concentration of indium, 500 p.p.m.

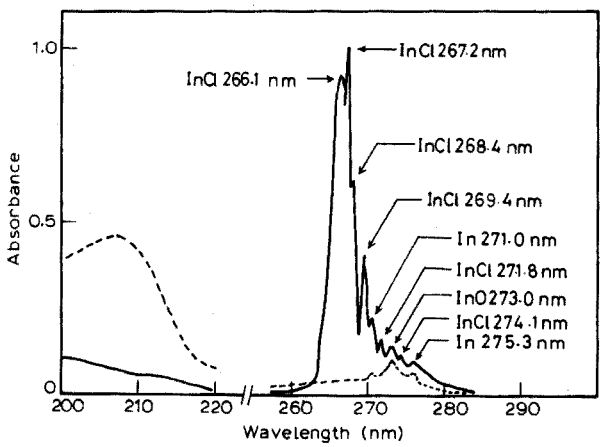

Fig. 4. Molecular absorption spectra of InCl and InO. Flame, argon (entrained air)—hydrogen; (—) hydrochloric acid (2.0 M) solution of indium (20000 p.p.m.); (---) nitric acid (2.0 M) solution of indium (20000 p.p.m.).

TABLE 4

Molecular emission intensities of indium hydride band headed at 454.1 nm in the cool flames
(5 p.p.m. In; 2000 p.p.m. Al; 5000 p.p.m. Mg)

Solution	Ar(air)—H_2		N_2(air)—H_2	
	Intensity[a] (cm)	Relative intensity	Intensity[a] (cm)	Relative intensity
In alone	22.2	1.00	13.0	1.00
In + Al	0.2	0.01	0.0	0.00
In + $MgCl_2$	21.0	0.95	14.0	1.08
In + $MgCl_2$ + Al	19.8	0.90	10.0	0.77
In + $MgBr_2$	24.4	1.11	15.0	1.15
In + $MgBr_2$ + Al	21.0	0.95	11.7	0.90
In + MgI_2	28.0	1.30	15.6	1.20
In + MgI_2 + Al	23.9	1.08	12.4	0.95
In + $Mg(NO_3)_2$	5.0	0.23	2.5	0.19
In + $Mg(NO_3)_2$ + Al	15.8	0.72	7.5	0.58

[a]Peak heights at 454.1 nm measured under the same experimental conditions.

contribute to the presence of InH molecules produced in the cool flames. Furthermore, indium solutions containing magnesium halides gave the spectra [21] of InI, InBr and InCl (Figs. 5—7), so that the existence of InI, InBr and InCl molecules in the cool flames is confirmed. The existence of InCl molecules in the cool flames is also indicated by the molecular absorption

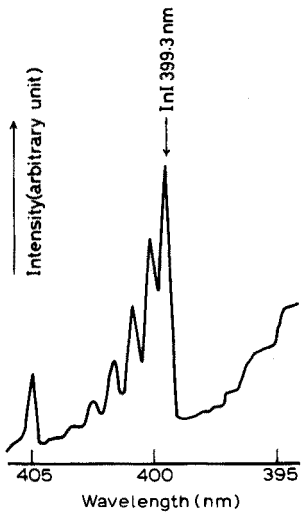

Fig. 5. Molecular emission band of InI. Flame, argon (entrained air)—hydrogen; concentration of indium, 500 p.p.m.; concentration of magnesium added as iodide, 5000 p.p.m.

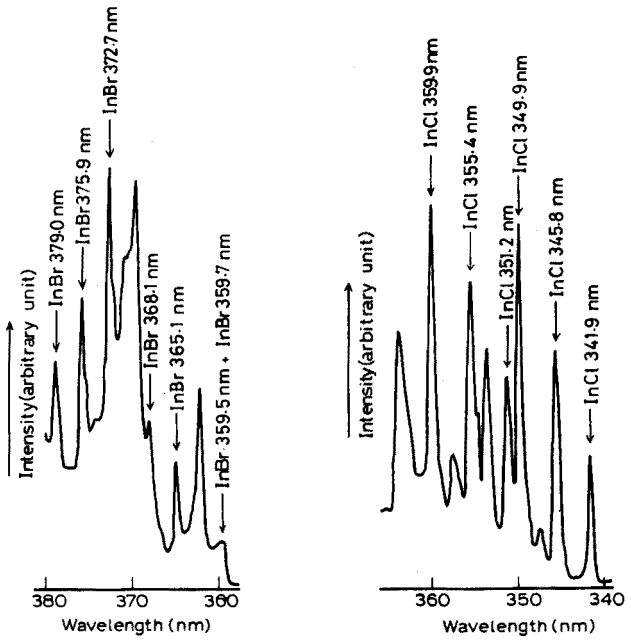

Fig. 6. Molecular emission bands of InBr. Flame, argon (entrained air)—hydrogen; concentration of indium, 500 p.p.m.; concentration of magnesium added as bromide, 5000 p.p.m.

Fig. 7. Molecular emission bands of InCl. Flame, argon (entrained air)—hydrogen; concentration of indium, 500 p.p.m.; concentration of magnesium added as chloride, 5000 p.p.m.

[9, 21] measurements (Fig. 4). Depressing interferences may occur through processes (1) and (2) rather than through processes (3) and (4) as indicated in Scheme 1.

The dissociation energies [20] of InI, InBr and InCl are 3.35, 4.0 and 4.5 eV; this order is the same as that of the interference-eliminating efficiency (Fig. 2) and of the relative intensities of the InH emission band (Table 4). Therefore, the mechanism of the interference-eliminating action of magnesium halides may be explained by the following scheme:

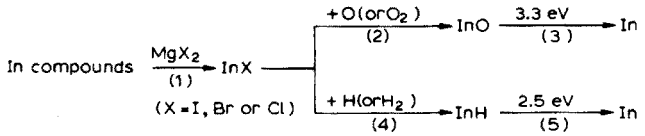

Scheme 2

The production of indium atoms presumably occurs to a greater extent through processes (1), (4) and (5) than through processes (1), (2) and (3) when magnesium halides are added, but a large part of the indium may be present as InO in the presence of the interfering elements.

Effect of organic solvents

Various organic solvent systems were studied to determine if greater sensitivity could be achieved. Solutions of 10, 20, 30, 40 and 50% (v/v) methanol, ethanol, acetone and iso-propanol gave no appreciable increase in sensitivity for indium over that observed in aqueous solutions.

Application of the method to some semi-conducting compounds of Groups III—V

On the basis of the above observations, the following procedures were designed for the determination of indium in some semi-conducting III—V compounds, e.g., $In_x Ga_{1-x} Sb$, $Ga_x In_{1-x} P$.

The semi-conducting compound (10—30 mg) was dissolved with 5 ml of concentrated nitric acid and 5 ml of concentrated hydrofluoric acid in a polyethylene bottle on a water bath (for $In_x Ga_{1-x} Sb$) or with 5 ml of concentrated nitric acid and 5 ml of concentrated hydrochloric acid on a hot plate (for $Ga_x In_{1-x} P$). After dissolution, the solution was diluted to 100 ml with distilled water. The sample solutions nebulized into the flame were prepared to contain 1000 p.p.m. of magnesium (as iodide). The indium in the samples was determined three times by referring to the calibration graphs prepared with 1000 p.p.m. of magnesium (as iodide) added to the standard indium solutions. The indium was measured at 303.9 nm in the premixed argon (entrained air)— and nitrogen (entrained air)—hydrogen flames under the optimal conditions mentioned above. The results of the

determinations with a precision of relative standard deviations of 2—3.5% (Table 5) agreed closely with the theoretical value.

The interest and encouragement of Professor Makoto Munemori in this work is gratefully acknowledged. The authors also acknowledge the assistance given by Mr. Wataru Taniguchi in the experimental work.

TABLE 5

Determination of indium in $In_xGa_{1-x}Sb$ and $Ga_xIn_{1-x}P$

x	Theor. value (wt. %)	Found (wt. %)	
		Ar(air)—H_2	N_2 (air)—H_2
$In_xGa_{1-x}Sb$			
0.0	0.00	0.00	0.00
0.1	5.86	5.84	5.88
0.2	11.49	11.47	11.48
0.3	16.78	16.75	16.80
0.5	26.71	26.74	26.72
0.7	35.93	35.94	35.95
1.0	48.50	48.49	48.45
$Ga_xIn_{1-x}P$			
0.0	78.98	78.95	78.90
0.1	72.94	72.90	72.80
0.13	71.18	71.10	71.15
0.4	53.78	53.75	53.70
0.455	50.06	50.01	50.09
0.695	30.62	30.60	30.59
0.79	21.93	21.92	21.95
0.87	14.06	14.05	14.02

REFERENCES

1 B. M. Gatehouse and J. B. Willis, Spectrochim. Acta, 17 (1961) 710.
2 J. E. Allan, Spectrochim. Acta, 18 (1962) 259.
3 W. Slavin, Appl. Spectrosc., 20 (1966) 281.
4 V. A. Fassel, V. G. Mossotti, W. E. L. Grossman and R. N. Kniseley, Spectrochim. Acta, 22 (1966) 347.
5 W. W. McGee and J. D. Winefordner, Anal. Chim. Acta, 37 (1967) 429.
6 C. E. Mulford, At. Absorption Newslett., 5 (1966) 28.
7 R. E. Popham and W. G. Schrenk, Spectrochim. Acta, Part B, 24 (1969) 223.
8 H. Spitzer and G. Tesik, Z. Anal. Chem., 241 (1968) 218.
9 H. Haraguchi and K. Fuwa, Chem. Lett., (1972) 913.
10 H. Haraguchi, M. Shiraishi and K. Fuwa, Chem. Lett., (1973) 251.
11 M. Miksovsky and I. Rubeska, Chem. Listy, 68 (1974) 299.
12 F. J. Langmyhr and S. Rasmussen, Anal. Chim. Acta, 72 (1974) 79.
13 A. Rattonetti, Anal. Chem., 46 (1974) 739.
14 T. Nakahara and S. Musha, Anal. Chim. Acta, 75 (1975) 305.

15 T. Nakahara, H. Date, M. Munemori and S. Musha, Bull. Chem. Soc. Jap., 46 (1973) 637.
16 T. Nakahara and S. Musha, Appl. Spectrosc., 29(4) (1975) 352.
17 C. H. Corliss and W. R. Bozman, Experimental Transition Probabilities for Spectral Lines of Seventy Elements, NBS Monograph No. 53, U.S. Department of Commerce, N.B.S., Washington, D.C., 1962, p. 154.
18 T. Nakahara, M. Munemori and S. Musha, Bull. Chem. Soc. Jap., 46 (1973) 639.
19 J. A. Dean and T. C. Rains, Flame Emission and Atomic Absorption Spectrometry, Vol. 1, Dekker, New York, 1969.
20 A. G. Gaydon, Dissociation Energies and Spectra of Diatomic Molecules, Chapman and Hall, London, 3rd. edn., 1968.
21 R. W. B. Pearse and A. G. Gaydon, The Identification of Molecular Spectra, Chapman and Hall, London, 3rd edn., 1965.

Analytica Chimica Acta, 80(1975)61—66

AN ATOMIC ABSORPTION METHOD FOR THE DETERMINATION OF 20 ELEMENTS IN LAKE SEDIMENTS AFTER ACID DIGESTION

HAIG AGEMIAN and A.S.Y. CHAU

Water Quality Laboratory, Canada Centre for Inland Waters, Burlington, Ontario L7R 4A6 (Canada)

(Received 21st April 1975)

The concentration of metals in lake or stream sediments is of particular importance in environmental and geochemical studies. Because of their environment, these sediments are somewhat different in their makeup from inorganic siliceous rocks; the essential difference is their higher organic matter content. Curtis [1] has discussed the incorporation of soluble organic matter into sediments and their association with trace metals. The correlation between organic matter and trace metal content of sediments is now well known for several elements [2]. Therefore, in the preparation of sediment samples, the important step of destruction of organic matter must be very rigorous.

The method of Bernas [3] for the analysis of silicates has been applied to several types of siliceous materials. Lerner et al. [4] decomposed soils, Buckley and Cranston [5] decomposed marine sediments, and Langmyhr and Paus [6,7] decomposed inorganic siliceous material by the hydrofluoric acid dissolution method. All of these techniques are very effective in dissolving siliceous material but they do not destroy the large quantities of organic matter present in some silt and clay lake sediments. A black residue remains, even after treating the sediment for extended periods of time with the aqua regia—hydrofluoric acid mixture used by Bernas [3]. Therefore it was necessary to develop a much stronger oxidizing mixture which would give complete recovery of as many metals as possible after the destruction of the organic matter.

Hartstein et al. [8] decomposed coals by first destroying the organic matter with fuming nitric acid in a teflon bomb and then dissolving the siliceous material with hydrofluoric acid. Gorsuch [9] compared the recoveries of a large number of metals from organic matter by different acid mixtures. A mixture of nitric and perchloric acids [10,11] was found to be the best for the majority of the metals. The use of sulfuric acid was omitted because of the low recoveries of lead [9] and the formation of barium sulfate [11].

The acid mixture employed must satisfy a few important conditions. It should dissolve the silica matrix of the sediment, it should destroy the organic matter and it should put all the metals into solution; no interfering ions should

be introduced. A mixture of nitric, perchloric and hydrofluoric acids satisfies these conditions. The nitric—perchloric acid mixture was adapted to the bomb technique and a mixture of the three acids was used to decompose the samples. This mixture was found to be excellent for all kinds of sediments ranging from fairly inorganic sand samples to organic-rich silt and clay samples. The method combines the efficient decomposing power of the triple acid system with the advantages [3,5] of the bomb technique to produce an effective means of recovering the total amount of an element from a sediment sample.

EXPERIMENTAL

Apparatus

A Parr 4745 acid digestion bomb (Parr Instrument Co., Moline, Ill. 61265) was used for the decompositions.

The atomic absorption spectrophotometer (Perkin-Elmer Model 403) was fitted with either a Boling (3-slot) air—acetylene burner or a nitrous oxide burner, and used with an A-25 Varian strip-chart recorder. All instrumental settings, including wavelength, slit and grating, were those recommended in the Perkin—Elmer Analytical Methods Book. Cd, Co, Cr, Cu, Fe, K, Li, Mn, Ni, Pb and Zn were determined by using an air—acetylene flame. A Boling 3 slot burner was used for all metals except Na and K, for which a 2-in. air—acetylene burner was used. Al, Ba, Be, Ca, Mg, Mo, Sr and V were determined with a nitrous oxide—acetylene flame. The burner position for all the metals was parallel to the hollow-cathode light path except for Ca, K, Mg and Na, when it was held perpendicular, in order to reduce the sensitivity since these metals were too concentrated in the solutions. Perkin—Elmer hollow-cathode lamps were used at the lamp currents specified on the lamps.

Reagents and samples

High-purity certified reagents were used for all analyses. All standards were prepared from certified atomic absorption reference standards (Fisher Scientific Co.).

Eight Lake Ontario sediments were taken for analysis: (1) fine sand, (2) mixed sand, (3) fine and medium sand, (4) fine sand, (5) medium sand, (6)—(8) silt and clay.

Procedure

Decomposition of sample

Frozen sediment samples were thawed and air-dried at room temperature. The dried sample was crushed to a fine powder and a representative sample of about 2 g was taken. This was further ground until a very fine powder passing through a 270-mesh sieve was obtained.

The prepared sample (100 mg) was transferred to the teflon cup, and 4.0 ml of nitric acid (concentrated), 1.0 ml of perchloric acid (60 %) and 6.0 ml of hydrofluoric acid (48 %) were added. The bomb was sealed and heated for 3.5 h at 140°C. After cooling, the contents of the teflon cup were quantitatively transferred to a 125-ml polypropylene bottle containing a solution of 4.8 g of boric acid in about 30 ml of deionized water to dissolve the precipitated metal fluorides. The solution was transferred to a 100-ml volumetric flask and made up to volume, and then stored in a 125-ml polypropylene bottle.

Analysis

All standards were made to contain 4.0 % (v/v) nitric acid, 1.0 % perchloric acid (60 %), 6.0 % hydrofluoric acid (48 %) and 4.8 % of boric acid. A blank sample was prepared similarly to the unknown samples and was taken through all the steps involved.

Some samples were spiked in the bombs before the decompositions, to obtain recovery values, and to check such factors as losses by volatilization, adsorption on the walls of the teflon container, or transference errors, as well as unsuspected chemical interferences.

Be, Cd, Cr, Co, Cu, Li, Mg, Pb, and Zn were determined by direct aspiration of the main sample solution. Chromium was determined by making all solutions and standards 2 % (w/v) in ammonium chloride to overcome interference [12,13] from iron. For molybdenum and vanadium, all solutions and standards were prepared [14,15] with 500 mg Al l^{-1} (as $AlCl_3$). Mn, Fe and Al were determined by diluting the main sample solution by a factor of 10 and analyzing by direct aspiration. For the determination of Ba, Ca and Sr, all sample and standard solutions contained 3000 mg Na l^{-1} (as NaCl), in order to remove the ionization interference in the nitrous oxide—acetylene flame. To prevent ionization interference in analyses for Na and K, all solutions contained 1000 mg Cs l^{-1} (as CsCl) [6].

The acid matrix used in the decomposition could suppress the signal of some metals. Nitric acid is known to suppress the signal for iron. Therefore, all reagents added to the samples were added to the standards in the same amounts.

RESULTS AND DISCUSSION

It was found that when a less oxidizing mixture than the one described above was employed, a black residue was left on the walls of the teflon cup. This residue was difficult to remove. The use of the nitric—perchloric acid mixture solves this problem.

The rate of decomposition of a sample is a function of temperature, hence as high a temperature as possible should be used. The manufacturer of the bomb suggests an upper limit of 150 °C, and 140 °C was chosen so as not to damage the bomb. It was found that heating the bomb at 140 °C overnight

produced similar results as heating for 3.5 h, which means that decomposition is complete after 3.5 h.

After the development of an acid mixture which would satisfactorily achieve complete dissolution of a resistant sediment sample, it was necessary to determine the degree to which the elements of interest could be recovered from the mixture. For this purpose, different levels of each element were added to the bomb before decomposition and the concentrations of the final solutions after decomposition were determined. For all elements except Al, Fe and Mn, 50, 100 and 150-μg amounts were added to the teflon cup together with the acid mixture, so that the expected increases in the concentration levels were 0.50, 1.00 and 1.50 $\mu g\ ml^{-1}$, respectively, for the final solutions.

For Al, Fe and Mn, 500, 1000 and 1500-μg amounts were added; with the 10-fold dilution of the main sample solution involved, the increase in concentration of the spiked samples was again 0.50, 1.00 and 1.50 $\mu g\ ml^{-1}$, respectively. These added levels were of the same order of magnitude as the actual concentration of the metal in the solution.

TABLE 1

Accuracy and precision of trace metal determination from the data on 8 lake sediments

Element	Amount added ($mg\ l^{-1}$)	Average recovery (%)	95 % conf. level ($mg\ l^{-1}$)	Element	Amount added ($mg\ l^{-1}$)	Average recovery (%)	95 % c level ($mg\ l^{-1}$
Ba	0.50	90	0.5±0.1	Mo	0.50	99	0.49±0
	1.00	98	1.0±0.1		1.00	101	1.01±0
	1.50	96	1.4±0.1		1.50	100	1.50±0
Be	0.50	101	0.51±0.01	Ni	0.50	95	0.48±0
	1.00	100	1.00±0.02		1.00	102	1.02±0
	1.50	101	1.51±0.02		1.50	98	1.47±0
Cd	0.50	99	0.49±0.02	Pb	0.50	99	0.50±0
	1.00	100	1.00±0.04		1.00	97	0.97±0
	1.50	100	1.49±0.05		1.50	96	1.44±0
Co	0.50	98	0.49±0.04	Sr	0.50	91	0.46±0
	1.00	97	0.97±0.04		1.00	92	0.92±0
	1.50	95	1.43±0.06		1.50	91	1.36±0
Cr	0.50	101	0.51±0.02	V	0.50	104	0.52±0
	1.00	96	0.96±0.02		1.00	105	1.04±0
	1.50	99	1.48±0.04		1.50	100	1.50±0
Cu	0.50	95	0.48±0.01	Zn	0.50	96	0.48±0
	1.00	94	0.94±0.01		1.00	95	0.95±0
	1.50	96	1.44±0.02		1.50	96	1.45±0
Li	0.50	99	0.50±0.01				
	1.00	99	0.99±0.01				
	1.50	99	1.49±0.02				

Tables 1 and 2 show the percentage recovery (accuracy) and the 95 % confidence limit (t-test) which gives a measure of the reliability of the recovery. The recovery at each of the spike levels was calculated by averaging the percentage recovery of each metal from the 8 sediment samples; this method was preferred to doing 8 replicate analyses on one sediment, because it shows that different matrices have no effect on the recovery and its limit of reliability. The recoveries ranged from an average of 91 % for strontium to 103 % for vanadium for the trace metals, and from an average of 96 % for sodium to 102 % for iron for the major elements. The recovery for strontium is a little low because of incomplete removal of matrix interferences [16, 17] in the nitrous oxide—acetylene flame. The possibility of loss of strontium by volatilization or retention on the walls of the teflon container was ruled out, when similar spikes in the main sample solution after decomposition gave similar recoveries.

Since complete dissolution of the samples was obtained, the recoveries also indicated the efficiency of the recovery of an element from the sediment.

TABLE 2

Accuracy and precision of major element determination from the data on 8 lake sediments

Element	Amount added ($mg\ l^{-1}$)	Average recovery (%)	95 % conf. level ($mg\ l^{-1}$)
Al	0.50	98	0.5±0.1
	1.00	99	1.0±0.1
	1.50	100	1.5±0.1
Ca	0.50	93	0.5±0.1
	1.00	100	1.0±0.1
	1.50	98	1.5±0.1
Fe	0.50	108	0.5±0.0
	1.00	101	1.0±0.1
	1.50	98	1.5±0.1
Mg	0.50	103	0.5±0.1
	1.00	96	1.0±0.1
	1.50	94	1.4±0.2
Mn	0.50	98	0.49±0.02
	1.00	98	0.98±0.01
	1.50	98	1.47±0.04
K	0.50	98	0.5±0.1
	1.00	98	1.0±0.1
	1.50	100	1.5±0.1
Na	0.50	93	0.5±0.0
	1.00	98	1.0±0.0
	1.50	98	1.5±0.0

The 95 % confidence limit depends jointly on the method of decomposition and on the detection limit for the element of interest in atomic absorption spectrometry.

All solution were stored for 40 days in the polypropylene bottles at room temperature. It was found that there was no appreciable loss of any of the 20 metals within this period of time. This should be long enough for the completion of any analyses.

Conclusions

The proposed method suggests a rigorous means of preparing a sediment sample by completely destroying the organic matter and thus effecting complete dissolution. Essentially no losses of elements occur during the preparation of the sample. The 95 % confidence limit data reflect not only the atomic absorption detection limits but the uncertainty involved in the method of decomposition.

Recovery experiments showed that there are no serious interferences other than those known in atomic absorption spectrometry. Methods of suppressing these interferences successfully provide a system in which complete matching of the matrix of the standards to that of the sample is not necessary.

SUMMARY

The teflon-lined bomb method for the decomposition of siliceous material is shown to be applicable for the determination of 20 elements in lake sediments. The sediment is digested at 140 °C with a mixture of nitric, perchloric and hydrofluoric acids; this destroys all organic matter as well as the silica matrix, and yields complete dissolution of the sediment. Quantitative recovery of 20 trace and major elements is obtained when atomic absorption spectrometry is used to complete the determinations.

REFERENCES

1 C.D. Curtis, in G.D. Hobson and M.C. Louis (Eds.), Advances in Organic Geochemistry, Pergamon Press, New York, 1966.
2 R.I. Thomas, Can. J. Earth Sci., 9 (1972) 636.
3 B. Bernas, Anal. Chem., 40 (1968) 1683.
4 L.A. Lerner, L.P. Orlova and D.N. Ivanov, Sov. Soil Sci., 3 (1971) 367.
5 D.E. Buckley and R.E. Cranston, Chem. Geol., 7 (1971) 273.
6 F.J. Langmyhr and P.E. Paus, Anal. Chim. Acta, 43 (1968) 397.
7 F.J. Langmyhr and P.E. Paus, At. Absorption Newslett., 7 (1968) 103.
8 A.M. Hartstein, R.W. Freedman and D.W. Plotter, Anal. Chem., 45 (1973) 611.
9 T.T. Gorsuch, Analyst (London), 84 (1959) 135.
10 G. Frederick Smith, Anal. Chim. Acta, 17 (1957) 175.
11 G.K. Hoops, Geochim. Cosmochim. Acta, 28 (1964) 405.
12 L. Barnes, Jr., Anal. Chem., 38 (1966) 1083.
13 A. Giammarise, At. Absorption Newslett., 5 (1966) 113.
14 R. Goecke, Talanta, 15 (1968) 871.
15 T.V. Ramakrishna, P.W. West and J.W. Robinson, Anal. Chim. Acta, 44 (1969) 437.
16 J.B. Willis, Appl. Opt., 7 (1968) 1295.
17 M.D. Amos and J.B. Willis, Spectrochim. Acta, 22 (1966) 1325.

Analytical Chimica Acta, 80(1975)67—74

A STUDY OF THE ABSORPTION AND FLUORESCENCE SPECTRA OF RIVANOL

DATTA V. NAIK and STEPHEN G. SCHULMAN
College of Pharmacy, University of Florida, Gainesville, Florida 32610 (U.S.A.)
(Received 18th March 1975)

Rivanol (2-ethoxy-6,9-diaminoacridinium lactate) is a potent antimicrobial agent which has been employed, as an amebicide, in the treatment of human dysentery and as a bactericide in the treatment of bovine streptomastitis [1]. As one of the highly basic 9-aminoacridine derivatives, rivanol is also potentially interesting as an absorbing and fluorescing probe of nucleic acid structure and of the interaction of aromatic cations with nucleic acids. The present study was taken in order to characterize the electronic absorption and fluorescence spectral properties of rivanol.

EXPERIMENTAL

Rivanol (Pfaltz and Bauer, Inc., Flushing, N.Y.) was recrystallized from absolute ethanol. Analytical reagent-grade sulfuric acid, sodium hydroxide (Mallinckrodt Chemical Works, St. Louis, Mo.) and trifluoromethanesulfonic acid (Willow Brook Laboratory, Inc., Waukesha, Wisc.) were used. Sulfuric acid solutions were prepared by dilution with distilled—deionized water; the corrected Hammett acidity scale of Jorgensen and Hartter [2] was employed to calibrate the sulfuric acid solutions. Solutions in the pH region 1—3 were prepared by dilution of sulfuric acid. Dilute sodium hydroxide solutions were employed for solutions of pH 11—14. To prepare solutions in the pH region 4—10, small amounts of sodium hydroxide or sulfuric acid were added to the aqueous solution. Absorption and fluorescence spectra were taken on $5.0 \cdot 10^{-5}$ M solutions of rivanol. The spectrophotometric titration procedures employed have been previously described [3]. pH was measured with an Orion model 801 digital pH meter with a combination silver—silver chloride glass electrode. Absorption spectra were recorded with a Beckman DB-GT spectrophotometer for 1-cm silica cells. Fluorescence spectra were recorded with a Perkin-Elmer MPF-2A fluorescence spectrophotometer whose monochromators were calibrated against the line emission spectrum of xenon. The polarized fluorescence excitation spectrum of the rivanol monocation, in glycerol at room temperature, was taken with the polarization accessory of the fluorescence spectrophotometer. The degree of polarization at a given wavelength was calculated from the following relationship [4]:

$$p = \frac{I_{\parallel} - I_{\perp}}{I_{\parallel} + I_{\perp}}$$

where $I_{\parallel}$ is the intensity of fluorescence when the analyzer is parallel to polarizer and $I_{\perp}$ is the intensity when the analyzer is perpendicular to the polarizer. The degree of polarization was not corrected for instrumental polarization, which was found negligible for present purposes [5].

RESULTS AND DISCUSSION

Rivanol has three basic nitrogen atoms and is capable of participating in three protolytic equilibria involving four distinct species. These species and the spectrophotometrically determined pK_a values corresponding to their interconversions determined absorptiometrically are depicted in Scheme 1. Also represented in Scheme 1 are the pK_a* values determined fluorimetrically, and corresponding to the observable excited-state protolytic processes.

Scheme 1

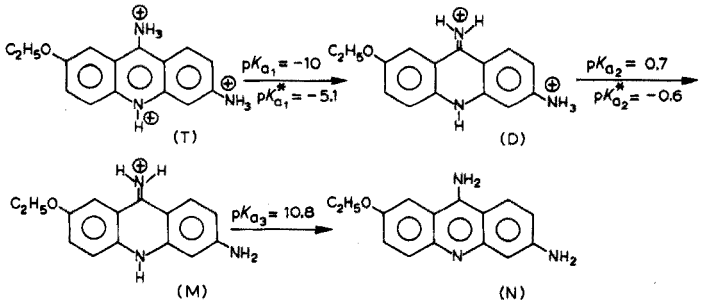

The principal features of the absorption and fluorescence spectra of these species are listed in Table 1 and the absorption spectra are shown in Fig. 1. The shifting of the absorption and fluorescence spectra of the trication (T) to shorter wavelengths, on dissociation to the dication (D), is anomalous for the dissociation of arylammonium ions. This phenomenon has also been observed in 9-aminoacridine [3] and is attributed to the iminoacridan structure of the singly charged 9-aminoacridinium cation. Apparently, the same type of structure is responsible for the short wavelength spectra of the rivanol dication and the unusually acidic pK_{a_1} of interconversion between T and D. Because of the electronegativity of the $-NH_3^{\oplus}$ group in the 6-position, pK_{a_1} for this equilibrium was, in fact, so acidic (ca. 1.5 log units more acidic than in 9-aminoacridine) that the absorptiometric titration from which this value (−10) was estimated was only half complete in the most concentrated sulfuric acid solution employed ($H_0 = -10.0$). In order to obtain the absorption spectra of the isolated trication (Table 1), it was necessary to take the absorption spectrum of rivanol in trifluoromethanesulfonic acid, an acid stronger than pure

TABLE 1

Long wavelength absorption ($\lambda_{^1L_a}$ and $\lambda_{^1L_b}$) and fluorescence (λ_f) maxima of rivanol in various states of protonation in aqueous and sulfuric acid media

Rivanol	$\lambda_{^1L_a}$ (nm)	$\lambda_{^1L_b}$ (nm)	λ_f (nm)[a]
Trication (T)[b]	450 (max.)	382 (0—0)	530 (max.)
Dication (D)	432 (0—0)	335 (0—0)	486 (max.)
	412 (max.)		(478)
Monocation (M)	423 (0—0)	362 (0—0)	502 (max.)
	409 (max.)		(455)
Neutral (N)	432 (0—0)	355 (0—0)	505 (max.)
	414 (max.)		(488)

[a]The wavelengths in the brackets are the fluorescence maxima at liquid nitrogen temperature, 77 K.
[b]The solvent was trifluoromethanesulfonic acid.

sulfuric acid. The conversion of the fluorescence of T to that of D, however, occurs in solutions some five orders of magnitude less acidic than the corresponding ground-state process. From the inflection region of the fluorimetric titration, the value of the dissociation constant of T in the lowest excited singlet state was estimated to be $pK^*_{a_1} = -5.1$.

The dissociation of D to form the monocation M is accompanied by a shift of the ^1L_b absorption and fluorescence bands to longer wavelengths and a shift of the ^1L_a absorption band to shorter wavelengths. These shifts are due to the liberation of the lone-pair of the 6-amino group, as a result of its dissociation. In the case of the ^1L_b band, the lone-pair of the β-amino group (the 6-amino group) furnishes the optical electron for the approximately longitu-

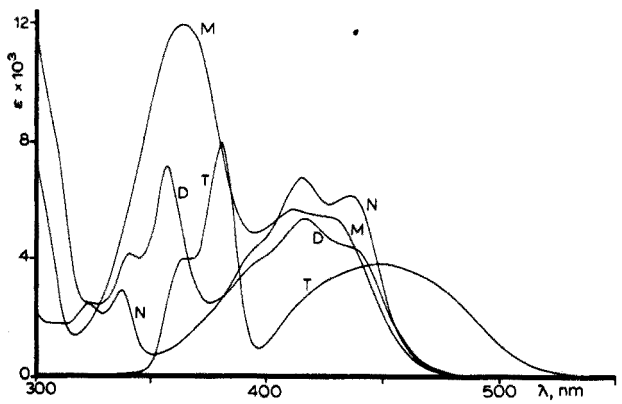

Fig. 1. Absorption spectra of rivanol; N = neutral, M = monocation, D = dication and T = trication.

dinally-polarized $^1L_b \leftarrow {}^1A$ transition. The lone-pair electrons of the 6-amino group are, in the ground electronic state, higher in energy than those of the β-ethoxy group, which contribute the optical electron for the $^1L_b \leftarrow {}^1A$ transition of D. As a result, the $^1L_b \leftarrow {}^1A$ transition of M lies at lower energy and the ^1L_b absorption band of M at longer wavelength than the corresponding transition and spectral band, respectively, of D. The effect of the β-amino group on the ^1L_a band is less direct than on the ^1L_b band. Although the $^1L_a \leftarrow {}^1A$ transition is polarized predominantly along the axis joining the heterocyclic nitrogen atom and the 9-amino group, the electron-withdrawing influence of the aromatic system attracts electronic charge from the 6-amino group into the aromatic ring. This phenomenon can be represented by a contribution of structure I to the ground state of the monocation. In essence then, the 6-amino

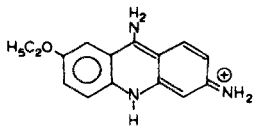

(I)

group increases the electron density at the exocyclic group in the 9-position, thereby inhibiting the transfer of electronic charge from the heterocyclic nitrogen atom to the amino group in the $^1L_a \leftarrow {}^1A$ transition. This raises the energy of the Franck—Condon ^1L_a state relative to the ground state and therefore decreases the wavelength of the ^1L_a band of M relative to that of D. The dissociation of M to form the neutral molecule (N), restores the aromaticity of the central ring of the acridine system resulting in a shift of the ^1L_a band to longer wavelengths as in 9-aminoacridine [3]. However, the loss of positive charge in the aromatic system caused by dissociation also diminishes the extent of transfer of charge from the 6-amino group to the aromatic ring, especially in the ^1L_b state, and as a result the ^1L_b band shifts to shorter wavelength on going from M to N.

The pK_a for the interconversion between the M and N species derived from rivanol was previously reported as 11.5 by Tolstoouhov [6] and 11.1 by Albert et al. [7]. The latter value was determined from measurements in aqueous 50 % ethanol corrected for the dielectric effect of the alcohol. The solvent in which the former value was obtained was unspecified. In the present studies, the value 11.5 was determined by spectrophotometric measurement of solutions initially containing $7 \cdot 10^{-5}$ M rivanol However, it was observed that at above pH 12 the neutral species precipitated. Upon repeating the absorptiometric titration with $5 \cdot 10^{-5}$ M rivanol, no precipitation was observed, but the value of pK_{a_3} was found to be 10.8. The precipitation of neutral rivanol would yield an apparent value of ϵ for the neutral species, which is smaller than the true value, at the analytical wavelength. The fraction of M calculated at any point in the inflection region of the titration will thus be greater, if precipitation of N occurs, than the true fraction of M. Hence, the apparent ratio of [N]/[M] will be smaller than the true ratio, and the apparent pK_a will be greater than the true pK_a. This argument supports the value of pK_{a_3} of 10.8 determined in these experiments.

The shift of the fluorescence of D to longer wavelength, on dissociation, is somewhat difficult to explain, because the ^1L_a (longest-wavelength) absorption band shifts in the opposite direction in the same process. It was first thought that, because the ^1L_b band of D also shifts to longer wavelength on dissociation, and substantially overlaps the ^1L_a band on its short wavelength side in M, the thermally equilibrated ^1L_b state of M might actually be stabilized enough by solvent relaxation to lie below the ^1L_a state of M. In this case fluorescence would likely occur from the ^1L_b state. However, the polarized fluorescence excitation spectrum (Fig. 2) of M in glycerol at room temperature, shows the highest degree of polarization in the spectral region corresponding to the ^1L_a band. This indicates that the absorption oscillator cor-

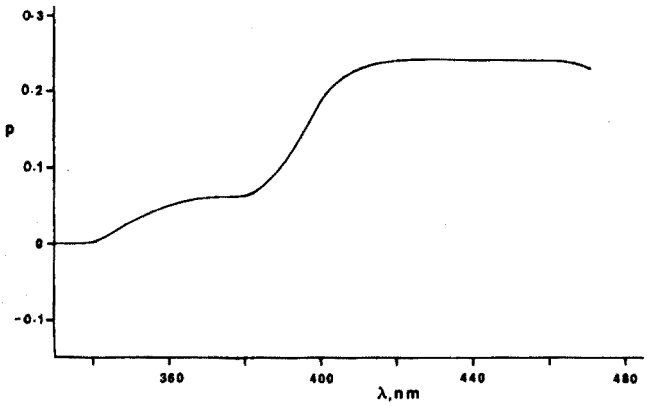

Fig. 2. Degree of polarization, p, in the fluorescence excitation spectrum of rivanol monocation, in glycerol, at 25 °C, as a function of excitation wavelength. Fluorescence emission was monitored at 495 nm.

responding to the ^1L_a absorption band, on average, makes a smaller angle with the emission oscillator giving rise to the fluorescence band, than does the ^1L_b absorption oscillatof. This may be taken as strong evidence that the fluorescence of M originates from the ^1L_a state. Moreover, in solvents of low dielectric strength, such as ethanol and chloroform, the fluorescence of D also shifts to longer wavelengths on dissociation, while the ^1L_a band of D shifts to shorter wavelengths on dissociation. Consequently, the anomalously long fluorescence wavelength of M cannot be explained on the basis of solvent relaxation phenomena or inversion of the ^1L_a and ^1L_b states.

In aqueous solutions, frozen in a liquid nitrogen bath, however, the fluorescence of M lies at shorter wavelength than that of D, paralleling the relative positions of the ^1L_a excitation bands of these species under the same conditions. The rigidification of the solvent prevents not only solvent relaxation, but also configurational relaxation, after excitation. In M, configurational relaxation in the excited state is most likely to involve the rehybridization of the planar 9-amino group to a tetrahedral configuration and of the tetrahedral

6-amino group to a configuration coplanar (or nearly so) with the acridine ring. These configurational changes would result from the gain by the 9-amino group and the loss by the 6-amino group, of electronic charge on excitation. Hence, in fluid solutions, the fluorescence arises from a thermally equilibrated excited state in which interaction of the 6-amino group with the aromatic system is great and whose structure is essentially that of a perturbed 3-aminoacridinium ion [8]. This conclusion is supported by the fact that the excited-state $pK_{a_2}^*$ corresponding to the dissociation of the 6-amino group (−0.6), determined by fluorimetric titrimetry, is more acidic than the corresponding ground-state pK_{a_2} (0.7). The shift of the fluorescence of D to longer wavelengths, on dissociation also indicates that the 6-amino group is electron-deficient in the thermally equilibrated excited state [9] while the shift of the ^1L_a band in the opposite direction, in the same process, indicates that the 6-amino group is more basic (electron-rich) in the Franck–Condon (ground-state configuration) excited state than in the ground state [9]. This shows that the anomalous fluorescence shift of D, on dissociation, is due to greater participation of the lone-pair of the 6-amino group in the aromatic system, in the thermally-equilibrated lowest excited singlet state. In rigid aqueous solutions, however, D and M are locked into the ground-state equilibrium solvent cage and atomic configurations, so that after excitation, configurational thermal relaxation does not occur. In this case, emission arises from atomic configurations identical to those of the absorbing ground-state species. Therefore, in the rigid media, the interaction of the 6-amino group with the aromatic system in the fluorescing state of the monocation, is weak. In this case, the fluorescing (thermally-equilibrated) state of M is essentially that of a weakly perturbed 9-aminoacridine, so that the shift of the fluorescence of D on dissociation, parallels that of ^1L_a absorption band.

The dissociation of M to form the neutral molecule is accompanied by a slight shift of the fluorescence spectrum to longer wavelength and parallels the corresponding shift of the ^1L_a band and of the fluorescence spectrum in rigid water at 77 K. This shift can therefore be attributed to the restoration of the aromatic (acridine) structure in the neutral molecule (N). The conversion of the fluorescence of M to that of N occurs with ground-state titration characteristics (i.e. centered at pH 10.8). This indicates that in M and N fluorescence occurs with rates much greater than those of dissociation of M and protonation of D in the lowest excited singlet state.

Above pH 11 the fluorescence of the neutral molecule is quenched with increasing pH, quenching being virtually complete at pH 14. However, in this pH region and for solutions up to 14.2 M NaOH (H_- 17.5), the absorption of N does not vary with pH. Quenching or shifting of the fluorescence spectrum in concentrated alkaline solutions is often observed in arylamines including 9-aminoacridine [3] and 3-aminoacridine [8] and is attributed to proton abstraction, in the lowest excited singlet state, by hydroxide. Presumably, this phenomenon, depicted for rivanol in Scheme 2, is also responsible for the pH-dependent quenching observed here. The failure of proton abstrac-

Scheme 2

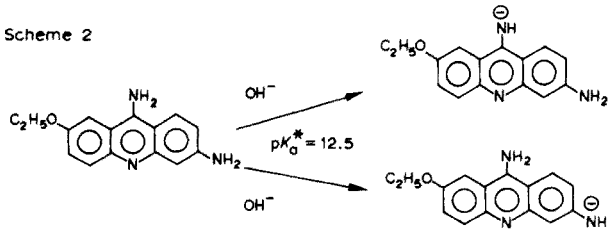

tion to be observed in the ground state (absorption spectrum), in concentrated alkaline solutions, indicates that the amino group from which proton abstraction occurs is more acidic in the excited state than in the ground state. This is certainly the case for most arylamines. However, in 9-aminoacridine [3] and 2-methoxy-6-chloro-9-aminoacridine [10], the 9-amino group is acidic enough to demonstrate visibly ground-state dissociation at pH higher than the corresponding excited-state process. The failure of rivanol to dissociate, in the ground state, in concentrated alkaline solutions, is probably due to the reduction of the acidity of the 9-amino group as a result of the electromeric interaction with the 6-amino group. 3-Aminoacridine itself is not sufficiently acidic to dissociate in the ground state, so it is not reasonable to expect the 6-amino group of rivanol to dissociate. However, in the lowest excited singlet state, both 9-aminoacridine and 3-aminoacridine demonstrate excited-state proton abstraction by hydroxide in the pH region 10—14. Consequently, it is at present uncertain whether the quenching of rivanol fluorescence in strongly alkaline solutions is due to proton abstraction from the 6-amino group or the 9-amino group (Scheme 2).

The fluorescence emissions of the rivanol M (λ_{ex} = 362 nm, λ_{em} = 502 nm) and D (λ_{ex} = 420 nm, λ_{em} = 482 nm) species are quite intense. In aqueous solutions of pH 3—9, where M is the predominant absorbing species, the fluorimetric detection limit, taken as the concentration of rivanol solution having a fluorescence intensity greater than twice the intensity of the solvent blank, is $5 \cdot 10^{-9}$ M (or 2 ng ml^{-1}). In ethanolic solution (λ_{ex} = 375 nm, λ_{em} = 482 nm), the limit of detection for M is the same as that for the aqueous solution. In 20—30 % sulfuric acid, where D predominates, the fluorimetric limit of detection for D is $5 \cdot 10^{-11}$ M (or 20 pg ml^{-1}).

SUMMARY

The electronic absorption and fluorescence spectra of the antibacterial 2-ethoxy-6,9-diaminoacridine lactate (rivanol) were studied as a function of pH and Hammett acidity. The dissociation of the doubly charged cation results in an unusual shifting pattern in the absorption and fluorescence bands. This is shown, by polarized excitation spectroscopy and low-temperature conventional emission spectroscopy, to be due to configurational reorganization in the excited state involving the amino groups. The doubly charged cation can be detected by its native fluorescence in concentrations as low as 20 pg ml^{-1}.

REFERENCES

1 C.O. Wilson and O. Gisvold, Textbook of Organic, Medicinal and Pharmaceutical Chemistry, Lippincott, Philadelphia, 4th edn., 1962, p.179.
2 M.J. Jorgensen and D.R. Hartter, J. Amer. Chem. Soc., 85 (1963) 878.
3 A.C. Capomacchia, J. Casper and S.G. Schulman, J. Pharm. Sci., 63 (1974) 1272.
4 G. Weber in D.M. Hercules (Ed.), Fluorescence and Phosphorescence Analysis, Wiley-Interscience, New York, 1966, Ch. 8.
5 T. Azumi and S.P. McGlynn, J. Chem. Phys., 37 (1962) 2413.
6 A.V. Tolstoouhov, Ionic Interpretation of Drug Action in Therapeutic Research, Chemical Publishing Co., New York, 1955, p.124.
7 A. Albert, S.D. Rubbo, R.J. Goldacre, M.E. Davey and J.D. Stone, Brit. J. Exp. Pathol., 26 (1945) 160.
8 S.G. Schulman, D.V. Naik, A.C. Capomacchia and T. Roy, J. Pharm. Sci., 64 (1975) 982.
9 P.J. Kovi and S.G. Schulman, Anal. Chim. Acta, 63 (1973) 39.
10 A.C. Capomacchia and S.G. Schulman, Anal. Chim. Acta, 79 (1975) 79.

Analytica Chimica Acta, 80 (1975) 75—83

SPECTROGRAPHIC DETERMINATION OF MERCURY IN ROCKS AND COAL

E. S. PECK

Lawrence Livermore Laboratory, University of California, Livermore, California 94550 (U.S.A.)

(Received 14th May 1975)

SUMMARY

An optical emission spectrographic method for the determination of 5—1000 p.p.b. mercury in rocks and coal is described. The method is applied to USGS rock and NBS coal standards, and the results are compared to other analytical procedures. Little or no sample preparation makes the procedure simple and rapid. The standard deviation is about 30%.

The abundance and distribution of mercury in the environment has been studied extensively in recent years. Although the mercury content of rocks and coal has long been studied for geological information, much of the current interest relates to pollution and the necessity for understanding the sources, contamination routes, and repositories of mercury. Recent reviews [1—5] cover both the geological and pollution aspects of mercury in the environment.

Most methods for determining mercury in rocks employ neutron activation [6—14], flameless atomic absorption [15—24], or atomic fluorescence [25, 26] analysis. For coal samples the procedures used are neutron activation [27—30], flameless atomic absorption [21, 30—32], and spark-source mass spectroscopy [33]. Neutron activation analysis requires highly specialized equipment, and the irradiation and decay processes take 1 d to 2 wk. After rock samples have been irradiated, lengthy chemical separations are necessary, although coal samples may be analyzed without chemical treatment. Two general types of atomic absorption procedures are used. One involves acid dissolution of the sample, reduction and/or oxidation reactions, and aeration of mercury vapor from solution. The other involves heating the sample to vaporize the mercury, which is then amalgamated with gold or silver and subsequently vaporized by heating. Various combinations of these steps have been described. In this laboratory an atomic absorption method similar to that given by Vaughn [15] has been used to determine mercury distribution in core samples. To supplement this method and to provide a semi-quantitative method for sorting or selecting samples for

further analysis, a simple, rapid, and direct spectrographic method was sought for determining mercury in rock and coal at concentrations below 1 p.p.m.

Emission spectrographic methods for mercury determination in geological samples have generally followed one of two approaches. In one, samples are excited in the discharge without chemical or physical pre-separation of the mercury. Such procedures have only moderate sensitivity with detection limits of 10—100 p.p.m. mercury. Examples are the determination of mercury in sphalerite [34, 35], ZnS ore [36], and coal ash [37]. In the second approach, which is generally more sensitive, mercury is separated from its matrix usually by a preferential vaporization process. Preuss [38], for example, vaporized 1—3-g samples of rocks and minerals in a 2270 K carbon tube furnace and directed the vapors into a carbon arc. For some samples the sensitivity approached 30—100 p.p.b. with an accuracy of ±30%. A double arc method with a sensitivity of 1 p.p.m. mercury on 0.1-g soil samples was developed by Shilling [39]. Sergeev [40] determined mercury in rocks semiquantitatively down to 300 p.p.b., using a steel—carbon "boiler" type electrode with a capacity of 0.4 ml; using an electrode of 6-ml capacity provided with a furnace for heating, he obtained a sensitivity of 10—20 p.p.b. His method is the basis for extensive studies of the geochemistry of mercury reported in the Russian literature. In a revision of Sergeev's method, Feges and Podobnik [41] used 5-g samples in graphite electrodes, obtained a standard deviation of 12% at 1 p.p.m. mercury and calculated a detection limit of 40 p.p.b. Veres and Perfil'ev [42] developed a method similar to that of Preuss [38] in which 10-g samples were heated to 1070 K to supply mercury vapor to the discharge; sensitivities of 0.1—1 p.p.b. were claimed.

In the double-arc method of Dall'Aglio et al. [43], 0.1—0.2-g sample charges were excited in an argon atmosphere, and a sensitivity of 10 p.p.b. was achieved for alluvium and soil samples. The method was extended to rock analysis [44] in which sample charges of 0.4 g gave a repeatability of 11% at 10 p.p.b. mercury.

This paper describes a simple, rapid, direct determination of 5—1000 p.p.b. mercury in rock and coal samples. The method is suitable for sorting samples for possible further analysis, and can be used as the primary method when high precision is not required.

EXPERIMENTAL

Standard preparation

The base material for the rock standards was well-ground, well-blended granite, which was heated in a muffle furnace to remove any mercury. Aliquots of solutions containing 0.1 and 1.0 mg Hg l^{-1} were added to 1-g portions of the granite in an agate mortar and then ground. Additional water was added with the smallest aliquots to ensure good mixing during grinding.

The ground slurries were dried under an infrared lamp and further mixed in a plastic vial on a dental amalgamator. Granite standards containing 0, 10, 25, 60, 150, 400, and 1000 p.p.b. mercury were prepared.

For coal standards, the base material was spectrographic graphite powder (< 200 mesh), which was heated to remove any mercury. Mercury(II) oxide (325—400 mesh) was mixed with graphite to give 10% mercury in graphite. A series of standards was prepared by step-wise dilution of this stock mixture with graphite. The lowest standards were equivalent in mercury content to the rock standards.

Sample preparation

Rock samples were ground to a fine powder with an agate mortar and pestle. Coal samples in the form of coarse or fine powders were analyzed as received. Coal samples of low ash content were diluted with graphite.

Equipment and spectrographic procedures

Table 1 summarizes the equipment and the operating conditions. A cut-away view of the electrode system used with rock samples is shown in Fig. 1. The electrodes and the boiler caps were heated in a muffle furnace at 650 K for at least 45 min, cooled in a desiccator, and charged with sample material. Relatively large sample sizes for both rocks and coal ensured that the samples were fairly representative of the material of interest.

TABLE 1

Equipment and spectrographic parameters

Spectrograph	Jarrell—Ash, 0.75-m, Czerny—Turner (f 6.3)
Grating	590 grooves mm^{-1}, 500 nm blaze, 440—560 nm region
Slit	0.010 mm × 4 mm
Slit filter	40%, transmitting
Illumination	A double convex lens focuses a magnified image of the electrodes on the slit
Photographic plates	Kodak, SA-1, 127 mm × 178 mm
Excitation	Jarrel—Ash, varisource, d.c. arc mode, 7.5 A
Electrodes	Anode: Ultra Carbon Products No. 120 for rock. A.S.T.M. Type S-3 for coal. Ultra Carbon Products No. 300 cap for rock and coal Cathode: Ultra Carbon Products No. 5001
Sample charge	Rock: 60 mg Coal: 55—85 mg Graphite: 85 mg
Analytical gap	5mm
Atmosphere	Argon, 0.1 $m^3 h^{-1}$
Exposure	Rock: 20 s Coal and graphite: 40 s, following 5 s preburn
Developing	Kodak D-19 for 3 min at 290 K
Microphotometer	Jarrell—Ash, recording, Model 23-500

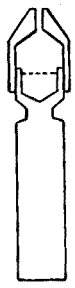

Fig. 1. Cut-away view of electrode system for rock samples showing position of cap and sample fill line.

The exposure times were set to allow complete vaporization of the mercury; filtering was necessary to prevent plate over-exposure. The discharge took place in a flowing argon atmosphere in a chamber that has been described previously [45]. The grating of the relatively fast spectrograph was set to take advantage of the second-order mercury line (253.652 nm), which falls near the grating blaze. Standard photometric procedures were used. The spectrum was scanned from 253.3 to 254.0 nm to obtain transmission values for both the mercury line and the background. A plate calibration curve was used to convert the transmission values to intensity values. The background intensity value was subtracted from the line plus background intensity to yield the true line intensity. The true mercury line intensity versus concentration in p.p.b. was plotted on a log—log scale as shown for rocks in Fig. 2.

Comments on procedures

The slurry preparation method yielded much more uniform mixtures of mercury in rock than did a direct powder mixing method; the latter did not result in reliable standards of 30 p.p.m. and less, probably because of unsatisfactory HgO particle size and resultant poor mixing. Even in the slurry method, non-uniform particle distribution is probably an important source of poor repeatability. The slurry method was not useful with the graphite standards; very fine graphite and HgO powders were needed to obtain satisfactory standard mixtures. In similar studies Feges and Podobnik [41] found the slurry method best while Dall'Aglio et al. [43, 44] preferred the powder mixing method.

In all methods for trace determination in the fractional p.p.m. range, contamination is a persistent problem. In this work, mercury contamination was found in crater electrodes, boiler caps, and graphite powder; all these contaminated samples came from supplies which had been opened at some time in the past and kept in their original boxes and jars in laboratory drawers. Mercury was not detected in freshly opened batches of electrodes or powder. To study mercury pick-up in the laboratory, a quantity of

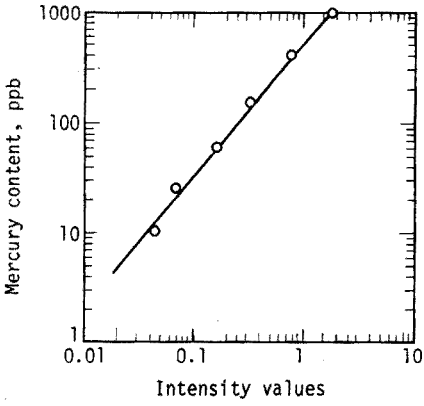

Fig. 2. Analytical curve for mercury in rocks.

graphite powder was placed in a watch glass on a bench top. Although no mercury was detected in this material after 20 h, an estimated 40 p.p.b. was found after 15 d. Thus no extraordinary procedures are required to prevent mercury contamination over a short term.

There was no memory effect or carry-over associated with the atmosphere chamber at the mercury levels usually encountered in this study. Any detectable mercury contamination in the electrodes, graphite, or blank rock could be removed by heating the material in a muffle furnace at 650 K for at least 45 min.

The crater electrodes could be reused for up to three different exposures. They were, of course, heated to 650 K each time, and only those electrodes which were used for materials containing less than 1000 p.p.b. mercury were reused. There was no obvious difference in repeatability between fresh and reused electrodes.

In moving plate studies, mercury was found to be volatilized from rocks in the 5—20-s time interval and from graphite in the 10—40-s time interval. In rocks the matrix was usually not disturbed, but in some sample exposures much matrix material was evolved and excited; in such cases it was impossible to determine mercury. This condition was usually obvious during arcing of the sample and occurred in about 10% of attempted determinations; the U.S. Geological Survey standard rocks AGV-1, BCR-1, and PCC-1 accounted for two-thirds of these failures and some core drillings for the other third.

A somewhat similar situation occurred with coal samples, especially those having high volatility and low ash content. Coal soot occasionally extruded from the cap and shorted out the discharge. This difficulty was overcome by using a smaller sample charge or diluting the coal with graphite. Several trial runs were necessary with unknown coals to establish a satisfactory sample charge. For coal samples, the boiler cap must fit snugly on the crater portion, otherwise the expanding gases may force off the cap during excitation. For coal samples, the opening at the top of the excitation chamber was enlarged to allow smoke to escape.

RESULTS AND DISCUSSION

Rocks

The applicability of this method was tested by determining the mercury content of eight USGS standard rocks. At the time this work was undertaken there were no certified values for mercury in these rock standards. Therefore a statistical procedure [49] was developed in which values from the literature were weighted according to their precision, and a weighted mean was determined for each standard. As additional values were reported, they were included in this procedure. Table 2 shows the spectrographic results, the weighted means, and recent USGS values [46] for the standard rocks. The analyses of the USGS standards were carried out over a period of 5 months except for the G-1 standard, which was analyzed five times in a 1-wk period. All synthetic standards and USGS rocks were analyzed at least ten times with only a few duplicate analyses made on any one day. All data obtained were used, except for exposures in which the matrix was volatilized and excited, usually obscuring the mercury line. Thus the precision data represents actual analytical practice.

The limit of detection, defined [47] as the concentration at which the standard deviation is 100%, was calculated to be 6 p.p.b.

Core samples

One of the purposes for developing this method was to sort and screen field samples, perhaps before analysis by atomic absorption. Atomic absorption analysis of core samples [48] had shown gross heterogeneity even in samples taken from the same core sections. Spectrographic determination of mercury in these samples was made, to compare the results of the two

TABLE 2

Comparison of mercury content values for USGS standard rocks

Standard	USGS	Weighted literature	This work		
	value [46] (p.p.m. Hg)	value (p.p.m. Hg)	Mean (p.p.m. Hg)	No. of detns.	s_r
G-1	0.097	0.0873	0.086	5	38
G-2	0.039	0.045	0.042	10	19
W-1	0.225	0.153	0.205	11	30
AGV-1	0.015	0.0135	0.027	10	28
BCR-1	0.0107	0.0114	0.025	10	34
DTS-1	0.0087	0.00717	0.0077	12	28
GSP-1	0.0155	0.0151	0.015	10	37
PCC-1	0.0072	0.0052	0.0097	10	35

methods. Each sample taken represented about four cubic inches of rock from the interior of the core sample. This piece of rock was broken, and separate small chunks were selected for analysis. Some chunks were analyzed by emission spectrography and others by atomic absorption. The results of these analyses are shown in Table 3. Spectrographic results include the average value, and the bounds of the range of values; 3—4 determinations were made for each chunk. The atomic absorption results, with an estimated accuracy of 20%, are shown for the separate chunks; these results show that the heterogeneity varies up to a factor of six for the 2561.6-m sample, and varies a factor of 14 over the depth interval studied. The spectrographic results show a maximum variation factor of only 1.7 at any one depth and an overall variation factor of 18. The differences between the spectrographic and the atomic absorption determinations are due in part to the sample heterogeneity. A similar variation of mercury throughout a coal sample has been reported [28].

Coal

Table 4 shows the results of the spectrographic determination of mercury in the National Bureau of Standards SRM 1630 (Trace Mercury in Coal). Also shown are the NBS certified value and other reported determinations. For the spectrographic results, both undiluted sample charges of 55 mg of the coal and diluted sample charges of 85 mg of half coal and half graphite

TABLE 3

Determination of mercury in core samples

Sample depth (m)	Sample type	Spectrographic Mean and range (p.p.b. Hg)[a]	A.a.s. [48] (p.p.b. Hg)
2561.6	Sandstone	102 ± 18	19, 97, 16
2561.6	Sandstone	151 ± 17	
2570.4	Sandstone/Siltstone	196 ± 36	46
2570.4	Sandstone/Siltstone	129 ± 16	
2572.2	Shale	30 ± 4	86
2572.8	Sandstone	19 ± 11	9.2, 4
2572.8	Sandstone	11 ± 8	
2573.3	Shale	107 ± 38	100, 32, 130
2573.3	Shale	102 ± 38	
2573.3	Shale	102 ± 10	
2574.2	Shale	135 ± 17	77
2575.7—6.0	Siltstone	87 ± 23	30, 30, 20
2575.7—6.0	Siltstone	68 ± 9	

[a]3 or 4 determinations of each sample.

TABLE 4

Comparison of mercury content values for NBS standard reference material 1630 (trace mercury in coal)

Method and reference	Mercury value (p.p.m.)	No. of detns.	s_r
This work, undiluted sample	0.12	10	26
This work, diluted sample	0.15	10	26
Neutron activation[a]	0.127	55	5
Neutron activation [29]	0.127	4	4
Atomic absorption [32]	0.139	7	5

[a]NBS Certificate of Analysis, November 1971.

were used. The blank graphite standard gave a weak signal at the mercury analytical line position, and the average intensity of that signal was subtracted from all standard and sample intensities. Two of the graphite standards were analyzed in quadruplicate by an atomic absorption method similar to Vaughn's [15], and the values of all standards were corrected proportionately to those results; the analytical curve was established by using a least-squares fit of the data from 10—1700 p.p.b. standards.

This work was performed under the auspices of the U.S. Energy Research & Development Administration. Portions of this work were presented at the National Meeting of the Society for Applied Spectroscopy, Dallas, Texas, September 1972.

REFERENCES

1 W. T. Pecora, Geological Survey Professional Paper 713, U.S. Government Printing Office, Washington D.C., 1970.
2 R. Hartung and B. D. Dinman, Environmental Mercury Contamination, Ann Arbor Science Publishers, Ann Arbor, Michigan, U.S.A., 1970.
3 H. T. Shacklette, J. G. Boerngen and R. L. Turner, Geological Survey Circular 644, U.S. Government Printing Office, Washington D.C., 1971.
4 I. R. Jonasson, Geol. Surv. Can. Pap., 70—57 (1970).
5 I. R. Jonasson and R. W. Boyle, Can. Inst. Mining Met. Bull., 65 (1972) 32.
6 D. F. C. Morris and R. A. Killich, Talanta, 11 (1964) 781.
7 A. Alian and R. Shabana, Microchem. J., 12 (1967) 427.
8 W. D. Ehmann and J. F. Lovering, Geochim. Cosmochim. Acta, 31 (1967) 357.
9 O. Landstrom, K. Samsahl and C. G. Wenner, in J. R. DeVoe and P. D. LaFleur (Eds.), Modern Trends in Activation Analysis, Vol. I, National Bureau of Standards Special Publication No. 312, U.S. Government Printing Office, Washington D.C., 1969, pp. 353—366.
10 G. H. Morrison, J. T. Gerard, A. Travesi, R. L. Currie, S. F. Peterson and N. M. Potter, Anal. Chem., 41 (1969) 1633.
11 J. C. Laul, D. R. Case, M. Wechter, F. Schmidt-Bleek and M. E. Lipschuz, J. Radioanal. Chem., 4 (1970) 241.

12 G. Marowsky, Z. Anal. Chem., 253 (1971) 267.
13 G. Marowsky and K. H. Wedepohl, Geochim. Cosmochim. Acta, 35 (1971) 1255.
14 P. J. Aruscavage, Geological Survey Professional Paper 800-C, U.S. Government Printing Office, Washington D.C., 1972, pp. 209—214.
15 W. W. Vaughn, Geological Survey Circular 540, U.S. Government Printing Office, Washington D.C., 1967.
16 W. R. Hatch and W. L. Ott, Anal. Chem., 40 (1968) 2085.
17 S. H. Omang and P. E. Paus, Anal. Chim. Acta, 59 (1971) 393.
18 B. G. Weissberg, Econ. Geol., 66 (1971) 1042.
19 S. R. Aston and J. P. Riley, Anal. Chim. Acta, 56 (1972) 349.
20 R. E. Cranston and D. E. Buckley, Environ. Sci. Technol., 6 (1972) 274.
21 C. Huffman, Jr., R. L. Rahill, V. E. Shaw and D. R. Norton, Geological Survey Professional Paper 800-C, U.S. Government Printing Office, Washington D.C., 1972, pp. 203—207.
22 J. Marinenko, I. May and J. I. Dinnin, Geological Survey Professional Paper 800-B, U.S. Government Printing Office, Washington D.C., 1972, pp. 151—155.
23 J. M. McNeal, N. H. Suhr and A. W. Rose, Chem. Geol., 10 (1972) 307.
24 A. M. Ure and C. A. Shand, Anal. Chim. Acta, 72 (1974) 63; A. M. Ure, Anal. Chim. Acta, 76 (1975) 1.
25 V. I. Muscat and T. J. Vickers, Anal. Chim. Acta, 57 (1971) 23.
26 V. I. Muscat, T. J. Vickers and A. Anders, Anal. Chem., 44 (1972) 218.
27 J. N. Weaver, Anal. Chem., 45 (1973) 1950.
28 J. V. O'Gorman, N. H. Suhr and P. L. Walker, Jr., Appl. Spectrosc., 26 (1972) 44.
29 E. Orvini, T. E. Gills and P. D. LaFleur, Anal. Chem., 46 (1974) 1294.
30 M. D. Schlesinger and H. Schultz, U.S. Bur. Mines Rep. Invest., 7609 (1972).
31 B. W. Bailey and F. C. Lo, J. Ass. Offic. Anal. Chem., 54 (1971) 1447.
32 T. C. Rains and O. Menis, J. Ass. Offic. Anal. Chem., 55 (1972) 1339.
33 J. A. Carter, Eastern Analytical Symposium, Paper No. 25A, New York, N.Y., November 1973.
34 I. Oftedal, Skrifter Norske Videnskaps-Akad. Oslo, I. Mat.-Naturv. Klasse, 1940 (1941) 103 pp.; see L. H. Ahrens and S. R. Taylor, Spectrochemical Analysis, Addison—Wesley Publishing Co., Reading, Mass., U.S.A., 2nd edn., 1961, p. 269.
35 F. Hegemann and H. Kostyra, Metall, 9 (1955) 849.
36 L. W. Strock, Amer. Inst. Mining Met. Engrs., Tech. Pub. No. 1866 (1945).
37 A. J. W. Headless and R. C. Hunter, Ind. Eng. Chem., 45 (1953) 548.
38 E. Preuss, Z. Angew. Mineral., 3 (1940) 8.
39 M. L. Shilling, Zavod. Lab., 22 (1956) 447.
40 E. A. Sergeev, Int. Geol. Rev., 3 (1961) 93 (English translation).
41 J. Feges and B. Podobnik, Věstn. Slov. Kem. Drus., 16 (1969) 5.
42 G. I. Veres and A. P. Perfil'ev, Zavod. Lab., 36 (1970) 248.
43 M. Dall'Aglio, D. Visibelli and F. Tonani, XV Colloquium Spectroscopium Internationale, Madrid, 1969; published as Comitato Nazionale Energia Nucleare Report RT/GEO(70)8, 1970.
44 M. Dall'Aglio and D. Visibelli, XVI Colloquium Spectroscopium Internationale, Heidelberg, October 1971, Preprint No. 70, pp. 45a—53a.
45 W. F. Morris and E. F. Worden, Appl. Spectrosc., 25 (1971) 305.
46 F. J. Flanagan, Geochim. Cosmochim. Acta, 37 (1973) 1189.
47 Methods for Emission Spectrochemical Analysis, American Society for Testing and Materials, E-2 SM 2—4, Philadelphia, Pa., 6th edn., 1971, p. 392.
48 J. H. Hill, Informal Report UCID-15943, Lawrence Livermore Laboratory, University of California, Livermore, Calif., December 1971.
49 E. S. Peck, Report UCRL-51819, Lawrence Livermore Laboratory, University of California, Livermore, California, May 1975.

Analytica Chimica Acta, 80(1975)85—95

THE ANALYSIS OF SURFACE WATERS FOR IRON, ZINC AND LEAD BY COPRECIPITATION ON IRON HYDROXIDE AND X-RAY FLUORESCENCE

E. BRUNINX and E. VAN MEYL

Philips Research Laboratories, Eindhoven (The Netherlands)

(Received 3rd April 1975)

Much has been published on the analysis of trace elements (concentration: 1—1000 $\mu g\ l^{-1}$) in surface water systems [1]. Such analyses are important not only for public health but also for studies of the chemical behaviour of all kinds of natural aquatic systems. In many cases, elements have been determined singly, e.g. by atomic absorption, but there are indications that not only the number of trace elements to be measured will increase but also the number of samples to be analysed, thus favoring multi-element methods which should be rapid, sensitive and reliable, with a preference perhaps for simultaneous methods.

Two workhorses of multi-element analysis are thus eliminated: neither neutron activation nor spark-source mass spectrometry are rapid, and their application is restricted to larger laboratories. The same argument excludes the routine use of emission spectrometry with a high-frequency plasma torch as excitation source. Polarography is also eliminated because: (a) it cannot deal with more than 4 or 5 elements, and (b) the presence of other chemicals in solution can give rise to interferences. This means that a direct multi-element analysis at this concentration level is impractical and therefore a preconcentration step is necessary: x-ray fluorescence (x.r.f.) then becomes a very attractive multi-element analysis method.

Of the preconcentration techniques, evaporation must be rejected because it is much too slow [2]. Chelating ion-exchange resins [3, 4], either on columns or in batch operation, require equilibration times of at least 15—20 min and around 100 mg of resin. Ion-exchange papers (or discs) [5, 6] are better as they yield the adsorbed elements in a thin disc ready for measurement e.g. by x.r.f. Repeated circulation of the sample through the ion exchanger is necessary to achieve complete adsorption.

Solvent extraction is very attractive and rapid as it requires the addition of only small amounts of chemicals, and the extracted elements in the organic phase are amenable to direct measurement [7]. Similar considerations are valid for organic coprecipitation [8].

Inorganic coprecipitation, e.g. with iron hydroxide, has been used extensively in sea water analysis [9]. The amount of iron(III) added can be kept down

to 1—10 mg l^{-1}; except for solvent extraction, all other preconcentration techniques require the addition of larger quantities of chemicals.

The iron coprecipitation technique has been chosen for use here because the method can easily be modified so that the trace elements are directly measured in the precipitate by means of x.r.f.; at the same time, iron forms a well-defined matrix and serves as an internal standard. Moreover, the hydroxide precipitate is very surface-active, so that non-ionic forms of trace elements can be collected. This is important since trace elements in surface waters are not always in well-defined ionic states (adsorbed, complexed, anions, cations etc.) [10]. Further advantages are that elements occurring in large concentrations such as Ca, Mg etc. are eliminated, which reduces the sample thickness irradiated by the x-ray beam; and that the number of chemical additions and manipulations is kept to a minimum.

The next section describes the method of analysis; the final section is devoted to the analysis of surface waters for Fe, Zn and Pb by this method, and comparative analyses are used to test the accuracy.

METHOD OF ANALYSIS

Coprecipitation

Preconcentration by means of iron hydroxide has both a physicochemical aspect and an analytical aspect. Physicochemical data will be reported elsewhere [11]; only those points essential for a reliable preconcentration step are considered here.

All experiments to determine the optimal precipitation conditions were done with solutions of potassium nitrate (10^{-2} M) acidified with hydrochloric acid to a pH of 1.5—2 and containing 10 mg l^{-1} of Fe^{3+}. The radioactive nuclides ^{65}Zn and ^{212}Pb were employed for measuring distribution ratios of Zn or Pb between the iron hydroxide and the solution. The precipitates were collected by suction on a membrane filter clamped between a glass chimney and a fritted glass plate. The instrument is similar to that described by Luke [8].

The distribution ratio is defined as $D = [Me]_{Fe}/[Me]_{sol}$, where $[Me]_{Fe}$ is the amount of Zn or Pb in the iron hydroxide precipitate and $[Me]_{sol}$ the amount of Zn or Pb in the entire volume of solution after the hydroxide has been filtered off. Two parameters are essential in this preconcentration step: the pH, and the amount of Zn or Pb to be concentrated. Raising the pH increases the distribution ratio D for both elements up to a maximum at pH 8.5 (see Fig.1). This pH was adopted in all further analyses and experiments.

Increasing the amount of Zn or Pb in the solution and keeping the volume and iron concentration constant results in a steady decrease in the value of D (see Fig.2). This is hardly a drawback as the fraction coprecipitated, $f = D/(1+D)$, remains close to unity up to 20 mg l^{-1} for lead and 2 mg l^{-1} for zinc and the method is used as a preconcentration step for traces, not for large amounts.

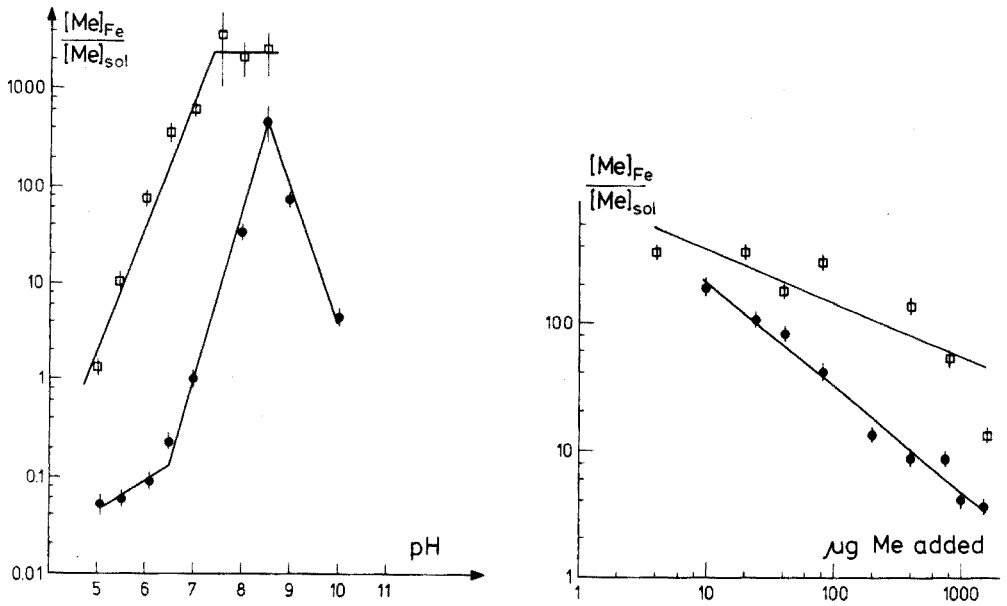

Fig.1. Distribution ratio for varying pH and fixed amount of metal. Volume 40 ml; Fe = 400 µg. (□) Pb, 4 µg. (•) Zn, 4 µg. Error bars indicate 1s counting statistics.

Fig.2. Distribution ratio with varying amounts of metal. Volume 40 ml; Fe = 400 µg. (□) Pb. (•) Zn. Error bars indicate 1s counting statistics.

At low lead concentrations the measured values of D have a fairly large uncertainty because of the poor counting statistics of the solution phase.

Other parameters such as the volume and the amount of iron added are kept constant so that, $C(\mathrm{Fe}) \geqslant 10\ \mathrm{mg\ l^{-1}}$. These two parameters can, under certain circumstances, influence the distribution ratio [11].

In an actual analysis of water samples the precipitate is dried at 80 °C for about 20 min. The size of the iron hydroxide particles after drying varies with the amount of iron and other coprecipitated elements, but usually lies between 10 and 50 µm. The precipitate adheres quite firmly to the membrane filter but not so well to filter papers.

x-Ray measurements

Any real sample, e.g. river water, may contain a certain quantity of iron. This means that the amount of precipitated iron on the membrane filter will be the sum of the added known amount and the amount of unknown iron in the sample. The x-ray analysis is done in two steps (all intensities are nett intensities).

(i) The iron analysis requires two measurements: the intensity of the Fe Kα

line, I(Fe), in the precipitate and the intensity of the Fe Kβ line, I_∞(Fe), in a thick iron sample. The thick iron is employed simply as a reference in order to correct possible fluctuations of the x-ray equipment, and the Kβ line is used in order to avoid excessively high count rates and dead-time corrections. The ratio I(Fe)/I_∞(Fe) is then converted to the total mass of iron by means of a calibration line as shown in Fig.3. This line was constructed by means of a series of precipitated iron hydroxide samples, the amount of iron varying between 0.2 and 2 mg. This is equivalent to 0.08—0.8 mg $Fe(OH)_3$ cm^{-2}; the thickness of the membrane filter is about 4.7 mg cm^{-2}.

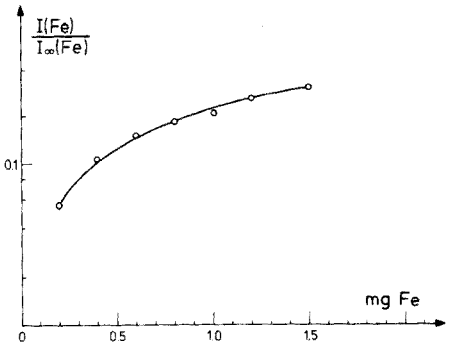

Fig.3. Iron intensity ratio for varying quantities of iron.

The amount of iron present originally in the sample is calculated as follows. The measured intensity ratio, I(Fe)/I_∞(Fe), is converted by means of the calibration line, as in Fig.3, to mg Fe(m_t). As the quantity of iron added, m_0, is known, it follows that the unknown amount of iron, m_x, present in the water sample is simply

$$m_x = m_t - m_0 \qquad (1)$$

(ii) The amount of Zn or Pb in the precipitate is deduced from the intensity I(Me) of the Zn Kα line or Pb-Lβ line and the already measured intensity I(Fe) of the iron. As precipitates of varying thickness are involved (varying amounts of iron), the calibration line is constructed as follows. A set of precipitated samples is prepared; each contains, e.g. 0.5—1.0—2.0 mg of iron, and varying amounts of Zn or Pb e.g. 1—50 μg. The intensity ratio I(Me)/I(Fe) was found to be a simple function of the mass ratio R:

$$R = \frac{m(\mathrm{Me})}{m(\mathrm{Fe}) + m(\mathrm{Me})}$$

where m(Fe) and m(Me) are the quantity of iron and zinc or lead in the precipitate respectively (see Fig.4).

The amount of Zn or Pb is thus found by converting the measured ratio I(Me)/I(Fe) to R by means of the calibration line. As m(Fe) is known, m(Me) is easily calculated.

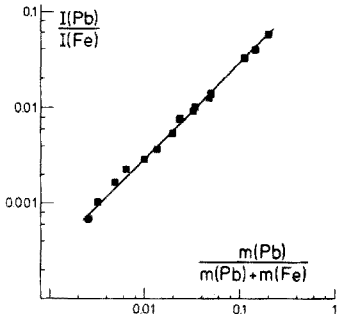

Fig.4. Calibration line for the determination of lead in iron hydroxide samples of varying mass (thickness). Zinc gives a similar curve.

The role of the Fe Kα intensity is therefore to take care of the variations in sample thickness and to correct for instrument fluctuations since it is related to the intensity of the thick iron standard. Thus the two calibration curves are valid over comparatively long periods of time.

Data treatment

Since most samples yielded only one analytical result, its standard deviation was computed from the spread of the data points on the calibration line. This method was adopted as it would require considerably more effort to extract — with statistical techniques — the same information from a repeated analysis of the same sample because of the difficulty of taking a representative, homogeneous sample from a medium as complex as river water.

The iron calibration line (Fig.3) and the trace metal calibration curve (Fig.4) can be represented by one of the following equations

$$y = ax; y = ax + b; y = ax + b + cx^2$$

The coefficients of these equations are calculated by means of least squares: the decision to choose one particular type was made by using the F test at the 95 % level as a criterion [12].

For iron the quadratic model best represents the calibration curve and the conversion of an observed y to x can be done by means of the coefficients a, b and c. Such a calculated value x_c (i.e. the total amount of iron) has an upper and a lower confidence limit: x_U and x_L (e.g. at 95 % level) [13]. These two values must satisfy the following inequality when substituted into the x position:

$$(b + ax + cx^2 - y_{obs})^2 < F^1_{n-3}(0.05).s^2.v$$

where a, b, c = coefficients of the iron calibration line
y_{obs} = observed value corresponding to x_c

$$s^2 = \sum_{i=0}^{i=n} \frac{(b + ax_i + cx_i^2 - y_i)^2}{n-3}$$

x_i, y_i are the data points (n) on the calibration line.
F^1_{n-3} = value of F-distribution at 95 % level for 1 and $n-3$ degrees of freedom

$$v = 1 + \frac{1}{n} + \frac{(x-\bar{x})^2}{m_2} + \frac{[(x-\bar{x})^2 - (x-\bar{x})m_3/m_2 - m_2/n]}{[m_4 - m_3^2/m_2 - m_2^2/n]}$$

$$m_j = \sum_i (x_i - \bar{x})^j$$

This formula in which x takes again the two values x_U and x_L looks complicated, but in the least squares analysis all products and sums are directly available and the value of x_U and x_L are obtained without any difficulty. Two remarks are necessary: (a) the confidence limits are not symmetrical around x_c; (b) since the standard deviation of x_c is required in further calculations, the average confidence limit is divided by 2 (the quantity F could also be used at the 67 % level, but this value is not found in most Tables).

Summarizing

$$s(x_c) = s(m_t) = \frac{x_U - x_L}{4}$$

Once the standard deviation, $s(m_t)$, of the total amount of iron is known it is easy to obtain the standard deviation, $s(m_x)$, of the amount of iron present in the sample. Formula (1) can be rearranged as

$$m_x = m_0 \left(\frac{m_t}{m_0} - 1\right) \qquad (2)$$

Experience has shown that m_t and m_0 are rather close to each other, so the following approximation is made:

$$m_t \simeq I' = \frac{I'(\mathrm{Fe})}{I_\infty(\mathrm{Fe})}$$

and $$m_0 \simeq I = \frac{I(\mathrm{Fe})}{I_\infty(\mathrm{Fe})}$$

Substitution in eqn.(2) gives

$$m_x = m_0 \left(\frac{I'}{I} - 1\right)$$

This approximation is sufficient for the derivation of the standard deviation except when m_t and m_0 have widely different values. Standard techniques of error propagation give

$$s(m_x) = \left(\frac{I'}{I} - 1\right) \left[s^2(m_t) + \frac{m_0^2}{(I'-I)^2} \cdot s^2(I') + \frac{(m_0 I')^2}{I^2 (I'-I)^2} \cdot s^2(I)\right]^{1/2} \quad (3)$$

In this formula the variance $s^2(m_0)$ has been replaced by $s^2(m_t)$: this is not entirely correct, but since both m_t and m_0 are usually rather close, the error is negligible. The term $s^2(m_t)$ thus also includes uncertainties arising from grain size, etc.

For the trace metal calibration line (Fig.4) the relation between $I(\mathrm{Me})/I(\mathrm{Fe})$ and $m(\mathrm{Me})/[m(\mathrm{Fe}) + m(\mathrm{Me})]$ can also be expressed by a linear or a quadratic function. In the case of a linear function, existing formulae [14, 15] can be used for converting observed intensity ratios to mass ratios (R) together with the standard deviation $s(R)$.

The standard deviation $s(\mathrm{Me})$ of the amount of Zn or Pb, $m(\mathrm{Me})$, is calculated as follows

$$\frac{m(\mathrm{Me})}{m(\mathrm{Me}) + m(\mathrm{Fe})} = R \pm s(R)$$

Since $m(\mathrm{Fe})$ (or m_t) and its standard deviation are already known, the usual techniques of error propagation give

$$s(\mathrm{Me}) = \frac{m(\mathrm{Fe})R}{(1-R)} \left[\frac{s^2(R)}{R^2(1-R)^2} + \frac{s^2(m(\mathrm{Fe}))}{m^2(\mathrm{Fe})}\right]^{1/2} \quad (4)$$

Technical procedures

Nuclide experiments

To 40 ml of 10^{-2} M KNO_3, add hydrochloric acid to give pH 1.5—2, 400 μg of Fe^{3+}, Zn or Pb carrier, ^{65}Zn or ^{212}Pb obtained by milking ^{228}Th, and ammonia solution to give the required pH. Allow to settle for 15 min, and filter on a 1.2-μm pore-size Sartorius membrane filter No. 13303 (useful filter diameter 28 mm). Count the entire precipitate and 5 ml of the liquid phase.

River water analysis

Acidify on the spot with 2 ml of 12 M HCl l^{-1}. Filter through a 1.2-μ pore-size membrane filter (as above). Add 10 mg Fe^{3+} l^{-1}, make alkaline, and proceed as for the nuclide experiments. Dry the precipitate at 80 °C for 20 min.

Calibration

Samples for construction of x-ray calibration curves (Fe, Zn or Pb) were precipitated in "synthetic river water" of composition (mg l^{-1}): $CaCl_2.2H_2O$, 294; NaCl, 216; $MgSO_4.7H_2O$, 86.1; KCl, 9.5; $(NH_4)_2HPO_4$, 7.3. The precipitation conditions were as for the river water analysis.

X-ray fluorescence

Philips, PW1540; W tube; 55 kV, 20 mA; fine collimator; scintillation

counter with pulse-height selection for each element; LiF(200); airpath. Counting time: at least 10^4 counts are collected. The iron hydroxide precipitate is oriented towards the x-ray beam.

Comparative analyses of river water

For iron, evaporate the sample to dryness, digest with perchloric and nitric acids, and measure spectrophotometrically by the *o*-phenanthroline procedure. [16]. For zinc, use atomic absorption with an air—acetylene flame (direct). For lead, evaporate the sample to dryness, digest with perchloric and nitric acids, extract with dithizone [17], reextract into water and measure by atomic absorption with a Massmann furnace.

RESULTS AND DISCUSSION

The coprecipitation data obtained from the radionuclide experiments constitute only a guideline, since the simplicity of this medium cannot be compared with the complexity of a river water sample.

To test the method, a number of water samples were analysed for Fe, Zn and Pb; the concentrations were ca. 1000 μg Fe l^{-1}, 100 μg Zn l^{-1} and 10 μg Pb l^{-1} Samples were taken from the Meuse river in the Netherlands, including known "dirty" and "normal" sites. The water was acidified on the spot; in the laboratory (3--4 h later), the water was filtered with a membrane filter and the filtrate was analysed for the three elements by means of the coprecipitation method and by the comparative analytical methods: iron by spectrophotometry with *o*-phenanthroline, zinc by flame atomic absorption spectrometry, and lead by atomic absorption in a Massmann furnace. The analyses were done with the addition of iron(III) at two different concentrations: 10 mg l^{-1} (recommended concentration) and 2 mg l^{-1}. Table 1 summarizes the results; all quoted standard deviations (1*s*) were calculated as described above (eqns.(3) and (4)).

Sample 1 was analysed repeatedly over a period of three weeks. The iron results showed a considerable scatter not only with the coprecipitation technique but also with the spectrophotometric method. The site involved was obviously dirty, as the zinc and lead results were also high: it cannot be excluded that some chemical interference influences strongly the behaviour of iron. The Zn and Pb results showed good reproducibility over this period: these elements were probably precipitated together with the added iron, while the iron naturally present in river water may either not coprecipitate or only to a small extent with the added iron.

The standard deviation calculated from the six individual analyses is 111 μg (8 %) for zinc and 11 μg (7 %) for lead. This is higher than the individual standard deviations calculated from the calibration line, but it is not possible at this stage to ascribe the difference definitely to sample inhomogeneities.

For samples 2, 5, 6, C and F, larger volumes (400 ml) were analysed: for low lead concentrations, the 100-ml sample volumes resulted in the lead

TABLE 1

Results of river water analyses

Sample number, volume (ml); mg Fe added	μg Fe l^{-1}	μg Zn l^{-1}	μg Pb l^{-1}
1. 100; 1.0	1500 ± 60	1420 ± 62	164 ± 7
100; 1.0	600 ± 30	1300 ± 59	175 ± 7
100; 1.0	1300 ± 50	1300 ± 61	172 ± 7
100; 1.0	1300 ± 50	1500 ± 65	176 ± 7
50; 0.5	1800 ± 110	1400 ± 88	157 ± 10
50; 0.5	2800 ± 150	1580 ± 91	190 ± 11
Comparative analysis	700 ± 35	1500 ± 75	190 ± 10
	3000 ± 150	—	—
	3200 ± 160	—	—
2. 400; 1.0	2200 ± 140	1210 ± 65	180 ± 10
100; 1.0	2100 ± 90	1020 ± 55	154 ± 7
Comparative analysis	2200 ± 100	1200 ± 60	165 ± 8
5. 400; 1.0	600 ± 20	273 ± 14	40 ± 2
	600 ± 20 [a]	243 ± 13 [a]	47 ± 2 [a]
100; 1.0	700 ± 30	286 ± 37	36 ± 4
Comparative analysis	600 ± 30	300 ± 15	47 ± 10
6. 400; 1.0	600 ± 20	260 ± 14	43 ± 2
100; 1.0	1000 ± 40	282 ± 38	27 ± 5
Comparative analysis	600 ± 30	300 ± 15	49 ± 1
9. 100; 0.2	1000 ± 200	215 ± 25 [b]	45 ± 4
100; 1.0	800 ± 30	232 ± 38 [b]	43 ± 9
Comparative analysis	1040 ± 50	230 ± 10	30 ± 3
	1120 ± 60 [c]	240 ± 12 [c]	35 ± 7 [c]
10. 100; 0.2	400 ± 50	113 ± 21	16 ± 3
100; 1.0	700 ± 30	133 ± 39	20 ± 9
Comparative analysis	340 ± 20	120 ± 10	9 ± 1
	420 ± 20 [c]	130 ± 7 [c]	~ 3 [c]
C. 400; 1.0	600 ± 20	212 ± 13	19 ± 2
400; —	400 ± 80	196 ± 32	13 ± 2
100; 1.0	500 ± 30	200 ± 37	19 ± 4
Comparative analysis	500 ± 30	230 ± 23	20 ± 2
E. 400; 1.0	1430 ± 70	135 ± 15	15 ± 2
100; 1.0	1500 ± 60	130 ± 40	14 ± 5
Comparative analysis	1000 ± 50	170 ± 17	17 ± 2
F. 100; 0.2	6400 ± 430	—	23 ± 7
100; 1.0	7000 ± 140	78000 ± 660	29 ± 13
5; 0.2	6000 ± 440	17200 ± 860	—
5; 1.0	—	23200 ± 810	—
Comparative analysis	5800 ± 100	21000 ± 1000	45 ± 5
	6500 ± 300 [c]	25000 ± 1200 [c]	46 ± 5 [c]

[a] After destruction with $HClO_4$ + HNO_3.
[b] No element observed in filtrate of coprecipitation phase.
[c] Analysed by high-frequency plasma emission [18].

analyses being done below the "limit of determination" [19]. For 1 mg of iron this limit lies around 3 μg for both lead and zinc Background fluctuations are one of the reasons for this somewhat high limit.

Sample F is interesting because it contains an enormous amount of zinc. Although the measured quantity of zinc in the 100-ml sample has a considerable error, through the extrapolation of the calibration line, the results for iron and lead are still reasonably good.

For all analyses the average of the percentage standard deviations is: Fe, 6 %; Zn, 10 %; Pb, 5 % (excluding points below the limit of determination). On average the standard deviation for zinc is higher than that for lead.

It is clear that this technique cannot always guarantee accurate data for iron concentrations. If, for example, only a small amount of iron is present in the sample compared with the added amount, then the result will be highly uncertain through the subtraction of two nearly equal quantities. To omit the addition of iron — as was done with sample C — is not advisable: indeed, if the quantity of iron in the sample is too low, then incomplete coprecipitation might result.

Each individual coprecipitation result was also compared with the corresponding comparative analysis result; the five iron results from sample 1 were omitted in the comparison. This tested, by means of least squares, whether $K = 1$ in the following "apparent equation": (coprecipitation result) = K. (comparative analysis result). This yielded the following values for K:

Fe: 1.11 ± 0.03 for 18 observations
Zn: 0.96 ± 0.03 for 23 observations
Pb: 0.92 ± 0.02 for 23 observations

The quoted standard deviations of K are probably too low as the standard deviation of each individual analysis was not included in the comparison. This means that it is impossible to decide unequivocally whether the deviations of K from unity are real. Further analyses with standardized samples could give a definite answer to the question of possible systematic errors.

In the construction of the trace metal calibration curve it was assumed that only iron, lead and zinc are present. If, in a real sample, some other elements are coprecipitated in appreciable quantities, then this may lead to errors in the amount of metal because the iron intensity is then no longer a measure of the total mass on the membrane. It was also assumed that the coprecipitation of one element does not influence the coprecipitation of another element. There are insufficient data available to settle this question definitely at present.

The overall analysis time is as follows: filtration and precipitation, 15 min; drying at 80 °C, 20 min (this could be speeded up); total counting time for the three elements, 10 min.

To conclude: an analysis of surface waters for trace elements can be done by concentrating the traces on iron hydroxide followed by x.r.f. measurements. The iron serves as an internal standard, and eliminates the need for frequent recalibrations. The selective character of the iron hydroxide means that all elements are not collected with the same efficiency. The coarse sus-

pended matter which is filtered off (particle size > 1.2 μm), can also be analysed [20, 21] by x.r.f. without further processing. In this way a total analysis of the surface water is possible with the same technique.

Compared with other multi-element analysis methods, the analysis time is short. If the method were extended to other coprecipitated elements the analysis time would not increase, since multichannel or energy-dispersive spectrometers could be used. The sensitivity of the x-ray method, however, is not yet as good as that of neutron activation.

The comparative analyses by Messrs. Bastings and van Kollenburg are gratefully acknowledged.

SUMMARY

Coprecipitation of trace amounts of zinc and lead on iron hydroxide has been studied. A simple method is described to measure by means of x-ray fluorescence the amounts of Zn, Pb and Fe in iron hydroxide precipitates of varying thickness. Surface waters with zinc and lead concentrations between 10 and 100 $\mu g\ l^{-1}$ have been analysed by this technique; the results show good agreement with independent analytical methods.

REFERENCES

1 No attempt is made to include all references in one particular field. Complete surveys can be found in: Biannual Reviews of Analytical chemistry; L. Ciaccio, Water and water pollution handbook, Vols.1—4, M. Dekker, New York, 1971.
2 W. Kölle, Y. Park and H. Sontheimer, Jahr. Wasser, 34 (1967) 31.
3 J. Riley and D. Taylor, Anal. Chim. Acta, 40 (1968) 479.
4 D. Leyden, 4th Ann. Symp. Recent Adv. Anal. Chem. Pollut., Basle, 1974.
5 W. Campbell, F. Spano and T. Green, Anal. Chem., 38 (1966) 987.
6 M. Blasius, S. Kerkhoff, R. Wright and C. Cothern, Water Res. Bull., 8 (1972) 704.
7 F. Marcie, Environ. Sci. Technol., 1 (1967) 164.
8 C. Luke, Anal. Chim. Acta, 41 (1968) 237.
9 J. Riley, Chemical Oceanography, Vol.2, Academic Press, New York, 1965.
10 R. Gibbs, Science, 180 (1973) 71.
11 E. Bruninx, to be published.
12 J. Mandel, The statistical analysis of experimental data, Interscience, New York, 1967.
13 H. Prins, Anal. Chim. Acta, to be published.
14 J. Mandel and F. Linnig, Anal. Chem., 29 (1957) 743.
15 M. Maurice, Z. Anal. Chem., 158 (1957) 271.
16 O. Koch and G. Koch, Handbuch der Spurenanalyse, Springer Verlag, Berlin, 1964.
17 G. Iwantscheff, Das Dithizon und seine Anwendung in die Mikro und Spurenanalyse, Verlag Chemie GmbH, Berlin, 1958.
18 P. Boumans and F. de Boer, Spectrochim. Acta, Part B, 27 (1972) 391.
19 L. Currie, Anal. Chem., 40 (1968) 586.
20 P. Burkhalter, Naval Research Laboratory Report NRL-7637, Washington, 1973.
21 J. Cann and C. Winter, Mar. Geol., 11 (1971) M33.

Analytica Chimica Acta, 80(1975)97—108

A SEPARATION SCHEME FOR THE DETERMINATION OF TRACE ELEMENTS IN BIOLOGICAL MATERIALS BY NEUTRON ACTIVATION ANALYSIS

P. LIEVENS*, R. CORNELIS** and J. HOSTE

Institute for Nuclear Sciences, Rijksuniversiteit Gent, Proeftuinstraat 86, 9000 Gent (Belgium)

(Received 3rd April 1975)

Neutron activation analysis (n.a.a.) coupled with Ge(Li) γ-ray spectrometry is a powerful method for the simultaneous determination of a number of trace elements in biological materials. Since high matrix activities prohibit the direct measurement of many isotopes, however, extensive separation schemes have been developed by several authors [1—8]; a chemical group separation combined with high-resolution γ-ray spectrometry [9, 10] offers the same possibilities. The chemical group separation outlined in this paper allows the determination of Ag, As, Cd, Co, Cr, Cs, Cu, Fe, Hg, K, La, Mn, Mo, Na, Rb, Sb, Se, Sc, Sn, and Zn; seventeen of these twenty elements can be determined within 5 d after irradiation. Accurate, rapid standardization is provided by the multi-isotopic ruthenium comparator.

STANDARDIZATION

The relative multiple comparator method, which has been described [11—14] elsewhere, eliminates the tedious chemical separations on a multi-element standard necessary to obtain an identical counting geometry, or avoids multiple measurements of single element standards (*cf.* ref.2). Determination of the infinite dilution resonance integrals [15, 16] extends the application of the method to a greater number of elements. Table 1 shows the ruthenium isotopes used as a comparator for the trace elements concerned. The specific activity of ^{105}Ru was calculated from the daughter activity ^{105}Rh, a case of non-equilibrium, as follows:

$$A_{sp}{}^{105}\mathrm{Ru} = \frac{A^{105}\mathrm{Rh}}{(1 - e^{-\lambda \mathrm{Rh} t}).e^{-\lambda \mathrm{Rh} t'}.w} \cdot \frac{I_{\mathrm{Ru}}}{I_{\mathrm{Rh}}} \cdot \frac{\lambda_{\mathrm{Ru}} - \lambda_{\mathrm{Rh}}}{\lambda_{\mathrm{Ru}}} \qquad (1)$$

where $A_{sp}{}^{105}\mathrm{Ru}$ = specific activity of ^{105}Ru expressed as counts mg^{-1} h^{-1} saturation factor^{-1} at the end of the irradiation;

$A^{105}\mathrm{Rh}$ = measured activity of ^{105}Rh;

*Research fellow of the I.W.O.N.L.

**Research associate of the I.I.K.W.

TABLE I

Nuclear data for the ruthenium isotopes and their respective use as comparator

Comparator							Classification of isotopes
Target nuclide	Isotope formed by (n,γ)	Half-life	Natural abundance θ (%)	γ-energy of most important transition and absolute abundance (%)	$I_0'/\sigma'(\sigma')$	Useful I_0/σ range	
^{96}Ru	^{97}Ru	69.1 h	5.5	216 keV 11.7 %	23.1(0.25)	$17 < I_0/\sigma$	^{117m}Sn, ^{113}Sn, ^{122}Sb, ^{86}Rb
^{102}Ru	^{103}Ru	39.5 d	31.6	496 keV 87.6 %	3.3(1.3)	$0 < I_0/\sigma < 8.2$	^{38}Cl, ^{51}Cr, ^{60}Co, ^{64}Cu, ^{59}Fe, ^{203}Hg. ^{42}K, ^{140}La, ^{56}Mn, ^{24}Na, ^{46}Sc, ^{69m}Zn, ^{65}Zn
^{104}Ru	^{105}Ru $\downarrow \beta^-$	4.44 h	18.6	316.5 keV 11.6 %	13.0(0.47)	$8.2 < I_0/\sigma < 17$	^{110m}Ag, ^{76}As, ^{115}Cd, ^{82}Br, ^{134}Cs, ^{99}Mo, ^{75}Se
	^{105}Rh	35.5 h		318.9 keV 19.3 %			

$\lambda_{Ru}, \lambda_{Rh}$ = decay constants of ^{105}Ru and ^{105}Rh;
t = irradiation time;
t' = decay time;
w = weight of the comparator
I = fraction of emitted γ-rays per disintegration.

Care should be taken to avoid interference of the 316.5-keV photopeak of ^{105}Ru with the 318.9-keV peak of ^{105}Rh by allowing a sufficient decay time (*e.g.* 57 h waiting time for 10 h irradiation). One single measurement of ^{97}Ru, ^{103}Ru and ^{105}Rh about 3 d after irradiation thereby ensures the standardization of the 20 elements to be determined.

The k-factors were determined by irradiating 50-μl solutions of the elements (Table 2) spotted on 1.5 g of dextrose (analytical grade) packed in a polythene box (16 mm diameter, 21 mm high) and surrounded by six Ru comparators (each 10 mg). The irradiation time varied between 0.5 and 7 h. The organic dextrose dilution avoids self-shielding effects as with the biological sample. The low water content (max. 10 %) comparable with a lyophilized sample minimizes the possibility of a flux increase, through elastic neutron scattering with water protons [17]. The average flux ratio in the irradiation facility used is $\phi_{th}/\phi_{epi} = 32$. To determine the epithermal and thermal flux gradients, tin and copper discs (20 mm diameter; 0.15 mm thick) are irradiated and divided into 32 parts. The tin pieces are dissolved in 2 ml of 6 M hydrochloric acid and the 159-keV peak of ^{117m}Sn is measured on a Ge(Li) detector. The 511-keV β^+-annihilation peak of the copper pieces is measured with a NaI(Tl) well-type crystal. The ^{117m}Sn activity is induced to an extent of 39 % by epithermal neutrons ($I_0/\sigma = 81$) and the ^{64}Cu activity to the extent of 4 % only ($I_0/\sigma = 1.3$). The average percentages of thermal and epithermal flux gradients, parallel to the reactor core, are 4 % cm^{-1} and 3 % cm^{-1} respectively. The radial average decrease of thermal and epithermal flux away from the reactor core is 4 % cm^{-1} and 13 % cm^{-1} respectively. Three ruthenium comparators were therefore placed above and beneath each sample to ensure a consistent mean value of flux and flux-ratios. Table 2 shows the k-values found experimentally for Ag, As, Cd, Co, Cr, Cs, Cu, Fe, Hg, La, Mn, Mo, Rb, Sb, Se, Sc, Sn and Zn. The k-factors of K and Na were determined four times with the Bowen Kale powder as a standard reference material. These values are also given, together with their reproducibility, in Table 2.

Simonits et al. suggested [18] the compilation of generalized k_0 factors, which are independent of irradiation and measuring conditions.

The k_0-factor is defined by eqn.(2):

$$k_0 = \frac{M'}{M} \cdot \frac{\theta}{\theta'} \cdot \frac{\gamma}{\gamma'} \cdot \frac{\sigma}{\sigma'} = \frac{A_{sp}}{A'_{sp}} \cdot \frac{\epsilon'_p}{\epsilon_p} \cdot \frac{\phi_{th}/\phi_{epi} + I'_0/\sigma'}{\phi_{th}/\phi_{epi} + I_0/\sigma} \qquad (2)$$

The parameters M', θ' etc. refer to the comparator, and parameters M, θ etc. to the isotope.

ϵ_p = photopeak efficiency for the measured γ-ray energy;
M = atomic weight;

θ = isotopic abundance;
γ = absolute abundance of the measured γ-ray;
$A_{sp}/A'_{sp} = k$ = the experimentally determined k-value.

TABLE 2

Standardization

Element	Compound [a]	Solvent	Concn. μg/50 μl	Isotope	γ-Energy
Ag	$AgNO_3$	H_2O	313.6	^{110m}Ag	657.5
					884.5
As	As_2O_3	0.4 M NH_4OH	13.65	^{76}As	559
					657
Cd	Metal	4.4 M HCl	23.09	^{115}Cd	527
				^{115m}In	335
Co	Co_2O_3	8.6 M HCl	463.7	^{60}Co	1173
					1332
Cr	Metal	1.2 M HCl	173.8	^{51}Cr	320
Cs	CsCl dried	H_2O	28.64	^{134}Cs	569
					796
Cu	Metal	0.8 M HNO_3	45.35	^{64}Cu	511
Fe	Metal	4.3 M HCl	970.8	^{59}Fe	1098
		0.5 M HNO_3			1192
Hg	Metal	0.7 M HNO_3	361.9	^{203}Hg	279
La	La_2O_3	5.6 M HNO_3	156.9	^{140}La	328.7
					487
					816
					1596
Mn	MnO_2	6 M HCl	104.11	^{56}Mn	846
Mo	MoO_3	1.4 M NH_4OH	17.63	^{99}Mo—^{99m}Tc	140
Rb	RbCl dried	H_2O	651.26	^{86}Rb	1076
Sb	Metal (etched)	6 M HCl; 0.3 M HNO_3	13.73	^{122}Sb	564
Se	Metal	0.7 M HNO_3	535.6	^{75}Se	120
		1.2% H_2O_2			136
					265
					279
					400
Sc	Sc_2O_3	12 M HNO_3	1.274	^{46}Sc	889
					1120
Sn	Metal	12 M HCl	755.6	^{117m}Sn	159
				^{113}Sn	391
Zn	Metal	1 M HCl	294.8	^{65}Zn	1115
Na	Bowen's kale		2506 [b]	^{24}Na	1368
					2754
K	Bowen's kale		24615 [b]	^{42}K	1527.7

[a] All materials were of p.a. grade.
[b] In $\mu g\ g^{-1}$.

TABLE 2 (continued)

I_0/σ	Comparator	k-Factor	Found k_0	Theor. k_0
12.2	^{105}Ru	2345	174.8	165.9
		1383	139.7	132.4
9.5	^{105}Ru	2202	245.0	255.3
		232.4		
11.4—77	^{105}Ru	63.0	3.59	1.43—2.20
		173.2	5.87	2.38—3.71
2.0	^{103}Ru	2446	181.1	171.4
		2184	180.1	
0.5	^{103}Ru	45.9	Not determ.	
12.0	^{105}Ru	11309	381	307
		51547	2052	1930
1.3	^{103}Ru	132.2	3.99	4.96
1.4	^{103}Ru	0.1653	0.0113	0.0097
		0.1096	0.0086	0.0076
0.83	^{103}Ru	55.9	1.544	1.657
1.3	^{103}Ru	125.4	3.14	3.79
		193.9	7.00	8.31
		69.27	3.81	4.34
		144.8	13.8	17.52
1.0	^{103}Ru	1078	59.8	65.4
9.2	^{105}Ru	511.0	Not determ.	
7.9—17	^{97}Ru	44.67	3.389	2.49—5.67
33.6	^{97}Ru	4524	203	161
8.2	^{105}Ru	871.3	10.98	11.50
		2912	36.63	39.45
		1723	38.94	41.15
		757	16.75	17.31
		473	7.46	8.23
0.5	^{103}Ru	5830	167.1	157.9
		4688	168.9	
81	^{97}Ru	8.42	Not determ.	
38.6	^{97}Ru	10.31		
2.2	^{103}Ru	10.69	0.693	0.806
0.66	^{103}Ru	2.580 ± 0.029 (1.12%)	1.191 ± 0.021 (1.77%)	
0.90	^{103}Ru	0.04938 ± 0.00045 (0.91%)		

The first part of eqn.(2) can be calculated from known nuclear constants (M, θ, γ and σ), yielding a theoretical k_0 value. By measuring a relative efficiency curve for the Ge(Li) detector used and converting the detection efficiency of the sample and comparator geometries to a point source geometry at 12-cm distance from the detector, it is possible to calculate ϵ'_p/ϵ_p and thus the experimental k_0-value. Both k_0-values are given in Table 2. The relative efficiency curve was experimentally determined by activity measurement of the following point sources at a fixed distance of 12 cm from the detector, to

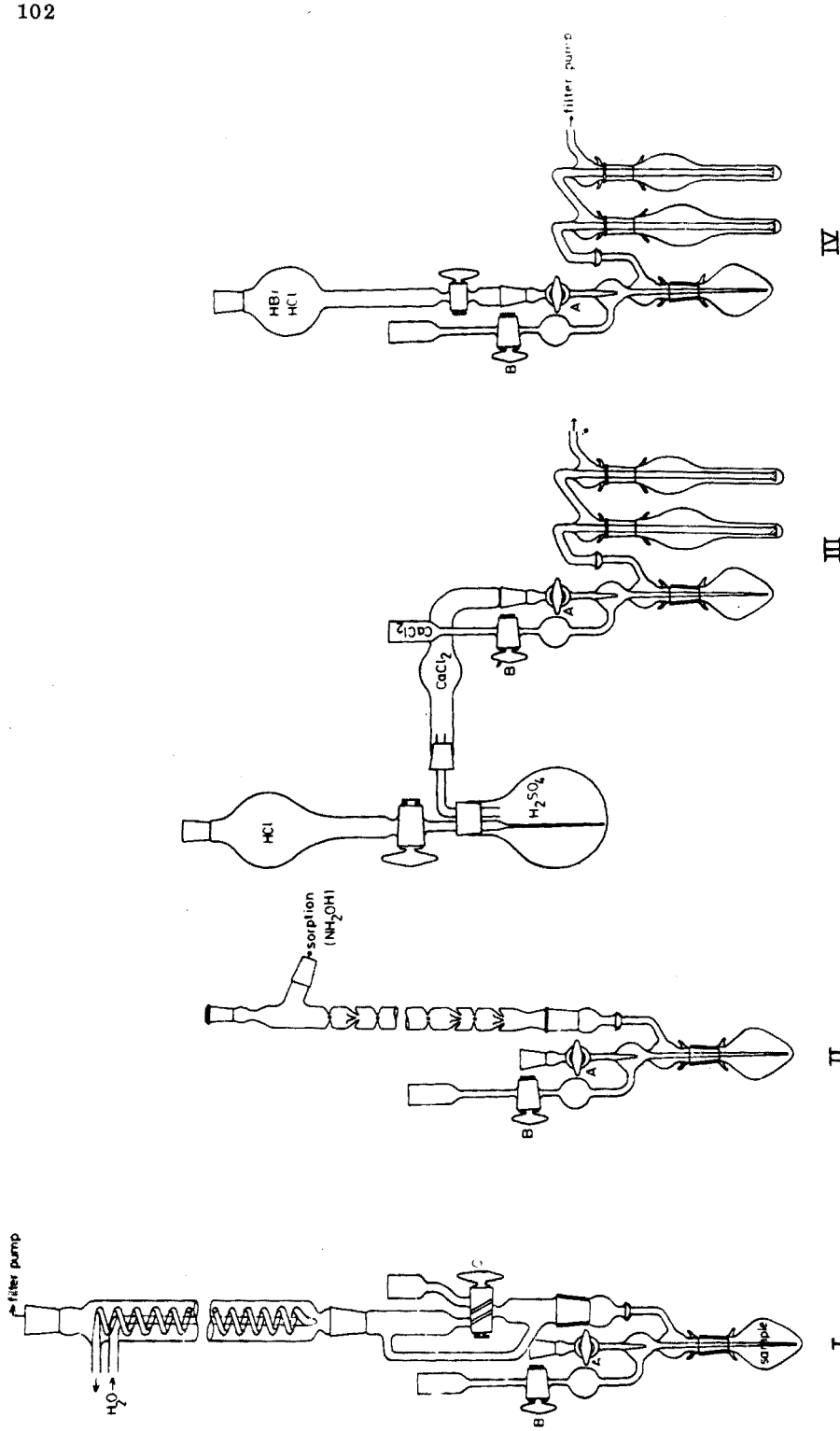

Fig.1. Apparatus. I. Destruction. II. Bromine volatilization. III. CrO_2Cl_2 distillation. IV. As, Hg, Mo, Sb, Se, Sn distillation.

avoid 'real' coincidence of cascade γ-rays: ^{152}Eu, ^{154}Eu, ^{182}Ta, ^{133}Ba, ^{82}Br, ^{110m}Ag, ^{75}Se. Additional measurements of some IAEA standard sources, e.g. ^{241}Am, ^{57}Co, ^{22}Na, ^{137}Cs, ^{54}Mn, ^{60}Co, allow the normalization of the relative curve to give an absolute curve for general use.

Once sufficient data are published, the general k_0-values enable the calculation of k-values for a given comparator, a given reactor spectrum, and a given detector, as can be seen from eqn.(3):

$$k = k_0 \frac{\phi_{th}/\phi_{epi} + I_0/\sigma}{\phi_{th}/\phi_{epi} + I'_0/\sigma'} \cdot \frac{\epsilon_p}{\epsilon'_p} \qquad (3)$$

All peak areas were determined by a suitable program [19] on a PDP 9 computor. In addition, a second program calculated specific activities of comparators, k_{anal}-values, an error estimate [13], a possible yield determination, and the element concentrations in routine analysis.

ANALYSIS OF SAMPLES

About 1.5 g of biological material was irradiated for 7 h in the Thetis reactor of the University of Ghent at a thermal neutron flux of $1.5 \cdot 10^{12}$ n cm^{-2} s^{-1}. One hour after the end of the irradiation, a 30-mg sample is measured for ^{24}Na and ^{42}K activities (12 cm distance) with the Ge(Li) detector (useful volume 70 cm^3; energy resolution (FWHM) 2.0 keV for the 1332-keV peak of ^{60}Co).

The remaining sample is digested with 15 ml of 12 M $HClO_4$ and 8 ml of 14 M HNO_3 in a 50-ml distillation flask (Fig.1). Carrier (10 μg) is added for each of the elements,Ag, As, Cd, Co, Cs, Cu, La, Mn, Rb and about 100 μg for Sb, Se, Hg and Sn, all dissolved in nitric acid, with 10 mg of chromic acid in aqueous solution also present. At the same time known amounts of ^{77}As (prepared [20] on silica gel from irradiated germanium) and of ^{124}Sb tracer are added for yield determinations. The mixture is agitated by an air stream, created by a filter pump, at the top of the Nimroth water-cooler. The reaction receiver is heated by an electrically heated bath containing Woods metal; the temperatures recorded below were measured in this surrounding bath.

Primary oxidation of the biological material during digestion is achieved with nitric acid at 120 °C for 15 min, whereupon the temperature is raised to 180 °C and kept constant for another 5 min. Then the receiver is heated at 230 °C with valve C closed. After about 5 min the green colour of the solution changes to orange-red (Cr(III)→Cr(VI)), indicating complete destruction. Loss of tracers through volatilization does not occur [21]. The next stage (Fig.2) is the volatilization of bromine, performed by adding, dropwise, 5 ml of 48 % hydrobromic acid at 110 °C during 15 min. Other possible volatile compounds reflux in the Vigreux column (Fig.1). The residual nitric acid and water is then distilled at 150 °C and collected in the two-trap receiver. Possible losses during the volatilization of bromine and the removal of nitric acid and water amount

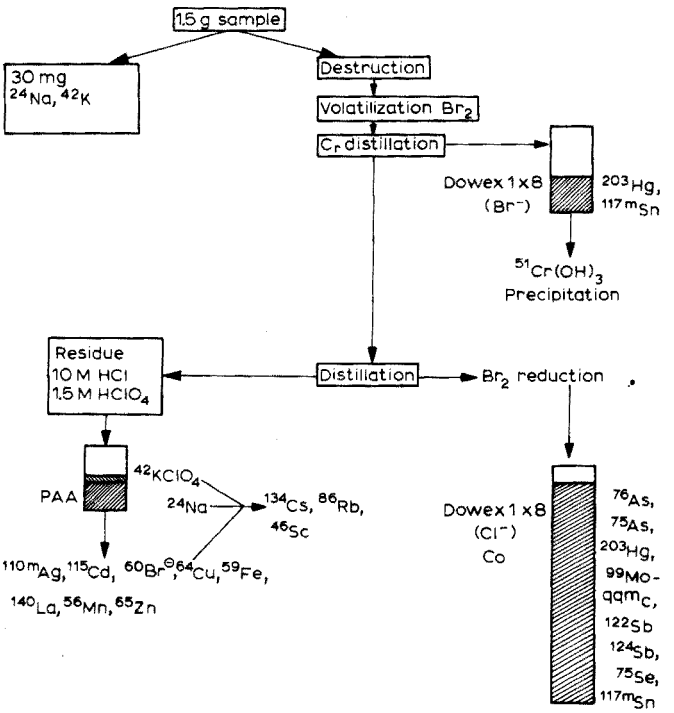

Fig. 2. Separation scheme.

to 3 % for Hg and to 0.7 % for As, Sb, Cr, Se, Sn and Mo. By raising the temperature to 210 °C and slowly introducing dried hydrogen chloride, CrO_2Cl_2 is distilled and collected in 30 ml of 48 % HBr—2 % NH_2OH (previously boiled for 1 min and cooled to room temperature). The two-trap receiver is ice-cooled. The distillation is repeated twice with 10 mg of CrO_3 carrier. Under these working conditions, more than 99 % of the As, Sb, Se and Mo remain in the distillation flask. However, the distillate appears to contain up to 40 % Hg and 55 % Sn which are now fixed on a 2-ml Dowex 1-X8 (200—400 mesh) column in the bromide form. Chromium(III) is not adsorbed and is precipitated as chromium hydroxide by adding 14 M ammonia solution up to pH 7, thus increasing the detection efficiency of the low-activity 320-keV γ-ray by a factor of 2 or 3. The quantitative distillation of As, Mo, Sb, Se and of the residual Sn and Hg is carried out by adding 100 ml of a mixture of HBr (48 %) and 12 M HCl (2 : 1) dropwise at 230 °C. Halfway through this distillation, 10 ml of 12 M $HClO_4$ is added to the distillation flask. Subsequently the bromine formed during the distillation is reduced to bromide by adding 8 g of hydroxyammonium chloride to the ice-cooled distillate and then heating gently in an Erlenmeyer flask fitted with a 60 cm-high spiral condenser. The six elements are next fixed on a 10-ml Dowex1-X8 (200—400 mesh) column in the bromide, chloride form. The two resin fractions are combined, homogenized

a 20-ml counting vial, and dried by suction with a filter stick. The resin can then be measured for ^{77}As, ^{76}As, ^{203}Hg, ^{99}Mo—^{99m}Tc, ^{122}Sb, ^{124}Sb, ^{75}Se, ^{117m}Sn activities.

The distillation residue is evaporated to about 2 ml of $HClO_4$ and taken up again in hot 12 M HCl (15 ml). This solution is treated on a 1-g PAA (polyantimonic acid) column; sodium is completely retained and K, Cs, Rb and Sc are retained partially, while $KClO_4$ partially precipitates at room temperature. The following elements are eluted quantitatively from the PAA with 5 ml of 12 M HCl: Cu, Mn, Zn, Co, Ag, Fe, La, Cd. The eluate is measured for the first time (12 cm distance) with the Ge(Li) detector for ^{64}Cu and ^{56}Mn. The highly energetic γ-rays of the residual ^{42}K cause a dead-time of 15 %. This high counting-rate results in pile-up losses of up to 8 % as shown by tracer experiments. On the basis of Anders' hypothesis [22] that these losses are equal for all the γ-energies over the entire spectrum, a second measurement of ^{42}K a few days later (when the dead-time is less than 2 %) yields the net activity of ^{42}K, and comparison with the first measurement allows the calculation of the pile-up losses for the 846-keV ^{56}Mn peak and the 511-keV annihilation peak of ^{64}Cu (corrected for β^+ annihilation of ^{42}K).

After total decay of ^{42}K (about 5 d after irradiation), ^{115}Cd—^{115m}In, ^{140}La, ^{59}Fe, ^{60}Co, ^{65}Zn and ^{110m}Ag are measured in the PAA eluate. After total decay of ^{24}Na (*ca.* 14 d), the PAA column is added to the PAA eluate and the solution is evaporated to dryness so that the quantitative measurement of ^{86}Rb, ^{46}Sc and ^{134}Cs becomes possible.

TABLE 3

Yield determinations tested by tracer experiments
(Two determinations were done unless otherwise specified)

Element	Yield (%)	Remarks
Rb [a]	99	80—92 % on PAA
Cd, Cu, Mn [a], Se [b], Sc, Zn	98	Av. 88 % on PAA for Sc
Co [a], Cs, Cr, La, Sn	96	91 % on PAA, 5 % in eluate for Cs
Ag, Fe, Mo	94	
As [c]	93	
Hg	90	
Sb [c]	80	80—95 % irreproducible

[a] 3 determinations.
[b] 5 determinations.
[c] 4 determinations.

RESULTS AND DISCUSSION

The yields for the 18 elements were tested by tracer experiments in the presence of 1.5 g of lyophilized pork liver (Table 3). The values are satis-

TABLE 4

Bowen's kale powder

Element	Found (p.p.m.)						Mean value (p.p.m.)	s_r (total) (%)	s_r (count) (%)	Best mean values or ranges [23]
Ag	< 0.04									< 0.01—0.5
As	0.134	0.127	0.122				0.128	6.0	2.4	0.14 (0.11—0.22)
Cd	1.07	0.95	0.90	1.02	0.94	1.07	0.99	8.3	3.5	0.80 (0.38—1.06)
Co	0.058	0.065	0.063	0.053	0.057	0.060	0.059	8.6	7.3	0.058 (0.04—0.08)
Cr	0.452	0.430	0.462	0.437	0.448	0.442	0.445	2.8	1.4	0.31 (0.18—0.42)
Cs	0.084	0.081	0.078	0.084	0.072	0.084	0.081	6.7	4.7	0.074 (0.069—0.77)
Cu	5.4	5.7	5.2	5.6	5.3	5.8	5.5	4.6	1.8	5.0 (3.6—6.5)
Fe	104	104	106	105	102	110	105	3.1	2.4	118 (88—157)
Hg	0.142	0.147	0.149				0.146	3.4	3.0	0.167 (0.11—0.23)
La	0.1073	0.1061	0.1062	0.1061	0.1851	0.1078	0.1067	0.91	1.6	0.087 (0.08—0.1)
Mn	15.2	16.3	15.9	16.5	15.2	16.7	16.0	4.8	0.30	14.7 (12.6—18)
Mo	1.93	2.07	1.97	2.15	2.01	2.04	2.03	4.3	0.54	2.28 (1.5—3.1)
Rb	48.6	48.0	51.4	47.8	48.6	47.3	48.6	3.4	0.49	52.2 (41—57)
Sb	0.065	0.058	0.059	0.057	0.068	0.055	0.060	9.5	3.2	0.069 (0.05—0.11)
Se	0.123	0.116	0.118	0.113	0.106	0.105	0.113	6.9	6.7	0.121 (0.02—0.15)
Sc	0.0120	0.0103	0.0104	0.0109	0.0111	0.0119	0.0111	6.9	1.6	0.008
Sn	< 0.6									0.26
Zn	31.1	31.2	33.7	32.4	31.1	32.4	32.0	3.7	1.0	33.2 (30—38)

factory with the exception of those for antimony, which required an independent yield determination. The good reproducibility and accuracy of the method can be seen from the 6 analyses of Bowen's kale powder [23] (Table 4) and the 2 analyses of NBS Bovine Liver, SRM-1577 (Table 5). The dry weight appeared to be 94.3 % for Bowen's kale powder (20 h drying at 90 °C) and 94.6 % for the Bovine Liver SRM-1577 (24 h freeze-drying). The chromium result for Bowen's kale is rather high, although the precision is excellent. The difference between the two chromium results for SRM-1577 may indicate inhomogeneity for this element. Interferences from $^{54}Fe(n,\alpha)^{51}Cr$, $^{56}Fe(n,p)^{56}Mn$ are negligible. According to Chauvenet's criterion [24] the fifth result for the lanthanum concentration in Bowen's kale powder was omitted from the mean value.

TABLE 5

Determination of trace elements in bovine liver
($\mu g\ g^{-1}$ dry weight)

Element	(67 % conf. lim.)	NBS value [a]	Element	(67 % conf. lim.)	NBS value [a]
Ag	0.051 ± 0.011	—	Mn	11.2 ± 0.5	10.3 ± 1.0
As	0.056 ± 0.004	(0.055)	Mo	3.19 ± 0.14	(3.2)
Cd	0.288 ± 0.035	0.27 ± 0.04	Rb	17.97 ± 0.60	18.3 ± 1.0
Co	0.223 ± 0.011	(0.18)	Sb	0.0048 ± 0.0005	—
Cr	0.074 ± 0.005	—	Se	1.02 ± 0.03	1.1 ± 0.1
	0.123 ± 0.006		Sc	< 0.0005	—
Cu	187 ± 8	193 ± 10	Sn	< 0.6	—
Cs	0.0149 ± 0.0022	—	Zn	135 ± 5	130 ± 10
Fe	236 ± 5	270 ± 20	Na	2632 ± 29	2430 ± 130
Hg	0.0223 ± 0.0013	—	K	10323 ± 258	9700 ± 600
La	0.0173 ± 0.0004	—			

[a] Values in parenthesis are not certified.

The standard deviation for a single measurement, calculated from the six results, determines the overall precision for one analysis. The error from the analytical treatment (assuming that the material is homogeneous) was calculated from the average counting error for a single analysis and from the overall precision.

In conclusion, the present method of trace analysis is applicable to any biological material, and is versatile, simple, and reproducible. A skilled analyst requires about five hours to perform all the required chemical manipulations after irradiation. The measurements of some γ-activities are rather time-consuming. Nevertheless, quantitative results for 20 elements are available within two weeks with the aid of ruthenium as a multi-comparator; this includes the processing of the data with a suitable computer program.

SUMMARY

A separation scheme for the determination of 20 trace elements by neutron activation analysis has been developed and tested on biological material. The method is based on a wet chemical destruction followed by distillation, ion exchange separation and column chromatography (polyantimonic acid) for the removal of the sodium matrix activity. The recovery of tracers added to liver samples has been studied for the following elements: Ag, As, Cd, Co, Cs, Cu, Cr, Fe, Hg, La, Mn, Mo, Rb, Sb, Se, Sc, Sn and Zn. The yields exceeded 90 % except for Sb. The accuracy and reproducibility can be deduced from repeated analyses of Bowen's kale powder and from the NBS bovine liver, standardised by the relative multiple comparator method. The reproducibility varied between 0.91 % and 9.5 % (counting statistics included).

REFERENCES

1 G. Aubouin and J. Laverlochère, Rapport C.E.A. No. 2359, 1963.
2 K. Sahmsahl, D. Brune and P.O. Wester, Int. J. Appl. Radiat. Isotop., 16 (1965) 273.
3 P. Van den Winkel, A. Speecke and J. Hoste, Nuclear Activation Techniques in the Life Sciences, IAEA, 1967, p.159.
4 K. Sahmsahl, Anal. Chem., 39 (1967) 12, 1480.
5 K. Sahmsahl, P.O. Wester and O. Landstrom, Anal. Chem., 40 (1968) 181.
6 J. Schuhmacher and W. Maier-Borst, Kerntechnik, 14 (1972) 4, 165.
7 P.S; Tjioe, J.J.M. de Goeij and J.P.W. Houtman, I.R.I. Rapport 133-72-10, 1972.
8 L.G. Nagy, G. Török, G. Fóti, T. Toth and L. Feuer, J. Radioanal. Chem., 16 (1973) 245.
9 G.H. Morrison and N.M. Potter, Anal. Chem., 44 (1972) 4,839.
10 B. Maziere, A. Gaudry, W. Stanilewicz and D. Comar, J. Radioanal. Chem., 16 (1973) 281.
11 R. Van der Linden, F. De Corte and J. Hoste, J. Radioanal. Chem., 20 (1974) 729.
12 R. Van der Linden, F. De Corte and J. Hoste, Anal. Chim. Acta, 71 (1974) 263.
13 R. Van der Linden, F. De Corte and J. Hoste, J. Radioanal. Chem., 13 (1973) 169.
14 T. Bereznai, F. De Corte and J. Hoste, Radiochem. Radioanal. Lett., 17 (1974) 3,219.
15 R. Van der Linden, F. De Corte, P. Van den Winkel and J. Hoste, J. Radioanal. Chem., 11 (1972) 133.
16 R. Van der Linden, F. De Corte and J. Hoste, J. Radioanal. Chem., 20 (1974) 695.
17 R.A. Johnson, Talanta, 11 (1964) 149.
18 A. Simonits, F. De Corte and J. Hoste, J. Radioanal. Chem., 24 (1975) 31.
19 J. Op de Beeck, presented at the 32nd Symp. Recent Developments in Neutron Activation Analysis, Cambridge, U.K., July 1973.
20 P. Lievens and J. Hoste, Anal. Chim. Acta, 70 (1974) 462.
21 J. Pyck, J. Hoste and J. Gillis, Proceedings of the International Symposium on Microchemistry 1958, Pergamon, Oxford, 1959.
22 O.U. Anders, Nucl. Instrum. Methods, 68 (1969) 205.
23 H.J.M. Bowen, J. Radioanal. Chem., 19 (1974) 215.

Analytica Chimica Acta, 80 (1975) 109—115

THE DETERMINATION OF PLATINUM AND PALLADIUM IN COPPER-BASED STANDARD REFERENCE MATERIALS BY NEUTRON ACTIVATION ANALYSIS

A. GOVAERTS*, R. GIJBELS and J. HOSTE

Institute for Nuclear Sciences, Ghent University, Ghent (Belgium)

(Received 30th May 1975)

SUMMARY

The determination of palladium and platinum by n.a.a. in 100—1 $\mu g\ g^{-1}$ Pd—Cu and Pt—Cu alloys is described. To avoid systematic errors, standards with approximately the same shape and composition as the samples were prepared by quantitative deposition of the noble metals from dilute hydrochloric acid medium on copper powder; after ignition in hydrogen, the powder was pressed to standard pellets. Platinum was determined by i.n.a.a. via ^{199}Au. For palladium an instrumental analysis via ^{111}Ag was possible only for the 100 $\mu g\ g^{-1}$ samples. For the lower concentrations copper was removed by cation exchange and palladium was determined via the ^{109}Pd—^{109m}Ag isotopes. The precision for each analysis was 2—3 % relative. The accuracy was checked by comparison with results from other laboratories.

There is a growing need for standard reference materials for noble metals, and the Bureau Eurisotop (Brussels) has been sponsoring the development of a copper metal matrix containing standardized platinum metal contents (100, 10 and 1 $\mu g\ g^{-1}$ palladium—copper and platinum—copper alloys). The proposed standards were prepared by successive dilutions of palladium or platinum metal in a copper metal matrix by means of high-frequency levitation melting [1]. The determination of palladium and platinum by n.a.a. in copper samples of various origins, one of which was chosen for the preparation of the alloys, will be described elsewhere [2]. This paper deals with precise n.a.a. for palladium and platinum in the proposed standard reference materials.

EXPERIMENTAL

The samples were disks with a diameter of 10 mm, a thickness of 1.5 mm and a weight of ca. 1 g. To avoid neutron self-shielding and, in the case of an instrumental determination, γ-attenuation and counting geometry problems, special palladium—copper and platinum—copper standards were prepared

*Research fellow of the I.I.K.W.

with approximately the same shape, weight, density and composition as the "100" $\mu g\ g^{-1}$ samples. This preparation involved the quantitative deposition of palladium or platinum from dilute hydrochloric acid medium on copper powder. After decantation of the supernatant liquid, the residue was dried and ignited in a Rose crucible under a stream of hydrogen. The reduced powder was pressed into pellets.

Preparation of the Pd(Cu) and Pt(Cu) pellets

Copper powder (10 g, particle size ca. 10 μm, Merck, p.a.) was weighed in a tall-form 250-ml beaker, and 50 ml of water and a drop of 2 M HCl were added as a wetting agent. The solution was vigorously stirred and 25 ml of a standard solution of palladium or platinum (1000 μg Pd or Pt; 0.1 M HCl for Pd and 0.2 M HCl for Pt) were added at a rate of 3 ml min^{-1}. After this addition the solution was continuously stirred for 80 (Pd) or 120 (Pt) min at 70 °C. The supernatant liquid was decanted and filtered through a Whatman filter paper in order to collect the small amount of copper powder which did not settle readily. The residue in the beaker was dried for several hours under an i.r. lamp to constant weight (ca. 10.5 g); after drying the weight variation must be less than 1 mg h^{-1}.

The initial acidity, temperature and stirring time for quantitative deposition were determined by radioactive tracer experiments; the procedure started with the preparation of standard solutions from irradiated Pd or Pt metal, and γ-counting was done via the ^{109}Pd—^{109m}Ag 88-keV and the ^{197}Pt 191.4-keV peaks. The results are presented in Table 1.

For the best working conditions, typically 0.3 % of the amount of noble metal added was lost in the filtrate (0.1 %) and in the small solid fraction on the filter paper (0.2 %). The homogeneity of the dried residue at the 1-g level was checked by dividing it into ten 1.05-g fractions which were dissolved in 10 ml of 6 M HNO_3; the nitric acid was removed by successive additions of 12 M HCl followed by evaporations to a syrupy consistency on a hotplate. The final residues were dissolved in 20 ml of water and the solutions were transferred to standard counting vials. Palladium and platinum contents of 100 ± 2 μg were found (theoretically 99.7 μg), which proves that the homogeneity at the 1-g level was better than 2 % relative.

As no mechanically resistant pellets could be pressed from the dried residue, the powder was first ignited in hydrogen to remove surface oxidation. Fractions of 1.05 g were reduced by heating in Rose crucibles under a stream of hydrogen until constant weight was obtained. The final weight was typically 0.995 g, which agrees with the 0.5 % copper lost in the filtrate (0.3 %) and on the filter (0.2 %).

The reduced powders were pressed at 160000 psi to pellets (diameter 10 mm; density 8.5 g cm^{-3}). The pellets were weighed (ca. 0.990 g) in polyethylene vials and the noble metal content was calculated on the assumption of homogeneous distribution (99.7 $\mu g \times 0.990/0.995 = 99.2\ \mu g$).

TABLE 1

Deposition of palladium and platinum from dilute hydrochloric acid medium on copper powder

Metal	Stirring time (min)	% in filtrate			% in lost solid fraction[a]		
Palladium		^{109}Pd		Cu[b]	^{109}Pd		Cu[b]
Room temp.; 0.03 M HCl	30	2.8/2.3					
	60	0.8/0.7					
70 °C; 0.03 M HCl	30	0.3					
	60	0.2					
	80	0.05		0.32	0.20		0.18
		0.09		0.24	0.17		0.14
		0.07		0.30	0.22		0.22
Platinum		^{197}Pt	^{199}Au	Cu[b]	^{197}Pt	^{199}Au	Cu[b]
70 °C; 0.03 M HCl	60	20	0.3				
70 °C; 0.06 M HCl	60	0.3	0.05				
		0.2	0.05				
	120	0.10	0.05	0.36	0.20	0.17	0.18
		0.07	0.02	0.40	0.17	0.17	0.20
		0.11	0.10	0.25	0.16	0.19	0.20

[a]The percentage in the solid fraction lost on the filter was established by dissolving the fraction in aqua regia and diluting with water before counting.
[b]The copper results were obtained by i.n.a.a. After the ^{109}Pd or ^{197}Pt activity of the filtrate and the dissolved fraction lost on the filter had been measured, known fractions of these solutions were irradiated together with spotted copper monitors.

Blanks prepared in the same way were analysed for palladium and platinum by r.n.a.a. [2]. They contained less than 50 ng Pd g^{-1} and less than 100 ng Pt g^{-1}, indicating that the content of the undoped copper powder and contaminations introduced during the preparation can be neglected.

Determination of platinum

Platinum was determined in the proposed standards by i.n.a.a. via the nuclear reaction ^{198}Pt (n, γ) ^{199}Pt (β^-) ^{199}Au.

Irradiation

Polyethylene vials containing the sample, the Pt(Cu) standard, two copper flux monitors (20-mg foils) and a spotted gold standard (ca. 3 μg Au on high-purity silica powder) were precisely centred above each other with polyethylene rings in the cylindrical irradiation container, in the order shown in Fig. 1. Most irradiations were performed in irradiation site number 10 of

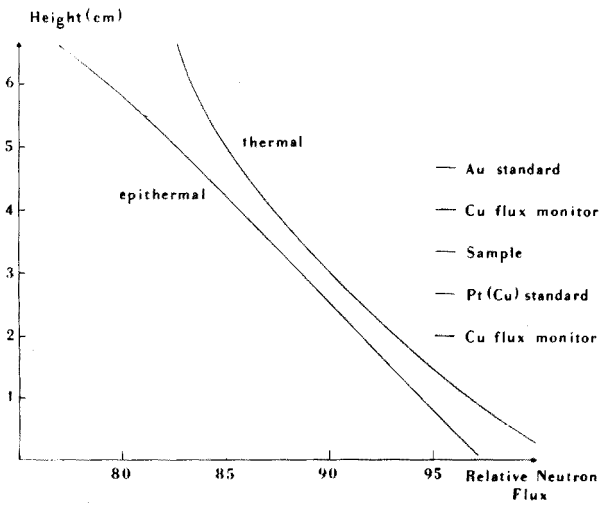

Fig. 1. The variation of the thermal and epithermal neutron flux as a function of the height in irradiation site number 10 of the Thetis reactor [3]. Position of the sample, flux monitors and standards for the determination of platinum.

the Thetis reactor for 3—7 h at a thermal neutron flux of 10^{12} n cm^{-2} s^{-1} ($\phi_{th}/\phi_{epi} \approx 30$). Although the I_0/σ_{th} values for the ^{63}Cu (n, γ) ^{64}Cu and ^{198}Pt (n, γ) ^{199}Pt reactions are quite different (1.3 and 13, respectively), ^{64}Cu can be used as internal flux monitor, as the ratio ϕ_{th}/ϕ_{epi} is practically constant at the irradiation site. Moreover, since the flux is approximately a linear function of the irradiation height, the flux correction can be calculated by linear interpolation between the ^{64}Cu activities of the copper foil flux monitors.

Counting

After a cooling time of one week, the copper flux monitors were measured with a 40-cm^3 Ge(Li) detector via the 511.0-keV annihilation radiation of ^{64}Cu. Internal ^{64}Cu flux monitoring was done by measuring the sample and the standard after 10 days. With both methods the same flux correction factor of 1.030 ± 0.005 was found.

After a cooling time of two weeks, the sample and the standard were measured again, and platinum was determined via the 158.4-keV γ-ray of ^{199}Au. The samples were measured for 1—15 h depending on the platinum content. The gold content of the samples, determined via the 411.8-keV γ-ray of ^{198}Au, was practically the same as that reported [2] for the undoped copper matrix (ca. 10 ng g^{-1}), hence the production of ^{199}Au via the ^{197}Au (n, γ) ^{198}Au (n, γ) ^{199}Au reactions can be neglected even for the 1 μg g^{-1} Pt(Cu) samples. The net peak area of the 158.4-keV photopeak was calculated on the assumption that the background was linear. By extrapolation, it appeared that for the 1 μg g^{-1} samples a systematic positive error of ca. 1 %

could be caused by the presence of the ^{198}Au back-scatter peak in the 158-keV region. For the 1 μg g^{-1} samples the standard deviation expected from counting statistics was 2 % relative. Figure 2 shows the γ-ray spectrum of an irradiated "1.19" μg g^{-1} Pt(Cu) sample measured two weeks after irradiation.

Determination of palladium

Palladium was determined in the "100 μg g^{-1}" Pd(Cu) samples by i.n.a.a. via the ^{110}Pd (n, γ) ^{111}Pd (β^-) ^{111}Ag reactions, and by r.n.a.a. via the ^{108}Pd (n, γ) ^{109}Pd (β^-) ^{109m}Ag reactions. As the sensitivity of the instrumental method was rather poor, r.n.a.a. was used for the more dilute samples. For this purpose, sample and standard were surrounded by two copper flux monitors (vertical flux gradient correction) and irradiated for 1 h at a thermal neutron flux of 10^{11} n cm^{-2} s^{-1} ("100" μg g^{-1} samples; $\phi_{th}/\phi_{epi} \approx 150$) or for 3 h at a flux of 10^{12} n cm^{-2} s^{-1} (for the more dilute samples; $\phi_{th}/\phi_{epi} \approx 30$).

Procedure

The procedure was essentially the same as that described for the determination of Pd, Pt and Au in the undoped copper dilution matrix [2]. The sample was dissolved in 10 M HNO_3 in the presence of 10 mg of Pd carrier. After dissolution and conversion to hydrochloric acid medium, the final residue was dissolved in 50 ml of 0.03 M HCl. The solution was passed through a Dowex 50W-X8 cation-exchange column (2 cm diameter, 12 cm high), and the resin was washed with 150 ml of 0.03 M HCl. The eluate was acidified to give a 0.5 M HCl solution and 3 ml of a 1 % solution of dimethylglyoxime in ethanol was added. The precipitate was collected on a Millipore filter and mounted on an aluminium counting tray.

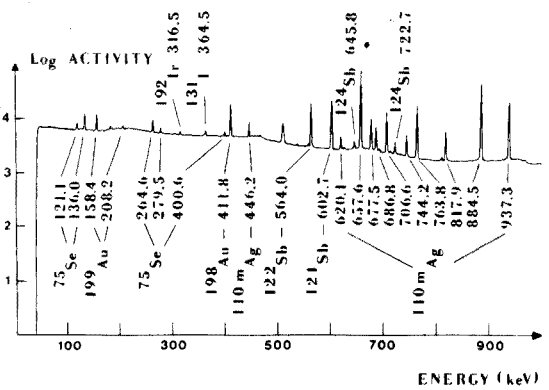

Fig. 2. γ-Ray spectrum of an irradiated "1.19" μg g^{-1} Pt(Cu) standard reference sample measured for 25 h, two weeks after irradiation.

Counting

The precipitates were counted with a 40-cm^3 Ge(Li) detector via the 88-keV γ-ray of ^{109m}Ag, a G.M. tube via ^{109}Pd, and a NaI(Tl) wafer via Ag x-rays.

Chemical yield

After ignition of the Millipore sandwich and reduction in hydrogen, the chemical yield was determined by weighing as the metal. Yields of 90 % were usually obtained.

The vertical flux gradient and chemical yield corrections were taken into account, and the concentrations were calculated from the mean of the ratios of the sample and standard $Pd(DMG)_2$ activities obtained by the three counting techniques.

I.n.a.a. via ^{111}Ag

Two weeks after an irradiation of 7 h at a thermal neutron flux of 10^{12} n cm^{-2} s^{-1}, the sample and the standard were counted for 15 h with a 40-cm^3 Ge(Li) detector; the 341.9-keV γ-ray of ^{111}Ag was used. The standard deviation expected from counting statistics was 2 % relative. Figure 3 shows the γ-ray spectrum of an irradiated "100" μg g^{-1} Pd(Cu) sample, measured two weeks after irradiation.

RESULTS AND DISCUSSION

The results are shown in Table 2, and the accuracy of the method in Table 3, which also gives the results obtained by other laboratories. The weighted mean of all analyses includes determinations by other techniques such as emission spectrography, x-ray fluorescence, isotope dilution methods, γ-ray and charged particle activation analysis. The agreement is good.

Thanks are due to the I.I.K.W. and the I.W.O.N.L., for financial support.

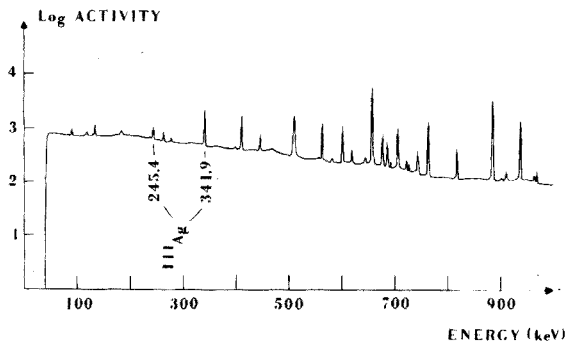

Fig. 3. γ-Ray spectrum of an irradiated "100" μg g^{-1} Pd(Cu) standard reference sample measured for 15 h, two weeks after irradiation (for other peaks see Fig. 2).

TABLE 2

Palladium and platinum content of the Pd(Cu) and Pt(Cu) alloys
(All values are given in $\mu g\ g^{-1}$)

Palladium	100[a]	11.9[a]	1.19[a]
RNAA	98 ± 2[b]	11.9 ± 0.3[b]	1.19 ± 0.03[b]
INAA	100 97		
Platinum	100[a]	11.9[a]	1.19[a]
INAA	97 ± 2[b]	11.6 ± 0.2[b]	1.17 ± 0.03[b]

[a]Expected content from the dilutions (calculations based on the copper and noble metal weights that were initially mixed).
[b]Mean of 6 determinations and standard deviation on one determination.

TABLE 3

Comparison with the results obtained by other laboratories

	100[a]	11.9[a]	1.19[a]
Palladium			
This work	98.3 ± 0.6[b]	11.9 ± 0.1[b]	1.19 ± 0.01[b]
N.a.a.[c]	97.7 ± 0.5	11.95 ± 0.05	1.20 ± 0.01
A.a.s.[c]	98.0 ± 0.1	11.70 ± 0.02	1.21 ± 0.02
Gravimetry[c]	99.7 ± 0.2	—	—
Mean[d]	98.2 ± 0.1	11.77 ± 0.02	1.20 ± 0.01
Platinum			
This work	97 ± 1[b]	11.6 ± 0.1[b]	1.17 ± 0.01[b]
N.a.a.[c]	101.1 ± 0.4	11.73 ± 0.04	1.19 ± 0.01
A.a.s.[c]	96.8 ± 0.3	11.75 ± 0.06	1.18 ± 0.03
Photometry[c]	98.5 ± 0.2	12.0 ± 0.3	1.13 ± 0.02
Mean[d]	98.5 ± 0.1	11.75 ± 0.03	1.18 ± 0.01

[a]Expected content from dilution.
[b]Standard deviation of the mean.
[c]Weighted mean of all results obtained by this technique.
[d]Weighted mean of all analyses.

REFERENCES

1 J. Van Audenhove and J. Joyeux, Nucl. Instrum. Methods, 102 (1972) 409.
2 A. Govaerts, R. Gijbels and J. Hoste, Anal. Chim. Acta, 79 (1975) 139.
3 R. Van der Linden, private communication.

Analytica Chimica Acta, 80(1975)117—123

DETERMINATION OF SULFUR IN NICKEL-BASE ALLOYS AND ALLOY STEELS BY ISOTOPE DILUTION MASS SPECTROMETRY

KAZUO WATANABE

Analytical Chemistry Laboratory, Japan Atomic Energy Research Institute, Tokai-mura, Ibaraki-ken (Japan)

(Received 1st May 1975)

Gravimetric, combustion, and evolution methods are generally used for the determination of sulfur in metals and alloys. The gravimetric barium sulfate method is reliable but insensitive; less than 0.005 % sulfur cannot be determined [1]. The combustion method is simple and rapid, but the recovery is sometimes incomplete although many attempts [2—4] have been made to improve it. The evolution method is effective only if sulfur is present as metal sulfides [5].

When total sulfur has to be determined, a decomposition procedure that converts all the sulfur to sulfate is preferable. Luke described a method of oxidizing sulfur to sulfate and then reducing to hydrogen sulfide [6], and applied it to the photometric determination of sulfur in metals and alloys [7]. Unfortunately, the reduction of sulfate to sulfide was not quantitative; the reagents which have been described for this reduction vary from a mixture of hydriodic acid, formic acid, and red phosphorus [8] to a mixture of hydriodic acid, acetic anhydride, and sodium hypophosphite [9].

The present work was designed to develop an accurate and precise method

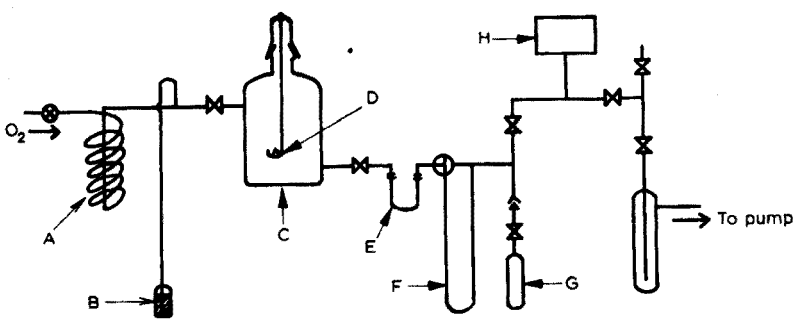

Fig. 1. Apparatus for the combustion of silver sulfide to sulfur dioxide. (A) Molecular sieve column; (B) Hg manometer; (C) oxygen combustion bottle (0.5 l); (D) Pt basket; (E) first U-tube containing P_2O_5; (F) second U-tube; (G) sampling bottle; (H) vacuum gauge.

for the determination of sulfur in nickel-base alloys and alloy steels; isotope dilution mass spectrometry (i.d.m.s.) that involves reduction of sulfate to hydrogen sulfide is described. Once the spike has been mixed thoroughly with the sample, quantitative separation of sulfur is not necessary because only isotope ratios are measured. A stable isotope dilution method has been used for the determination of milligram quantities of sulfur in organic compounds [10].

EXPERIMENTAL

Apparatus

The oxygen combustion apparatus shown in Fig. 1 was used.

Isotopic analysis of sulfur was performed with a CEC 21-103C mass spectrometer equipped with a Cary 401 M vibrating reed electrometer and a strip-chart recorder. Preliminary experiments with an Atlas CH-4 mass spectrometer showed that it was unsuitable for microgram quantities of sulfur because of serious adsorption losses of sulfur dioxide in the inlet system.

Reagents and special solutions

Reagent-grade chemicals were used except for hydrochloric and nitric acids which were of super special grade. Enriched ^{34}S isotope (elemental sulfur) was obtained from the Oak Ridge National Laboratory. Nitrogen was purified by passing it through columns of silica gel and potassium hydroxide pellets.

Spike solution

5 mg of 45 % enriched ^{34}S isotope was burned in a 500-ml flask by the oxyge combustion method [11], and absorbed in 20 ml of 10 % (1+2) 100-vol. hydro gen peroxide solution. Then 10 ml of 1 % sodium hydroxide solution was added. After boiling, the solution was diluted to volume with water in a 50-ml volumetric flask.

Standard potassium sulfate and sodium sulfate solutions

Potassium sulfate (minimum 99.6 %) and sodium sulfate (minimum 99.5 %) were dissolved in water to give a sulfur concentration of 300 $\mu g\ g^{-1}$ of solution.

Reducing solution

Hydriodic acid (500 ml, 57 %), hydrochloric acid (816 ml, 12 M), and hypophosphorous acid (245 ml, 50 %) were mixed. This reducing mixture was the same as that used by Thode et al. [12].

Procedure

All the samples were dissolved in 15 ml of a mixture (1+1+1) of 12 M hydro-

chloric acid, 16 M nitric acid and water, plus 3 drops of hydrofluoric acid, except for Inconel 713 and Hastelloy X, which did not dissolve in this mixture.

Dissolution of most samples

Dissolve 1 g of sample (chips or turnings) in 15 ml of the acid mixture in a 100-ml conical beaker covered with a watch glass; heat if necessary. After complete dissolution, add 1 ml of 16 M nitric acid and boil for several minutes. Add 1 g of 100 μg S g^{-1} spike solution. Evaporate to dryness and remove nitrate by repeated evaporation with 2-ml portions of 12 M hydrochloric acid. Dissolve the residue in 5 ml of 12 M hydrochloric acid with heating.

Dissolution of Inconel 713 and Hastelloy X

Dissolve 1 g of Inconel 713 in 50 ml of 12 M hydrochloric acid—16 M nitric acid mixture (3+2) by heating at about 150 °C for 2—3 h. Dissolve 1 g of Hastelloy X in 40 ml of 12 M hydrochloric acid—16 M nitric acid mixture (3+1) by heating at about 150 °C for 2—3 h. Then continue as described above.

Reduction of sulfate

Transfer 25 ml of reducing mixture to a 300-ml round-bottom flask with a reflux condenser. Remove any sulfur compounds present by passing a stream of nitrogen at a flow rate of 35 ml min^{-1} through the mixture heated at 200 °C for 1.5 h. Allow to cool for 30 min, then add the spiked sample solution and reflux at 180 °C with the stream of nitrogen for 1.5 h. Bubble the evolved hydrogen sulfide through water and absorb in a mixture of 10 ml of 0.1 M cadmium acetate and 20 ml of water. Convert cadmium sulfide to silver sulfide by adding 10 ml of 0.1 M silver nitrate. After ageing by heating, filter the silver sulfide precipitate through medium-texture paper, and wash with ammonia liquor and then with water. Dry the precipitate in an oven at 120 °C.

Burning

Cut off the upper part of the filter paper. Roll up loosely the bottom part which contains the silver sulfide. Place it in a platinum basket (Fig. 1). Flush the combustion bottle with oxygen and burn the sample in the usual manner described for organic materials [11].Absorb the water generated in phosphorus pentoxide in the first U-tube trap. Trap the evolved sulfur dioxide and carbon dioxide in the second trap which is cooled with liquid nitrogen. Pump off the remaining oxygen till the pressure drops below $1 \cdot 10^{-3}$ mmHg. Transfer the sulfur dioxide and carbon dioxide to the bottom part of a sampling bottle which is held at liquid nitrogen temperature, by replacing the liquid nitrogen of the second trap with a cooling mixture at about −20 °C. Remove carbon dioxide by pumping the sample at −108 °C, which is attained by using an isobutanol slush.

Isotope analysis

Measure the isotope ratio of sulfur in sulfur dioxide. From eight scans of

the mass peaks *m/e* 64 and *m/e* 66 in consecutive order, calculate the isotope ratio of $^{34}S/^{32}S$ by using the value [13] of the oxygen isotope ratio, $^{18}O/^{16}O$ = 0.00204, for correction.

Spike calibration

The spike solution was calibrated by i.d.m.s. mainly by using standard potassium sulfate solution. Later it was checked by using the standard sodium sulfate solution.

Weigh 2 g of spike solution and 1 g of standard solution in the same weighing bottle and carry out the reduction and burning as described above.

Blanks

Run a blank through the entire procedure.

RESULTS AND DISCUSSION

Isotope analysis

The relative standard deviation of single determinations of the $^{34}S/^{32}S$ ratio was better than 0.3 % for natural sulfur and better than 0.2 % for the 45 % enriched ^{34}S isotope. No appreciable fractionation of sulfur isotopes resulted from the sample preparation or during isotope measurement. Table 1 shows the $^{34}S/^{32}S$ ratios in some reagents and steels. It is well-known that the $^{34}S/^{32}S$ ratio for natural sulfur varies by a few percent or more depending on its origin [12]. But this variation in the isotope ratio has a very small effect on the accuracy of the determination of sulfur by i.d.m.s. For example, if the $^{34}S/^{32}S$ ratio in the sample varies by 3 %, its relative contribution to the atomic weight will be 0.009 % and that to the determination of 100 μg of natural sulfur will be 0.4 %. In this work the average value, $^{34}S/^{32}S$ = 0.04516, was used for calculations.

The isotope ratios for the enriched ^{34}S isotope, which was burned to sulfur

TABLE 1

Sulfur isotope ratios in reagents and steels

Material	Av. $^{34}S/^{32}S$	s	No. of scans
Elemental sulfur	0.044278	0.000089	10
Sodium sulfate	0.044912	0.000112	8
Potassium sulfate	0.045636	0.000119	8
Steel, BCS 211/1	0.045007	0.000105	8
Steel, JSS 152-4	0.045967	0.000092	8
Average	0.045160	0.000660	

dioxide in the combustion apparatus without any reduction procedure, were found to be 0.00886 (± 0.000009) for $^{33}S/^{32}S$, 0.82171 (± 0.00034) for $^{34}S/^{32}S$, and 0.000323 (± 0.000013) for $^{36}S/^{32}S$. The values are the averages of seven determinations with eight scans. From nuclidic mass data [14] the atomic weight of enriched ^{34}S isotope is calculated to be 32.873.

Spike calibration

Table 2 shows calibration data for the spike solution. Six mixtures were prepared by weighing standard solutions and the spike solution. The values obtained with potassium sulfate and sodium sulfate are in excellent agreement.

TABLE 2

Calibration of the spike solution

Calibrating material	Spike taken (g)	S found in spike (μg)	Concentration of spike (μg S g^{-1})
Sodium sulfate	2.0227	211.7_1	104.6_7
	2.0262	212.0_3	104.6_4
	2.0206	210.9_6	104.4_0
Average			104.5_7 ± 0.15
Potassium sulfate	2.0042	209.5_8	104.5_7
	2.0083	210.0_8	104.5_9
	2.0139	210.5_7	104.5_7
Average			104.5_8 ± 0.01

Determination of sulfur in standard samples

Table 3 shows the results obtained for JAERI (Japan Atomic Energy Research Institute) nickel-base alloy standards. Table 4 shows the results for NBS, BCS, and JSS (alloy steel standards); the value given for the BCS 211/1 is the average of eleven determinations over six months, during which two different spike solutions were used. In Tables 3 and 4, the method blank (μg S) was subtracted from the detected sulfur (μg). The method blank was usually 3.28 ± 0.19 μg (five determinations) of sulfur, but when reagent-grade hydrochloric and nitric acids were used instead of the super-special grade acids, the blank increased to 5.12 ± 0.78 μg (five determinations).

The results obtained by i.d.m.s. for the nickel-base alloys and alloy steels are consistently lower than the certified values. The most likely cause of these low results was thought to be loss of sulfur as hydrogen sulfide and/or sulfur dioxide during the decomposition. In order to examine this, two different procedures were tried: in the first, the sample was dissolved in a more strongly

TABLE 3

Determination of sulfur in nickel-base alloy standards

Sample	Isotope dilution (p.p.m. S)		Combustion method (% S)	
	Average[a]	s	Range	Average
Inconel X750 R1	38.5	0.4_1	0.004 —0.007	0.005[b]
Inconel X750 R2	40.1	0.6_1	0.003 —0.008	0.004[b]
Inconel X750 R3	45.9	1.3_4	0.003 —0.007	0.005[b]
Inconel 713 R4	42.3	2.4_7	0.004 —0.006	0.005[b]
Inconel 600 R5	17.9	0.5_6	0.002 —0.006	0.004[c]
Inconel 600 R6	47.5	1.1_4	0.004 —0.008	0.006[b]
Incoloy 800 R7	41.0	0.4_4	0.004 —0.008	0.006[c]
Incoloy 800 R8	31.0_7	0.07	0.004 —0.006	0.005[c]
Hastelloy X R9	3.3_2	0.3_5	0.0002—0.008	0.002[b]

[a]The values are the averages of 3—4 determinations, except for Hastelloy X (5 determinations).
[b]Thirteen laboratories participated in the analysis organized by the Sub-Committee on the Analysis of Reactor Materials, JAERI. Different combustion techniques and methods of completing the determination were used in most of the laboratories.
[c]Standard value of the Japanese Standards of Iron and Steel (JSS), Iron and Steel Institute of Japan, Tokyo. Eleven laboratories participated in the analysis.

TABLE 4

Determination of sulfur in alloy steels

Sample	Certified value (% S)	Isotope dilution (p.p.m. S)		
		Average	s	No. of detns.
13% Cr rustless steel, BCS 211/1	0.032	302.7	3.6	11
Ni—Cr steel, NBS 32e	0.021	171.5	0.8	5
Ni steel, NBS33d	0.010	86.1	1.1	3
Cr—Mo steel, NBS72f	0.024	196.9	1.5	6
Ni—Cr steel, JSS508-2	0.017	150.1	3.2	7

oxidizing solution (1 ml of bromine plus 15 ml of acid mixture); in the second, the evolved gas was collected in an oxidizing solution (10 ml of 7 % hydrogen peroxide plus 10 ml of 1 % sodium hydroxide solution) during dissolution. The first modification was applied to NBS 32e and the second to JAERI R7; both procedures were applied to BCS 211/1, NBS 72f, and JSS 508-2. None of the results obtained by these methods showed significant differences, indicating that no sulfur was lost during the decomposition. Therefore, all the results were included in the calculation of average values.

The precision of the gravimetric determination is within 0.002 % S in normal

ranges, and the addition of a known amount of sulfate is desirable for less than 0.015 % S [15]; thus the results obtained in this work are in reasonably good agreement with the certified values. The accuracy of the accepted combustion procedures depends very largely on the accuracy of the calibration standards used, and no reliable standards are available for less than 0.005 % S.

In this work, carbon steels which could evolve hydrogen sulfide easily during dissolution were not analyzed, but the proposed method should be applicable if a strong oxidizing reagent were used in the dissolution with an oxidizing absorbent for volatile sulfur compounds.

The author is grateful to Mr. S. Tamura, and Dr. T. Komori, JAERI, for valuable advice, and to Dr. T. Sakaki, Japan Special Steel Co. Ltd., for some NBS samples.

SUMMARY

An isotope dilution mass spectrometric method has been developed for the precise determination of 3—300 p.p.m. of sulfur in nickel-base alloys and alloy steels. The sample is dissolved in mixed acids, a spike is added, and nitrate ions are removed. Sulfate is reduced with a mixture of hydriodic, hypophosphorous, and hydrochloric acids; the hydrogen sulfide evolved is absorbed in cadmium acetate solution and converted to silver sulfide, which is burned to sulfur dioxide, for the isotope analysis. The relative standard deviation at the 50-p.p.m. level for 1-g samples is less than 3 %.

REFERENCES

1 Amer. Soc. Test. Mater., Proc., E350 (1974).
2 K.E. Burke, Anal. Chem., 39 (1967) 1727.
3 R. Kajiyama and K. Hoshino, Analyst (London), 96 (1971) 835.
4 T.S. Harrison and R.J. Spikings, Anal. Chim. Acta, 67 (1973) 145.
5 C.L. Luke, Anal. Chem., 29 (1957) 1227.
6 C.L. Luke, End. Eng. Chem., Anal. Ed., 15 (1943) 602.
7 C.L. Luke, Anal. Chem., 21 (1949) 1369.
8 C.M. Johnson and H. Nishita, Anal. Chem., 24 (1952) 736.
9 J.B. Davis and F. Lindstrom, Anal. Chem., 44 (1972) 524.
10 A.D. Kirshenbaum and A.V. Grosse, Anal. Chem., 22 (1950) 613.
11 A.M.G. MacDonald, in C.N. Reilley (Ed.), Advances in Analytical Chemistry and Instrumentation, Vol. 4, Interscience—Wiley, New York, 1965, p. 75.
12 H.G. Thode, J. Monster and H.B. Dunford, Geochim. Cosmochim. Acta, 25 (1961) 159.
13 A.O. Nier, Phys. Rev., 77 (1950) 789.
14 J.H.E. Mattauch, W. Thiele and A.H. Wapstra, Nucl. Phys., 67 (1956) 1.
15 B. Bagshawe and A.L. Pill, Analyst (London), 80 (1955) 796.

Analytica Chimica Acta, 80 (1975) 125—133

THE EXCITON EFFECT IN DIKETONATE COMPLEXES AND ITS APPLICATION TO THE SPECTROFLUORIMETRIC DETERMINATION OF EUROPIUM

S. J. LYLE and R. MAGHZIAN*

Chemical Laboratory, University of Kent at Canterbury, Kent CT2 7NH (England)

(Received 5th May 1975)

SUMMARY

A method based on a new analytical principle is described for the determination of μg quantities of europium in lanthanides. The fluorescence intensity from europium(III) in a pulverized solid is measured at 611 nm, with excitation at 366 nm. The solid, prepared by coprecipitation from solution, consists of mixed crystals formed by isomorphous replacement of lanthanum in a host lattice of $[pip][La(bta)_4]$, where bta^- is derived from 1,1,1-trifluoro-4-phenylbutane-2,4-dione and pip is the piperidinium cation. A large constant amount of lanthanum (200 mg) is added to the sample containing < 5 mg of lanthanide; complete precipitation of the lanthanides is unnecessary. The solid sample is measured directly in a demountable cell in a holder, which fits the cell compartment of a commercial spectrophotofluorimeter. A rectilinear relation exists between the fluorescence intensity and the europium content over a wide range of concentrations. Of the lanthanides and yttrium, only cerium and neodymium interfere if their respective ratios to added lanthanum exceed 1/1000 (w/w). The precision attained is less satisfactory, but interferences from other lanthanides are less serious, than those found in solution methods involving diketonate complexes. Higher sensitivity can be obtained by minor modifications.

The absorption and emission of light by europium(III) complexes with β-diketones has received considerable attention in recent years because of earlier promise in laser systems. Irradiation of many tris- and tetrakis-complexes of this type in the near u.v. spectral region produces orange—red fluorescence characteristic of the europium(III) ion. The emission may be observed in solution or in the solid, the intensity being dependent on the nature of the complex. A great deal of work has been done on the mechanism whereby light initially absorbed by the ligand is transferred to the metal ion [1]. It is widely considered that the transfer is an intramolecular process following the energy path, singlet (ground) → singlet (excited) → triplet states (all on the ligand) → metal ion. However, Curran and Shepherd [2] reported recently that in the complex $[pip][Gd(bta)_4]$ light absorbed by its ligands could be passed on to excite europium(III) present as impurity

*On leave from the University of Isfahan, Isfahan, Iran.

even at considerable dilution of the latter. [In the formula, pip is the piperidinium cation and bta^- the ligand derived from 1,1,1-trifluoro-4-phenylbutane-2,4-dione(Hbta)]. Several lanthanide ions, e.g. lanthanum(III) and gadolinium(III) do not accept excitation energy as described above from the ligand. Thus Curran and Shepherd were able to show that the energy transfer in this instance was intermolecular, probably occurring by a "bound" triplet exciton process. The effect is therefore confined to solids.

It has been found in the course of the work reported here that the effect also occurs in [pip] [$La(bta)_4$] when europium(III) is present at low concentrations. Some preliminary work to explore the potential of this complex as a matrix for the spectrophotofluorimetric determination of small amounts of europium is described below.

EXPERIMENTAL

Reagents

Standard solutions of 0.14 M $La(NO_3)_3$ and 0.05 M $Eu(NO_3)_3$ were prepared in 95% (v/v) ethanol. From the europium solution, further dilutions in 95% ethanol were made as required. The metal nitrates and those, except cerium, used in interference tests were prepared from oxides of 99.9% purity (Koch-Light Ltd.). The other reagents used were $Ce(NO_3)_3 \cdot 6H_2O$ (Hopkin and Williams Ltd.), ^{152}Eu and ^{154}Eu, in admixture, of high specific activity (Radiochemical Centre, Amersham) Hbta and other diketones (Koch-Light, "pure"), and piperidine (reagent grade, Fisons Scientific Apparatus Ltd.).

Preparation of the complex

The total lanthanide content of the sample should not exceed about 5 mg in the nitrate form in 95% ethanol. To it is added 200 mg of lanthanum(III), i.e. 10 ml of 0.14 M $La(NO_3)_3$ stock solution, and the mixture is poured into a freshly prepared solution consisting of Hbta (0.9 g) and piperidine (0.5 ml) in 95% ethanol. The precipitate of [pip] [$La(Eu)(bta)_4$] is obtained by evaporating the solution, initially about 50 ml in volume, under reduced pressure at 40—50°C until the volume is about 15 ml. The concentrate is cooled in an ice bath to induce precipitation. The precipitate is collected by filtration under suction, washed with cold 50% (v/v) ethanol/water solution (10 ml), and dried at 80—90°C for 20 min. The total time required for a single complete preparation is about 50 min.

Instrumentation

An Aminco-Bowman spectrophotofluorimeter was used for the measurements. The light source is a mercury—xenon lamp but measurements can also be performed satisfactorily, albeit with lower fluorescent emission

output, with a xenon lamp. (Both lamps are available with the instrument.)

Cell and cell-holder

The cell housing supplied with the instrument to take quartz cells of square cross-section 1.2 cm edge (external) and 4.5 cm long, for measurements on liquid samples was adapted to take the specially designed cell and holder shown in Figs. 1 and 2. Figure 1 provides 4 plans and corresponding

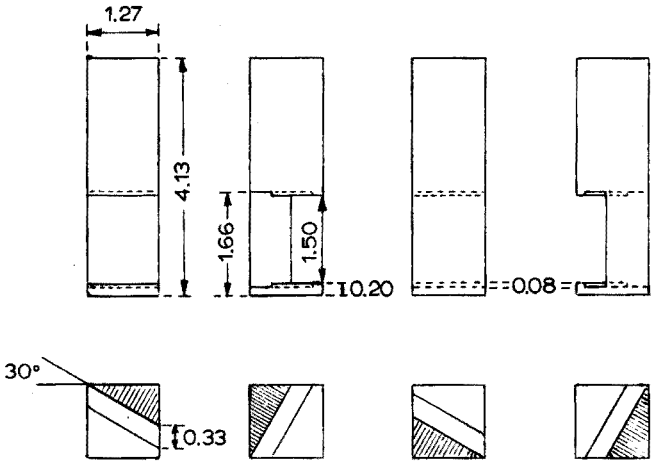

Fig. 1. The aluminium cell holder in plan and elevation. (Dimensions in cm.)

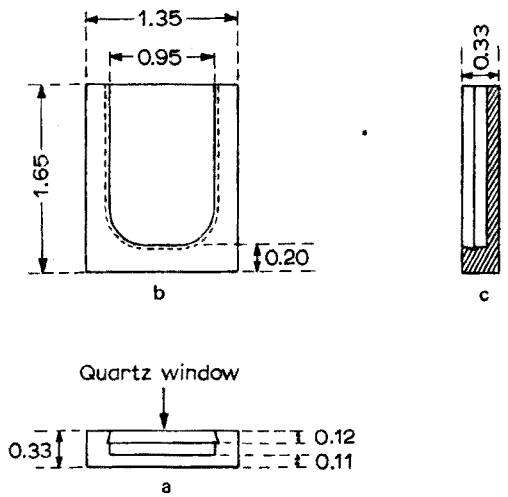

Fig. 2. The cell assembly (a) in plan, (b) in elevation and (c) in side view. The quartz window, dovetailed to the aluminium body of the cell, is detachable. (Dimensions in cm.)

elevations of the holder which was machined from aluminium rod of square cross-section. A part of the rod was cut away to the point where the new internal face passed through one corner making an angle of 30° with the remaining complete side of the rod. The floor and ceiling of the cut-away section each had a shallow channel 0.33 cm wide and 0.075 cm deep cut as shown to enable the cell to slide into place in the holder.

The assembled cell with demountable quartz window but otherwise constructed from aluminium is shown in plan (Fig. 2(a)), elevation (Fig. 2(b)) and side view (Fig. 2(c)). A dovetail fit of window to metal base ensures constancy of geometry.

Measurement

The dry precipitate was pulverized in an agate mortar and 30—40 mg transferred to the cell; uniformity of packing was achieved by tapping the cell and contents. The cell-holder with cell in position was placed in the sample compartment of the fluorimeter in such a way that excitation radiation of 366 nm struck at 30° to the quartz window. The emission intensity at 611 nm was determined for each sample at room temperature. Slit widths of 0.5 mm were used.

The radioactive europium-containing precipitates (10 mg of each) were dissolved in 2 ml of 12 M hydrochloric acid and diluted to 12 ml with ethanol. A 10 ml portion of each solution was counted with an annular type Geiger—Muller counter.

RESULTS AND DISCUSSION

Preliminary experiments with [pip][$La(bta)_4$] showed that, with the quality of La_2O_3 used, the europium content was below that detectable by its fluorescence at 611 nm. However, the addition of 100 p.p.m. (w/w) of europium to the lanthanum in the complex, for example, gave a strong fluorescence not observed from a similar amount of europium in the absence of lanthanum. Likewise dissolution of the mixed lanthanide complex in pure ethanol or EPA (ether:isopentane:ethanol in the ratio 5:5:2, (v/v)) solvent mixture (40 mg in 5 ml of each solvent) resulted in total loss of europium fluorescence. It can therefore be concluded that, as in the work of Curran and Shepherd [2] on [pip][$Gd(Eu)(bta)_4$], the europium(III) excitation is an intermolecular exciton process confined to the solid state. Gadolinium is considerably more difficult to produce free from europium than lanthanum, which is therefore more economical in an analytical context.

Earlier work [3] on a range of diketones showed that the tetrakis complexes of europium(III) formed from 1-phenylbutane-1,3-dione (Hba), 1,3-diphenylpropane-1,3-dione (Hdbm) and 1,1,1-trifluoro-4-(2-thienyl)-butane-2,4-dione (Htta) as well as Hbta had high fluorescence output. (It should be noted that in Ref. 3, Table 3, [$Eu(tfa)_4$][pip] ought to read

$[Eu(tta)_4][pip]$.) Table 1 compares the relative intensities from 100 p.p.m. (w/w) europium in the corresponding lanthanum complexes. The $[pip][La(Eu)(tta)_4]$ complex is difficult to prepare pure in a reasonable time by the method given here. It is unlikely to be suitable for analytical purposes and consequently was omitted from the comparison. It is seen that for europium(III) excitation dependent on an exciton process, the bta^- complex is more efficient than the corresponding ba^- or dbm^- complexes.

A plot of intensity of fluorescence against europium content, measured by the europium to lanthanum ratio in the solution from which the mixed complex $[pip][La(Eu)(bta)_4]$ was precipitated, is shown in Fig. 3. It is probably linear over a considerably greater range than that presented. However, there is some scatter about the curve and this is reflected in the reproducibility of the whole determination. The mean fluorescence intensity recorded and the standard deviation of the mean for 10 separate complete determinations of 100 p.p.m. (w/w) europium in lanthanum were 21.2 and 2.2, respectively. About half this scatter was associated with filling the cell and making the measurement, e.g. for 10 fillings, from a common source of sample, the mean and standard deviation were 19.8 and 1.2, respectively.

In none of the precipitations of the mixed diketonate complexes described

TABLE 1

Comparison of the relative fluorescence intensities of diketonate complexes containing europium

Matrix complex	$[pip][La(bta)_4]$	$[pip][La(ba)_4]$	$[pip][La(dbm)_4]$
Relative intensity	260	120	20

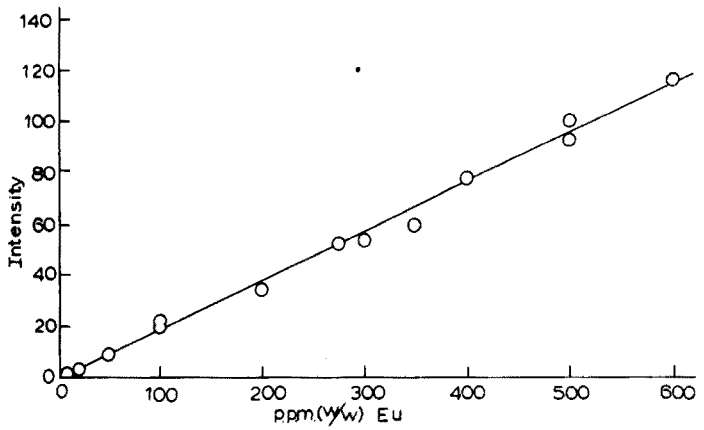

Fig. 3. A plot of fluorescence intensity at 611 nm against europium content (measured in p.p.m., (w/w) relative to lanthanum) of the mixed complex $[pip][La(Eu)(bta)_4]$.

here was any attempt made to obtain complete precipitation, or indeed precipitation of a fixed fraction of the total lanthanides present. The method assumes that the relation

$$(Eu/La)_{Solid} = (Eu/La)_{Total} \quad (1)$$

holds for all practically convenient ratios and fractions of the total lanthanum precipitated. Experiments based on europium labelled with an admixture of ^{152}Eu and ^{154}Eu of constant specific activity were used to demonstrate the validity of the assumptions embodied in eqn. 1 to the extent that they are relevant here. Table 2 gives the results of experiments in which various ratios of europium to lanthanum were used in the precipitation of [pip] [La(Eu)(bta)$_4$], under the conditions given in the experimental section. The activities normalized to that corresponding to 100 p.p.m. of europium are constant within experimental error, as would be expected if eqn. (1) held. The relative fluorescence intensities observed fit on the line shown in Fig. 3, so that the samples were typical of those produced in the course of the work. (It may be noted in this context that frequent checks on the quality of the [pip] [La(Eu)(bta)$_4$] precipitates were made through determination of the C, H and N content). Experiments in which two batches of crystals were produced successively from a common mother liquor gave the same activity per unit weight of precipitate, thus demonstrating the independence of the ratio in eqn. (1) on the fraction of lanthanum precipitated. Provided that the europium(III) and lathanum(III) complexes with Hbta are isostructural, as is almost certainly the case, coprecipitation will follow from isomorphous displacement of "carrier" by trace component in the host crystal. Application of either of the two applicable limiting laws [4], representing homogeneous and logarithmic distributions of minor component, to the system will give eqn. (1) if their coefficients, D and λ respectively, are set equal to unity. This means that segregation of europium and lanthanum does not occur during precipitation. Since the procedure devised for each precipitation is such that the total amount of lanthanum is always held

TABLE 2

Coprecipitation of labelled europium with lanthanum

Eu p.p.m. (w/w)	Measured activity (c.p.m.) /mg ppt.	Normalized activity[a]	Relative fluorescence intensity
25	360	1440	5.0
100	1530	1530	21.5
200	2770	1385	40.0
300	4430	1477	57.5

[a]Normalized to that expected if 100 p.p.m. europium had been used in the precipitation.

effectively constant, it follows from eqn. (1) that the europium content of the crystalline product, [pip][La(Eu)(bta)$_4$], is directly proportional to the total europium present in the original sample irrespective of the fraction of lanthanum precipitated.

In testing for interferences from other elements it was assumed that the method would only be applied to mixtures of lanthanides, perhaps with yttrium present, obtained from a group separation of elements. Some data derived from the tests are presented in Table 3. Not all lanthanides were tested but those excluded from the Table, and yttrium, are not expected to interfere up to at least 10000 p.p.m. (w/w) relative to lanthanum when each is taken separately with europium. Cerium and neodymium interfere when more than 1000 p.p.m. of each is present. The [pip][Ce(bta)$_4$] complex has a bright orange colour which may be due to surface oxidation of the crystals giving cerium(IV). When cerium is coprecipitated with lanthanum, the normally colourless crystals acquire the orange colour at cerium concentration levels reflected in the results presented in Table 3. Attempts to prevent the colour formation by the addition of small amounts of reducing agents, e.g. hydroxylamine or hydrazine, to the reaction mixture were unsuccessful. The presence of the colour in the mixed crystals may be used as an indicator for cerium interference in a determination of europium. Neodymium interferes for reasons discussed at some length by Curran and Shepherd [2] in work in which [pip][Gd(bta)$_4$] was used as the matrix crystal. In a light rare earth fraction, cerium is likely to be the most abundant element present (besides lanthanum) and a preliminary separation would be necessary unless a sufficiently small sample can be taken to ensure

TABLE 3

Interference tests with M^{3+} in [pip][La(Eu,M)(bta)$_4$] (M^{3+} is a lanthanide ion. Each sample had 100 p.p.m. (w/w) of europium and the amount of M^{3+} given in column 2, both with respect to lanthanum.)

M^{3+}	Amount present (p.p.m., w/w)	Relative fluorescence intensity
—	—	20.5
Ce	10000	2.5
	5000	8.2
	1000	19.2
Nd	5000	11.0
	1000	19.5
Sm	10000	20.5
Gd	10000	21.3[a]
Tb	10000	21.6[a]
Yb	10000	21.5

[a] After accounting for europium originally present in M^{3+} by a method of addition.

that the Ce/La ratio in the preparation of the complex does not exceed 1/1000 (w/w). This latter consideration also applies to neodymium which will normally be considerably less abundant, at least in mixtures of natural origin [5]. Fortunately cerium is readily separated from all other lanthanides so that the neodymium content of a sample may present the only serious problem. In spite of this limitation, the general tolerance to other lanthanides is markedly better in this method than in the method in which the fluorescence from a europium(III) diketonate complex is measured in solution [6]. Indeed some lanthanides capable of promoting exciton-induced fluorescence in europium when mutually incorporated in complexes formed from Hbta may only interfere when the quantity present has a significant diluting effect on the lanthanum host on mixed crystal formation. For quantitative purposes the maximum amount of host crystal capable of being produced in each determination must remain effectively constant. The total lanthanide content of the sample should therefore be restricted as suggested in the Experimental section for preparation of the mixed complex.

The method has been used to analyse various synthetic samples of europium in the absence and in the presence of other lanthanides. Table 4 gives some results for samples prepared without the analyst having prior knowledge of the lanthanide content. It is seen that the discrepancies between the observed and corresponding arranged values are not usually more than 10%. Furthermore, the method is probably capable of much higher sensitivity than that displayed in these measurments. The sample having 100 p.p.m. (w/w) of europium relative to lanthanum in the measuring cell of the spectrofluorimeter will contain just under 40 ng of europium. Considerably less europium can be determined by using a higher sensitivity setting on the spectrofluorimeter and the amount could possibly be reduced further by making use of a mercury line at a shorter wavelength to increase the intensity of excitation. With these instrumental changes the sensitivity could probably be increased by two orders of magnitude, thus taking the europium content in the measuring cell down to pg levels. Further experimentation is in progress to improve the precision, sensitivity and scope of the method.

TABLE 4

Results for some synthetic lanthanide samples containing europium

M^{3+}	M^{3+} present (p.p.m., w/w)	Relative intensity	Eu found (p.p.m., w/w)	Eu present (p.p.m., w/w)
—	—	7.5	40	50
—	—	21.2	110	100
—	—	39.0	205	200
Y + Ce + Nd + Yb	1000 of each	15.0	79	80
voluit × 4	voluit × 4	19.2	101	100
		20.5	107	100
		21.0	110	100
		39.2	210	200

REFERENCES

1 G. A. Crosby, Mol. Cryst., 1 (1966) 37.
2 J. S. Curran and T. M. Shepherd, J. Chem. Soc., Faraday II, 69 (1973) 126.
3 S. J. Lyle and A. D. Witts, J. Chem. Soc., Dalton, (1975) 185.
4 N. A. Bonner and M. Kahn in A. C. Wahl and N. A. Bonner (Eds.), Radioactivity Applied to Chemistry, Wiley, New York 1951, Ch. 6.
5 O. A. Songina, Rare Metals, U.S. Dept. of the Interior and the Nat. Science Foundation 1970, Ch. VI. (Translated from the Russian, Redkie Metally, 3rd edn. by J. Schmorak.)
6 D. E. Williams and J. C. Guyon, Anal. Chem., 43 (1971) 139.

Analytica Chimica Acta, 80(1975)135—141

KINETIC DETERMINATION OF TRACES OF MANGANESE(II) BY ITS CATALYTIC EFFECT ON THE OXIDATION OF ACID BLUE 45 WITH HYDROGEN PEROXIDE

SHIGEKI ABE, KUNIO TAKAHASHI and TSUTOMU MATSUO
Department of Applied Chemistry, Yamagata University, Yonezawa (Japan)
(Received 2nd April 1975)

Recently, increasing numbers of analytical applications of the kinetic method of analysis have been published and a variety of catalyzed reactions has been proposed for the determination of manganese(II) at low concentrations. Fernandez et al. [1] used the catalytic oxidation of leucomalachite green by sodium periodate for trace determination of manganese in blood serum. Mottola and Harrison [2] have shown that manganese(II) can catalyze the reaction of periodate with malachite green. Janjic et al. [3] determined manganese by its effect on the hydrogen peroxide—alizarin red S reaction; the sensitivity of the method is 0.3 ng Mn ml^{-1}. Catalytic oxidation of some aromatic amines — *p*-phenetidine [4], *p*-anisidine and *o*-dianisidine [5] — by potassium periodate has also been applied for the kinetic determination of manganese. Although these catalyzed rate methods offer highly sensitive and selective analyses, only a few attempts have been made to elucidate the mechanism of the reaction, mainly because of the complexity of the systems and the nature of the results obtained. Less complicated indication reaction systems are desirable from an analytical point of view.

In connection with an investigation into the use of manganese(II) as a catalytic titrant, a considerable increase was observed in the rate of oxidation of aminoanthraquinone dyes by hydrogen peroxide in hydrogencarbonate media [6]. Kinetic studies of the manganese(II)-catalyzed oxidation of acidic dyes showed that Acid blue 45 (C.I. 63010; the disodium salt of 1,5-diamino-4,8-dihydroxyanthraquinone-3,7-disulfonic acid) possesses satisfactory stability in alkaline solution and good sensitivity to a manganese catalyst. The present paper describes a kinetic method for the determination of trace amounts of manganese based on this catalytic effect. The method allows the determination of as little as 2 ng Mn ml^{-1}.

EXPERIMENTAL

Reagents and apparatus

All chemicals, except the anthraquinone dyes used, were of reagent grade and deionized—distilled water was employed throughout.

Standard manganese(II) solution, 500 μg Mn ml^{-1}

An aqueous solution of manganese(II) sulfate was prepared and standardized by titration with EDTA and eriochrome black T indicator. The stock solution was diluted as required immediately before use.

Hydrogen peroxide, 1.02 M

Hydrogen peroxide solution (30 %, w/w) was diluted with water and standardized iodimetrically, using starch as indicator.

Acid blue 45 (C.I. 63010)

A commercial dye (Solway Blue BN, Imperial Chemical Industries Ltd.) was purified by an adaptation of the method of Robinson and Mills [7]. It was recrystallized several times from saturated sodium acetate solution. The solution of dye was prepared by dissolving the required weight in water. The molar absorptivity of Acid blue 45 in 0.28 M ammonium carbonate solution is $1.53 \cdot 10^4$ at 595 nm.

For preliminary experiments, some readily available sulfonated derivatives of anthraquinone dye were used, i.e. alizarin red S (C.I. 58005), Acid blue 25 (C.I. 62055), Acid violet 43 (C.I. 60730) and Acid green 25 (C.I. 61570).

A Hitachi Model 139 spectrophotometer with 10-mm cells, a Hitachi–Horiba Model M-5 pH meter and a Toa Model EPR-2TC thermo-recorder equipped with a glass thermistor were used for kinetic measurements. The cell compartment of the spectrophotometer was thermostated at 25 ± 0.1 °C by circulating water.

Procedure

The reaction was followed spectrophotometrically by measuring the rate of change in absorbance of Acid blue 45 at 595 nm. All reactants were kept in a thermostated bath at 25 ± 0.1 °C before the beginning of the reaction.

Place an aliquot of manganese(II) solution into a calibrated volumetric flask (50 ml). Add 10 ml of 2 M ammonium carbonate solution and 2 ml of 0.05 % Acid blue 45 ($1.055 \cdot 10^{-3}$ M) solution, and dilute with distilled water to 48 ml. Then add 2 ml of 0.5 M hydrogen peroxide to the test solution and shake well. Start the timer right after the addition of hydrogen peroxide. Transfer a portion of reaction mixture to a thermostated 10-mm spectrophotometer cell and follow the reaction by recording the absorbance at various reaction times. Calculate the rate of the reaction from the slope of the absorbance–time curve.

The reaction conditions were chosen so that the rate of the uncatalyzed reaction was very small compared with that of the catalyzed reaction.

RESULTS AND DISCUSSION

Manganese(II)-catalyzed oxidation of Acid blue 45 with hydrogen peroxide

Reaction rate studies were made by following the rate of change in absorbance at 595 nm, at which Acid blue 45 has an absorption maximum in carbonate media.

A typical plot of absorbance versus time for the catalytic oxidation of Acid blue 45 is shown in Fig.1. Besides manganese(II), copper(II) also catalyzed the reaction in ammonium carbonate solution. In both cases, a linear relationship was obtained between absorbance and time, suggesting zero-order kinetics for the oxidation of the dye under the experimental conditions.

In any catalytic reaction system, the uncatalyzed reaction proceeds at a finite rate, and the kinetic aspects of some anthraquinone dyes were therefore investigated. The results are shown in Fig.2. In contrast to the uncatalyzed oxidation of alizarin red S, which is known to follow first-order kinetics [3], the oxidation of Acid blue 45 proceeds linearly with time. Apparently Acid blue 45 is much more stable than alizarin red S towards attack by hydrogen peroxide.

Effects of reaction variables

The effect of hydrogen peroxide on both the uncatalyzed and the manganese(II)-catalyzed oxidation of Acid blue 45 is shown in Fig.3. In the presence of manganese, the variation in the reaction rate slope (tg α) showed a half-order response to hydrogen peroxide concentration, whereas the rate of the uncatalyzed reaction increased linearly, indicating first order with respect to hydrogen peroxide.

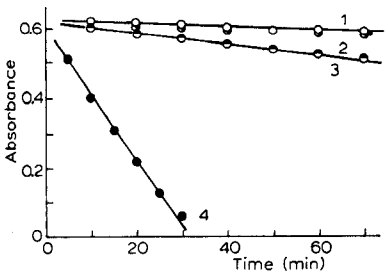

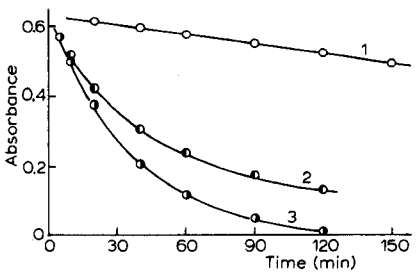

Fig.1. Metal ion-catalyzed oxidation of Acid blue 45 in ammonium carbonate solution. (1) Blank (○); (2) Co^{2+}, 24.0 ng ml^{-1} (◑); (3) Cu^{2+}, 29.6 ng ml^{-1} (◓); (4) Mn^{2+}, 18.8 ng ml^{-1} (●). Reaction conditions: $4.22 \cdot 10^{-5}$ M Acid blue 45, $4.0 \cdot 10^{-1}$ M $(NH_4)_2CO_3$, $4.08 \cdot 10^{-2}$ M H_2O_2.

Fig.2. Uncatalyzed oxidation of anthraquinone dyes with hydrogen peroxide. (1) Acid blue 45 (○, 595 nm); (2) alizarin red S (◐, 515 nm); (3) acid violet-43 (◑, 572 nm). Reaction conditions are: $4.22 \cdot 10^{-5}$ M dye, $4.0 \cdot 10^{-1}$ M $(NH_4)_2CO_3$, $4.08 \cdot 10^{-2}$ M H_2O_2.

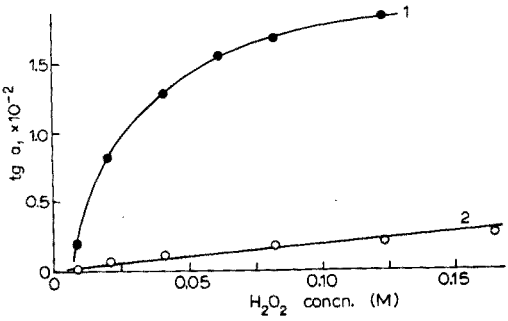

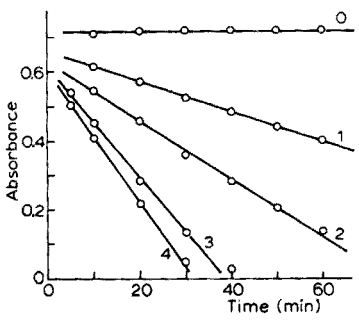

Fig.3. Effect of hydrogen peroxide concentration on catalyzed and uncatalyzed oxidation of Acid blue 45. (1) Mn^{2+}-catalyzed reaction ($2.34 \cdot 10^{-7}$ M Mn, ●); (2) uncatalyzed reaction (○). Reaction conditions are: $4.22 \cdot 10^{-5}$ M Acid blue 45, $2.8 \cdot 10^{-1}$ M $(NH_4)_2CO_3$.

Fig.4. Effect of carbonate concentration on catalyzed oxidation of Acid blue 45. $(NH_4)_2CO_3$: (0) nil; (1) 0.1 M; (2) 0.2 M; (3) 0.3 M; (4) 0.4 M. Reaction conditions: $3.42 \cdot 10^{-7}$ M Mn^{2+}, $4.22 \cdot 10^{-5}$ M Acid blue 45, $2.04 \cdot 10^{-2}$ M H_2O_2.

The effect of the ammonium carbonate concentration on the reaction rate was studied (Fig.4). The rate of the catalytic reaction depended linearly on the carbonate concentration up to about 0.3 M, but then showed a slower change at higher carbonate concentrations. Subsequent reaction rate studies were made at a carbonate concentration of 0.28 M.

The pH-dependence of the system was studied for mixtures of ammonium carbonate and ammonium hydrogencarbonate giving a total carbonate concentration of 0.28 M. From Table 1, it is evident that the manganese-catalyzed oxidation of the dye was first order with respect to hydrogencarbonate concentration and that the rate was inversely proportional to the square root of the hydrogen ion concentration in the pH range 8.4—9.7. It was confirmed that manganese(II) showed no catalytic action on the oxidation of anthraquinone dyes with hydrogen peroxide in sodium carbonate solution (pH 12). Similar phenomena have been observed for the catalytic oxidation of aromatic amines such as *p*-anisidine, *p*-phenetidine and *o*-dianisidine [8]. The role of hydrogencarbonate and hydrogen ions will be discussed later.

The rate of the manganese-catalyzed reaction increased about 1.3 times with a rise of temperature from 20 to 30 °C. The dependence of the rate on temperature indicated that the activation energy is relatively small for this catalyzed reaction.

Rate equation

On the basis of the kinetic investigation, the following kinetic equation is suggested for the manganese(II)-catalyzed oxidation of Acid blue 45 with hydrogen peroxide in hydrogencarbonate media.

$$-\frac{d[\text{Dye}]}{dt} = K[H^+]^{-\frac{1}{2}}[HCO_3^-][H_2O_2]^{\frac{1}{2}}[Mn^{2+}] + k[H_2O_2]$$

TABLE 1

Dependence of reaction rate on hydrogen and hydrogencarbonate ions

Composition (mol l^{-1})		tg α ($\cdot 10^{-3}$)	$[H^+]$ ($\cdot 10^{-10}$)	$[HCO_3^-]$ ($\cdot 10^{-1}$)	$\frac{\text{tg } \alpha}{[H^+]^{-1/2}[HCO_3^-]}$ ($\cdot 10^{-7}$)
$(NH_4)_2CO_3$	NH_4HCO_3				
—	0.28	2.41	38.0	2.74	5.43
0.02	0.26	3.61	19.1	2.72	5.81
0.04	0.24	5.05	11.8	2.70	6.42
0.08	0.20	6.16	7.95	2.66	6.53
0.12	0.16	7.09	5.50	2.58	6.43
0.16	0.12	7.50	4.17	2.52	6.07
0.20	0.08	8.80	2.82	2.41	6.13
0.28	—	8.92	2.00	2.28	5.52

where [Dye] is the concentration of Acid blue 45, and K and k are the conditional rate constants. The values of K and k were found to be $1.1 \cdot 10^{-3}$ and $1.9 \cdot 10^{-6}$, respectively, for the experimental conditions used.

Although at the present time it is difficult to describe the mechanism of this catalytic reaction completely, the rate equation that has been derived is adequate for discussion of the use of the reaction in the catalytic determination of manganese. The rate of the Acid blue 45 oxidation is zero order with respect to dye concentration, so that the dye does not participate in the rate-determining step. In the absence of the anthraquinone dye, the thermometric response for the manganese(II)-catalyzed decomposition of hydrogen peroxide was investigated. The reaction was exothermic in hydrogencarbonate media, a sharp rise of temperature being observed on the addition of manganese catalyst, whereas no appreciable temperature change was found in sodium carbonate solution (pH 12). Manganese(II) showed no catalytic action toward hydrogen peroxide in formate solution of pH 7.9. These facts indicate that the reaction involving manganese(II), hydrogen peroxide, hydrogencarbonate ion and reaction product must be rate-determining and must give rise to some oxidizing species that will react rapidly with the dye. Seemingly, an intermediate hydrogen peroxide complex with hydrogencarbonate is involved in the manganese(II)-catalyzed oxidation of anthraquinone dyes.

It is known that α,β-unsaturated ketones such as naphthoquinone are oxidized with hydrogen peroxide in basic media and naphthoquinone rings are easily cleaved [9].

Calibration curve

For experimental convenience, the tangent method was applied and the rate of the catalyzed reaction was plotted as a function of manganese concentration.

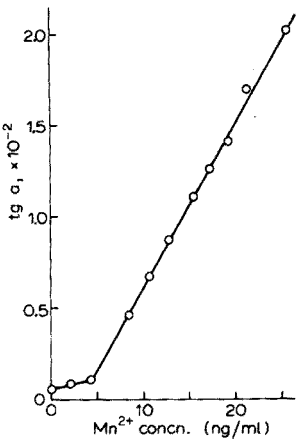

Fig.5. Calibration graph for manganese (II). Reaction conditions: $4.22 \cdot 10^{-5}$ M Acid blue 45, $2.8 \cdot 10^{-1}$ M $(NH_4)_2CO_3$, $2.04 \cdot 10^{-2}$ M H_2O_2.

The calibration graph (Fig.5) is linear in the concentration range 4—25 ng Mn^{2+} ml^{-1}. The limit of determination is 2 ng ml^{-1}. The relative standard deviation for ten determinations of 12.9 ng Mn ml^{-1} was 1.9 %.

Study of interferences

In order to assess possible analytical applications of the reaction, the influenc of foreign ions on the reaction rate in the presence of manganese(II) was exam-

TABLE 2

Influence of foreign ions
($2.34 \cdot 10^{-7}$ M manganese(II) present)

Foreign ion	$\frac{[Ion]}{[Mn^{2+}]}$	tg α ($\cdot 10^{-3}$)	Foreign ion	$\frac{[Ion]}{[Mn^{2+}]}$	tg α ($\cdot 10^{-3}$)
—	—	8.7	Nitrate[d]	100	8.6
Mg(II)[a]	100	8.6	Chloride[d]	100	8.5
Ni(II)[a]	100	8.6	Sulfate[e]	100	8.4
Zn(II)[b]	100	8.2	Phosphate[f]	100	8.5
Cd(II)[a]	100	8.5	Tartrate	100	7.7
Pb(II)[b]	100	8.3		10	8.4
Cu(II)[c]	10	2.6			
	1	4.1			

[a] Added as chloride.
[b] Added as nitrate.
[c] Added as sulfate.
[d] Added as ammonium salt.
[e] Added as potassium salt.
[f] Added as sodium salt.

ined. The results are summarized in Table 2. With regard to cation interferences, copper(II) showed significant interference and must be absent from the solution (cf. Fig.1). Iron(III) was omitted from this study as it could not be kept in the alkaline solution and was therefore of little practical importance as an interferent.

Common anions such as chloride, nitrate, sulfate and phosphate did not interfere, while tartrate in a 100-fold amount retarded the reaction appreciably.

Application of indication reaction to titrimetry

Several manganese(II)-catalyzed oxidation reactions have already been used for end-point indication in titrimetric analysis. Weisz and Pantel [10] have discussed the principles of such applications of catalyzed reactions.

The Acid blue 45 system has been utilized to indicate the end-point of titrations of manganese with EDTA [6]. It has an advantage over other dye indicators that no appreciable fading was observed near the end-point, and accurate results were obtained.

SUMMARY

A catalytic method is described for the determination of trace amounts of manganese(II) based on its catalytic effect on the hydrogen peroxide oxidation of an anthraquinone dye, Acid blue 45 (C.I. 63010). The reaction is followed spectrophotometrically by measuring the rate of change in absorbance of the dye at 595 nm. The calibration graph (rate constant (tg α) vs. manganese concentration) is linear in the range 4—25 ng Mn ml^{-1}, the relative standard deviation being 1.9 % at the 13 ng Mn ml^{-1} level. There are few interferences. The kinetic parameters of the reaction were investigated and the role of hydrogen peroxide and hydrogencarbonate ions is discussed.

REFERENCES

1 A. Fernandez, C. Sobel and S. Jakobs, Anal. Chem., 35 (1963) 1721.
2 H.A. Mottola and C.R. Harrison, Talanta, 18 (1971) 683.
3 T. Janjic, G.A. Milovanovic and M.B. Celap, Anal. Chem., 42 (1970) 27.
4 I.F. Dolmanova, V.P. Poddubienko and V.M. Peskova, Zh. Anal. Khim., 25 (1970) 2146.
5 I.F. Dolmanova, N.T. Yatsimirskaya, V.P. Poddubienko and V.M. Peskova, Zh. Anal. Khim., 26 (1971) 1540.
6 S. Abe and K. Takahashi, Bunseki Kagaku, 23 (1974) 1326.
7 C. Robinson and E. Mills, Proc. Roy. Soc., Ser. A, 182 (1944) 335.
8 S. Abe, K. Takahashi and T. Matsuo, Nippon Kagaku Kaishi, (1973) 963.
9 L.F. Fieser and M. Fieser, Reagents for Organic Synthesis, John Wiley, New York, 1967, p.466.
10 H. Weisz and S. Pantel, Anal. Chim. Acta, 62 (1972) 361.

Analytica Chimica Acta, 80(1975)143—151

SPECTROPHOTOMETRIC DETERMINATION OF ULTRA-TRACE AMOUNTS OF TITANIUM, IRON, VANADIUM AND ALUMINUM IN FUSED SILICA

K.F. SUGAWARA and YAO-SIN SU

Research and Development Laboratories, Corning Glass Works, Corning, New York 14830 (U.S.A.)

(Received 2nd April 1975)

Impurities extending to the parts per billion ($\mu g\ kg^{-1}$) concentration level in pure fused silica significantly diminish the optical transmittance in the ultraviolet, visible and near infrared regions of the energy spectrum [1—4]. Thus, with the introduction of advanced optical waveguides, the accurate analysis of fused silica for ultra-trace impurities assumed paramount importance. In the work described here, six different boules of fused silica were analyzed spectrophotometrically for titanium, iron, vanadium and aluminum. As with all trace analytical procedures, extreme care was taken to minimize inhomogeneity of the sample and preclude contamination. This paper is concerned essentially with the analytical preparation of the fused silica samples, procedural details of the spectrophotometric methods and comparison of the spectrophotometric data with that obtained by other trace techniques. Particular attention was given to Tölg's thorough discussion of extreme trace analysis of the elements [5].

Since considerable emphasis has been placed on the high sensitivities attainable by modern analytical instrumentation, it is not always remembered that similar sensitivities are possible by simple spectrophotometric methods, which can also provide other valuable information. For example, in numerous instances, particularly at the ultra-trace level, results are often reported but not substantiated by either standards or data obtained by alternative methods. In this respect, since fused silica standards for impurities at the ultra-trace level were not available, the spectrophotometric data contributed significantly toward establishing the probable level of certain ultra-trace impurities by supporting data obtained by other techniques. Although not used in this study, an Ultrex grade of silicon dioxide (J.T. Baker No. 4909) analyzed mainly by d.c.-arc spectrography is commercially available.

Generally, the most sensitive spectrophotometric methods are those based on measurements of metal—organic complexes directly in the organic phase. For titanium, the trioctylphosphine oxide—cyclohexane extraction of the titanium thiocyanate complex reported by Young and White [6] and Hibbits et al. [7] proved very satisfactory. For iron, the hexanol extraction of the

iron—bathophenanthroline complex [8] was established as the most appropriate. These procedures for titanium and iron exhibited excellent precision, sensitivity and selectivity at the ultra-trace level. For vanadium, three methods [9—11] were investigated in an effort to select one possessing adequate characteristics for trace analysis. The method of Donaldson [9], based on a chloroform extraction of the vanadium—N-phenyl-benzohydroxamic acid complex, proved the most satisfactory. This method was similar to, but more efficient than, that described by Priyadarshini and Tandon [10] because complete oxidation of trace vanadium was assured by boiling with ammonium persulfate. The extraction method reported by Siroki and Djordjevic [11], in which tetraphenylarsonium chloride is used with 4-(2-pyridylazo)resorcinol, resulted in a very sensitive method for vanadium but suffered from poor precision. For aluminum, the 8-hydroxyquinoline—chloroform separation [12] and an aqueous catechol violet spectrophotometric procedure [13], were examined. The former method was very selective and reliable but lacked high sensitivity and was time-consuming; the latter method was selective, sensitive, rapid and reliable, and was therefore chosen for this study.

EXPERIMENTAL

Reagents

Ammonia solution, 10—12 M

Cool 500 ml of water in an ice bath and pass in anhydrous ammonium gas, (Merck) using a plastic tubing with a porous tip at the end for more efficient dissolution of ammonia.

Bathophenanthroline solution, 0.002 M

Dissolve 0.066 g of 4,7-diphenyl-1,10-phenanthroline (Eastman) in 50 ml of ethanol and gradually add 50 ml of water with stirring.

Hexamine buffer solution

Dissolve 150 g of hexamethylenetetramine in 350 ml of water, transfer to a 500-ml graduated cylinder, add 8.4 ml of ammonia solution and dilute to 500 ml.

Hydroxyammonium chloride solution

Adjust an aqueous 10 % (w/v) hydroxyammonium chloride solution to pH 4 with dilute ammonium hydroxide and transfer to a separatory funnel. Extract the iron with 2 ml of the above bathophenanthroline solution and 5 ml hexano

Nitric acid, hydrofluoric acid and sulfuric acid were of Ultrex grade (J.T. Baker). Other chemicals were obtained from Eastman or J.T. Baker.

All solutions were prepared with distilled water deionized freshly before use

Apparatus

A laminar flow hood (Model Lab One, Environmental Air Control, Inc.), rigid teflon bottles (250 ml, Laboratory Supplies Co.) and 125-ml teflon separatory funnels (Ace Scientific) were used.

An Hitachi—Perkin-Elmer Model 139 spectrophotometer was used with semimicro 1.00-cm pathlength optical cells (Type 9, Heat Systems—Ultrasonics, Inc.).

Sample preparation

The sections of fused silica reserved for analysis were surface ground to eliminate all markings and surface contamination. They were then washed with methanol, warm (1+9) hydrofluoric acid, and distilled—deionized water, and carefully air-dried between filter papers. The portions were then protected with polyethylene sheets and crushed with an iron mallet into small pieces about 0.25—0.50 in. in diameter. After washing with warm (1+9) hydrochloric acid and distilled—deionized water and again carefully air-drying between filter papers, the samples were stored in plastic bottles.

Sample dissolution

Dissolve the samples in heavy-walled 250-ml Teflon bottles with screw-on lids using 10 ml of distilled—deionized water, 30 ml of hydrofluoric acid, 0.5 ml of sulfuric acid and 1 ml of nitric acid. Digest for at least 48 h on a hot plate at low heat (ca. 120 °C), then remove the lids and transfer the contents to 100-ml teflon evaporating dishes. Evaporate to light sulfur trioxide fumes twice, and subsequently analyze for titanium, iron and vanadium. For the determination of aluminum, omit sulfuric acid from the dissolution step, and evaporate the solution to dryness at low heat on a hot plate. Reagent blanks are carried through the respective procedures. Dissolution, evaporations, and color development steps should all be completed in the clean room.

Determination of titanium

Transfer the solution from the teflon dish to a platinum dish with the addition of 3—4 drops of nitric acid and 6 ml of sulfuric acid. Then evaporate to strong sulfur trioxide fumes, cool in a cold water bath and dilute to 20 ml. Transfer the cooled solution to a 125-ml separatory funnel with 5 ml of distilled—deionized water, and add 2 ml of mercaptoacetic acid (98 %), and 3 g of ammonium thiocyanate with mixing. Extract the titanium for 5 min with exactly 20.0 ml of 0.02 M trioctylphosphine oxide in cyclohexane. Drain the aqueous phase and discard it, and scrub the organic phase with 20 ml of 6 M sulfuric acid containing 0.5 ml of mercaptoacetic acid. After discarding the scrub solution, transfer the organic phase to a test tube and measure the

absorbance at 430 nm in 1.00-cm cells. Take a reagent blank through the complete procedure to obtain the net absorbance for the sample. Determine the concentration of titanium in the sample from a calibration curve prepared with standard titanium solutions.

Determination of iron

Transfer the sample solution from the teflon dish to a platinum crucible with several drops of nitric acid and distilled—deionized water, evaporate to strong sulfur trioxide fumes and then transfer to a 30-ml beaker. Dilute to about 10 ml, cool in a cold water bath, and add 1 ml of 10 % hydroxyammonium chloride solution, 2 ml of 10 % (w/v) sodium acetate solution and 1.0 ml of 0.002 M bathophenanthroline solution. Adjust the pH to 4.0 with dilute ammonia solution using a pH meter. Extract the iron with exactly 2.00 ml of hexanol. After discarding the aqueous phase, pass the organic phase into a 3-ml test tube and centrifuge. Measure the absorbance at 533 nm in 1.00-cm cells. Take a reagent blank through the complete procedure to obtain the net absorbance for the sample. Establish the iron concentration from a calibration curve prepared from standard iron solutions.

Determination of vanadium

Transfer the sample solution from the teflon dish to a platinum crucible with several drops of nitric acid and distilled—deionized water and evaporate to sulfur trioxide fumes. Cool in a cold water bath and transfer to a plastic graduated cylinder with 2—3 ml of distilled—deionized water. Then add 1 ml of 12.5 M sulfuric acid, 0.8 ml of hydrofluoric acid, 0.5 ml of 10 % (w/v) iron(II) ammonium sulfate solution and 0.6 ml of 10 % (w/v) ammonium persulfate solution with mixing. Dilute to about 6 ml and transfer to a 30-ml teflon beaker with about 0.5 ml of distilled—deionized water. Warm the sample on a hot plate while mixing magnetically for 10 min, and cool in a cold water bath. Extract the solution for 5 min with 1.50 ml of N-phenyl-benzohydroxamic acid (0.1 % in chloroform) in a teflon separatory funnel, pass the organic phase into a 3-ml test tube, and centrifuge. Transfer the chloroform layer to a 1.00-cm cell, and measure the absorbance at 475 nm. Take a reagent blank through the complete procedure to obtain the net absorbance for the sample. Establish the vanadium content from a calibration curve prepared from standard vanadium solutions.

Determination of aluminum

Transfer the fused silica solution to a teflon evaporating dish and take to dryness; evaporate the final 1—2 ml of solution very slowly at low heat. Add 10 ml of 0.1 M hydrochloric acid, dissolve the aluminum in the residue by warming, cool and transfer to a 30-ml beaker. Add 10 drops of the hydroxy-

ammonium chloride solution and 10 drops of aqueous 0.1 % (w/v) 1,10-phenanthroline solution followed by 1.00 ml of aqueous 0.038 % (w/v) catechol violet solution. Adjust the pH of the solution to exactly 6.10 ± 0.05 with hexamine buffer solution, transfer to a 25.0-ml volumetric flask and dilute to volume. Allow the color to develop for 30 min, and measure the absorbance at 580 nm. Take a blank through the complete procedure. Establish the aluminum concentration in the sample from a calibration curve prepared from standard aluminum solutions.

RESULTS AND DISCUSSION

The extent to which trace ions can be detected by spectrophotometric methods depends primarily upon the characteristics of the sample, purity of reagents, sample preparation and contaminant pickup. For this investigation, very careful attention was given to all these factors to enhance the reliability of the data. Unlike most other types of samples, impurities in fused silica can be readily concentrated to a very small volume through volatilization of silicon as silicon tetrafluoride. Thus, the chemical characteristics of fused silica make it particularly well suited for trace analysis. Purity of reagents involved primarily hydrofluoric acid because of the relatively large volume consumed during the decomposition of the glass. Ultrex-grade hydrofluoric, sulfuric and nitric acids each containing very low ($\mu g\ l^{-1}$) concentration levels of most individual metallic contaminants were used. Contaminant pickup, particularly for trace iron from stainless steel hoods, has always proved troublesome in this laboratory. Blanks were generally erratic. To surmount this problem a small room was converted into a trace laboratory by installing two relatively small laminar flow hoods and a clean work bench area. Air passing through the hoods and over the clean bench was purified by a high-efficiency filter which removed 99.99 % of all particulate matter of 0.3 μm and larger. The interior of the laminar flow hood was lined with Kynar (polyvinylidene fluoride), a material which is hard, readily cleaned and chemically resistant to all common acids and bases used in the laboratory. This project, in particular, required a clean working environment. The laminar flow hood and clean bench contributed significantly toward this end.

The spectrophotometric determination of elements at the 500-$\mu g\ kg^{-1}$ level and lower in fused silica required a 5-g sample size and procedures with sensitivities capable of determining 2 μg of the respective elements. The dissolution of this relatively large sample presented no problems other than the control of the blanks which was readily accomplished by the use of the Ultrex-grade acids. The determination of elements at the 2-μg level was more involved because spectrophotometric procedures are normally used only for higher levels. Thus, in the procedures for vanadium and iron, with N-phenylbenzohydroxamic acid and bathophenanthroline, respectively, the detection limits were lowered by decreasing the volume of extractant. Since absorbance measurements were completed directly in the organic phase, the determination

of as little as 2 μg was quite feasible. Figure 1 summarizes the respective calibration curves, final volumes for color development and types of cells used for the absorbance measurements.

Precision of analysis for blanks

Tölg [5] indicated that the blank values depend on instrumental as well as procedural variations, e.g., electronics, voltage fluctuations, dissolutions, preconcentration and determination. Thus, to be meaningful, the signal for the elements to be determined must be greater than the total blank value and its variations. A signal of three standard deviations above the blank was suggested as the minimum reporting value. Based on this criteria, all positive spectrophotometric values reported for iron, titanium, vanadium and aluminum are at least three standard deviations greater than the mean value for the blank. Since the blank values depended on the particular lot of hydrofluoric acid used, blanks were always run simultaneously with the samples. The standard deviations for the blanks (Table 1) were all run on the same lot.

Titanium

Table 1 shows the reagent blank absorbances with Ultrex and reagent-grade hydrofluoric acids, and no hydrofluoric acid. The difference between the Ultrex and reagent-grade acids is significant, and emphasizes the importance of using ultrapure grades. The amount of titanium impurity in Ultrex hydro-

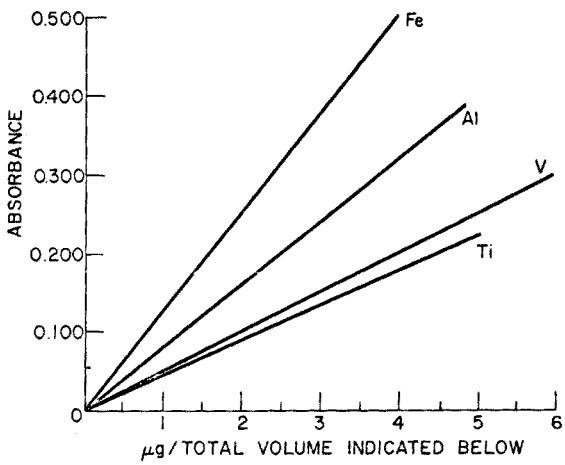

Fig. 1. Calibration curves for iron, titanium, vanadium and aluminum. Fe: Bathophenanthroline complex extracted in 2.00 ml of hexanol and measured in 1.00-cm semi-micro cell. Ti: Thiocyanate complex extracted in 20.00 ml of TOPO—cyclohexane and measured in 1.00-cm cell. V: N-phenylbenzohydroxamic acid complex extracted in 1.00 ml of chloroform and measured in 1.00-cm semi-micro cell. Al: Catechol violet complex in 25.0 ml of aqueous solution and measured in 1.00-cm cell.

TABLE 1

Comparison of reagent blanks for titanium, iron, vanadium and aluminum

	Absorbance			
	Ti	Fe	V	Al
30 ml Ultrex HF + 10 ml H_2O	0.078±0.0096[a]	0.047±0.0091[a]	0.032±0.0021[a]	0.092±0.0118[a]
30 ml reagent grade HF + 10 ml H_2O	0.712, 0.725	0.340, 0.340	0.026, 0.028	0.400, 0.315
40 ml H_2O	0.010	0.010	0.035	0.080, 0.100

[a]Mean of 4 results and standard deviation.

fluoric acid appears to be ca. 50 p.p.b., which is higher than the certified value of 30 p.p.b. but not unreasonably so, considering the low level involved and the possible leaching of minute amounts of titanium from the apparatus used.

The detection limit for titanium by the TOPO—cyclohexane extraction spectrophotometric procedure is excellent and, if necessary, it could be lowered further by using less extractant. Experimentally, however, the lower detection limit was governed by the reproducibility of the blank. Table 2 lists the results obtained for titanium by the proposed method and by three other techniques. The results of spectrophotometry, atomic absorption and mass spectrometry generally agree quite well; a slight discrepancy exists on sample 6, where the results of spectrophotometry and atomic absorption exceed 2000 $\mu g\ kg^{-1}$, while mass spectrometry and voltammetry indicate significantly lower values.

Iron

Dependable results were obtained for trace iron determinations only after the experimental work had been restricted to the laminar flow hood and the clean bench. The data on reagent blanks in Table 1 indicate that Ultrex hydrofluoric acid provides a significant improvement over the reagent-grade acid.

When the small-scale bathophenanthroline extraction procedure was applied, the detection limit was improved considerably, becoming comparable with that of a.a.s. Comparison with the results by other techniques (Table 2) indicates reasonable agreement with atomic absorption; samples 1 and 2 contained more iron than the remaining samples.

TABLE 2

Analysis of fused silica boules

(All results in $\mu g\ kg^{-1}$.)

	Boule no.	Method[a]				
		Spectr.	A.a.s.	N.a.a.	S.s.m.s.	Volt.
Ti	1	220, <220	500		600	<2000
	2	<200, <200	<100		440	<2000
	3	<200, <200	400		190	<2000
	4	<200, <200	200		140	<2000
	5	<200, <200	300		550	<2000
	6	3200, 2600	3500		1900	<2000
Fe	1	240, 150	370	<80		<2000
	2	240, 220	400	<150		<2000
	3	<100, <100	270	<80		<2000
	4	<100, <100	67	<50		<2000
	5	<100, <100	250	<500		<2000
	6	<100, <100	185	<200		<2000
V	1	320, 380	240	990	250	500—1500
	2	340, 440	220	700	94	500—1500
	3	370, 500	250	760	22	500—1500
	4	<200, <200	<50	<300	26	500—1500
	5	<200, <200	<50	<100	20	500—1500
	6	<200, <200	<50	890	32	500—1500
Al	1	590, 550	1000		<9500	
	2	<200, <200	340		960	
	3	350, 270	340		470	
	4	<200, <200	390		4300	
	5	<200, <200	26		1500	
	6	2700, 3100	3200		<7800	

[a] Spectrophotometry, atomic absorption spectrometry, neutron activation analysis, spark-source mass spectrometry, and differential pulse voltammetry (for V) or differential pulse anodic stripping (for Ti, Fe, Al).

Vanadium

The determination of vanadium at the $\mu g\ kg^{-1}$ level required a micro-extraction technique with a reduced volume of extractant. The absorbance of the reagent blank for the vanadium procedure was consistently low (< 0.050 absorbance), regardless of whether Ultrex or reagent-grade hydrofluoric acid was used, hence reagent blanks presented no problem. After the N-phenylbenzohydroxamic acid—chloroform extraction, small droplets of water adhering to the organic phase were transferred to the test tubes; but, when the chloroform phase was carefully decanted into the optical cell, the

water remained on the tube wall, so that separation of the organic phase for measurement was clean. A comparison of the data (Table 2) indicates relatively good agreement between spectrophotometry and atomic absorption. Samples 1, 2, and 3 contain significantly more vanadium than the other samples. Neutron activation indicated a significantly higher level of vanadium in samples 1, 2, 3 and 6.

Aluminum

The spectrophotometric catechol violet method for aluminum is particularly suitable for trace work because of its simplicity and sensitivity. A significant factor is the relatively high absorbance obtained with reagent-grade hydrofluoric acid compared to the Ultrex grade (Table 1); aluminum was not detectable in the latter acid, but the certified value for aluminum is only 1 p.p.b. A comparison of the data (Table 2) for the aluminum levels in the fused silica samples indicates fair agreement with atomic absorption. Both techniques showed a high aluminum content in sample 6. Mass spectrometric results were considerably higher in most cases, but neutron activation and voltammetry data were not obtained.

The authors would like to acknowledge the efforts of S.S.C. Tong, J.L. Elzie (currently at Chevron Research Company), W.R. Strzegowski, W.M. Wise and G.A. Machajewski in obtaining the data by other analytical methods.

SUMMARY

The spectrophotometric determination of ultra-trace levels of Ti, Fe, V and Al in pure fused silica is described. Titanium is determined by extraction of the thiocyanate complex with TOPO in cyclohexane, iron with 4,7-diphenyl-1,10-phenanthroline, vanadium with N-phenylhydroxamic acid, and aluminum with catechol violet. The results are generally in reasonable agreement with those obtained by other techniques. The metal contaminant levels in reagent-grade and Ultrex-grade hydrofluoric acid are compared.

REFERENCES

1 M. Zief and J. Horvath, Amer. Lab., 6(10) (1974) 81.
2 P.C. Schultz, J. Amer. Ceram. Soc., 57 (1974) 309.
3 D.E. Campbell and P.B. Adams, Develop. Appl. Spectrosc., 8 (1970) 115.
4 D.E. Campbell and P.B. Adams, Glass Technol., 10 (1969) 29.
5 G. Tölg, Talanta, 19 (1972) 1489.
6 J.P. Young and J.C. White, Anal. Chem., 31 (1959) 393.
7 J.O. Hibbits, A.F. Rosenberg and R.T. Williams, Talanta, 11 (1964) 1509.
8 G.F. Smith, W.H. McCurdy and H. Diehl, Analyst (London), 77 (1952) 418.
9 E.M. Donaldson, Talanta, 17 (1970) 583.
10 U. Priyadarshini and S.G. Tandon, Anal. Chem., 33 (1961) 435.
11 M. Siroki and C. Djordjevic, Anal. Chim. Acta, 47 (1971) 301.
12 R. Villarreal, J.R. Krsul and S.A. Barker, Anal. Chem., 41 (1969) 1420.
13 W.K. Dougan and A.L. Wilson, Analyst (London), 99 (1974) 413.

Analytica Chimica Acta, 80 (1975) 153—161

END-POINT CONSTRUCTION AND SYSTEMATIC TITRATION ERROR IN LINEAR TITRATION CURVES — PRECIPITATION REACTIONS

P. M. J. COENEGRACHT and H. J. METTING

Laboratory for Pharmaceutical and Analytical Chemistry, Antonius Duesinglaan 2, Groningen (The Netherlands)

(Received 10th March 1975)

SUMMARY

The systematic titration error which is introduced by the intersection of tangents to hyperbolic titration curves is discussed for precipitation reactions. A simple expression for the systematic titration error is derived, and S/C_x^2 is proposed as a measure of the sharpness of the titration curve. The effects of the conditional solubility product (S), the concentration of the unknown component (C_x), and the ranges used for the construction of the end-point, are considered. A graphical method is presented for the selection of pairs of ranges which result in small systematic titration errors. For equal values of S/C_x^2 and $1/KC_x$, the optimum combinations of ranges are different for precipitation and complexation titrations. The differences are not large for values smaller than about 0.002. For titration curves with a reversed L-shape, the error is calculated when the end-point is constructed by the intersection of the tangent to the second branch of the curve with volume axis; in this case equal ranges result in the same titration error for equal values of S/C_x^2 and $1/KC_x$. The systematic titration error is equal to $-S/C_x^2$ when the tangent to the curve is taken at $f_a = 3.0$.

The end-point of hyperbolic titration curves is usually constructed as the intersection of two tangents drawn to "linear" segments (ranges) on the two branches that form the titration curve. Several authors [1—5] have given different procedures for the construction of the end-point of linear precipitation titrations, especially for strongly bent titration curves. However, the tangent method and the practically equivalent method of linear extrapolation of portions of the titration curve to their intersection, are normally applied. Premature termination of the titration is a common failure, and causes negative titration errors as has been shown by Kolthoff, et al. [6, 7] for the titration of halides with silver solutions. Langer and Stevenson [2] and Mar'yanov [5] have pointed out that the tangent method can give erroneous results if the ratio of the solubility product and the initial concentration of the component in the sample is too large.

It has recently been shown [8] that the systematic titration error in linear complexiметric titrations can be minimized if tangents are drawn to properly chosen ranges of f (f is the ratio of equivalents of titrant to those of sample). A graphical procedure for the selection of the ranges has been given, and the

equivalence of the tangent method and the linear extrapolation of relatively small portions of the titration curve has been demonstrated. The present paper is concerned with linear precipitation titrations. An expression for the systematic titration error is derived. Measurement errors are not considered. A criterion for a sharp end-point is proposed and it is shown that the tangents will intersect at $f = 1$, i.e. the titration error will be zero, if the abscissae of the points of contact before, f_b, and after the end-point, f_a, fulfil a simple condition. The graphical method for the selection of ranges that minimize the systematic titration error, as described for complexiметric titrations [8], is now extended for precipitation titrations, and the results are compared. As pointed out earlier [8], it may be advantageous to construct an end-point by intersection of the volume axis by the tangent to the second branch of a titration curve of a reversed-L shape, instead of the usual intersection of two tangents. It is then necessary to extrapolate ranges selected well after the end-point; this is possible by analog correction of the recorded tiration curve for dilution of the sample with the titrant [9, 10]. The systematic titration errors of the methods are discussed.

THEORETICAL CONSIDERATIONS

The titration reaction of a component X with a titrant T to yield an insoluble 1 : 1 product XT can be represented by

$$X + T \rightleftarrows XT \tag{1}$$

for which the conditional solubility product is

$$S = [X]\,[T] \tag{2}$$

It is assumed that the product XT is present at the start of the titration. This permits the entire titration curve to be described by a single equation and avoids a discontinuity caused by the first appearance of the precipitate [1, 2]. If the titration curve is recorded by monitoring the concentration of only one compound involved in the reaction, if only this compound contributes to the measurement, and if the measured property is directly proportional to the monitored concentration, then the relationship between titration parameter, f, and [X] is represented [11] by

$$f = -\frac{[X]}{C_x} + \frac{S}{C_x[X]} + 1 \tag{3}$$

and the titration curve is L-shaped. The relationship between f and [T] is given by

$$f = \frac{[T]}{C_x} - \frac{S}{C_x[T]} + 1 \tag{4}$$

and the titration curve has a reversed-L shape. Equation (4) will be used in the following discussion. The symbols have the same meaning as defined in the previous paper [8].

Calculation of the systematic titration error

Case A

The end-point is found by the intersection of two tangents, one at a point, $[T]_b$, f_b, before the end-point, and another at a point, $[T]_a$, f_a, after the end point. From the equations of the tangents, a general expression for the titration parameter at the point of intersection, f_i, can be found (eqn. (8), ref. 8). Differentiation of eqn. (4) with respect to [T] and inversion of the resulting expression yields

$$\frac{d[T]}{df} = \frac{C_x [T]^2}{S + [T]^2} \tag{5}$$

which is the general equation for the slope of a tangent to the titration curve. Using eqns. (4) and (5) one can express f_i in terms of S, C_x, $[T]_b$ and $[T]_a$. After simplification, rearrangement and subtraction of 1, the systematic titration error is given by

$$E_i = \frac{2([T]_b [T]_a - S)}{([T]_b + [T]_a)C_x} \tag{6}$$

or

$$E_i = \frac{2([T]_b [T]_a - S)/C_x^2}{([T]_b + [T]_a)/C_x} \tag{6a}$$

E_i can be calculated for given values of S/C_x^2, f_b and f_a by expressing $[T]_b/C_x$ and $[T]_a/C_x$ in these terms after solving eqn. (4) for [T], which gives after rearrangement

$$[T]/C_x = \tfrac{1}{2} \{f - 1 + [(f-1)^2 + 4\, S/C_x^2]^{\frac{1}{2}}\} \tag{7}$$

Since $[T]/C_x$ cannot be negative, the negative root is inadmissible. It is obvious from eqns. (7) and (6a) that the form of the normalized titration curve and the magnitude of the systematic titration error are directly determined by S/C_x^2. Consequently, we propose the term S/C_x^2 as a measure of sharpness of the titration curve.

If the titration error is equal to zero, it follows from eqn. (6) that

$$[T]_b [T]_a = S \tag{8}$$

Combination of this relation with the expression for the sum of f_b and f_a, obtained from eqn. (4), leads to a simple condition for zero titration error

$$E_i = 0: \quad f_b + f_a = 2 \tag{9}$$

The intersection of the tangents at $f_b = 0$ and at $f_a = 2$ to the compleximetric titration curve results in a systematic titration error of $-1/KC_x$, and has been proposed [12] as a criterion of sharpness: $KC_x \geqslant 1000$, for $E_i \leqslant -0.1\%$ (K is the conditional stability constant). The intersection of these tangents gives zero titration error for precipitation titrations in accordance with eqn. (9), and does not lead to a sharpness criterion. But it can easily be

shown that the systematic titration error is approximately equal to S/C_x^2 in precipitation reactions, if the end-point is taken as the intersection of tangents at $f_b = 0$ and $f_a = 3$; if $S/C_x^2 \leqslant 0.001$, then the maximum titration error is 0.1%.

The systematic titration error, E_i', for an L-shaped titration curve, described by eqn. (3), is found in the same manner

$$E_i' = \frac{2(S - [X]_b\,[X]_a)}{([X]_b + [X]_a)C_x} \tag{10}$$

and is equal to the titration error given by eqn. (9). This is readily shown by substitution of $[X] = S/[T]$ in eqn. (10), and would be expected from symmetry considerations.

Case B

The end-point is found by the intersection of the volume axis with the tangent at point $[T]_a, f_a$, when the titration curve is of the reversed-L type. The relation between the titration parameter at the point of intersection, f_s, and the ordinate of the point of contact, $[T]_a$, is found as described before [8] and can be expressed in terms of S, C_x and $[T]_a$, by means of eqns. (4) and (5). After simplification of the result, and subtraction of 1, the systematic titration error, E_s, is given by

$$E_s = -\frac{2S}{C_x[T]_a} \tag{11}$$

The titration error may be expressed in terms of S/C_x^2, f_a and the fractional deviation from complete reaction. The fractional deviation (after the end-point), Δ_a, is defined as the difference between the real and "ideal" concentration of the titrant, normalized to the analytical concentration, C_x, of the component, (eqn. (15), ref. 8). This results in

$$E_s = -2S/\{C_x^2(f_a - 1 + \Delta_a)\} \tag{12}$$

The systematic titration error decreases with increasing values of f_a, but remains negative. The error is approximately $-S/C_x^2$ for $f_a = 3$. The same error, but with opposite sign, results from the intersection of the same tangent at $f_a = 3$ with the tangent at $f_b = 0$.

RESULTS

Case A

Systematic titration errors were calculated for $S/C_x^2 = 0.01; 0.004; 0.002$ and 0.001, when the end-point is constructed by the intersection of the tangent to the curve at the points $f_b = 0.0; 0.1; 0.2; 0.3; 0.4; 0.5$ with tangents at points f_a varying from 1.0 to 4.0. Plots of the systematic titration error, E_i, in per cent as a function of f_a at constant f_b are given in Fig. 1. The systematic titration error as a function of f_b at constant f_a is shown in Fig. 2,

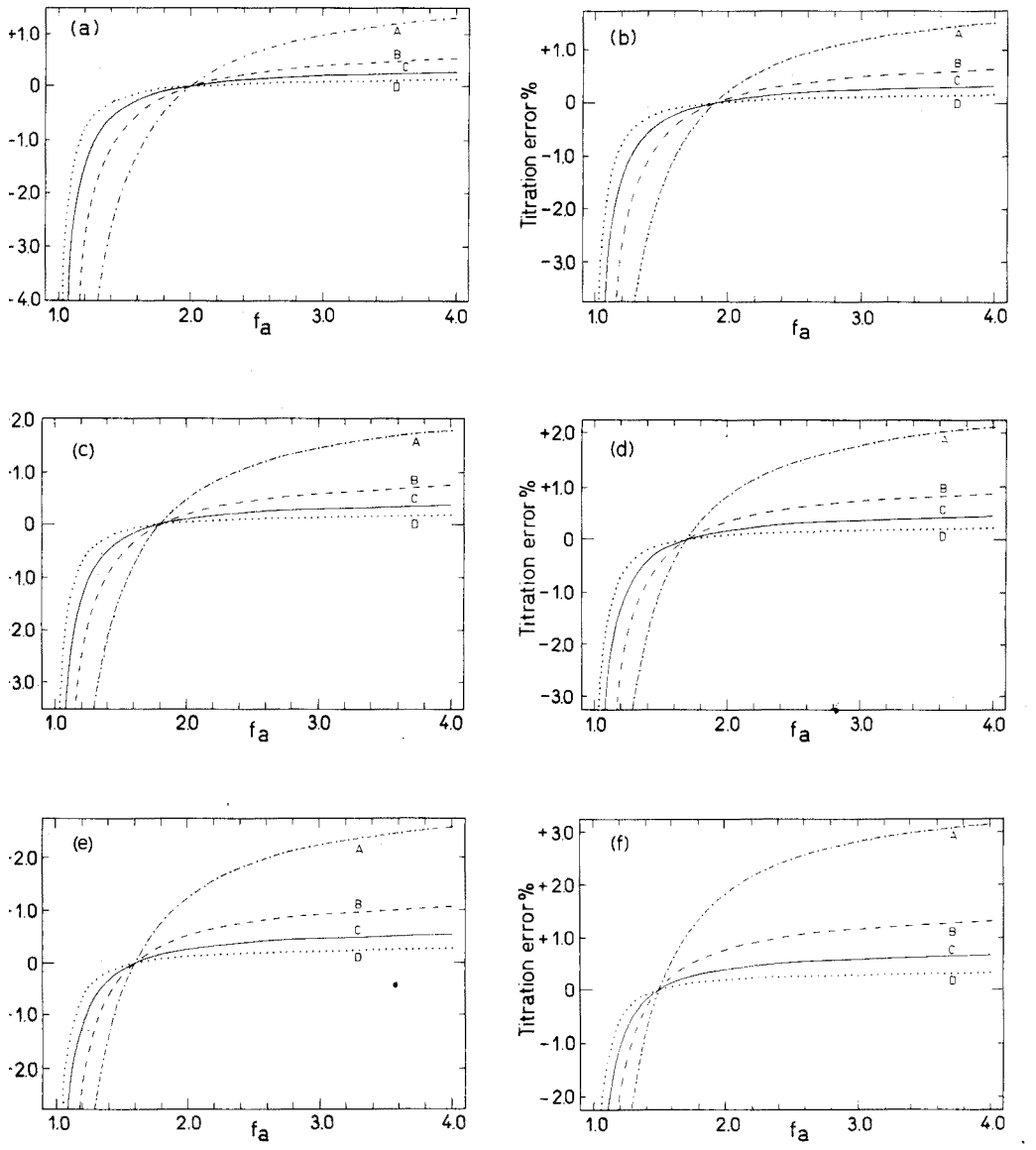

Fig. 1. Plots of the systematic titration error, E_i, as a function of f_a at discrete values of f_b for different values of S/C_x^2: (A) $S/C_x^2 = 0.01$; (B) $S/C_x^2 = 0.004$; (C) $S/C_x^2 = 0.002$; (D) $S/C_x^2 = 0.001$. (a) $f_b = 0.0$. (b) $f_b = 0.1$. (c) $f_b = 0.2$. (d) $f_b = 0.3$. (e) $f_b = 0.4$. (f) $f_b = 0.5$.

for $f_a = 1.5; 2.0; 2.5; 3.0$. Several combinations of ranges of f_b with ranges of f_a, which result in a given maximum absolute titration error for a given value of S/C_x^2, can be selected from these figures by procedures analogous to those given for complexim etric titrations [8]. For example, the combination 0.0—0.7 with 1.5—2.5, found from Figs. 2(a), 2(c), curve B, results in a

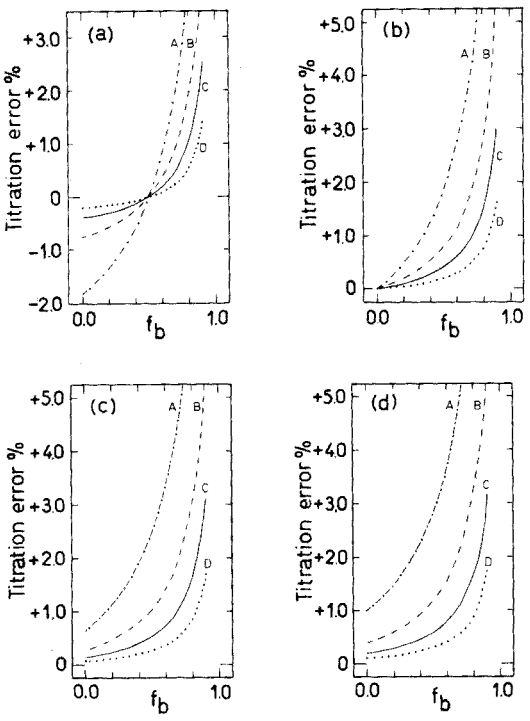

Fig. 2. Plots of the systematic titration error, E_i, as a function of f_b at discrete values of f_a for different values of S/C_x^2: (A) $S/C_x^2 = 0.01$; (B) $S/C_x^2 = 0.004$; (C) $S/C_x^2 = 0.002$; (D) $S/C_x^2 = 0.001$. (a) $f_a = 1.5$. (b) $f_a = 2.0$ (c) $f_a = 2.5$. (d) $f_a = 3.0$.

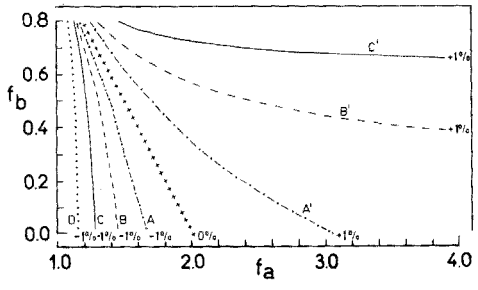

Fig. 3. Nomogram giving ±1 % limits of the systematic titration error, E_i, as a function of f_b and f_a for different values of S/C_x^2: (A, A') $S/C_x^2 = 0.01$; (B, B') $S/C_x^2 = 0.004$; (C, C') $S/C_x^2 = 0.002$; (D) $S/C_x^2 = 0.001$. D' lies outside the figure. The crossed line gives zero error for all values of S/C_x^2.

titration error of ±2% for $S/C_x^2 = 0.004$.

Figure 3 was constructed from Figs. 1 and 2 and additional calculations. This nomogram shows the ±1% error limits for $S/C_x^2 = 0.01; 0.004; 0.002; 0.001$. It permits an easy selection of combinations of ranges that give a maximum absolute titration error of 1%. Combinations are found by fitting rectangles between the positive and negative error limits for a given value of S/C_x^2 with their sides parallel to the coordinate axes. The vertical side gives the range of f_b, and the horizontal side gives the range of f_a. The central crossed line corresponds to the points of intersection of the curves of Figs. 1 and 2 and is represented by eqn. (9). The line indicates the pair of tangents at f_b and f_a which give zero titration error for every value of S/C_x^2.

The titration error as a function of both points of contact f_b and f_a is depicted as the curved surface in Fig. 4 for $S/C_x^2 = 0.01$. The model shows the relationship between Figs. 1, 2 and 3. Sections through the model perpendicular to the f_b- and f_a-axis give the curves A of Figs. 1 and 2 respectively. Curve A, A′ and the central crossed line in Fig. 3 are given by sections through the model perpendicular to the E_i -axis for $E_i = -1\%, +1\%$ and 0%.

Case B

The end-point was constructed by intersection of the volume axis with tangents at f_a values varying from 1.0 to 4.0 for a reversed L-shaped titration curve. Systematic titration errors, E_s, were calculated for the same values of S/C_x^2 as above and are presented as a function of f_a in Fig. 5. The figure shows, in accordance with eqn. (12), that the titration error is directly proportional

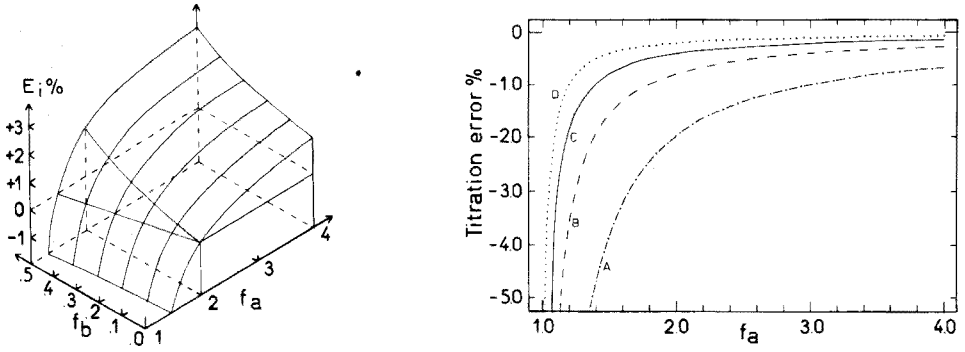

Fig. 4. Model showing interrelationships between the systematic titration error, E_i, and f_b and f_a.

Fig. 5. Plots of the systematic titration error, E_s, as a function of f_a for different values of S/C_x^2: (A) $S/C_x^2 = 0.01$; (B) $S/C_x^2 = 0.004$; (C) $S/C_x^2 = 0.002$; (D) $S/C_x^2 = 0.001$.

to S/C_x^2 and approximately directly proportional to $2/(f_a-1)$. Thus the titration error at $f_a = 2.0$ is twice the error at $f_a = 3.0$.

DISCUSSION

In practice it is often difficult to choose linear ranges on a hyperbolic titration curve. The calculation of their positions from theory makes the choice more objective. Careful selection of such ranges may enhance accuracy and precision, and save time by optimization of experimental conditions. However, the exact selection of ranges yielding a given titration error for a given value of S/C_x^2 requires the conditional solubility product and the stoichiometric end point to be known. But if the end-point can be estimated from the titration curve, then one can find combinations of ranges which result in relatively small titration errors for S/C_x^2 values of 0.01, or smaller, from Figs. 1, 2 and 3. A few examples, which are easily found from Fig. 3, are: 0.0—0.3 with 1.7—2.1; 0.0—0.5 with 1.5—2.4 and 0.0—0.7 with 1.3—2.3. However, different ranges, that do not start at $f_b = 0.0$, can also be found. This may be advantageous when the first measurements of the titration curve deviate because of the initial formation of precipitate.

It is possible to cover the parts of Figs. 1(a) and 1(f) for which $f_a \leqslant 2$ with the inverted Figs. 2(b) and 2(a), respectively. This shows that the variation of the titration error with f_a at constant f_b is equal to the variation of the error with f_b at constant f_a, but moves in an opposite sense with increasing values of the titration parameter. The constant values of f_b and f_a must be at equal distances from $f = 1$. This can be expressed as follows: $E_i(f_b; f_a) = -E_i(f_b'; f_a')$ provided that $f_b + f_a' = 2$ and $f_b' + f_a = 2$. The notation, $E_i(f_b; f_a)$, indicates the titration error that results from the intersection of tangents at f_b and f_a to the curve. This relation also follows from eqns. (6), (8) and (9) and may be used for obtaining the end-point as the mean of two points of intersection that have the same error with opposite sign.

Examination of Figs. 1 and 2 shows that the titration error is approximately directly proportional to S/C_x^2 for small titration errors (< 5%). It has been found [8] that the titration error is approximately directly proportional to $1/KC_x$ in complexiметric titrations. Comparison of precipitation and complexation titrations shows that the plots of the titration error against f_b and f_a differ for equal values of S/C_x^2 and $1/KC_x$. For example, in precipitation titrations $E_i(0.0; 2.0) = 0$ and $E_i(0.0; 3.0) = S/C_x^2$, whereas in complexation titrations [8] $E_i(0.0; 2.0) = -1/KC_x$ and $E_i(0.0; 3.0) = 0$. However, for values of 0.002 and smaller, the optimum combinations of ranges do not differ very much. When the end-point is found by intersection of the tangent to the second branch of the titration curve with the volume axis, almost the same titration error is found for complexation and precipitation titration curves of a reversed L-shape. For equal values of S/C_x^2 and $1/KC_x$ the plots of the titration error against f_a in Fig. 5 are identical with those given in

Fig. 6 of ref. (8) for complexiметric titrations. Examination of the normalized titration curves with a reversed L-shape for $S/C_x^2 = 1/KC_x = 0.1$ shows that the second branch of the complexiметric curve has almost the same form as the precipitation curve.

In the amperometric titration of chloride with silver, Kolthoff and Kuroda [6] took the point of intersection of the extrapolated reagent line with the residual current as the end-point. They reported results which were 10—15% too low in the titration of 10^{-4} M chloride solutions at 28 °C, if the reagent line was drawn through points of f_a between 1.2 and 1.7. Calculation of the approximate titration error with $E_s = -2S/C_x^2(f_a - 1)$ for $S = 1.8 \cdot 10^{-10}$ yields negative titration errors of 5—18%. The same authors titrated 10^{-4} M chloride solutions at 0° and 5 °C with an accuracy and precision of 1—2%, when the excess reagent line was drawn after 25 % excess of silver had been added. The calculated titration error for $S = 2.6 \cdot 10^{-11}$ (at 5 °C) and $f_a = 1.25$ is approximately −2 %. The agreement between calculated and experimental errors is fairly good.

REFERENCES

1 V. Majer, Z. Elektrochem., 42 (1936) 123.
2 A. Langer and D. P. Stevenson, Ind. Eng. Chem., Anal. Ed., 14 (1942) 770.
3 E. Grunwald, Anal. Chem., 28 (1956) 1112.
4 J. A. Goldman and L. Meites, Anal. Chim. Acta, 30 (1964) 280.
5 B. M. Mar'yanov, Zh. Anal. Khim., 26 (1971) 637.
6 I. M. Kolthoff and P. K. Kuroda, Anal. Chem. 23 (1951) 1306.
7 I. M. Kolthoff and J. T. Stock, Analyst, 80 (1955) 860.
8 P. M. J. Coenegracht, A. J. M. Duisenberg, Anal. Chim. Acta, in press.
9 P. M. J. Coenegracht, Anal. Chem. 45 (1973) 1675.
10 H. Hauer, MPI Applications Notes, 9 (1974) 17.
11 G. den Boef, Grondslagen van de analyse in waterige oplossingen, Agon Elsevier, Amsterdam, 1968, p. 89.
12 F. Freese, Ph.D. Thesis, Amsterdam 1971.

Analytica Chimica Acta, 80(1975)163—169

Short Communication

THE SEPARATION AND ATOMIC-ABSORPTION MEASUREMENT OF TRACE AMOUNTS OF LEAD, SILVER, ZINC, BISMUTH AND CADMIUM IN HIGH-NICKEL ALLOYS

M. KIRK, E.G. PERRY and J.M. ARRITT

Huntington Alloy Products Division, The International Nickel Company, Inc., Huntington, West Virginia 25720 (U.S.A.)

(Received 17th March 1975)

Accurate determinations of trace quantities (less than about 10 p.p.m.) of lead, silver, zinc, bismuth, and cadmium in nickel alloys have been difficult to achieve. Classical analytical methods are not suitable because of the complexity of the alloys and the low levels of those elements present.

This communication describes a procedure that has the high sensitivity and selectivity necessary for determination of the low concentrations involved. The procedure is based on the use of an ion-exchange technique to separate the elements from the matrix. The separated elements are then concentrated to permit measurement by atomic-absorption spectrometry.

Experimental

Reagents

Reagent-grade chemicals were used in preparation of all standards and eluants. Stock solutions (1000 p.p.m.) of Pb, Ag, Zn, Bi, or Cd were made with either the pure (99.999 %) metal or commercially prepared solutions (J.T. Baker "Dilute-it") that contained the elements in substrate form.

Ion-exchange columns

Anion-exchange columns contained BioRex 9 (100—200 mesh, Cl^- form) resin in a plexiglass column. The resin bed was 14 cm deep and 2.5 cm in diameter. The column was preconditioned with 100 ml of 1.5 M hydrochloric acid.

Cation-exchange columns contained BioRad AG50-X8 (100—200 mesh, H^+ form) resin. The resin bed was 7 cm deep and 2.5 cm in diameter. The column was preconditioned with 100 ml of 0.1 M hydrofluoric acid.

Equipment

A Perkin-Elmer Model 303 atomic-absorption spectrophotometer was used. It was equipped with a three-slot burner and Perkin-Elmer hollow-cathode source lamps.

Calibration standards

Two sets of calibration standards were prepared for each element. One set was a low standard for the 10X scale, and the other a high standard for the 1X and 2X scales. The lead and bismuth contents were 1, 2, and 3 p.p.m. for the low standards and 5, 10, and 15 p.p.m. for the high standards. The zinc and cadmium contents were 0.25, 0.50, and 0.75 p.p.m. for the low standards, 0.50, 1.0, and 1.5 p.p.m. for the high standards. Silver contents were 0.1, 0.2, and 0.3 p.p.m. for the low standards and 1, 2, and 3 p.p.m. for the high standards. Each calibration standard contained the same amount and type of acid as the final solution to be measured.

Ion-exchange procedure

Published data from several sources [1—6] were used in the development of the ion-exchange procedure. Figure 1 illustrates the procedure used to separate the lead, silver, zinc, bismuth, and cadmium from the alloy matrix.

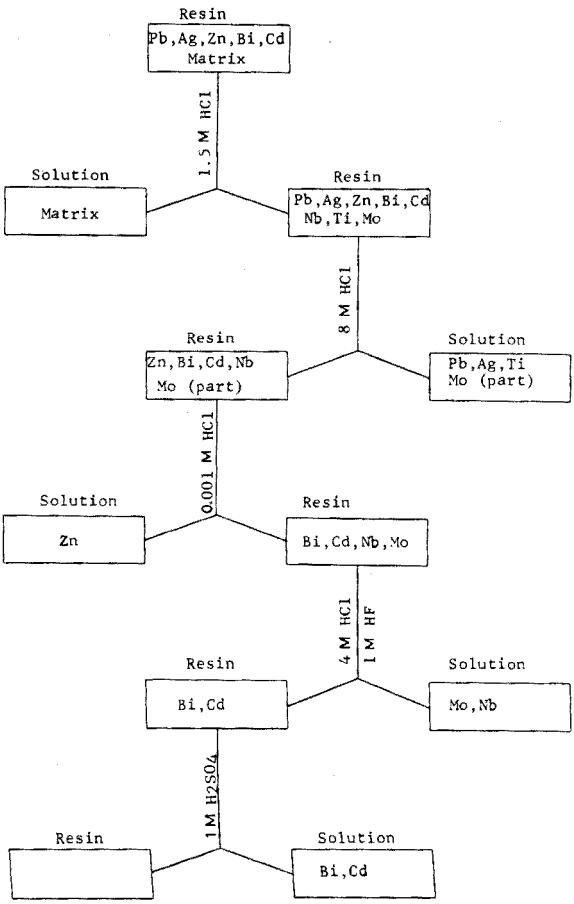

Fig. 1. Elution sequence for the anion-exchange column.

Dissolve a 10-g sample of the alloy in appropriate acids, usually a mixture of hydrochloric and nitric acids. After the reaction ceases, add 1 ml of hydrofluoric acid (40 %) and evaporate the solution to dryness. Add 20 ml of 12 M hydrochloric acid and evaporate to dryness. Repeat the addition and evaporation of 12 M hydrochloric acid until all nitric acid is expelled. To ensure that all the salts are soluble, dissolve the residue in 50 ml of 12 M hydrochloric acid and evaporate to dryness on a steam bath. To produce the 1.5 M HF solution required for the column, add 5 ml of hydrofluoric acid (40 %) and 100 ml of water, and heat to redissolve the salts. Transfer the HCl/HF solution of the sample to the anion-exchange column, and elute most of the matrix with 100 ml of 1.5 M HCl.

Elute the lead and silver from the column with 200 ml of 8 M HCl; this fraction will also contain part of any titanium and molybdenum present in the sample, but these are later separated from the lead and silver by cation exchange. Elute the zinc with 200 ml of 0.001 M HCl. Remove any organic compounds present in this eluate by addition of 5 ml of nitric acid and evaporation to dryness. At this point in the elution sequence, elute any remaining molybdenum or any niobium that may have been partially adsorbed on the column with 300 ml of 4 M HCl—1 M HF solution; discard the eluate.

Elute the bismuth and cadmium with 300 ml of 1 M sulfuric acid. Remove any organics in the eluate by adding 5 ml of 16 M nitric acid and evaporating to fumes of sulfur trioxide. Then cool, transfer to a glass beaker, and evaporate to dryness.

Remove titanium and molybdenum from the lead/silver fraction by the cation-exchange procedure shown in Fig. 2. First remove any organics present in the eluate by addition of 20 ml of 16 M nitric acid and evaporation to dryness. Convert the metals to fluorides by addition of 10 ml of 40 % hydrofluoric acid, and evaporation to dryness. Produce the 0.1 M HF solution required for the column by adding 5 ml of water and 2 ml of 40 % hydrofluoric acid, redissolving the salts by heating, and diluting with 300 ml of

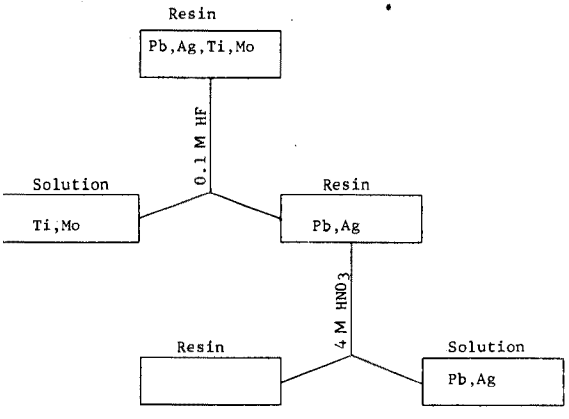

Fig. 2. Elution sequence for the cation-exchange column.

water. Transfer the solution to the cation-exchange column, and elute the titanium and molybdenum with 300 ml of 0.1 M HF. Then elute the lead and silver with 300 ml of 4 M HNO_3. Obtain the chloride medium needed for spectrometry by addition and evaporation of 12 M hydrochloric acid until all nitric acid is removed from the eluate.

The separated and concentrated elements in the three (Pb/Ag, Zn, and Bi/Cd) elution fractions can now be prepared for the a.a.s. measurement. To determine the quantities of the trace elements that may have been introduced by the reagents, take a reagent blank through the entire procedure with the same amounts of reagents used for the sample, and deduct the reagent blanks from the sample values.

TABLE 1

Flask sizes and concentration ranges for 10-g samples and instrumental parameters

Element	Flask size (ml)	Concn. range (p.p.m.)	Scale expansion	Wavelength (nm)	Slit
Lead[a]	5	< 1.5	10X	283.3	4[c]
		1.5—7.5	2X		
Silver[b]	5	< 0.15	10X	328.1	4
		0.15—1.5	1X		
Zinc[a]	25	< 1.9	2X	213.9	4
		1.9—3.8	1X		
Bismuth[a]	5	< 1.5	10X	223.1	3
		1.5—7.5	2X		
Cadmium[b]	5	< 0.15	10X	228.8	4
		0.15—0.38	1X		

[a] Air—acetylene flame.
[b] Air—propane flame.
[c] Slit 4 corresponds to 0.7 nm, and 3 to 0.2 nm.

Atomic-absorption measurement

The sizes of volumetric flasks used are listed in Table 1. If concentration ranges other than those listed are involved, dilute the samples accordingly. A chloride medium is needed for lead and silver, and the lead/silver fraction is transferred to flasks with 5 % (v/v) hydrochloric acid. Zinc, bismuth and cadmium require a nitrate medium, and those fractions are transferred with 5 % (v/v) nitric acid. The instrumental parameters used are listed in Table 1; in general, the instrument settings correspond to those recommended in the analytical methods supplied with the unit. Obtain an absorbance value for each element, and establish the concentrations from calibration curves. Figure 3 shows all the curves plotted on the same scale to indicate relative sensitivities.

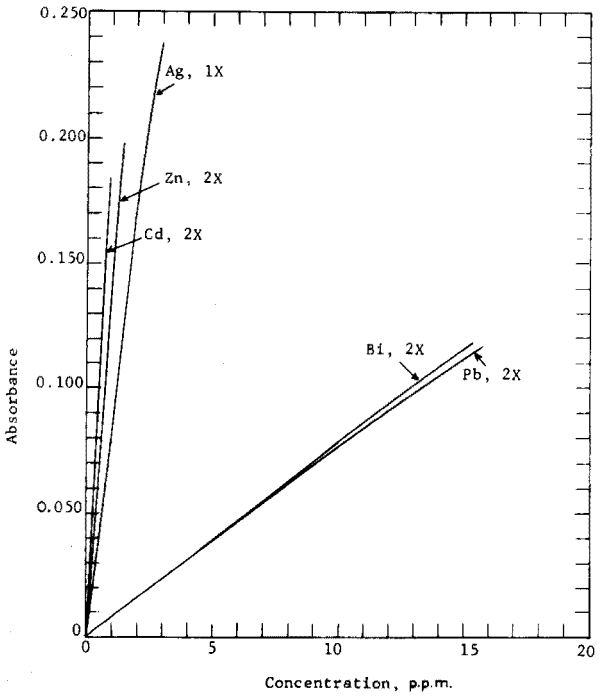

Fig. 3. Composite plot of calibration curves for the atomic-absorption spectrophotometer.

Discussion

A hydrochloric acid medium could be used to separate lead, silver, zinc, bismuth, and cadmium from the matrix of simple alloys, but complex alloys required an HCl—HF medium. Distribution coefficients could not be found for silver and cadmium in an HCl—HF medium. It was observed, however, that only slight differences existed between the hydrochloric acid and the HCl—HF media for lead, bismuth, and zinc. Since silver and cadmium do not form strong fluoride complexes in the HCl—HF medium, it was assumed that their distribution ratios for that medium would parallel those for hydrochloric acid. This assumption was verified by the elution data.

Eluant volumes were determined by adding lead, silver, zinc, bismuth, and cadmium to eight different nickel alloys and then applying the proposed procedure to the samples. The eluates were collected in 10-ml fractions, and the quantities of the added elements were determined for each fraction. The elution curves shown for Inconel alloy 600 (76 % Ni, 15.5 % Cr, 8 % Fe) in Fig. 4 are typical of the results; eluant volumes for the other alloys varied by only about 10 ml.

Cation exchange was chosen to separate titanium—molybdenum from lead—silver. Those eluant volumes were also arrived at by collection of 10-ml eluate

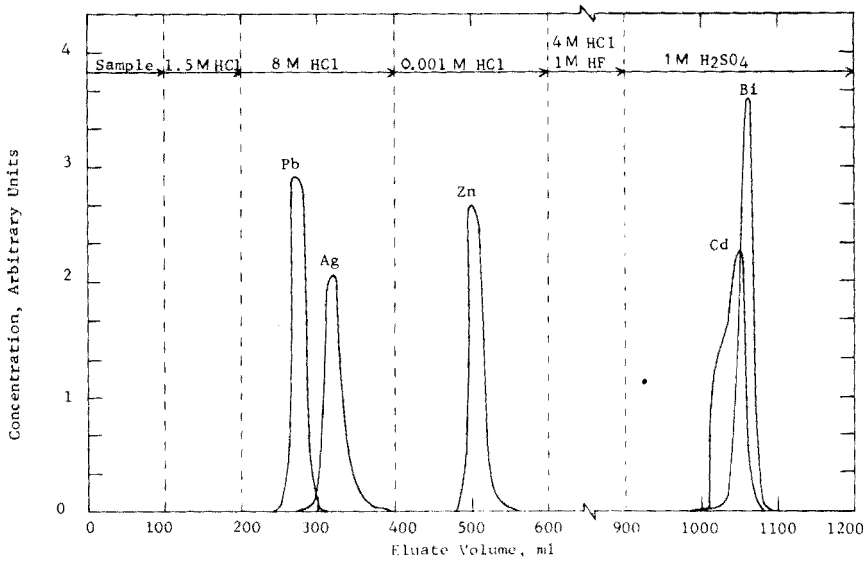

Fig. 4. Elution curves for Inconel alloy 600 on the anion-exchange column.

fractions, and determination of the lead and silver in each fraction. Typical elution curves, again for the Inconel alloy 600 matrix, are shown in Fig. 5.

The degree of recovery of the trace elements was determined by applying the elution sequence to samples of high-purity nickel pellets to which known amounts of each element had been added. A sample of the same material without the added elements was also taken through the elution sequence for

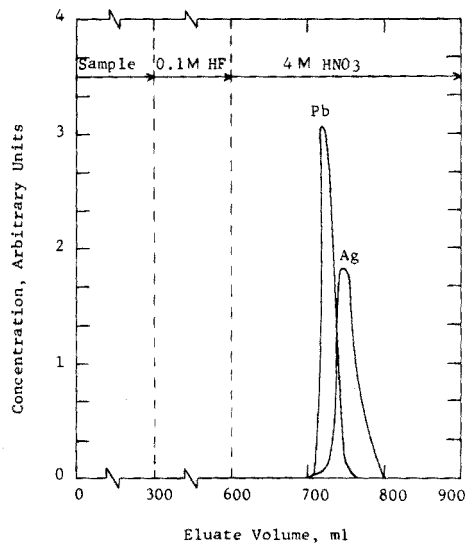

Fig. 5. Elution curves for Inconel alloy 600 on the cation-exchange column.

TABLE 2

Recovery of trace elements from samples[a] of high-purity nickel pellets and analysis of NBS SRM 361

High-purity nickel pellets					NBS SRM 361	
Element	Initial amount found (p.p.m.)	Amount added (p.p.m.)	Final amount found (p.p.m.)	Recovery (%)	Published value ($\cdot 10^{-3}$ %)	Amount found ($\cdot 10^{-3}$ %)
Lead	0.04	2.00	2.03	99.5	0.025	0.03
Silver	0.001	1.00	0.96	95.9	0.40	0.34
Zinc	0.03	5.00	5.03	100	0.10	0.17
Bismuth	0.00	2.00	1.92	96.0	0.40	0.49
Cadmium	0.00	1.00	0.92	92.0	—[b]	0.0011

[a] Based on 10-g samples.
[b] Cadmium value not supplied.

comparison. The results, given in Table 2, ranged from 92.0 % to 100 % recovery.

Analyses performed on National Bureau of Standards reference materials showed good correlation with the published values (Table 2).

REFERENCES

1 F. Nelson and K.A. Kraus, J. Amer. Chem. Soc., 76 (1954) 5916.
2 F.W.E. Strelow and C.J.C. Bothma, Anal. Chem., 39 (1967) 595.
3 J.A. Marinsky, Ion Exchange, M. Dekker, New York, 1966.
4 J.S. Fritz, B.B. Garralda and S.K. Karraker, Anal. Chem., 33 (1961) 882.
5 F.W.E. Strelow, R. Rethemeyer and C.J.C. Bothma, Anal. Chem., 37 (1965) 106.
6 F. Nelson, R.M. Rush and K.A. Kraus, J. Amer. Chem. Soc., 82 (1960) 339.

Analytica Chimica Acta, 80(1975)170—175

Short Communication

DESIGN AND PRELIMINARY EVALUATION OF A SIMPLE DISCRETE SAMPLER FOR FLAME SPECTROMETRIC ANALYSIS

MALCOLM S. CRESSER

Soil Science Department, Aberdeen University, Old Aberdeen, AB9 2UE (Scotland)

(Received 30th May 1975)

One of the primary advantages of electrothermal atomizers in analytical atomic spectrometry is that they employ small, discrete aliquots of sample solution for analysis. Their use in flame spectrometric analysis has largely been confined to heated cups, boats and filaments, however, although the direct nebulization of pulses of sample solutions offers a highly selective method of analysis when sample availability, and not detectability, is the limiting factor. The injection of discrete samples, either into a flowing water stream [1] or directly into a pneumatic nebulizer [2—5], has been suggested; the precision attainable with such methods is restricted by the reproducibility of the rates of injection. Ultrasonic nebulization of discrete samples has also been employed [6], but requires additional apparatus. The device described in this communication is not dependent upon an injection rate, is simple and inexpensive to manufacture, and may be substituted quickly for the flexible capillary of a conventional pneumatic nebulizer.

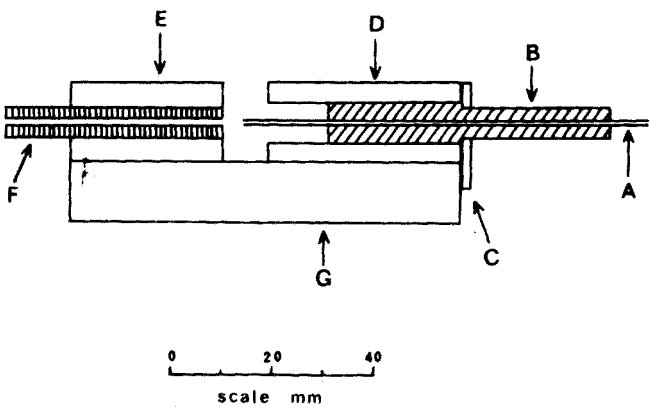

Fig. 1. Discrete sampling device: A, stainless steel capillary; B, brass piston; C, plate to limit outward travel of piston; D, brass barrel with circular hole for piston B; E, brass support for glass capillary which also serves to limit the inward travel of the piston; F, glass capillary (with internal diameter slightly larger than the external diameter of the steel capillary) to contain samples; G, brass base.

Experimental

The device is shown in Fig. 1. The length of the glass capillary, F, is chosen so that when piston B is pushed inwards, the steel capillary just enters a thread of solution contained in the glass capillary, thus ensuring smooth nebulization without break-up of the liquid thread: the precise length depends on the internal diameter of the glass capillary, which must be very slightly larger than the external diameter of the steel capillary. Samples of between 5 and 90 μl were introduced into the glass capillary with a 100 μl graduated pipette, fitted with a laboratory-made, curved plastic tip to facilitate sample manipulation. The sample is then nebulized by pushing the piston inwards from the position shown in Fig. 1.

The device was tested with EEL 140 and 240 atomic absorption spectrophotometers, with a Bryans 29000 chart recorder or a storage oscilloscope (connected to the photomultiplier via a fast-response d.c. amplifier) as the read-out system.

Results and discussion

A preliminary investigation indicated that, for the EEL 140 nebulizer/burner system, a 60 μl aliquot of sample solution gave a signal identical to that from continuous nebulization (Fig. 2). However, the amplifier response times of both the model 140 and the model 240 spectrophotometers are so slow that, even for 90-μl samples, the recorder signals were significantly smaller than those obtained from continuous nebulization. This may not occur in other instruments with more rapid response times, particularly those which may be used without modification with electrothermal atomizers. The signal duration is quite long compared with that of some other atomization systems.

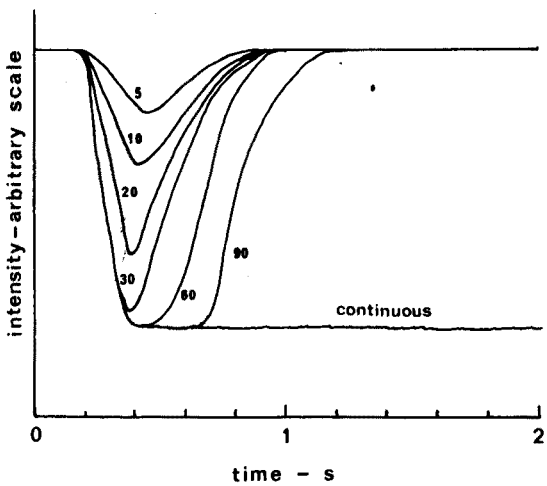

Fig. 2. Intensity—time plots for 1μg ml^{-1} magnesium for 5, 10, 20, 30, 60 and 90-μl aliquots and for continuous nebulization; as recorded on a storage oscilloscope.

For samples of less than 50μl, the maximum free atom concentration in the flame is less than the steady state concentration when continuous nebulization is employed. The useful working range may therefore be extended by employing smaller sample volumes (Fig. 3). This could be useful in atomic fluorescence spectrometry for eradicating the possibility of ambiguous results which arise from the negative slope of the calibration plots at high analyte element concentrations when line excitation sources are employed.

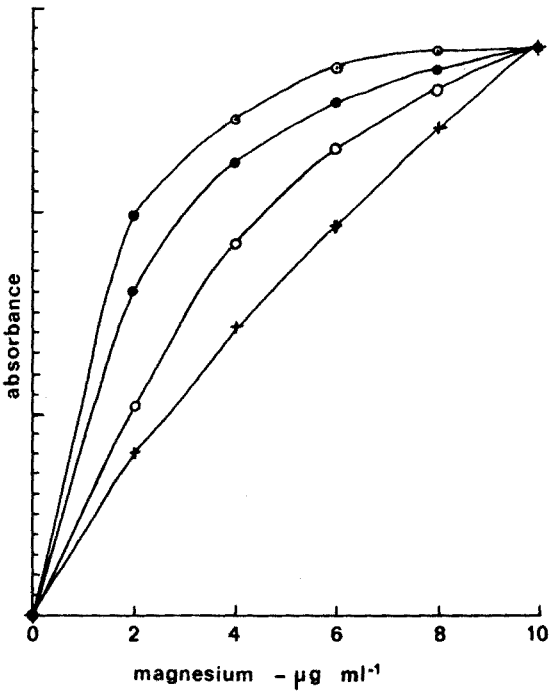

Fig. 3. Calibration curves for magnesium at 285.3 nm in an air—acetylene flame: (+) 10μl; (○) 20μl; (●) 50μl; (⊙) 90μl.

To obtain an indication of the precision attainable, the variation in the percentage standard deviation with sample volume was studied for cadmium at 228.8nm in a normal 100-mm air—acetylene flame: the results are shown in Table 1. For cadmium, and for other elements studied subsequently, the precision attainable with a 50-μl sample aliquot compares favourably with that obtained by continuous nebulization, provided that the concentration is well above the detection limit (obtained by continuous nebulization). The poorer precision for smaller sample volumes (e.g. 20μl) is attributable primarily to the poorer sampling reproducibility. Sample volumes greater than 80μl were susceptible to breaking-up during nebulization: this also reduced the precision by distorting the shape of the recorder trace. As the sample concentration approached the detection limit, the decrease in both the true and the apparent (electronic damping effect) signal had a deleterious effect upon

precision and detectability when small, discrete samples were used, particularly when 20μl samples were nebulized.

TABLE 1

Variation in relative standard deviation (s) with sample volume

Element	Concn. (μg ml^{-1})	Sample vol. (μl)	Absorbance[a]		s_r[b]
			Mean	Range	
Cd	0.1	20	not detectable		—
	0.1	50	0.027	0.023—0.032	14.0
	0.1	90	0.041	0.035—0.048	11.0
	0.1	Continuous	0.046	0.041—0.051	9.5
	0.5	20	0.033	0.022—0.041	77.0
	0.5	50	0.080	0.076—0.086	3.8
	0.5	90	0.175	0.168—0.187	4.8
	0.5	Continuous	0.312	0.297—0.323	3.0
	5.0	20	0.117	0.108—0.124	5.0
	5.0	50	0.184	0.181—0.187	1.0
	5.0	90	0.306	0.292—0.312	2.8
	5.0	Continuous	0.469	0.462—0.475	1.2
Zn	1.0	50	0.137	0.131—0.143	3.6
	1.0	Continuous	0.395	0.377—0.415	3.0
Cu	0.6	50	0.066	0.063—0.075	7.3
	0.6	Continuous	0.160	0.155—0.174	3.7
Mg	0.2	50	0.430	0.400—0.458	4.4
	0.2	Continuous	0.654	0.638—0.678	2.2

[a] Arbitrary scale expansion used.
[b] Based on ten absorbance values.

Although chemical matrix interferences are now well-known in flame atomic absorption spectrometry, the effect on the incidence or extent of such interferences of nebulizing small, discrete samples has not been studied. The effect of sample volume on some well-known interferences was therefore investigated, as shown in Fig. 4. The effect of aluminium on calcium and magnesium absorbance became significantly more serious as the sample volume was decreased. This effect is possibly attributable to a different size distribution of aerosol particles in the nebulizer spray when pulse nebulization is used. This hypothesis was supported to some extent by the results obtained for calcium when the mixer paddle, which reputedly serves also to remove larger droplets from the aerosol, was removed from the spray chamber: the enhancement of the interference effect for small sample volumes then became even more pronounced. The interference enhancement was less pronounced for phosphate on calcium (both present at 20 μg ml^{-1}). Lanthanum, at a final concentration

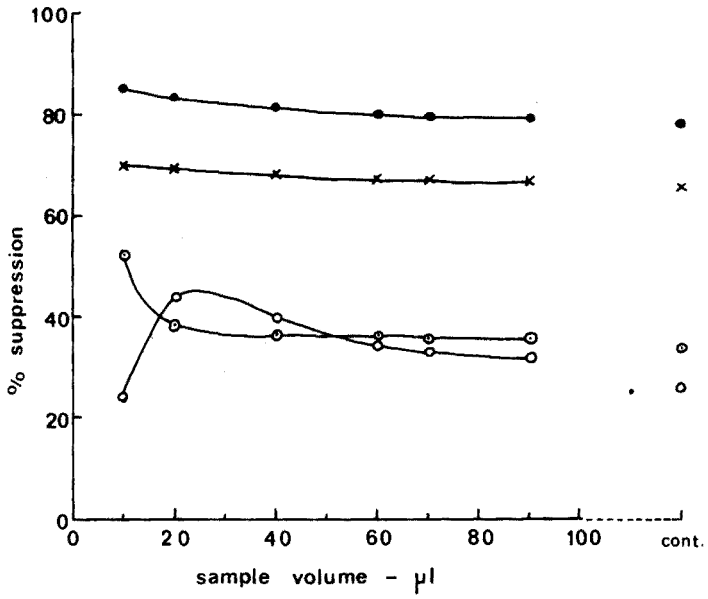

Fig. 4. Effect of sample volume on degree of interference. (O) 100μg ml^{-1} iron on 5μg ml^{-1} chromium; (●) 20μg ml^{-1} aluminium on 20μg ml^{-1} calcium; (×) 20μg ml^{-1} aluminium on 1μg ml^{-1} magnesium; (Θ) 5μg ml^{-1} aluminium on 20μg ml^{-1} calcium, mixer-paddle removed.

of 2000 μg ml^{-1}, effectively eradicated the above interferences, regardless of the sample volume used.

The effect of decreasing sample volume on the interference of iron in the determination of chromium differed significantly from the effects described above. For the smallest sample volume (10μl), the iron interference was slightly less although at higher volumes the more typical pattern was again observed. This effect may be attributable to a variation in the reducing properties of the air—acetylene flame with the rate of introduction of water into the flame.

Two additional advantages are associated with the direct nebulization of discrete samples, apart from that of small sample requirement. The first is the virtual elimination of the tendency of burners towards clogging. This effect, which arises primarily from the far smaller total amount of nebulized solution, has been discussed briefly by other workers [2] for the direct injection method. This has been found particularly useful for the analysis of soil extracts containing very large amounts of dissolved organic and inorganic species: these extracts tend to cause serious clogging, particularly of nitrous oxide—acetylene burners, when large numbers of samples are being analyzed. The second advantage is that organic solvents which may cause the flame to become excessively fuel-rich on continuous nebulization, even when the acetylene flow is reduced to the minimum safe level, or which may generate

toxic combustion products or possibly extinguish the flame, may be nebulized in small amounts. Benzene, toluene, chloroform and carbon tetrachloride could be nebulized in this way. Small changes in background absorption at certain wavelengths, which could limit detectability for elements with resonance lines in these regions may, however, be caused by these solvents; this aspect is undergoing further investigation. This type of device might also be used successfully without desolvation in conjunction with a high-efficiency, heated spray-chamber.

REFERENCES

1 F.S. Chuang, J.R. Sarbeck, P.A. St. John and J.D. Winefordner, Mikrochim. Acta, (1973) 523.
2 E. Sebastiani, K. Ohls and G. Riemer, Z. Anal. Chem., 264 (1973) 105.
3 E. Jackwerth and H. Berndt, Anal. Chim. Acta, 74 (1975) 299.
4 I. Harris and D.C. Newton, Varian Techtron Atomic Absorption Symposium, London, September, 1971.
5 S. Greenfield and P.B. Smith, Anal. Chim. Acta, 59 (1972) 341.
6 N.E. Korte, J.L. Moyes and M.B. Denton, Anal. Chem., 45 (1973) 530.

Analytica Chimica Acta, 80(1975)176—179

Short Communication

RAPID DETERMINATION OF RUTHENIUM IN ORGANOMETALLIC COMPOUNDS, SUPPORTED CATALYSTS AND ORGANOMETALLIC POLYMERS BY x-RAY FLUORESCENCE

LEONARDO LEONI

Istituto di Mineralogia e Petrografia dell'Università di Pisa, via S. Maria 53, 56100 Pisa (Italy)

GIUSEPPE BRACA, GLAUCO SBRANA and ENZO GIANNETTI

Istituto di Chimica Organica Industriale dell'Università di Pisa, via Risorgimento 35, 56100 Pisa (Italy)

(Received 3rd March 1975)

The determination of ruthenium in organometallic compounds by conventional methods is often complicated, and appreciable errors can arise especially when second or third row main group elements such as sulphur and phosphorus are present [1]. Atomic absorption spectrometry is satisfactory only for ruthenium compounds which are soluble in water [2] or in suitable organic solvents [3]. Serious difficulties are encountered in analyses for ruthenium in organometallic complexes which are insoluble in water or in organic solvents, and in supported catalysts and organometallic polymers. For catalysts and polymers determination of ruthenium is extremely important not only for characterization of the product but also in checking the metal losses during catalytic reactions.

x-Ray fluorescence is well recognized as an accurate, rapid and sensitive technique, for the determination of heavy elements in organometallic complexes [4,5] and organometallic polymers [6].

However, no details have been reported on the x.r.f. determination of ruthenium [7]. It is shown here that x.r.f. provides a simple, convenient metho of solving the above-mentioned problems.

Experimental

Apparatus

A Philips PW 1540/10 manual x-ray spectrometer, a LiF 220 analyzing crystal and a tungsten target tube were used. The ruthenium $K\alpha$ intensities were measured with a scintillation counter. All readings were corrected for the background, measured immediately before and after the angular position of the Ru $K\alpha$ characteristic line. No interferences from other elements were encountered. To achieve a high degree of reproducibility, measurements were related to an external standard.

Reagents

The standards used were metallic ruthenium (99.9%; Metaux Precieux, Neuchatel, Switzerland), ruthenium tris(acetylacetonate) crystallized twice from ethanol—water [8], and di-μ-chloro-bis(chlorotricarbonylruthenium) [9], $[Ru(CO)_3Cl_2]_2$.

The organometallic phosphorus-containing compounds analyzed were new hydrido carboxylato ruthenium complexes [10] prepared by reaction of $RuH_2(PPh_3)_4$ and $RuH_2CO(PPh_3)_3$ with carboxylic acids [11]. The organometallic polymers were prepared as described elsewhere [12].

The matrix for analysis of solid insoluble samples was dry silica (U 40 grade; J. Crosfield and Co.); this was also used as the carrier for the supported ruthenium catalysts [13].

Procedure

Standards and samples were prepared as powder pellets or as benzene or methanol solutions. To prepare the pellets, a small amount of the organometallic complex or polymer (10—50 mg) was dispersed in very fine silica (1 g), by mixing in an agate mortar for about 15 min; the samples were then compressed to discs of approximately constant thickness (2 mm, 0.46 g cm^{-2}) under constant pressure. The thickness indicated is very close to infinite thickness. The samples were then irradiated so that the standard counting error for the net peak was about 0.5%. The silica-supported catalysts were analyzed directly without dispersion in the matrix.

Calibration curves were obtained by plotting the count-rate vs. the ruthenium concentration as percent by weight, with metallic ruthenium and di-μ-chloro-bis(chlorotricarbonylruthenium) as standards. The curve computed by least-squares regression analysis was practically linear in the range 0.2—2% ruthenium by weight; the ruthenium content could be calculated from the relation

$$Ru\ \% = I_{Ru K\alpha} \times 2.4571 \cdot 10^{-4} - 67.7 \cdot 10^{-4}$$

For the analysis of solutions, series of standard solutions of ruthenium tris(acetylacetonate) in benzene or methanol (0.08—0.200 g Ru l^{-1}) were prepared. The calibration curves were linear over the range mentioned. Benzene or methanol solutions from catalytic experiments with heterogeneous ruthenium catalysts were analyzed directly for ruthenium. When solutions were analyzed, 8.5—10 ml sufficed to provide a depth of 27 mm, corresponding to infinite thickness for the geometry used.

Results and discussion

Table 1 shows the results obtained for organometallic complexes, organometallic polymers and supported ruthenium catalysts, as well as comparative results produced by other techniques. The agreement between the theoretical and found results is good for organometallic complexes (maximum error 3 %), and the results for organometallic polymers and supported catalysts are very close to those obtained by other methods.

TABLE 1

Analyses of solid pellets by x.r.f.

Compound	Theor.	x-Ray	Comparative method
$\{RuH[P(C_6H_5)_3]_2CO\}_2[OCO(CH_2)_2OCO]$	14.18	14.42 ± 0.06	13.78[a]
$\{RuH[P(C_6H_5)_3]_2CO\}_2[OCO(CH_2)_4OCO]$	13.91	14.13 ± 0.09	
$RuH(OCOCH_2OH)[P(C_6H_5)_3]_3$	10.48	11.06 ± 0.06	
$RuH[OCOCH(OH)C_6H_5][P(C_6H_5)_3]_3$	9.72	10.10 ± 0.06	
$RuH(OCOCH_2COOH)[P(C_6H_5)_3]_3$	10.19	10.63 ± 0.06	
$[Ru(CO)_3Cl_2]_2$ on phosphinated silica		0.66 ± 0.003	0.62[a]
$[Ru(CO)_3Cl_2]_2$	39.48	39.21 ± 0.2	39.34[b]
$RuBr(C_3H_5)(CO)_2$(PPST)[c]	10.50[d]	9.78 ± 0.06	
$RuBr(C_3H_5)(CO)_2$(P4VP)[e]		19.01 ± 0.1	19.43[a]

[a] Neutron activation analysis.
[b] Atomic absorption spectrometry in solution.
[c] PPST = polyphenylphosphinostyrene.
[d] Based on bromine determination, assuming a 1:1 Ru/Br ratio in the polymeric sample.
[e] P4VP = poly-4-vinylpyridine.

TABLE 2

Analyses of solutions by x.r.f.

Sample	Solvent	Nominal Ru content ($g\ l^{-1}$)	X.r.f. ($g\ l^{-1}$)
1	Benzene	0.0763	0.0764
2	Benzene	0.1080	0.1040
3	Benzene	0.1525	0.1620
4	Benzene	0.2160	0.2110
5	Methanol	0.0813	0.0826
6	Methanol	0.0992	0.0958
7	Methanol	0.1630	0.1680
8	Methanol	0.1980	0.1940

Table 2 shows some results for direct analyses of samples in benzene and methanol solutions; the differences between the nominal and determined contents are below 0.010 g Ru l^{-1}.

The precision depends essentially on the standard counting error, which is about 0.5 %; the accuracy depends only on the sample preparation, as the matrix effect and the deviation from linearity of the calibration curves are negligible. The sensitivity for a counting time of 100 s is about 25 p.p.m. for pelleted samples and 0.002 g Ru l^{-1} for solutions.

The method has the following advantages: (i) dilution of solid samples with

fine silica, or the use of solutions, eliminates matrix effects; (ii) it is possible to analyze insoluble compounds and heterogeneous catalysts, for which atomic absorption spectrometry or x.r.f. on filter paper [4,6] are unsatisfactory; (iii) the method is rapid, requiring ca. 15 min to weigh, homogenize and analyze one sample; (iv) the method is sensitive and requires only 10—100 mg of product.

This work was supported by C.N.R. (Rome).

REFERENCES

1 C.V. Banks and J.W. O'Laughlin, Anal. Chem., 29 (1957) 1412.
2 B. Montford and S.C. Cribbs, Anal. Chim. Acta, 53 (1971) 101.
3 G. Braca, R. Cioni, G. Sbrana and G. Scandiffio, At. Absorption Newslett., 14(2)(1975) 39.
4 J.M. McCall, D.E. Leyden and C.W. Blount, Anal. Chem., 43 (1971) 1324.
5 S.J. Anderson, D.S. Brown and A.H. Norbury, J. Organometal. Chem., 64 (1974) 301.
6 D.E. Leyden, J.C. Lennox and C.U. Pittman Jr., Anal. Chim. Acta, 64 (1973) 143.
7 M. Shelef and H.S. Gandhi, Metal Platinum Rev., 18 (1974) 2.
8 C. Barbieri, Atti Accad. Lincei, 23 (1914) 334.
9 G. Braca, G. Sbrana, E. Benedetti and P. Pino, Chim. Ind. (Milan), 51 (1969) 1245.
10 G. Braca, G. Sbrana and E. Giannetti, unpublished data.
11 S.D. Robinson and M.F. Uttley, J. Chem. Soc. Dalton, (1973) 1912.
12 G. Braca, G. Sbrana, C. Carlini and F. Ciardelli, Int. Symp. on the Relations between Heterogeneous and Homogeneous Catalytic Phenomena, Bruxelles, 23—25 Oct. 1974, D 1.1.
13 K.G. Allum, R.D. Hancock, S. McKenzie and R.C. Pitkethly, Proc. 5th Int. Congress on Catalysis, Amsterdam, 1972.

Analytica Chimica Acta, 80(1975)180—182

Short Communication

A HIGHLY SENSITIVE FLUORESCENT REACTION FOR TELLURIUM(VI) APPLICATION TO THE DETERMINATION OF TELLURIUM IN SELENIUM

M. BOVAY and M. MARCANTONATOS

Department of Inorganic and Analytical Chemistry, University of Geneva, 1211-Geneva-4 (Switzerland)

(Received 8th May 1975)

Numerous spectrophotometric methods have been proposed for the determination of tellurium, but the highly sensitive photoluminescence techniques have only found a few applications. Most of the colorimetric methods are based on the formation of complexes with ligands having oxygen, sulfur or O,S coordination sites; a few methods involve the formation of colored ionic associates between acid tellurium complexes and organic bases [1].

Fluorescent associates have been obtained with rhodamine S derivatives [1(a)] and these, like the coloured associates and the other absorbing complexes, permit the determination of tellurium in the $\mu g\ ml^{-1}$ range. The formation of fluorescent tellurium chelates does not seem to have been reported; the only fluorimetric method proposed so far for the determination of tellurium is based on the formation of ion associates with rhodamine S (or derivatives).

1,1′-Dianthrimide reacts with tellurium species in concentrated sulfuric acid, to give a 1:1 coloured complex [2,3]. In this solvent, fluorescent chelates are formed between orthotelluric acid and hydroxy-2-benzophenone ligands, which also form highly luminescent chelates with the tetra(hydrogensulfato)borate monomeric anion [4—6]. Most of the benzophenones studied in the present work gave coloured chelates with $Te(OH)_6$ and two of them — 2-hydroxy-5-methoxybenzophenone and 2,4,4-trihydroxybenzophenone (THB) — formed chelates which were also highly fluorescent. The THB ligand was found to be the most appropriate for analytical purposes, and permits the precise determination of tellurium in the $ng\ ml^{-1}$ range.

Boron—THB chelates, which are negligibly excited at 426 nm (maximum excitation of Te-THB), do not interfere.

Experimental

Reagent-grade orthotelluric acid and sulfuric acid (d 1.84; Merck) were used. 2,4,4-Trihydroxybenzophenone (Aldrich) was purified by double recrystallization with triple-distilled water—ethanol (70+30). Solutions of telluric acid in sulfuric acid were prepared from an aqueous $5 \cdot 10^{-2}$ M solution. A Perkin—

Elmer MPF-2A spectrofluorimeter was used.

Results and discussion

Spectral investigations, as well as studies on the kinetics and equilibria of complex formation, showed that THB, in excess over $Te(OH)_6$, forms successively 1:1 and 2:1 THB—$Te(OH)_6$ fluorescent chelates [7]. The 1:1 chelate is readily formed at room temperature, while the 2:1 chelate, on which the proposed analytical method is based, is formed by heating the THB—$Te(OH)_6$ solutions in sulfuric acid at 90 °C for 120 min. This is due to the structure of the 1:1 complex in which the tellurium moiety is deprived of sites capable of being readily coordinated by a second THB molecule. The formation of the 2:1 chelate, therefore, requires opening of a probably highly stabilized ring in the 1:1 complex.

The maximum excitation and fluorescence emission wavelengths of the 2:1 chelate lie at 426 and 465 nm, respectively. At these wavelengths, the apparent fluorescence emission efficiency, ϕ_{21}, for a moderately sensitive arrangement of the fluorimeter, is of the order of 10^8 M^{-1} cm^{-1}, thus permitting ng ml^{-1} levels of tellurium to be determined with acceptable precision. The ϕ_{11} value of the 1:1 chelate is about 10^2 times lower than the ϕ_{12} value, showing the predominant intraligand transition character of the absorption and emission bands of these complexes.

Analytical curves were determined by repeating single fluorescence measurements for each tellurium concentration over several weeks. Repeatability was satisfactory, and the straight-line slopes were reproducible. The linear regression coefficients were never lower than 0.995 and the relative errors did not exceed ± 16% and ± 3% for 9 ng Te ml^{-1} and 65 ng Te ml^{-1}, respectively.

Foreign ions such as Li^+, Mg^{2+}, Ca^{2+}, Sr^{2+}, Ba^{2+}, B^{3+}, Al^{3+}, V^{4+}, Mn^{2+}, Fe^{2+}, Co^{2+}, Ni^{2+}, Co^{2+}, Zn^{2+}, Cd^{2+}, Sn^{2+}, Pb^{2+}, Sb^{3+}, Bi^{3+}, NO_3^-, NO_2^- and CO_3^{2-} in 100-fold(molar) concentrations over $5 \cdot 10^{-7}$ M tellurium, did not interfere. Chromium(VI) and iron(III) doubled the fluorescence intensity, while chloride caused a 30% diminution in the intensity, when these ions were present in 100-fold amounts; they did not interfere when present in 10-fold amounts.

Direct determination of tellurium in high-purity selenium: Tellurium can be determined without any preliminary separation, by dissolving the selenium in hot 96% sulfuric acid, adding 0.5 ml of THB solution (10^{-5} M) in sulfuric acid to aliquots of sample solution, and then forming the 2:1 chelate in a total volume of 5 ml (in an oven at 90 °C for 180 min); the fluorescence is measured at 465 nm (exc. 426 nm) versus a blank solution.

The analytical results for a sample of relatively pure selenium are given in Table 1. The mean result obtained by the external standard method was 0.104% (s = 0.005) and that obtained by the standard addition method was 0.089% (s = 0.005). The average result, 0.096%, is not in accordance with the maximum limit of impurity of tellurium given by the manufacturer. The high result cannot be explained by possible interferences from iron and chromium, because the

contents of these elements in the sample were far lower than the tolerance limits for the procedure.

TABLE 1

Fluorimetric determination of tellurium in selenium
(The selenium was a B.D.H. AnalaR sample with the maximum limits of impurity given as 0.05 % Te, 0.006 % Fe. P, initial sample solution in sulfuric acid; V_a, volume of aliquot (total volume, 5 ml); F, fluorescence intensity.)

P (g ml^{-1})	V_a (ml)	External standard		Internal standard	
		F	% Te	F	% Te
1.2765	0.2	68	0.099	82	0.093
1.2765	0.2	51	0.093	57	0.075
1.0361	0.07	25	0.123	37	0.073
1.0361	0.1	—	—	47	0.090
0.20722	0.2	15	0.10	49	0.10
0.20722	0.3	23	0.10	56	0.099

REFERENCES

1 I.I. Nazarenko and A.N. Ermakov, Analytical Chemistry of Selenium and Tellurium. Halsted Press, New York (1972), (a) page 115.
2 O.B. Skaar and F.J. Langmyhr, Anal. Chim. Acta, 23 (1960) 175.
3 F.J. Langmyhr and G. Norheim. Anal. Chim. Acta, 41 (1968) 341.
4 M. Marcantonatos, A. Marcantonatos and D. Monnier, Helv. Chim. Acta, 48 (1965) 194.
5 M. Marcantonatos and B. Liebick, Chimia, 24 (1970) 447.
6 M. Marcantonatos and C. Menzinger, Inorg. Chim. Acta (in press).
7 M. Marcantonatos and M. Bovay, unpublished results.

Analytica Chimica Acta, 80(1975)183—187

Short Communication

THE DETERMINATION OF TOTAL PHOSPHATE IN NATURAL WATERS

P.D. GOULDEN and P. BROOKSBANK
Canada Centre for Inland Waters, Burlington, Ontario (Canada)
(Received 18th March 1975)

Phosphorus is one of several key elements essential for the growth of algae in water; it is often the growth-limiting nutrient, and the determination of phosphorus levels in natural waters has therefore become increasingly important. The "total" phosphorus analyses consist of two general steps [1]: (a) conversion of condensed phosphates and organic phosphorus compounds to orthophosphate, and (b) colorimetric determination of soluble orthophosphate. The method currently in use in these laboratories involves digesting the sample with potassium persulfate in a dilute sulfuric acid medium to convert all the phosphorus to orthophosphate, which is then treated with ammonium molybdate and tin(II) chloride to form molybdenum blue which is measured colorimetrically. In attempts to improve the precision, accuracy and detection limits of this method, two significant problems were identified. First, the reagent additions must be made precisely in the normal preparation of samples for digestion, which is best done with automated pipetters and "semi-automation" of the manual digestion, or by a completely automated digestion procedure; secondly, "blank" corrections are necessary because of turbidity in the sample, which could be minimized by the inclusion of an extraction step for the molybdenum blue. This extraction also serves to concentrate the color with a consequent improvement in the detection limit.

Two recommended alternatives for a total phosphorus analysis are described below. The first is a semi-automated autoclaving, and the second a fully automated procedure involving the use of u.v. digestion to break down organophosphorus compounds. Both of these methods incorporate steps to remove interference from arsenic, and extraction of the molybdenum blue.

Method I — Semi-automated autoclaving

The manifold used is shown in Fig. 1. The sample which has been previously autoclaved in the sample tube is mixed with sodium metabisulfite and sodium thiosulfate in a delay coil to reduce arsenate to arsenite [2]. Ammonium molybdate and tin(II) chloride are added to form molybdenum blue, which is then extracted into isobutanol for measurement.

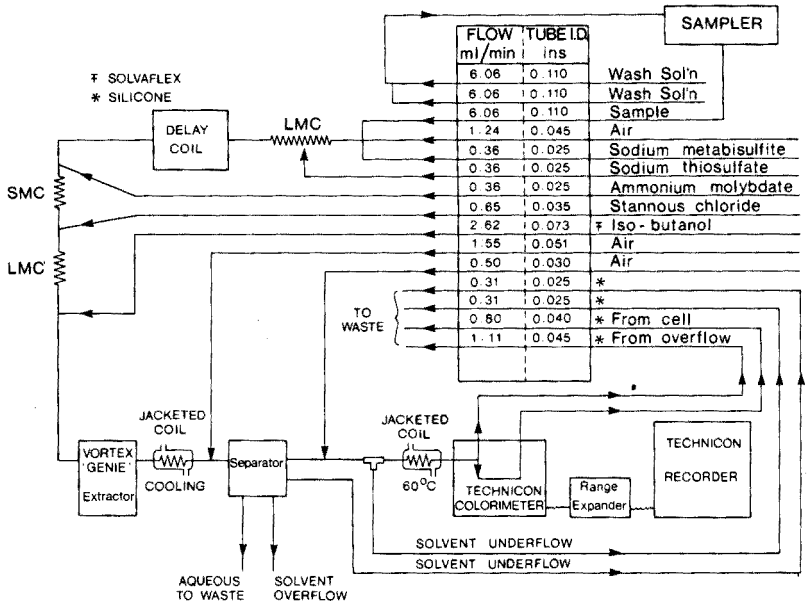

Fig. 1. Manifold for semi-automated "total" phosphorus determination.

Apparatus

The tubes used in the sampler and autoclaving are culture tubes 25 mm × 100 mm long, and graduated at the 25-ml volume. Small beakers (20 ml) cover the tubes in the autoclave (a "Castle" No 999-C electrically heated model). Fisher "Volustats" or similar dispensing devices are used for reagent additions before autoclaving. The sampler is an Industrial Sampler (Technicon), modified [3] to prevent air entering the system during the sample arm transfer. The pump is a 20-channel proportioning pump (Carlo Erba). The extraction and solvent separation are as previously described [3]. The color is measured with a Technicon AAI Colorimeter with a 50-mm flowcell at a wavelength of 660 nm.

Reagents

Deionized water is used throughout. The wash solution is 0.5 % (v/v) 18 M sulfuric acid. For the "strong" acid, 25 ml of 18 M sulfuric acid is added to 600 ml of water, and 1 ml of 18 M nitric acid is added to the cooled solution which is diluted to 1 l. The other solutions are: aqueous 4 % (w/v) $K_2S_2O_8$; a solution of 25 g of $(NH_4)_6Mo_7O_{24} \cdot 4H_2O$ in 175 ml of water, added to a mixture of 180 ml of 16 M sulfuric acid and 400 ml of water and diluted to 1 l; aqueous 15 % (w/v) $Na_2S_2O_5$; and aqueous 3 % (w/v) $Na_2S_2O_3$.

For the stock tin(II) solution, 5 g of $SnCl_2 \cdot 2H_2O$ is dissolved in 25 ml of 12 M hydrochloric acid, and this is diluted to 500 ml with water; this solution is stable for 2 weeks at 5 °C. For the working solution 30 ml of stock solution and 25 ml of 12 M hydrochloric acid are diluted to 500 ml.

Standard phosphate solutions are prepared from dipotassium hydrogenphosphate and sodium tripolyphosphate ($Na_5P_3O_{10}$).

Procedure

To the culture tubes are added standard solutions or samples to the 25-ml mark. "Strong" acid (1.0 ml) and 2.5 ml of persulfate solution are then added to the tubes, which are covered with 20-ml beakers and autoclaved at 15 p.s.i.g. for 30 min. After cooling, the tubes are loaded directly into the sampler for analysis.

Method II — Automated u.v. digestion

The sample is mixed with acid and persulfate and then pumped through a silica coil around a u.v. lamp (1200 W). By controlling the cooling, the solution is maintained at 85 °C in the coil; this oxidizes the organic phosphates and hydrolyzes the condensed phosphates in the same step. Sodium metabisulfite and thiosulfate are added to reduce arsenate, and the molybdenum blue produced as above is extracted for measurement.

Apparatus

The manifold is shown in Fig. 2. The sampler and pump are as described above. The u.v. lamp is a 1200-W mercury arc lamp (model 189A-16, Englehard Hanovia Inc.). A silica coil 27 m long and 3 mm i.d. wound in a 12-cm

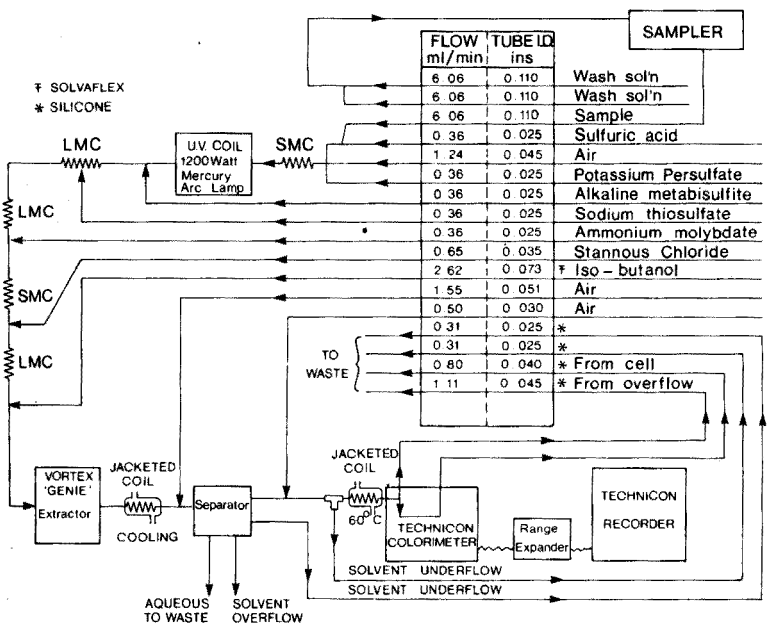

Fig. 2. Manifold for automated "total" phosphorus determination.

diameter coil is placed symmetrically around the lamp. The solvent extraction and separation are as previously described [3].

Reagents

Deionized water is used throughout. The wash solution is 0.3 % (v/v) 18 M sulfuric acid in water. The sulfuric acid solution is 37 % (v/v) 18 M sulfuric acid in water. For the ammonium molybdate, 25 g of $(NH_4)_6Mo_7O_{24} \cdot 4H_2O$ is dissolved in 175 ml of water, added to a mixture of 80 ml of 18 M sulfuric acid and 400 ml of water and diluted to 1 l. Other solutions are: aqueous 1 % (w/v) $K_2S_2O_8$; an alkaline sodium metabisulfite solution prepared by dissolving 14.4 g of sodium hydroxide pellets and 5 g of $Na_2S_2O_5$ in 100 ml of water; and other reagents as in the semi-automated method.

Procedure

The samples are poured directly into the sampler tubes and loaded into the sampler along with a number of standards interspersed among the samples, so that any change can be readily detected and the calibration curve checked. Standards normally used consist of orthophosphate and tripolyphosphate covering the range of expected concentration. The concentration of phosphate in the samples can then be determined directly from the peak heights on the chart.

Results and discussion

The two methods described above are designed to analyse natural water samples containing phosphorus in the range 0.2—4.0 $\mu g\ l^{-1}$, that have been preserved by addition of 1 ml of 30 % (v/v) 18 M sulfuric acid to a 100-ml

TABLE 1

Comparison of the results for total phosphate in lake water samples

	Standard method ($\mu g\ l^{-1}$)	Semi-automated ($\mu g\ l^{-1}$)	Fully automated ($\mu g\ l^{-1}$)
Sample 1	16.0	16.0	15.0
Sample 2	30.0	30.5	29.5
Sample 3	23.0	23.0	22.5
Sample 4	24.0	24.0	24.0
Sample 5	17.5	18.0	16.5
Sample 6	41.0	41.0	39.5
Sample 7	8.5	8.5	8.0
Sample 8	6.0	6.0	6.0
Average for 40 samples	20.80	20.74	20.29
Recovery*	—	100 %	97 %

*Relative to standard method.

aliquot of sample. Unacidified samples can be analyzed if the acid concentration in the system is adjusted to the optimum for formation of molybdenum blue.

Synthetic samples and standard solutions containing orthophosphate, tripolyphosphate and adenosine-5-monophosphate were analysed by both methods with 100 % recovery of total phosphorus. The detection limit for both methods is 0.2 μg P l^{-1}. Many water samples from the Great Lakes were analysed by both methods, and by the standard method [4]. The manual digestion method gave 100 % recovery and the u.v. digestion method gave 97 % recovery (Table 1).

At the 10 μg l^{-1} level based on 10 replicate determinations, the relative standard deviation was 2.3 % for the fully automated procedure and 3.4 % for the semi-automated procedure. Turbid samples were not a problem because the turbidity was not carried over into the solvent phase.

Initially, the procedure of Henriksen [5] based on extraction of the yellow molybdophosphoric acid with isobutanol, was examined; in this method, reduction with tin(II) is done in the organic phase, or the yellow molybdophosphate itself is measured. However, it was found that greater sensitivity could be obtained by forming the molybdenum blue in the aqueous phase and then extracting with isobutanol for the measurement.

In the automated digestion, changing the concentration of the reagents did not increase the oxidation for natural water samples. The temperature of the solution leaving the u.v. coil is fairly high, and additional heat is generated by addition of alkaline metabisulfite, so that a delay coil is not needed for the arsenate reduction. The addition of alkali is necessary to decrease the acidity before the formation and reduction of molybdophosphate, because the relative amounts of sulfuric acid and molybdate are important for optimum reactions [4].

The only important interference is arsenate, and this can be eliminated by reduction with thiosulfate in an acidic medium [2]. In the present method arsenate up to 1 mg l^{-1} does not interfere.

REFERENCES

1 Standard Methods for the Examination of Water and Wastewater, American Public Health Association, American Water Works Association, and Water Pollution Control Federation, New York, 13th edn., 1971.
2 P.D. Goulden and P. Brooksbank, Limnology and Oceanography, 19 (July 1974) 4.
3 P.D. Goulden, P. Brooksbank and J.F. Ryan, Amer. Lab., 5 (8) (1973) 10.
4 J. Murphy and J.P. Riley, J. Mar. Biol. Ass. U.K., 37 (1958) 9.
5 A. Henriksen, Analyst (London), 90 (1965) 29.

Analytica Chimica Acta, 80(1975)188—191

Short Communication

NOTE SUR L'UTILISATION DE L'OXYDE D'ARGENT(II) DANS LE TITRAGE DU PLUTONIUM

P. CAUCHETIER, C. GUICHARD et F. REGNAUD

Département de Recherche et Analyse/SCAPE, Centre d'Etudes Nucléaires, BP no. 6 — 92260 Fontenay-aux-Roses (France)

(Reçu le 30 mai 1975)

L'oxyde d'argent(II) est d'un emploi commode pour obtenir le plutonium(VI) dans les titrages qui font intervenir le système oxydoréducteur Pu(VI)/Pu(IV). La méthode a été décrite et utilisée avec différentes variantes [1, 2]; elle est appliquée couramment dans de nombreux laboratoires et nous avons essayé de l'adapter à des dosages demandant un haut niveau de précision: étalonnage de références, analyses de matières fissiles pour l'établissement de données neutroniques.

Pour l'analyse du plutonium, la méthode de travail du laboratoire consiste à prendre comme référence secondaire une solution de sulfate cérium(IV) 10^{-2} M. Cette solution est titrée au moyen d'étalons certifiés par le National Bureau of Standards: l'oxalate de sodium et l'anhydride arsénieux ou le plutonium métallique. Dans ce dernier cas, deux méthodes de titrage peuvent être utilisées, ayant pour principe soit l'oxydation de Pu(III) en Pu(IV) après réduction du plutonium par le titane(III) [3], soit la réduction de Pu(VI) en Pu(IV) après oxydation du plutonium par l'oxyde d'argent(II) [2]. A plusieurs reprises nous avons noté que cette dernière méthode présentait, par rapport aux autres, un écart systématique que nous avons cherché à expliquer.

Rappel du mode opératoire — Hypothèse sur l'origine de l'écart systématique

Le plutonium, en solution acide HNO_3M—H_2SO_4 0,5 M, est oxydé par 300 mg d'oxyde d'argent(II). Après destruction de l'excès d'oxyde par chauffage modéré et addition d'acide sulfamique, pour s'affranchir des nitrites, et de nitrate d'aluminium pour complexer les ions fluorure, Pu(VI) est réduit par une quantité connue de Fe(II) ajoutée en excès. La solution de Fe(II) et l'excès sont titrés par cérimétrie. Le point équivalent est déterminé par photométrie de l'orthophénanthroline ferreuse [4]. Les titrages et les prélèvements de solutions sont faits par pesée dans des conditions similaires à celles décrites par ailleurs [5].

Le titre de la solution de sulfate de cérium(IV) obtenu par cette méthode est d'environ 0,2 % plus faible que celui obtenu par oxydation de Pu(III) en Pu(IV) ou au moyen des autres étalons d'oxydoréduction. Les potentiels d'équilibre

des systèmes Ag(I)/Ag(0) et Fe(III)/Fe(II) étant voisins, nous avons émis l'hypothèse que Ag(I) oxydait une petite quantité de Fe(II) en Fe(III) [6]. La vérification expérimentale de cette hypothèse est donnée dans les essais suivants.

Partie expérimentale

Observation d'argent métallique

Lorsque l'on ajoute une solution sulfurique 0,5 M de fer(II) $2{,}5 \cdot 10^{-2}$ M à une solution sulfonitrique d'argent(I) obtenue par destruction à chaud d'oxyde d'argent(II), on peut observer l'apparition de particules brillantes. La dilution consécutive au mélange ne peut favoriser la précipitation de sulfate d'argent: seule la formation d'argent métallique peut expliquer ce phénomène.

D'autre part, le dosage de $0{,}15 \cdot 10^{-3}$ mole de fer(II) dans le même milieu sulfonitrique, en déterminant le point équivalent par potentiométrie à intensité constante [2], s'est révélé impossible en présence de $3{,}5 \cdot 10^{-3}$ mole d'argent ajouté sous forme $AgNO_3$. La perturbation est encore plus importante si l'on opère en milieu H_2SO_4 2M: l'une des électrodes de platine se recouvre d'un dépôt noir. Ces observations montrent que l'erreur observée est imputable à la présence d'ions Ag^+ et non à une destruction incomplète de l'oxyde d'argent(II).

Tracé des courbes voltampérométriqués

Les courbes voltampérométriques représentées sur la Fig.1 ont été obtenues à l'aide d'un polarographe potentiostatique PRG3 Tacussel en utilisant une électrode tournante de carbone vitreux. L'électrolyte support a la composition suivante: HNO_3M—H_2SO_4 0,5 M—HSO_3NH_2 $2{,}5 \cdot 10^{-3}$ M. Elles confirment que dans ce milieu, les potentiels des couples de l'argent et du fer sont très proches. En outre, le potentiel d'une solution d'argent(I) dépend beaucoup de sa concentration ($E = E_0 + 0{,}06 \log [Ag^+]$, alors que celui d'une solution de fer dépend du rapport $[Fe^{3+}]/[Fe^{2+}]$: dans les conditions du dosage, la concentration des ions Ag^+ est environ 20 fois plus importante, ce qui favorise la réaction envisagée.

Dosage de fer(II) en présence d'argent(I)

La figure 2 montre l'influence, sur le dosage d'une quantité constante de fer(II), de la quantité d'argent présent. L'argent est ajouté dans le milieu réactionnel habituel sous forme d'oxyde d'argent(II) que l'on détruit par chauffage avant l'introduction du fer(II). Pour éliminer l'influence éventuelle de l'instabilité de la solution fer(II), compte tenu du niveau de précision recherché, nous avons comparé chaque résultat à celui que nous avons obtenu pour une même prise d'essai en l'absence d'argent dans un intervalle de moins de 3 h. Nous avons vérifié que dans le même laps de temps, l'écart relatif obtenu entre deux dosages effectués en l'absence d'argent était inférieur à $2 \cdot 10^{-4}$. Pour 300 mg de AgO, quantité habituellement utilisée dans nos dosages de

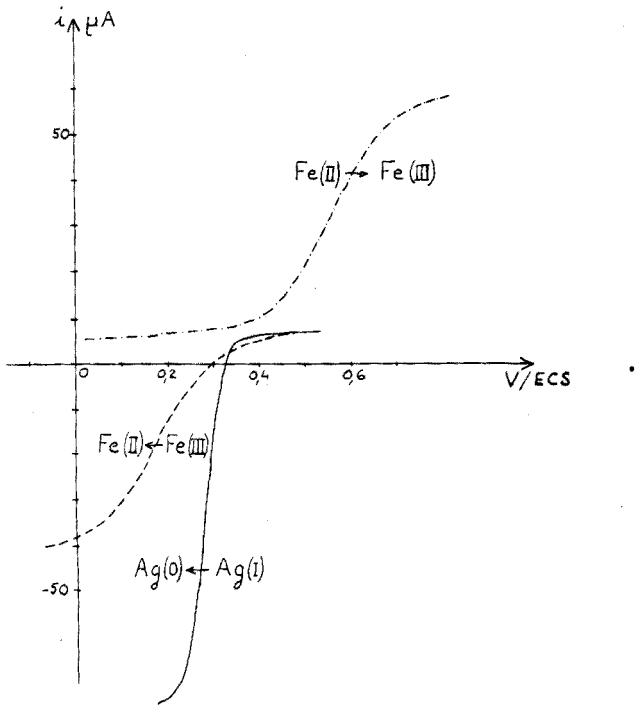

Fig.1. Courbes voltampérométriques de solutions sulfonitriques de fer(II) et (III), $1{,}6 \cdot 10^{-3}$ M et d'argent(I) $2{,}3 \cdot 10^{-3}$ M.

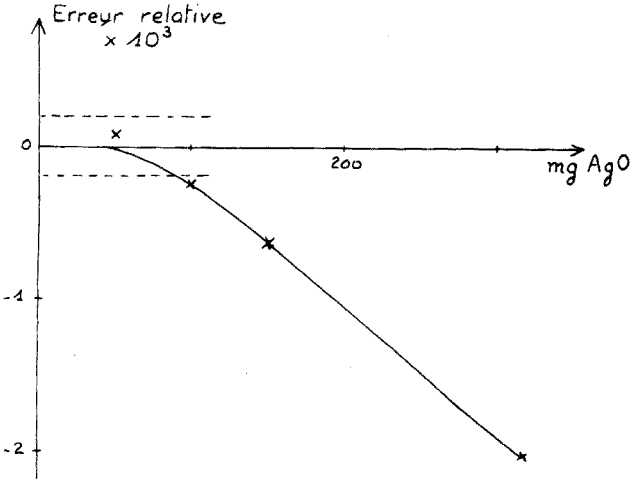

Fig.2. Variation de l'erreur relative dans le dosage de $0{,}37 \cdot 10^{-3}$ mole de Fe(II) en fonction de la quantité d'argent ajoutée.

plutonium, la quantité de Fe(II) oxydée par Ag(I) est d'environ $0{,}7 \cdot 10^{-6}$ mole. Il est probable que cette quantité dépend également de la quantité de Fe(II) présent et du rapport Fe(III)/Fe(II). Toutefois, l'influence de ces paramètres semble plus faible.

Titrage du plutonium

Un échantillon de plutonium métallique, dont la teneur en uranium était inférieure à $3 \cdot 10^{-5}$ g g^{-1} et celle en fer inférieure à $2 \cdot 10^{-5}$ g g^{-1} a été dissous en milieu perchlorique. La solution obtenue a été fractionnée en dix parties. Sur cinq d'entre elles, le plutonium a été dosé par la méthode au titane(III). Sur les cinq autres, la méthode à l'oxyde d'argent(II) a été appliquée dans les conditions suivantes: Pu $\simeq 0{,}2 \cdot 10^{-3}$ mole, AgO $\simeq$ 300 mg, Fe(II) $\sim$ $0{,}67 \cdot 10^{-3}$ mole. Les différentes déterminations ont été effectuées au cours d'une même journée, en utilisant la même solution cérium(IV).

Cette solution de référence avait été préalablement étalonnée au moyen d'anhydride arsénieux NBS (83 c) d'une part, et de plutonium NBS (949 c) par la méthode au titane(III), d'autre part. Les titres exprimés en équivalent/gramme de solution étaient respectivement: $(0{,}98948 \pm 0{,}00030)10^{-5}$ et $(0{,}98954 \pm 0{,}00026)10^{-5}$. Les teneurs en plutonium obtenues sont respectivement:

(100,015 ± 0,024) % pour la méthode au titane(III)

(100,227 ± 0,009) % pour la méthode à l'oxyde d'argent(II)

L'écart observé est significatif; il est du même ordre de grandeur que ceux observés dans les diverses comparaisons effectuées ces dernières années. Il correspond à l'oxydation d'environ $0{,}8 \cdot 10^{-6}$ mole de fer(II) par les ions Ag^+, ce qui est comparable aux résultats concernant le dosage du fer seul.

Conclusion

Les ions Ag^+ formés à partir de l'oxyde d'argent(II) interfèrent sur l'exactitude du titrage du plutonium(VI). Compte tenu de la reproductibilité des résultats, l'emploi de l'oxyde d'argent(II) reste néanmoins valable à condition d'étalonner la solution cérium(IV) au moyen d'un plutonium de référence, suivant un mode opératoire identique à celui utilisé pour le plutonium à doser.

BIBLIOGRAPHIE

1 C.A. Seils, R.J. Meyer et R.P. Larsen, Anal. Chem., 35 (1963) 1673.
2 J. Corpel et F. Regnaud, Anal. Chim. Acta, 35 (1966) 508.
3 J. Corpel et F. Regnaud, Anal. Chim. Acta, 27 (1962) 36.
4 C.E. Caldwell, Anal. Chem., 34 (1962) 346.
5 P. Cauchetier et C. Guichard, Rapport CEA R-4233, 1971.
6 P. Cauchetier, Standard reference materials and meaningful measurements, 6th Materials Research Symposium, NBS, Gaithersburg, 1973.

Analytica Chimica Acta, 80(1975)192—197

Short Communication

DIREKTTHERMOMETRISCHE BESTIMMUNG VON BLEI IN BLEISILICATGLÄSERN

K. DOERING

VEB Jenaer Glaswerk Schott und Gen., Jena (D.D.R.)

(Eingegangen den 6. Mai 1975)

Die bekannten Verfahren der masseanalytischen und volumetrischen Bleibestimmung in silicatischen Materialien [1,2] sind trotz ihrer Zuverlässigkeit zeitaufwendig und deshalb wenig geeignet für betriebsanalytische Serienuntersuchungen. Die laufende Kontrolle des Bleigehaltes von Bleisilicatgläsern während des Produktionsprozesses bedarf des Einsatzes einer rationellen Bestimmungsmethode. Dieser Forderung wird das auf Enthalpieänderungen von Reaktionen basierende Analysenverfahren mit direktthermometrischer Indikation gerecht [3,4].

Grundlagen der direktthermometrischen Analysenmethode

Fast jede in wässrigem Medium verlaufende chemisch-analytische Reaktion wird von einer mehr oder weniger grossen Enthalpieänderung $\Delta_R H$ begleitet. Die dabei auftretenden Energiebeträge sind den Mengen der reagierenden Stoffe proportional. Experimentell wird der Reaktionsablauf durch Beobachten der Temperaturänderung verfolgt, die bei adiabatischer Arbeitsweise gleichfalls den umgesetzten Stoffmengen proportional ist. Der Zusammenhang zwischen Temperaturänderung ΔT und umgesetzter Stoffmenge C [Mol] kann ausgedrückt werden durch die Beziehung

$$C = \Delta T \cdot k/\Delta_R H \qquad (1)$$

In Gleichung (1) bezeichnet k die Wärmekapazität des Gesamtsystems, die sich zusammensetzt aus den Wärmekapazitäten der Messapparatur, der Prüf- und Reagenslösung. Wird der Quotient $k/\Delta_R H$ durch geeignete Versuchsbedingungen konstant gehalten, dann ändert sich die Temperatur der Lösung im linearen Verhältnis zur analytischen Konzentration. k bleibt konstant, wenn jede Bestimmung in derselben Apparatur durchgeführt wird, die Prüflösung auf dieselbe Weise vorbereitet und ihr Volumen bei jeder Bestimmung das gleiche ist und die Prüflösung immer mit der gleichen überschüssigen Menge Reagenslösung der gleichen Konzentration auf einmal versetzt wird. Auf Grund der einmaligen Reagenszugabe im Überschuss wird die gesamte Reaktionswärme sofort freigesetzt. $\Delta_R H$ ist konstant, wenn stets die gleichen Ausgangsbedingungen eingehalten werden und sich immer derselbe Endzustand der Reaktion einstellt

Das wird erreicht, indem die Prüflösungen so vorbereitet werden, dass die Ionenstärke, Acidität und Ausgangstemperatur gleich sind. Damit kann die Gleichung (1) auch formuliert werden

$$C = \text{konst} \cdot \Delta T \qquad (2)$$

Mit Proben bekannten Komponentgehaltes wird eine Eichgerade aufgenommen, die dann zur Ermittlung unbekannter Gehalte dient.

Die direktthermometrische Methode ist für exotherm und endotherm ablaufende Reaktionen anwendbar. Wesentlich ist, dass eine ausreichend grosse Reaktionsenthalpie auftritt, die Reaktionsgeschwindigkeit hoch und die ausgewählte Bestimmungsreaktion selektiv ist. Der direktthermometrischen Indikation ist eine Vielzahl Neutralisations-, Fällungs-, Komplexbildungs- und Redoxvorgänge zugänglich.

Direktthermometrisch indizierbare Reaktionen des Bleis

Die in der Literatur für Blei mitgeteilten thermometrischen Titrationsstudien beziehen sich vorwiegend auf Untersuchungen wässriger Bleisalzlösungen. So wird über die Reaktion des Blei (II) mit Carbonat [5], Hydroxid [6], Oxalat [7] und Hexacyanoferrat (II) [8] berichtet. Auf der mit Enthalpieänderung verbundenen Löslichkeit des Blei(II)-oxids in verdünnter Essigsäure entwickelte Scholl [9] ein automatisch-thermometrisches Verfahren zur Bestimmung des Bleioxidgehaltes von "Grauoxid". Einige Autoren [10,11] titrieren thermometrisch wässrige Bleisalzlösungen mit Na_2—ÄDTA. Die exotherme Fällungsreaktion des Bleichlorofluorids wird zur quantitativen Bleibestimmung empfohlen [12]. Sajó und Sipos [13,14] benutzt die Fällung des Blei(II) als Bleisulfid auch zur direktthermometrischen Bleibestimmung in Gläsern.

TABELLE 1

Direktthermometrisch indizierte Reaktionen des Blei(II)

Reaktionsmedium (mol l^{-1})	Reagens	ΔH_{298} (kcal mol^{-1})
Komplexbildungsreaktion		
H_2O	Na_2—ÄDTA(H_2O)	−12,7 ±0,1
pH 5,5 (NH_4-ac.)	Na_2—ÄDTA(H_2O)	− 5,5 ±0,2
pH 7,0 (Hexamethylentetramin)	Na_2—ÄDTA(H_2O)	− 8,4 ±0,2
H_2O	NaOH	− 8,0 ±0,1
Fällungsreaktion		
0,1 NH_4-ac., pH 4,5	$K_2Cr_2O_7$(H_2O)	−10,9 ±0,1
H_2O	KBr+NaF(H_2O)	− 7,3 ±0,2
H_2O	KJ(H_2O)	−13,8 ±0,1

Wir versuchten, die exotherm verlaufende Chelatbildung des Blei(II) mit Na_2—ÄDTA für die direktthermometrische Bleibestimmung in Bleisilicatgläsern anzuwenden. Bleisilicatgläser lassen sich durch Eindampfen der Probe mit einem Flusssäure—Schwefelsäure-Gemisch leicht und schnell aufschliessen [15]. Der Rückstand von Bleisulfat löst sich [16] in Ammoniumacetat zum Kationenkomplex $[PbCH_3COO]^+$. Bei der Chelatbildung zwischen Pb(II) und Na_2—ÄDTA in acetathaltiger Lösung muss das Metallion zunächst aus dem Acetatkomplex verdrängt werden. Wie aus der Tabelle 1 hervorgeht, liegt der direktthermometrisch bestimmte $\Delta_R H$-Wert [17] daher weit unter dem für rein wässrige Lösungen gültigen und ausserdem in einem Bereich, der gegen die Verwendung der Reaktion für analytische Zwecke spricht. Dagegen erwies sich die Fällungsreaktion des Bleichromats in acetathaltiger Lösung als direktthermometrisch indizierbar [18]. Diese Reaktion wird zur direktthermometrischen Bleibestimmung in Gläsern angewendet.

Experimentelles

Analysenapparatur

Es wird das thermometrische Analysengerät "Directhermom" der Firma Ungarische Optische Werke (MOM) Budapest benutzt. Direktthermometrische Analysen sind nach dem Eichgeradenverfahren oder durch Direktanzeige des Konzentrationswertes ausführbar. Die Bestimmung des Bleis erfolgt nach dem Eichgeradenverfahren. Die Messzelle des Analysengerätes "Directhermom" besteht aus einem Dewar-Gefäss mit einem Plastbehälter zur Aufnahme der Probelösung. Der vertikal bewegliche Messkopf gewährleistet nach dem Einführen der Messelemente in die Prüflösung einen hermetischen Abschluss zur Umgebung, so dass während des Messvorganges quasi-adiabatischer Zustand herrscht.

Reagenslösung

26 g Kaliumdichromat z.A. werden in 1 l destilliertem Wasser gelöst.

Bleinitrat-Stammlösung (10 mg PbO ml^{-1})

14,839 g Bleinitrat z.A. werden in einen 1-l Messkolben eingewogen und zu 1 l in destilliertem Wasser gelöst.

Eichlösungen

10, 20, 30 und 40 ml der Bleinitrat-Stammlösung, die den Bleigehalten von 100, 200, 300 und 400 mg PbO entsprechen, werden in 250-ml Messkolben pipettiert, jeweils mit 25 ml Ammoniumacetatlösung (8 % ig) versetzt, und mit destilliertem Wasser wird bis zu den Eichmarken aufgefüllt.

Glasaufschluss und Analysenlösung

Die Einwaagengrössen der zu analysierenden Gläser werden so bemessen,

dass die vermuteten Bleigehalte in den Bereich der Eichkonzentrationen zwischen 150 und 300 mg PbO fallen. Die in der Achatreibschale feingemahlene Glasprobe wird in eine 50-ml Platinschale eingewogen, mit 3—5 Tropfen Wasser befeuchtet und zweimal mit je 15 ml Flusssäure (38—40 % ig z.A.) auf dem Wasserbad bis zur Trockene eingedampft. Zu dem Abdampfrückstand werden insgesamt 10 ml konzentrierte Schwefelsäure (z.A.) vorsichtig zugetropft, und es wird auf dem Sandbad bis zum Aufhören der SO_3-Entwicklung erhitzt. Dem in der Platinschale befindlichen Rückstand werden 25 ml Ammoniumacetatlösung (8 % ig in destilliertem Wasser) zugegeben. Der Schaleninhalt wird unter Rühren schwach erwärmt, wobei das Bleisulfat in Lösung geht. Die bleihaltige Aufschlusslösung wird quantitativ in einen 250-ml Messkolben überführt, und nach dem Abkühlen auf Raumtemperatur wird das Volumen mit destilliertem Wasser bis zur Eichmarke ergänzt.

Ausführen der Messungen

Die Eich-, Analysenlösungen und das Reagens werden auf die Ausgangstemperatur des Messzelleninnenraumes mit ± 0,1 °C eingestellt. Die Prüflösung wird in den als Messgefäss dienenden Plastbecher, in den vorher der Magnetrührkern eingelegt wird, eingegossen. Der Plastbecher wird dann in das Dewargefäss des Messgerätes eingesetzt. Die Immersionspipette wird mit 15 ml Reagenslösung gefüllt, aussen mit wenig destilliertem Wasser abgespült, mit einem weichen Tuch abgewischt und in der am Messkopf vorgesehenen Halterung befestigt. Durch Einfahren des Messkopfes gelangen die Messelemente in die Prüflösung, und die Messzelle wird verschlossen. Das Magnetrührwerk wird in Betrieb gesetzt. Der Temperaturausgleich zwischen Prüflösung, Reagens in der Immersionspipette und Messzellenumgebung findet innerhalb 5 Minuten statt. Die Messbrücke wird eingeschaltet. Nach Kontrolle auf vollständigen Temperaturausgleich wird der Galvanometerausschlag bei Messempfindlichkeit "2X" (ΔT = 0,5 °C = 1000 Skalenteile) mit dem "Grob"- und "Fein"-Potentiometer auf Null abgeglichen, das Reagens aus der Tauchpipette in die Prüflösung eingespritzt und der sich einstellende Galvanometerausschlag in Skalenteilen abgelesen.

Ergebnisse und Diskussion

Die Abhängigkeit der Temperaturänderung des Reaktionsgemisches von der analytischen Konzentration folgt entsprechend Gleichung (2) der linearen Funktion $y = a + bx$. Die Konstanten a und b werden aus den Eichdaten für x (mg PbO) und y (Skt.) mittels vereinfachter Regressionsrechnung [19] erhalten. Das Analysenergebnis ergibt sich dann zu

$$\text{Masse-\% PbO} = \frac{y_A - a}{b} \cdot 100/\text{mg Glaseinwaage} \qquad (3)$$

worin y_A den Messwert der Analysenprobe bezeichnet. In der Tabelle 2 sind

TABELLE 2

Vergleich zwischen direktthermometrisch und volumetrisch bestimmten Bleigehalten für einige Bleisilicatgläser

Bleisilicatglas	PbO Masse-%	
	Direktthermometrisch	Volumetrisch
1	3,0	2,7
2	28,5	28,7
3	60,8	61,0
4	80,4	80,1

TABELLE 3

Bewertung des Verfahrens der direktthermometrischen Bleibestimmung von Gläsern (Eichgeradenverfahren, Konzentrationsbereich: 100—400 mg PbO)

Standardabweichung in der Mitte des Messbereiches	
$s = \frac{1}{b}(s_0^2 (\frac{1}{n} + \frac{1}{m}))^{1/2}$	s = 1,6 mg PbO für n = 4 und m = 4[a]
Vertrauensintervall des in der Mitte des Messbereiches liegenden Konzentrationswertes	
$\Delta\bar{x} = t(P, f) \cdot s$	$\Delta\bar{x} = \pm 6{,}8$ mg PbO für $f = 2$[b]

[a] b = Regressionskoeffizient. s_0^2 = Varianz zwischen gemessenen y_i- und berechenbaren Y_i-Werten. n = Zahl der Parallelbestimmungen. m = Zahl der Eichproben.
[b] P = Statistische Sicherheit = 95 %. f = Freiheitsgrade = $m - 2$.

für einige Bleisilicatgläser die direktthermometrisch erhaltenen Analysenergebnisse den volumetrisch als Pb—ÄDTA bestimmten Bleigehalten gegenübergestellt. Der Vergleich zeigt Übereinstimmung.

Direktthermometrisch ist es möglich, Blei bis herab zu einer Konzentration von 34 mg PbO reproduzierbar zu erfassen. Das direktthermometrische Verfahren der Bleibestimmung ist vor allem von Vorteil für die Analyse von Gläsern, die gleichzeitig Barium enthalten.

Der Zufallsfehler des Verfahrens wurde ermittelt nach den von Doerffel [20] für eichbedürftige Analysenmethoden gegebenen Hinweisen und ist aus der Tabelle 3 ersichtlich. Der Zeitbedarf für eine Doppelbestimmung beträgt zwei Stunden. Der günstige Zeitfaktor und die gute Reproduzierbarkeit lassen den Einsatz des Verfahrens der direktthermometrischen Bleibestimmung in der Betriebskontrolle empfehlen.

LITERATUR

1 I.A. Voinovitch, J. Debras-Guedon und J. Louvrier, The Analysis of Silicates, Israel Program for Scientific Translations, Jerusalem, 1966, S. 343.
2 H. Bennett und R.A. Reed, Chemical Methods of Silicate Analysis, Academic Press, London, 1971, 3. Aufl., S. 165.
3 J.C. Wásilewski, P.T.-S. Pei und J. Jordan, Anal. Chem., 36 (1964) 2131.
4 I. Sajó, Termometria, Müszaki Könyvkiadó, Budapest, 1971.
5 P.T. Priestley, Analyst (London), 88 (1963) 194.
6 P. Dutoit und E. Grobet, J. Chim. Phys., 19 (1922) 324.
7 C. Mayr und J. Fisch, Z. Anal. Chem., 76 (1929) 418.
8 R. Paris, C.R. Acad. Sci., 199 (1934) 863.
9 F. Scholl, Z. Anal. Chem., 245 (1969) 49.
10 J. Jordan und T.G. Alleman, Anal. Chem., 29 (1957) 9.
11 P.T. Priestley, W.S. Sebborn und R.F.W. Selman, Analyst (London), 90 (1965) 589.
12 C.E. Johansson, Talanta, 17 (1970) 739.
13 I. Sajó und B. Sipos, Kohászati Lapok, 101 (1968) 484.
14 I. Sajó und B. Sipos, Építöanyag, 22 (1970) 274.
15 R. Bock, Aufschlussmethoden der anorganischen und organischen Chemie, Verlag Chemie, Weinheim, 1972, S. 47.
16 B.C. Purkayastha und R.N. Sen-Sarma, J. Indian Chem. Soc., 23 (1946) 31.
17 K. Doering, Z. Anal. Chem., 258 (1972) 177.
18 J. Barthel, N.G. Schmahl und K. Lenz, Z. Anal. Chem., 233 (1968) 328.
19 E.L. Bauer, A Statistical Manual for Chemists, Academic Press, New York, 2. Aufl., 1971, S. 116.
20 K. Doerffel, Statistik in der analytischen Chemie, Grundstoffindustrie, Leipzig, 1966, S. 172.

Analytica Chimica Acta, 80(1975)198—203

Book Reviews

A. Zlatkis and L.S. Ettre (Eds.), *Advances in Chromatography, 1974*, Elsevier, Amsterdam, 1974, xv + 772 pp., price $61.50, Dfl 160.00.

This special volume, reprinted from Volume 99 of the *Journal of Chromatography*, contains the texts of the 61 papers presented at the Ninth International Symposium on Advances in Chromatography, held at Houston, Texas on November 4—7, 1974. It seems little short of miraculous that editors and publishers should have achieved the publication of a major volume such as this, excellently edited and complete with author and subject indexes, before the end of 1974, so enabling all those unable to attend the Symposium to benefit from having the opportunity to read the papers so shortly after their presentation. The old problem of slowness of publication of the proceedings of major international symposia, from which the authors of papers have suffered as much as those unable to attend, now seems to have been overcome. Rapid publication and wide distribution of the information released at such meetings is important; the personal communication between scientists participating in the meeting is simply an additional bonus.

The papers presented at this Symposium were uniformly of a very high standard, and it is clear that developments in all aspects of chromatography are still forthcoming. It is amusing to recollect that in 1959, when the desirability of organizing a major conference on chromatography was under consideration, a leading British analytical chemist held the view that chromatography was running out of steam. At Houston last November, the emphasis was clearly on the revival of liquid chromatography and its transformation into high-pressure systems. Developments along these lines must be expected for some time yet.

The contents of this volume are divided into 5 major themes: New Horizons (5 papers); Chromatographic columns and stationary phases (8 papers); Theoretical and practical aspects of chromatography (23 papers); Biomedical applications (17 papers); and Environmental applications (8 papers). In addition, details of the citations are given for the award of the M.S. Tswett Chromatography Medal.

All those who consider themselves active chromatographers will have to consult this volume, which contains a great deal of thought-provoking material. The editors and publishers are to be congratulated on the production of this volume; its robust binding will ensure that it will stand up to the constant handling it will certainly receive.

D.M.W. Anderson

Wesley W. Wendlandt, *Thermal Methods of Analysis*, Wiley, New York, 2nd Edn., 1974, xvii + 505 pp., price £14.00.

The first edition of this book was published in 1964, and Professor Wendlandt claims that the field of thermal analysis has undergone a period of tremendous growth since that time. This second edition is intended to serve as an introduction to the modern techniques and applications of thermal analysis, and for this purpose it is excellent. No attempt has been made to develop a comprehensive treatment; indeed, each of the chapters could be expanded to a full-length book.

This text differs greatly from the first edition. The chapter on thermal analysis has undergone the least revision; dynamic thermogravimetry, differential thermal analysis and differential scanning calorimetry are discussed in greater detail than the other techniques, and there are two entirely new chapters — on nomenclature and on the application of digital and analog computers.

The references cited at the end of each chapter indicate how thoroughly the author has up-dated his original text. At the present time this book gives advanced students an excellent introduction to the theory and modern practice of thermal methods of analysis, and it can be strongly recommended.

John P. Phillips, Henry Feuer and B.S. Thyagarajan (Eds.), *Organic Electronic Spectral Data, Volume X (1968)*, Wiley, New York, 1974, xiii + 1034 pp., price £18.00.

This large book extends the massive co-operative task, undertaken in 1956, of abstracting in formula order all the ultraviolet—visible spectra of organic compounds published in the major chemical journals. The first two volumes covered the period 1946—1955; thereafter a volume was published in alternate years until 1966, when annual publication was begun.

The amount of work involved in producing a book of this kind is enormous; it is not surprising that publication of the compilation for 1968 was not achieved until December 1974. Processing of the data provided by the contributors to this Volume was undertaken at the University of Louisville; more than 50 chemists scanned over 100 journals. There can be nothing but praise for their efforts. All entries in the compilation are organised according to the molecular formula index system used by *Chemical Abstracts*; compounds are named in terms of the *Chemical Abstracts* system of nomenclature; data for the solvent, λ_{max} and log ϵ are quoted and the original reference is given. To round off a massive task, a complete author index, with cross-references, is provided.

This is clearly an essential reference work that should be available in all chemistry libraries. It is a pleasure to record that the price quoted represents excellent value by present standards.

D.M.W. Anderson

A. R. Butler and M. J. Perkins (Eds.), Organic Reaction Mechanisms, — 1973. J. Wiley, London, 1975, 579 pp., price £19.50.

Under its new Editors, the latest volume in this series continues in much the same vein as its predecessors. There are alterations in the order of chapter headings to facilitate the publication of separate parts of the book, thus encouraging a wider distribution. The chapter on photochemistry has been discontinued, because the subject is reviewed comprehensively elsewhere. This, no doubt, has contributed to the smaller size of the book.

As before, over 5000 references have been cited and many are discussed in detail. The chapter on radical reactions is quite the largest and testifies to the enormous activity in this field. Throughout, the standards of previous volumes have been maintained. The general format and diagrams are as usual very good.

E. J. Forbes

R. A. A. Muzzarelli, Natural Chelating Polymers, Pergamon Press, Oxford, 1974, vii + 253 pp., price £4.95.

This monograph continues Professor Muzzarelli's efforts over the past several years to convince his readers that the use of certain natural chelating polymers is of vital importance to analytical chemistry. His methods have not been widely emulated and it is unlikely that this Monograph will correct the situation. It opens with a rambling egotistic Preface, in which the views expressed are rather difficult to sustain, and the entire book could well have benefited from an increased measure of editorial attention. Obscure or even meaningless passages abound, and scant attention seems to have been given to proof-reading. As a result, this is a somewhat dangerous book for the novice. As a review of the essentials of polysaccharide chemistry, the text is considerably outdated, and its attempts to bridge the gap between polysaccharide and analytical chemistry are not entirely successful. It is difficult to recommend this book to any particular class of reader.

A. E. Martell and R. M. Smith, *Critical Stability Constants*, Vol. 1, Amino Acids, Plenum Press, New York, 1974, xiii + 469 pp., price $27.60.

Unlike the compilation of Martell and Sillen, published by the Chemical Society, the present series of publications presents values of protonation and metal complex stability constants, including ΔH and ΔS values, which, in the opinion of the authors, are the best values available. The first volume contains information not only on the compounds normally known as amino acids, but on a much larger number of ligands which contain amine and carboxylic acid functions. Thus, a wide collection of iminodiacetic acid compounds (EDTA derivatives, xylenol orange, for example) is included, as

well as pyridine carboxylic acids, anthranilic acid, etc. There is also a section on peptides. Full references are given to all constants reported.

The information contained in this, and subsequent volumes, will be invaluable to all who have reason to obtain quickly the most reliable equilibrium constant data available for metal complexes. The presentation of the information, although clear, leads to a great deal of wasted space on the very large pages (27 × 21 cm). The quality of the paper, too, has led to an excessively thick (3.6 cm for 470 pp.) and heavy (ca 5 lb) book. These factors detract from ease of use, but not from the value of its contents.

Modern Physical Techniques in Materials Technology, Edited by T. Mulvey and R. K. Webster, Oxford University Press, London, 1974, xiv + 321 pp., price £9.50.

Based on an interdisciplinary course offered at the Harwell Education and Training Centre, this book deals with the characterization of materials by physical instrumental techniques. Of the twenty chapters, thirteen are concerned with diffraction and electron microscopic methods. After a general introduction to crystallography and diffraction, diffraction techniques based on x-rays, neutrons and electrons are described in separate chapters. Accounts of field-ion and optical microscopy are followed by chapters on transmission, high-voltage and scanning electron microscopy, electron-probe microanalysis and Auger spectroscopy. The spectrometric methods described include mass, x-ray, atomic emission and atomic absorption; activation analysis, and Mössbauer and magnetic resonance spectroscopy are also discussed.

Each technique is covered within 10—20 pages, so that the treatment can only be superficial. For example, in the chapter on electron-probe microanalysis, a 2-page introduction precedes a section (6 pp.) on the principles of instrumentation, spectrometers, recording and quantitative analysis, a short paragraph on instrumentation, a section on applications (2 pp.) and a rather outdated reference list.

The claim that the information given will suffice for decisions to be made on the potentialities of each technique in problem solving seems a trifle optimistic, for the outlines of what has been accomplished in useful applications are woefully inadequate. However, the text summarizes skillfully what each technique is about and so should be useful for teaching purposes in materials science.

J. N. Done, J. H. Knox and J. Loheac, *Applications of High-Speed Liquid Chromatography*, Wiley, London, 1975, vii + 238 pp., price £6.50.

High-pressure, or high-speed, liquid chromatography (h.p.l.c.) is steadily increasing in importance for the analysis of materials which are not readily amenable to gas chromatography, but its possibilities and limitations are not

yet very widely appreciated. This eminently practical book should help to convert the unbelievers whose primary contact with the technique has been the instrument manufacturer's literature. The techniques and theory of h.p.l.c. are recounted briefly in 42 pages, which is probably adequate for the practical chemist, although some words of advice on ill-behaved columns would have been a useful adjunct to all the information on well-behaved columns. The main part of the book comprises 142 chromatograms which have been drawn to a standard format and are listed with the experimental parameters such as column size and packing, solvent, pressure, temperature, detection system, etc. It is worth noting that about 90% of these chromatograms were obtained with u.v. detection, and there is obviously a wide-open field for the development of other less limited sensitive detectors. Author, formula and compound indexes are provided.

The method of presentation is space-consuming, and the whole book might have been compressed almost to review length by extensive tabulation of essential data. Yet, because of the computer setting, the cost is by no means excessive for the amount of information conveyed, and the book can be recommended to all practising chemists.

A. L. Wilson, *The Chemical Analysis of Water—General Principles and Techniques*, The Society for Analytical Chemistry, London, 1974, viii + 188 pp., price £7.50.

Analysis of natural and potable waters is of great importance, and this text has been written to provide authoritative guidance for the increasing number of chemists with inadequate analytical training or experience now becoming involved in all aspects of environmental analysis. The book appears as Analytical Sciences Monograph No. 2 from the Society for Analytical Chemistry (now the Analytical Division of the Chemical Society).

The first few chapters contain discussions on what results are required and why they are needed — matters which must always be decided before suitable methods can be selected intelligently — and on sampling, storage, accuracy and reporting of results, and the general precautions necessary to ensure reliable analytical results. These excellent discussions are essential reading for newcomers to water analysis, and provide much useful advice for any student of analytical chemistry. Analytical methods, from gravimetry to x-ray fluorescence and reactor activation, are then reviewed; one of the few criticisms of this book is that the space used in describing the basic principles and practice of instrumental techniques could more beneficially have been devoted to more extensive information on the application of these methods tc waters. The final chapters provide useful surveys of automated and on-line analyses and of data handling.

This is a very useful book. It does not contain recommended procedures, but the chemist who has absorbed all the sensible advice given should be in a strong position to make his own selection among the many available methods.

R. C. Chirnside and J. H. Hamence, *The Practising Chemists — A History of the Society for Analytical Chemistry 1874—1974*, The Society for Analytical Chemistry, London, 1974, xv + 225 pp., price £3.00.

The Society for Analytical Chemistry celebrated its Centenary in 1974. The authors of this history have charted the progress and activities of the Society from its foundation as the Society of Public Analysts by a small group of analysts concerned about ill-designed legislation on the adulteration of foods, to its emergence as the Analytical Division of the Chemical Society at the beginning of 1975. The intervening years have seen many changes in direction of the Society's activities and massive extensions in its areas of interest. From the start, the members of the Society seem to have been a contentious lot, as ready to lift a vituperative pen as a test tube, and the recounting of some of these episodes lends vitality to what could have become a dry straightforward history.

This volume will be of interest to those with a taste for historical byways. Significantly, the organization of practising chemists as a single body was being discussed in 1874, but only in 1975 did this in fact happen in the U.K. with the unification of the major chemical societies. How successful this will be must depend largely on the goodwill of succeeding generations of "Practising Chemists".

Analytica Chimica Acta, 80 (1975) 204—207

ANNOUNCEMENTS

International Union of Pure and Applied Chemistry

CRITICAL SURVEYS OF STABILITY CONSTANTS OF METAL COMPLEXES

(Guidelines for prospective authors)

Critical Surveys of Stability Constants of Metal Complexes is a continuous series, edited by the IUPAC Commission on Equilibrium Data. Each Critical Survey will be published in the official journal of IUPAC, *Pure and Applied Chemistry*, enabling the series to be bound at a later date in a more permanent, hard-cover volume. The aim of the series is to evaluate the most reliable equilibrium constants from the available and frequently conflicting data.

Each survey is prepared by an expert, working actively in the field of thermodynamics of complexes. The papers are normally written by solicited authors. Unsolicited authors should first send an outline of their intended survey to avoid parallel work. Each survey, written by either solicited or unsolicited authors, is circulated among and commented on by the Members of the Commission on Equilibrium Data. It follows from the nature of the data considered, however, that even the recommended values cannot be regarded as "official" ones and further research may change the suggestion.

In a Critical Survey reference should be made to all published data, but the numerical values should not necessarily be mentioned. The data are handled in four categories: recommended, tentative, doubtful, rejected. It must definitely be stated why certain data are rejected and particularly why certain data are regarded as reliable.

(a) Data should be recommended if the results of at least two independent groups are available and they are in good agreement; if the surveyor has no doubt as to the adequacy of the applied experimental and calculation procedure; if the consideration of the activity-concentration relation is correct and the standard state is unambiguous. The given error of such a constant must be less than ±0.05 logarithmic unit.

(b) Data should be regarded as tentative if all the conditions mentioned in connexion with the recommended category are fulfilled, except the first, or if the surveyor observes some deviation from the necessary rigorousness, but this probably caused no serious mistakes. The given error of such a constant cannot exceed ±0.2 logarithmic unit.

(c) Data should be considered as doubtful if the surveyor found some mistake in the evaluation of the constants, which are nevertheless of

semiquantitative value. The probable error of such a constant should not exceed ±1 logarithmic unit.

(d) Data determined by an inadequate method, or obtained under undefined conditions, or where any serious objection is found in the evaluation, should be rejected.

Only published data should be included in the surveys. Quotations such as "unpublished data", "personal communication", etc., should be omitted. Even the published data can be considered only if the presented experimental details permit assessment of the degree of reliability of the constants.

A Critical Survey should preferably be written on the different complexes of a certain ligand or family of ligands, although in certain cases other groupings are accepted (e.g., complexes of a certain metal ion or a family of metal ions). Besides stability constants. ΔH and ΔS data should be included where available. For these data the same rules should be applied as for the equilibrium constants.

Arrangement of the Paper

Although strict uniformity in the format of papers is not expected, the following rules should be followed.

1. In the Introduction, the general characterization of the treated ligand (or metal ion) and of the complexes should be given. Stress should be laid on the problems connected with the determination of the stability constants, for the particular ligand.
2. The order of metal ions should follow the order applied in the volumes of *Stability Constants of Metal-Ion Complexes*, inorganic section, independently of whether the ligand in question is organic or inorganic. When a family of ligands is considered, it is suggested that the data be treated in an order permitting meaningful comparison.
3. To conclude the consideration of the constants referring to a certain equilibrium or set of equilibria, a constant or set of constants should be given, indicating the degree of reliability. In doing this the rules mentioned above should be applied.
4. Although a low degree of reliability is an immediate indication of the subjects requiring further work, it is suggested that fields be indicated where further careful studies are particularly desirable.
5. The reference numbers should be given in parentheses in the text or in the tables. The same bibliographic system should be applied as in Stability Constants: the last two digits of the year of publication and the initial of the family name of the first author. A list of references should be given in alphabetical order at the end of the paper.
6. All manuscripts should be sent in duplicate to the Chairman of the Commission on Equilibrium Data, who is at present:

Prof. G. H. Nancollas
Department of Chemistry
State University of New York
Acheson Hall
Buffalo, New York 14214
USA

or to the Project Leader, who is at present:

Prof. M. T. Beck
Institute of Physical Chemistry
Kossuth Lajos University
H-4010 Debrecen
Hungary

Surveys Received

The following Critical Surveys have been compiled and are at present being prepared for publication by the Commission on Equilibrium Data:

Survey on EDTA Complexes	G. Anderegg
Survey on Cyano Complexes	M. Beck
Critical Evaluation of Some Equilibrium Constants involving Alkylammonium Extracts	A. S. Kertes

First European Symposium on Thermal Analysis, Salford, September 20—24, 1976

This symposium is organized by the Thermal Methods Group of the Analytical Division of the Chemical Society, at the University of Salford. The deadline for submission of abstracts of papers is December 31, 1975. Further information can be obtained from: Dr. D. Dollimore, Department of Chemistry, University of Salford, Salford M5 4WT, England.

Interan '76 — Analysis of Geological Materials, Prague, August 23—27, 1976

This conference is organized under the auspices of the International Association for Geochemistry and Cosmochemistry. Working languages will be English, Russian, Czech and Slovak. The deadline for submission of abstracts of papers is September 30, 1975. The Conference will be held in the International Hotel, Prague. Further information can be obtained from: Ing. N. Bajova, House of Technology, SVTS, 011 80 Zilina, Czechoslovakia.

Fifth Biennial International CODATA Conference, Boulder, Colorado, June 28—July 1, 1976

CODATA is an interdisciplinary committee of ICSU concerned with data compilation and evaluation, and improvement of the quality of data collections and data accessibility. The Fifth Conference will cover: Methodology of data evaluation: Correlation, extrapolation and estimation of data; Mathematical modelling, technological impact assessment; Existing and planned data compilation; Machine techniques for storage and dissemination.

The Conference will be held in the University of Colorado, Boulder, Colorado, U.S.A. The deadline for submission of abstracts of papers is November 1, 1975. Further information can be obtained from Dr. H. van Olphen, National Academy of Sciences, 2101 Constitution Avenue, Washington, D.C. 20418, U.S.A., or from the CODATA Secretariat, 51 Boulevard de Montmorency, 75016 Paris, France.

VIIth International Symposium on Organic Sulphur Chemistry, Hamburg, Germany, July 12—16, 1976

This Symposium will be organized by the Gesellschaft Deutscher Chemiker. The topics covered will be: Synthesis including stereochemistry; Theoretical and structural chemistry; Natural products; Borderlines to inorganic chemistry. Further details can be obtained from: Dr. W. Fritsche, Gesellschaft Deutscher Chemiker, Postfcah 90 04 40, D-6000 Frankfurt/M 90, Federal Republic of Germany.

Analytica Chimica Acta, 80 (1975) 208

Erratum

M. Nanjo and G. G. Guilbault, Amperometric determination of alcohols, aldehydes and carboxylic acids with an immobilized alcohol oxidase enzyme electrode, Anal. Chim. Acta, 75 (1975) 169—180. On p. 179 of this paper, acknowledgement should have been made for the financial assistance of the National Institutes of Health under Grant No. 17268.

(Continued from page 4 of cover)

Short communications

Printed in The Netherlands

CONTENTS

(Continued on inside page of cover)